TECHNISCHE UNIVERSITÄT DARMSTADT

Investigations on the influences of paper intrinsic properties and flame retardants on paper materials fire properties

vom Fachbereich Chemie

der Technischen Universität Darmstadt

zur Erlangung des akademischen Grades eines

Doctor rerum naturalium (Dr. rer. nat.)

genehmigte

Dissertation

von

M.Sc. Felix Schäfer
aus Wiesbaden

Erstgutachter:	Prof. Dr. Markus Biesalski
Zweitgutachter:	Prof. Dr. Rudolf Pfaendner

Darmstadt 2023

Tag der Einreichung: 20.02.2023

Tag der mündlichen Prüfung: 03.04.2023

Schäfer, Felix: Investigations on the influences of paper intrinsic properties and flame retardants on paper materials fire properties
Darmstadt, Technische Universität Darmstadt
Jahr der Veröffentlichung der Dissertation auf TUprints: 2023
URN: urn:nbn:de:tuda-tuprints-236575
Tag der mündlichen Prüfung: 04.03.2023

Acknowledgement

First, I would like to thank Prof. Dr. Markus Biesalski for giving me the opportunity to do my PhD in the field of paper and macromolecular chemistry. Furthermore, thank you for the excellent supervision, the interesting discussions, the understanding in all matters and the guidance to develop myself personally. I would also like to thank Prof. Dr. Rudolf Pfaendner for preparing the second expert opinion and Prof. Dr.-Ing. Samuel Schabel and Dr. Torsten Gutmann for their professional examinations.

My gratitude also goes to Dr. Andreas Geißler, who contributed a lot to this work with his knowledge and support. In addition, I would like to thank Martina Ewald, who not only helped with the organization and questions in the lab, but also generally always had an open ear and was always up for a laugh. In addition, thank you to Vanessa Schmidt and Bärbel Webert for the good cooperation and the willing support of any kind.

A big thank you also goes to the members of the Biesalski and Andrieu-Brunsen working groups for their cooperation and inspiration on any issues. We had a great time together besides work and created memories that are unforgettable. Above all, a big thank you to Nicole Rath and Adnan Khalil who proofread this work and helped me a lot. Furthermore, a big thank you also goes to Niels Postulka, as he supported me immensely in creating the computer-based evaluation. In addition, thank you to the BAMP! team. The interdisciplinary work that we had to learn together was an exciting challenge besides the scientific work and I enjoyed it very much. To my interns Cynthia Cordt, Jan-Lukas Schäfer, Jan-Paul Siebert, Nicolai Schmitt, Ursula Menges and Tim Kircher I would like to say thank you for the good cooperation and the good results. It was fun to supervise you.

Furthermore, I would like to thank Dr. Federico Carosio of the Polytechnic University of Turin and Lais Weber & Daniela Goedderz of the Fraunhofer LBF Institute Darmstadt for the helpful and reliable support during the cone calorimeter measurements. Further thanks go to the working group of Prof. Dr. M. Retsch of the University of Bayreuth for performing the lock-in thermography measurements and to Mark Höfler of the working group of Prof. Dr. G. Buntkowsky for the analysis of the solid-state NMR spectroscopy. Thanks also to Dipl. Ing. Claudia Fasel from the group of Prof. Dr. R. Riedel of the TU Darmstadt for help with the TGA-FTIR-MS measurements. Final thanks go to PTS Heidenau for performing the mercury porosimetry.

A special thanks goes to my wife Alina Schäfer. You always supported me during this time and showed understanding for all my peculiarities and also bravely endured difficult times. I would also like to thank my parents and my sister Nora for your support and the now and then necessary motivation.

A final thank you goes to my former fellow student David Stock. Thank you for the time with you, even if it was limited.

Summary

Diese Arbeit ist Teil des interdisziplinären Projekts BAMP! - "Bauen mit Papier", in dem die Vorteile von Papier als Werkstoff für die Bauindustrie systematisch erschlossen werden sollen. Die generelle Notwendigkeit den Einsatz nicht nachhaltiger Baustoffe zu reduzieren, ist in Verbindung mit der Reduzierung von CO_2-Emissionen das Hauptziel des BAMP! - Projekts.

In diesem Rahmen ist es das Ziel dieser Arbeit Faktoren zu ermitteln, die das Brennverhalten und den Flammschutz von Papier beeinflussen. Dabei soll ein Verständnis geschaffen werden, wie das Verbrennungsverhalten von Papier durch die Veränderung von intrinsischen Parametern beeinflusst wird. Zudem werden Papiere aus gebleichtem und ungebleichtem Zellstoff gegenübergestellt, um weitergehend den Einfluss von Restlignin auf das Brandverhalten zu untersuchen. Die daraus erhaltenen Erkenntnisse werden anschließend verwendet, um mit Hilfe von Flammschutzmitteln flammgeschützte Papiere herzustellen. Im Sinne des Projekts werden dazu zwei biobasierte Flammschutzmittel, welche derzeit keine kommerzielle Anwendung im Bereich der Papierherstellung finden, eingesetzt und mit einem nicht biobasierten kommerziellen Flammschutzmittel verglichen. Bei den drei eingesetzten Flammschutzmittel handelt es sich um phosphorbasierte Flammschutzmittel. Da das Flammschutzmittel immer auf das zu schützende Material angepasst sein sollte, wird auch hierbei der Einfluss des Restlignins auf die Funktionsweise der Flammschutzmittel sowie mögliche Veränderungen im Zersetzungsverhalten untersucht, um somit ein Verständnis für wichtige Parameter der Flammhemmung auf Papier zu schaffen. Darüber hinaus werden die durch die Modifikation mit Flammschutzmittel erhaltenen mechanischen Eigenschaften untersucht, um final eine Schlussfolgerung aus den erhaltenen Ergebnissen für die Anwendbarkeit von Papier im Bauwesen ziehen zu können.

Im ersten Teil der Arbeit wurde zur Bestimmung des Brandverhalten von Papier eine Matrix aus Papierproben mit unterschiedlichen intrinsischen Eigenschaften erstellt. Dabei wurde über eine Kalandrierung die Verpressung und über die Grammatur das Gewicht der einzelnen Proben eingestellt. Diese Papiere wurden aus gebleichtem und ungebleichtem Zellstoff der gleichen Zusammensetzung hergestellt, um somit den Einfluss von verbleibendem Lignin auf den Fasern zu untersuchen. Um das Brandverhalten der unterschiedlichen Papierproben exakt analysieren zu können, wurde hierfür erstmals eine computerbasierte Auswertemethode entwickelt. Dabei wurde ein Video des Abbrennens aufgezeichnet und das Fortschreiten die Flammfront anschließend computerbasiert ausgewertet. Bei dieser Untersuchung wurden sowohl die horizontale als auch die vertikale Brennrichtung analysiert, um gleichzeitig unterschiedliche Verbrennungsmechanismen studieren zu können. Hinsichtlich des Einflusses der Kalandrierung konnte dadurch erstmals gezeigt werden, dass widersprüchlich zu der

Annahme, dass verdichtet Materialien langsamer brennen, die stärker kalandrierten Papiere schneller brennen. Zudem zeigte sich, dass die ligninhaltigen Proben ebenfalls schneller brannten als die Papiere aus gebleichtem Material. Um dieses untypische Verhalten der Zunahme der Brandgeschwindigkeit bei stärkerer Verdichtung und auch den Einfluss des Lignins erklären zu können, wurden die Veränderungen der intrinsischen Eigenschaften analysiert. Dabei wurden Faktoren, wie Porosität, Restfeuchte, thermischer Abbau sowie Kristallinität und Wärmeleitfähigkeit untersucht. Hierbei konnte gezeigt werden, dass für die Papierproben eine Abhängigkeit zwischen einer Steigerung der Wärmeleitfähigkeit aufgrund der Kalandrierung und der Brandgeschwindigkeit besteht. Daraus ließ sich Schlussfolgern, dass der entscheidende Faktor für den Anstieg der Wärmeleitfähigkeit die Zunahme der Dichte mit dem steigenden Verpressungsgrad ist, während sich die Temperaturleitfähigkeit und die Wärmekapazität durch die Kompression nur geringfügig ändern. Dieser Effekt ist jedoch nur bei dünneren Proben zu erkennen und hebt sich mit der Dicke der Proben auf. Der Unterschied zwischen dem Brandverhalten von ligninhaltigen und gebleichten Papieren, konnte mit Hilfe von thermogravimetrischen Analysen auf das frühere Einsetzen der Zersetzung bei niedrigeren Temperaturen zurückgeführt werden.

Im zweiten Teil der Arbeit wurden die Auswirkungen und Einflüsse von Flammschutzmitteln auf gebleichte und ungebleichte Papiere sowie die Veränderungen im Abbauprozess untersucht. Dazu wurden auf die gebleichten und ungebleichten Papiere mit den langsamsten Brenngeschwindigkeiten, aus dem ersten Teil der Arbeit, drei verschiedene Flammschutzmittel auf Phosphorbasis - Ammoniumpolyphosphat, eine mit Phosphat- und Carbamatgruppen modifizierte Stärke und Ammoniumphytat - in drei unterschiedlichen Mengen aufgebracht. Die verwendeten Mengen der Flammschutzmittel wurden nach drei Kriterien ausgewählt: nicht flammgeschützt, flammgeschützt und ein Übermaß an Flammschutzmittel. Um die Wirksamkeit der drei Flammschutzmittel zu bestimmen, wurden die Wärmefreisetzungsrate, die Gesamtwärmefreisetzung und die Rauchentwicklungsrate mit Hilfe der *Cone Calorimetry* ermittelt. Es wurde eine Korrelation zwischen der Menge und Art des aufgebrachten Flammschutzmittels und der Abnahme der Spitzenwärmefreisetzungsrate und der Gesamtwärmefreisetzung beobachtet werden. Hierbei konnte festgestellt werden, dass sich die jeweiligen Flammschutzmittel unterschiedlich auf den gebleichten und ungebleichten Papieren verhalten. Die besten Ergebnisse wurden dabei mit Ammoniumpolyphosphat und Ammoniumphytat erhalten. Aus den Ergebnissen konnte anschließend die Hypothese aufgestellt werden, dass aufgrund des Lignins die Effektivität der Phosphatgruppen in den Flammschutzmitteln reduziert ist. Da Lignin weniger Hydroxygruppen als Cellulose aufweist, fällt die Kondensationsreaktion im ersten Schritt des Flammschutzmechanismus quantitativ geringer aus und verringert somit die Effektivität der Flammschutzmittel. Um diese Hypothese weiter zu bestätigen

wurde der Mechanismus der Flammschutzmittel anhand der entstehenden Zersetzungsprodukte untersucht. Es konnte unterschiedliche Einflüsse auf die Wirkungsweise der Flammschutzmittel und Unterschiede zwischen den Papiertypen festgestellt werden. Primär gab es eine Verschiebung innerhalb der Zersetzungsprodukte, was ebenfalls auf ein Ausbleiben des durch die Kondensationsreaktion aus den Hydroxy- und Phosphatgruppen entstehenden Wassers zurückgeführt werden konnte, was die voran gegangene Hypothese unterstützte. Des Weiteren wurde der Einfluss der Flammschutzmittel auf die mechanische Stabilität der Papiere untersucht und die unterschiedlichen Einflüsse anhand der chemischen Zusammensetzung und Struktur diskutiert. Dabei ergab sich für die zur Cellulose chemisch ähnliche modifizierte Stärke das beste Ergebnis wohingegen das Aufbringen von Ammoniumpolyphosphat zur geringsten mechanischen Stabilität führte.

Insgesamt konnte somit ein grundlegendes Verständnis für die Einflussfaktoren auf das Verbrennungsverhalten von Papier abhängig der intrinsischen Eigenschaften geschaffen werden. Außerdem konnte der Einfluss von Restlignin in einer Papiermatrix auf den Flammschutz ermittelt werden. Die Kombination dieser Informationen mit den Ergebnissen der Untersuchungen über den Einfluss der Flammschutzmittel auf die mechanischen Eigenschaften der Papiere konnten im Rahmen des Projekts „Bauen mit Papier“ somit neue Möglichkeiten für Papier als Anwendungsmaterial im nachhaltigen Bauen eröffnet werden.

Contents

1. Introduction

Due to their outstanding combination of properties, polymeric materials, being used in all sorts of application areas such as construction, packaging and medicine, have added greatly to the quality of modern life. This applies not only to plastics but also to biopolymers such as cellulose and starch. For each individual application, these polymeric materials must be modified accordingly to meet the criteria of the application area. One example of this is flammability. The basic structure of the polymers, consisting of carbon and hydrogen, lends itself to good flammability. Every year there are about 200.000 residential fires in Germany that cause considerable losses of life and property.[1] These fire hazards imply that both government regulators and industry must address these issues to reduce the risk of fire.[2] In this context the typical approach is to either coat or mix the polymeric materials with a so-called flame retardants to improve the performance of the polymer by negating combustion. The flame retardant reduces the flammability of the polymer by interfering with the chemistry and/or the physics of the burning process both in solid and gas phases.[3] Historically primarily halogenated flame retardants were used to protect materials from burning, but in recent times their use has been reduced due to their impact on health and environment. During thermal decomposition of these halogenated flame retardants, various decomposition products are formed, which are toxic to humans when inhaled.[4] In addition, the high persistence of the compounds leads to an accumulation of halogens in the environment.[5] Due to these problems, the use of halogen-containing compounds has been increasingly restricted by new guidelines, which has led to an increased interest in new halogen-free flame retardants. Besides mineral, borate and nitrogen containing flame retardants, the development of new flame retardants is focused on phosphorous-containing compounds.[6,7] To achieve an optimised efficiency of these flame retardants, they must be specifically adapted to the material and its final application.[8,9]

This thesis is part of the interdisciplinary project BAMP! – "Building with Paper" in which the advantages of paper as a material consisting of polymeric building blocks for the construction industry are to be systematically developed. The general need to reduce the use of non-sustainable building materials, in combination with the reduction of CO_2 emissions, is the main objective of the BAMP! – project. In 2018, the construction sector accounted for 36 % of the world's final energy consumption and 39 % of energy- and process-related carbon dioxide emissions, of which 11 % were due to the production of construction materials such as steel, cement and glass. In this framework, paper as a sustainable resource represents untapped potential.[10,11] In addition, the acute need for alternative building materials is growing, driven by sand shortages in some parts of the world, which is needed for the production of concrete and as a bulk material.[12] Thus, the use of paper as a building material could both reduce CO_2 emissions and, because it is a renewable resource, reduce raw material

deficiencies. Paper has desirable properties for this purpose, including a relatively high stability at low weight compared to concrete or steel. In addition, paper is made from fibres separated from wood and reassembled during the production process, and therefore has uniform and adjustable mechanical properties. Paper in no way intended to displace the other materials, but it does offer the possibility of temporary buildings that are more sustainable due to their recyclability. However, paper also has some properties that make it unsuitable as a building material, including susceptibility to environmental influences, which can drastically reduce the safety and stability of these constructions. Since it is a natural material, the natural degradation of paper by bacteria and fungi, as well as the inherent flammability of the material must be addressed. Furthermore, the paper must be protected against the damaging effects of the environment, such as moisture or UV radiation. In addressing the flammability of paper, there are already a variety of flame retardants, such as inorganic fillers or silicates, which are already being used commercially. In recent years the aspect of environmental compatibility is also increasingly being taken into account. In these studies, the various criteria surrounding the effectiveness of the flame retardants are mostly determined and the effects of the flame retardants on the mechanical properties of the paper are only examined in individual cases. What is neglected in the studies, however, are the influencing factors of the base material. Since paper is a natural product and the wood pulping process also has an influence on the composition of the cellulose fibres, this can have a strong impact on the effectiveness and functionality of the flame retardants.

Based on these requirements, the objective of this thesis is to investigate the burning behaviour and flame retardancy of paper designed for use in construction. Through this, a basic understanding of the influences of the material on the fire properties should be developed. In accordance with the mission of the project, it is aspired to study bio-based flame retardants that are adapted to the material to be protected, as described above.

2. Theory

2.1. Fire

The ability to start and control fire was a huge improvement for the Neanderthals approximately 50.000 years ago and to this day fascinates young and old.[13] It is also impossible to imagine our daily lives without fire, as the combustion of organic compounds with oxygen is still a crucial part of the production of useful energy. However, just as useful it is, it also poses immense dangers. But what is fire? Fire is a rapid exothermic oxidation reaction that releases light, heat and a variety of reaction products during a combustion process. To start a fire, three crucial requirements must come together. A fire starts if a combustible or flammable substance in combination with a sufficient quantity of an oxidizer is exposed to a source of heat at ignition temperature. The oxidizer does not necessarily have to be oxygen, but can also be an oxygen-rich compound. If all three components are present in adequate quantity and ratio, they are able to sustain the oxidation reaction, which leads a chain reaction to occur that further keeps the fire burning. The heat generated during combustion causes the burning material to decompose into further combustible gases and at the same time creates a suction, which draws new oxygen into the fire.[14,15] This correlation between the components and the chain reaction is commonly visualised as the fire tetrahedron (Figure 1). By removing, interruption or depletion of one of the fire tetrahedron components the fire extinguishes.

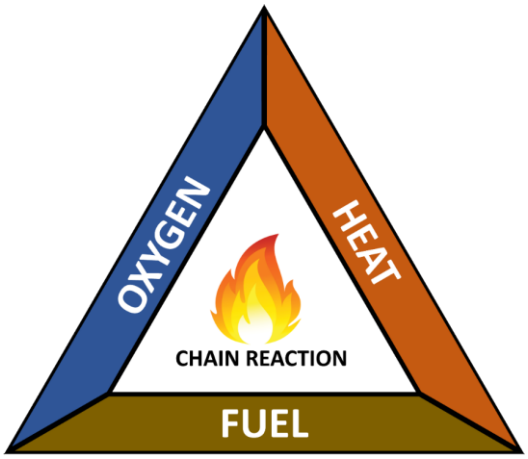

Figure 1: The fire tetrahedron, which visualises the interrelationship of the components of a fire.

The visible part of the fire is called flame. The flame consists of a mixture of reacting gases and solids, which emit electromagnetic radiation from ultraviolet, visible and infrared radiation range. The emitted radiation results out of both solid-state radiation and the radiation of gaseous molecules. The solid-state radiation is emitted from particles of the fuel or soot that arises within the flame. These particles emit radiation over the entire spectral band and this spectrum corresponds approximately to that of a black body, even though the particles are too small to behave like perfect black bodies. Black bodies have a characteristic frequency spectrum they emit depending on the body´s

temperature.[16,17] The gaseous molecules and atoms, however are heated up by the exothermic reaction, which can excite their electrons to a higher energetic level. When they fall back to an energetically lower state, the difference in energy is emitted as photons. In case of the molecules, vibrational and molecular bands are occupied, which leads to broader emission spectrum, whereas for atoms, a line spectrum is emitted. Because of this, the radiation of the gaseous molecules and the atoms varies greatly, depending on the combustion of the burning material and its intermediates. This shifts the colour of the flames individually.[18–20] These different aspects of a fire are displayed in the following Figure 2.

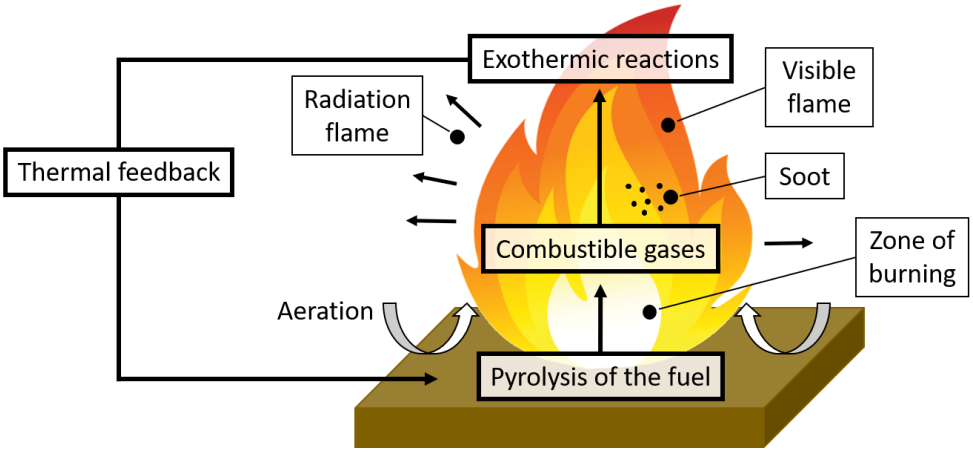

Figure 2: Processes during combustion in a fire.

To start a fire, the decomposition of the combustible material must first be initiated with the help of an ignition or heat source, as previously mentioned. The decomposition of the material is an endothermic reaction as the fuel must first be heated up to the activation energy of the bond cleavage. The resulting gaseous degradation products, together with the oxygen from air as oxidant, then form a combustible mixture, which is ignited. Even without an ignition source like a flame or spark, the mixture can ignite itself when it is heated to the autoignition temperature. Within the flame a multitude of different exothermic reactions take place. The high-energy hydrogen and hydroxyl radicals produced by the decomposition of the burning material act as catalysts in this combustion process. Chain propagation, chain branching and polymer degradation reactions, which are caused by the highly reactive hydrogen and hydroxyl radicals, lead to the generation of carbon radicals. These carbon radicals can then oxidise with the present oxygen, releasing large amounts of thermal energy to form carbon dioxide or further participate in the radical degradation of the fuel (Scheme 1).[3,21,22]

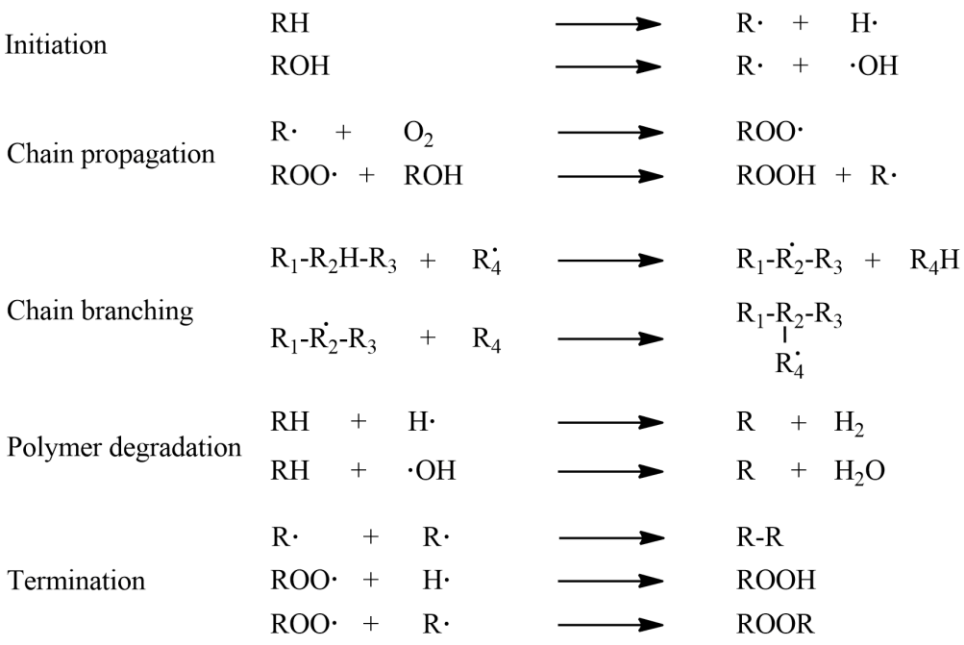

Scheme 1: Schematic representation of the radical reactions within a fire.[23,24]

Thereby the driving force of the burning with the most released heat is the conversion of the weak oxygen double bond of the molecular O_2 to stronger bonds in the reaction products carbon dioxide and water. Per mole O_2, approx. 418 kJ of energy are released, of which the new formation of oxygen bonds accounts for ¾, independent of the decomposing organic material.[25] The released energy of the decomposition reactions leads to further decomposition of the fuel in the thermal feedback and thus initiates the chain reaction for a sustained fire that does not require any further energy source from outside.

2.2. Cellulose based construction materials

Despite the increased flammability of bio-based materials compared to concrete or steel, the idea of using these sustainable materials as building materials has been around for years. Due to the ever-increasing attention to minimising the use of plastics and non-recyclable materials, the focus is shifting towards increasing the use of natural materials. Nature offers a very wide range of natural building materials that are ideal for construction: wood, natural stones, ceramic building materials, plants, fungi and animal products such as sheep's wool can be used for many different purposes.[26] In the following, the materials wood and paper are described in detail and their advantages and disadvantages are explained.

2.2.1. Wood

Wood as a material can be divided into two major categories: softwood and hardwood. The softwood comes mainly from coniferous trees and the hardwood from deciduous trees. The terms softwood and hardwood do not refer to the hardness of the wood, as there are hardwoods that are softer than

softwoods. The main difference between the two types of wood is that hardwoods have vessels in their anatomy that transport water. Softwoods, on the other hand, don't have vessels, but have so-called longitudinal tracheid, which perform a dual role of conducting the water and support in stability of the tree (Figure 3).[27] Further softwoods tend to have longer fibres with a length of 3.5 to 6 mm in comparison to hardwood with 1 to 1.5 mm. This difference in length is very important for the paper industry as it affects the properties of the papers.

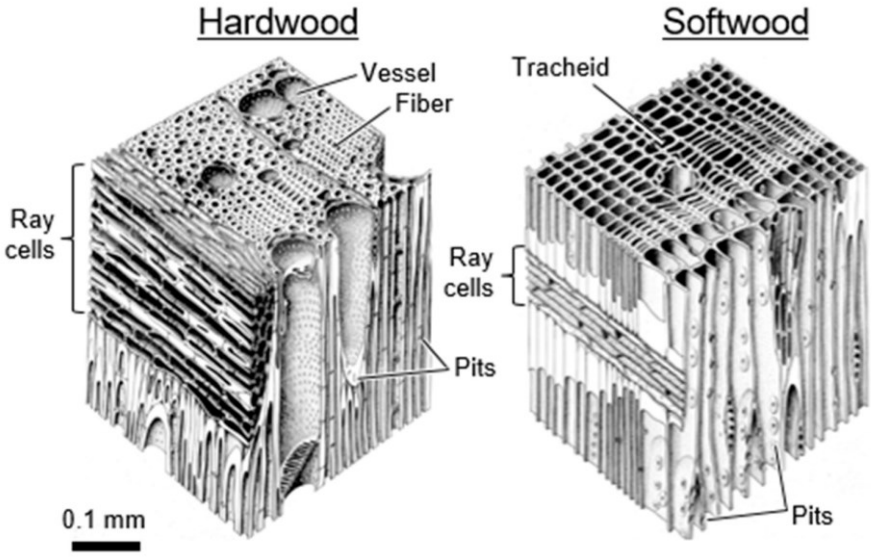

Figure 3: Illustration of the cellular structure of hardwood and softwood.[28]

Chemically, both types of wood are composed of the same three polymeric materials: cellulose, hemicellulose and lignin. These three components make up to 95-98 % of the wood while the remaining 2-5 % are lower molecular weight components or trace elements, so-called extractives. However, the chemical composition of the wood with the three polymers is not only dependent on the type of tree but also varies greatly within a tree and is dependent on the growing environment. An average composition of both wood types can be found in the Table 1 below.[27]

Table 1: Average chemical composition of softwood and hardwood.[27]

Components	Softwood [%]	Hardwood [%]
Cellulose	42 ± 2	45 ± 2
Hemicellulose	27 ± 2	30 ± 5
Lignin	28 ± 3	20 ± 4
Extractives	3 ± 2	5 ± 3

Cellulose, as the main component of wood, is a linear polysaccharide consisting of β-(1-4) glycosidic

linked D-glucopyranose units. The degree of polymerisation (DP) of cellulose in wood is highly dependent on the source but can range from 7000 – 10000 and even reach 15000. An average DP of 10000 corresponds to an approximately 5 µm long polymer chain. The building block of cellulose is the β-cellobiose, which is the smallest repeating unit in cellulose and consists of two D-glucose units. The individual pyranose rings along the cellulose chain, the so-called anhydroglucose units (AGU) are alternately rotated by 180° and adopt the energetically favourable $^4C_1$ chair conformation (Figure 4).[29,30]

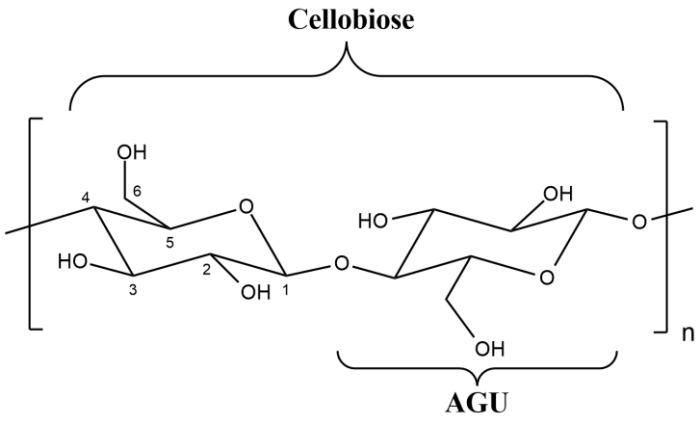

Figure 4: Molecular structure of cellulose with the AGU building blocks.

This conformation enables the linear cellulose polymer to stiffen itself by intramolecular hydrogen bonds. In addition, chains are arranged in parallel and held together by intermolecular hydrogen bonds. The combination of inter- and intramolecular hydrogen bonds leads to the formation of elementary, micro- and macrofibrils from which the actual fibre is built. The intramolecular hydrogen bonds can form between the hydroxyl group at C_3 and the oxygen atom of the neighbouring pyranose ring and the hydroxyl groups at C_6 and C_2 of the neighbouring glucose units. Intermolecular hydrogen bonds are formed in between the hydroxyl groups at C_3 and C_6 of adjacent chains as displayed in Figure 5.[31,32]

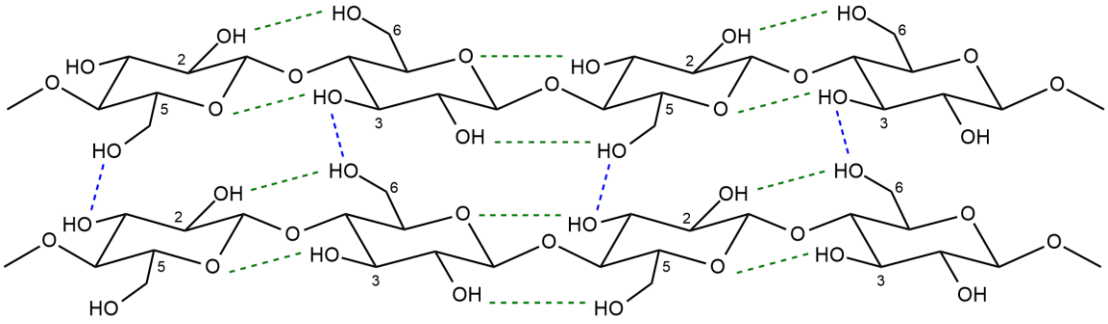

Figure 5: Supramolecular structure of cellulose I. Green links reflect the intramolecular and the blue the intermolecular hydrogen bonds of the cellulose polymer chains.[33]

These extremely high number of hydrogen bonds cause a very high lateral association of the cellulose molecules. This cohesion of the individual molecular chains leads to a high spatial order, which results in the formation of crystalline structures. These crystalline, highly ordered areas are surrounded by amorphous areas. A cellulose polymer chain integrates through several of these areas, resulting in a tightly connected network of several different cellulose chains. Depending on the origin of the cellulose, the proportion of crystalline regions can be up to 65 %.[27,31,34,35] The high number of hydrogen bonds also lead to a comparatively high glass transition temperature T_g of the cellulose fibres in the same range as the decomposition temperature.[36] Cellulose can exist in five different allomorphic forms, which can be distinguished based on their hydrogen bonds and elementary cells.[33] The natural, most widespread form is cellulose I, also called native cellulose. This is usually present as a mixture of cellulose I_α and I_β, whereby cellulose I_β is the thermodynamically more stable form. This is also found predominantly in plants and trees, which is why it is also most relevant in paper production. The assembly of the cellulose can be influenced by a chemical treatment of the native cellulose, whereby the inter- and intramolecular bonds are influenced and consequently further the modifications of cellulose II – IV can be obtained. Cellulose II (regenerative cellulose), for example, can be obtained by regeneration or mercerisation. Mercerisation is achieved by treating the cellulose with a 13.5 w% NaOH solution, in which the reagent is deposited in the lattice of the cellulose and causes the existing hydrogen bonds to be broken and a shift in the cellulose lattice to occur.[37]

Hemicelluloses, which is a collective term for the polyoses found in wood, are, like cellulose, polymers consisting of anhydrous sugar units. They differ from cellulose in that polyoses usually are a branched molecules and are composed of several different sugar units. In addition, polyoses are small molecules, compared to cellulose, with a DP of only 150 to 200 units. Their main building blocks are D-glucose, D-galactose, D-xylose, D-mannose, L-arabinose and 4-0-methyl-D-glucuronic acid. Within the natural fibre composite wood, the polyoses connect the hydrophilic cellulose and the hydrophobic lignin. They are partially covalently bonded to the lignin and form hydrogen bonds with the cellulose and hence increases the mechanical performance of the natural fibre composite wood immense.[38–40]

Lignin, with its very complex and branched three-dimensional structure serves as a stabiliser of the tree. Whereas the cellulose in the wood absorbs the loads caused by tensile stress, the lignin provides rigidity and absorbs compression. Furthermore, it is hydrophobic due to its chemical structure and thus prevents rapid enzymatic degradation of the polysaccharides. It is an amorphous aromatic or polyphenolic polymer, which is composed of three basic components: p-coumaryl alcohol, coniferyl alcohol and sinapyl alcohol (Figure 6).[41] These three building blocks are, for the most part, connected to each other via a β-O-4 bonds.[42] α-O-4 ether bonds as well as β-5 and 5-5 C-C linkages are among the more frequently occurring connections between the lignin building blocks. These three components and their most frequently occurring connections are displayed in Figure 6.

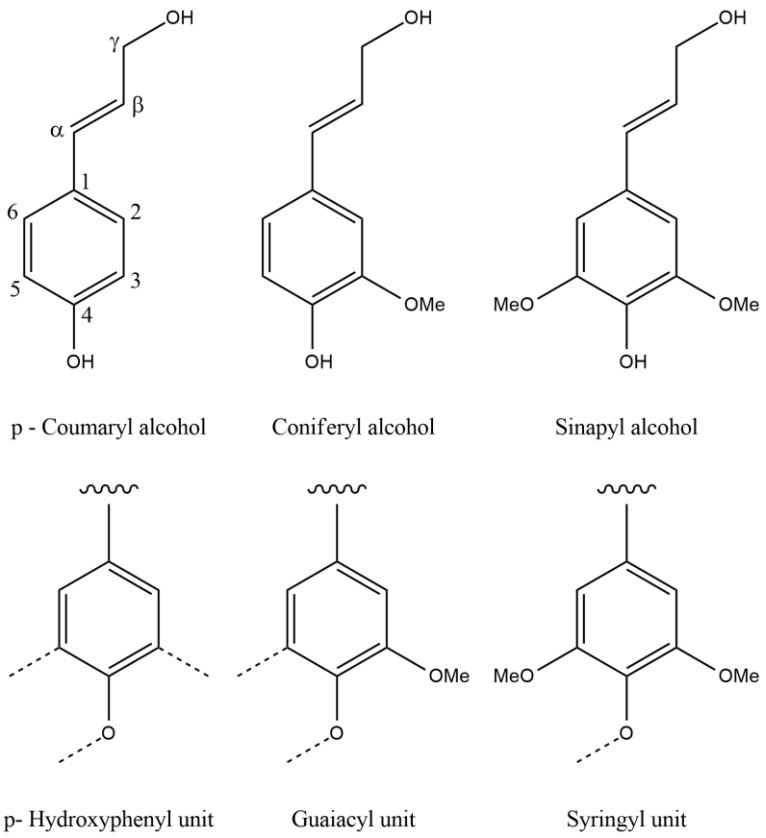

Figure 6: Structure of the three monomer building blocks (monolignols) of lignin and their structure in the incorporated Lignin.[43]

Due to this selection of different building blocks and connection possibilities, a large number of different lignin molecules can be created, which vary greatly among tree species. Even today, the exact structure of lignin has not been fully elucidated. Due to the properties of lignin, its isolation in unaltered form is still not possible, as the extraction either changes its native structure or only fractions of the lignin can be extracted unchanged. There are suggestions that a tree may contain only a few very large lignin molecules linked together throughout the whole trunk, but this has not yet been proven.[35,43] Currently, lignin, which is a by-product of the extraction of fibres for the paper industry, is burned to produce energy, but in recent years the search for material uses has become increasingly important.

2.2.2. Paper

Paper is a material consisting essentially of cellulose fibres of vegetable origin. The production of paper consists of a cascade of production steps. In the next part, the sub steps of wood pulping, fibre bleaching, and paper production will be discussed in detail.

Pulping

In order to obtain the desired fibres from wood for the production of uniform papers, the wood is first debarked and then chipped. This chopped wood can then be pulped using various methods to obtain

fibres with desired properties. The main categories of pulping are mechanical, biological, semi-chemical and chemical pulping. The pulp produced from each process differs due to the fibre properties being modified differently. This makes the various pulps suitable for different applications. However, the primary goal of all pulping processes is to obtain fibres or fibre bundles that further can be used for paper production. The chemical methods additionally strive for the removal of the lignin from the cellulose fibres while the entire fibre structure remains intact. Furthermore, for some application areas it is in the interest of the paper manufacturer that, to some extent, the hemicellulose remains on the cellulose fibres as this leads to a higher binding capacity within the later paper.[44,45]

Mechanical pulping

About 25 % of the wood pulp production in the world today is accounted by mechanical pulping.[46] Mechanical pulping is divided into “wood pulping” and “refiner wood pulping”. In the former, whole logs or log sections are ground on a grindstone and in the latter wood chips and smaller wood pieces are ground in a refiner. By using grinders and refiners, wood is broken down and mechanical force is used to cause fibre separation.[47] During this process, the lignin remains in the fibres, which leads to a high fibre yield. This, combined with the high mechanical stress on the fibres, produces fibres with relatively poor mechanical properties, softness and brightness. To counteract the deterioration of the mechanical properties, softwood is increasingly used in this process, as its longer fibres lead to a higher number of fibre-fibre contact points in the processed product.[47,48] Since the lignin cannot be separated from the cellulose fibres by pure mechanical force, thermo-mechanical or chemi-thermo-mechanical pulping processes can be used, in which the lignin is first softened by the use of steam and/or softening chemicals such as hydroxides or peroxides. This allows a better separation of the fibres during pulping, since the breakage of the structure is reduced in the fibre and increased in the softened lignin, which has a positive effect on the mechanical properties of the pulp obtained.[46,49,50]

Biological pulping

The biological pulping process is a more environmentally friendly, pre-treatment method developed to reduce the hazardous and environmentally damaging chemicals used in the subsequent chemical digestion process. For biological pulping, the wood chips are treated with white-rot fungi or enzymes that are capable of degrading lignin.[51,52] White-rot fungi have the ability to hydrolytically and oxidatively degrade wood components, which is why they are already used extensively in large parts of the biological pulping process. This targeted degradation, in which only the lignin is addressed during this pre-treatment step, saves energy during the pulping process and significantly improves the quality of the pulp, due to a milder approach.[48,53] Afterwards, however, the wood chips must be broken

down further by a mechanical or chemical process. Nevertheless, due to the savings in energy and the amount of chemicals required, biological pulping is a viable option for the future of the pulp and paper industry.[54]

Semi-chemical pulping

Semi-chemical pulping describes a two-staged process in which the wood chips are pulped using both chemical and mechanical pulping processes. First the wood chips are partially softened with chemicals to reduce the strength of the inter-fibre bonding by the removal of hemicellulose and lignin. After this, softened wood is mechanically refined to individual fibres. By varying the chemicals used and the level of mechanical stress on the material, the pulp obtained can be adjusted for specific applications.[55] The most significant semi-chemical process is the neutral sulphite semi-chemical process. It gained impetus due to the higher yields of usable pulp in comparison to conventional chemical processes. This results from the reduced extraction of lignin and hemicellulose, which is why stiffer fibres are generally obtained in this process. This property of the fibres is particularly advantageous for the production of corrugated board.[56,57]

Chemical pulping

Chemical pulping is the most widely used pulping method for producing high quality fibres.[46] For this pulping method, the wood chips are treated with chemicals in an aqueous solution at an elevated temperature and pressure to remove lignin and hemicellulose without damaging the cellulose fibres. These removals lead to very flexible fibres and an increased fibre-fibre contact area, which later results in papers with higher mechanical properties. However, the strength and durability of the fibres gained through this pulping process comes at the expense of pulp yield, which is almost half that of mechanical pulping (40-55 % yield).[58,59] Two basic processes can be distinguished in the chemical pulping of wood. Firstly, there is the Kraft-process, also known as sulphate process and secondly the sulphite process. Globally the Kraft-process is the most used pulping process and uses sodium hydroxide and sodium sulphide as pulping chemicals at a pH-level of 12.[60] The sulphite process, on the other hand digests the wood chips with an aqueous solution of sulphur dioxide and calcium, sodium, magnesium, or ammonium bisulphite. A great advantage of the sulphite digestion is, that it can be carried out at different pH values.[61] The choice of material to be used for this process is however limited to wood species with a low extractive content, as these extractives can interfere with the pulping process due to initiating condensation reactions with the lignin or causing a reduced accessibility into the wood. This is not the case for the Kraft process, as both hard and softwood can be utilized. The receiving pulps of each process differ in that the sulphite pulp is brighter, has a dependence of the yield correlating with the pH-level and later forms less porous sheets that can hold an increased amount of water,

whereas the Kraft pulp in general has better mechanical properties. A disadvantage of the sulphite process is, that it is less environmentally friendly as the chemicals used in this process are more difficult to recover and the cooking cycles are longer, what utilizes a higher energy input. The Kraft process, on the other hand, allows the used chemicals, which include the extracted lignin, hemicellulose, and extractives, to be recycled by going to a chemical recovery plant where the dissolved materials are burnt to generate new energy and steam for the process. Additionally, Kraft mills use their waste for making supplementary energy via anaerobic digestion.[62]

Bleaching

After pulping, the fibres still contain a proportion of lignin and other chromophore structures. To destroy and partially remove these from the fibres, the fibres can be bleached both oxidatively and reductively. This gives the pulps a higher degree of brightness, softness and cleanliness, which is of particular interest for manufacturing of many products like printing paper, tissue paper, sanitary papers, absorbent products and more. In case of paper, the remaining lignin on the fibres would cause the paper to yellow more quickly and become brittle when exposed to oxygen. The previous pulping process plays an important role for bleaching, since more lignin remains on the fibres during Kraft pulping than during sulphite pulping, which further requires a more intense treatment. The bleaching is accomplished with various chemicals as chlorine or chlorine containing compounds as well as oxygen and alkali extractions in multiple stages.[63] The use of different bleaching chemicals in different stages of the process increases the efficiency as each of the chemicals will react differently with the complex structure of lignin. The bleaching methods can be divided into three groups: chlorine process, elemental chlorine-free process (ECF) and total chlorine-free process (TCF).[64] The focus on increasing the environmental sustainability of the bleaching process and minimising the use of absorbable organic halides (AOX) in bleaching agents has promoted the ECF and TCF processes. The TCF process does not use chlorine or chlorine-containing chemicals, but only oxygen-based compounds. These are oxygen molecules, hydrogen peroxide, ozone and peroxy acids. The disadvantage of these processes is that the peroxides and oxygen can only reduce the lignin content to a certain extent. However, they are often used upstream of other processes because of their environmental compatibility. The ECF process in contrast to the TCF process utilizes compounds containing bound chlorine. This is mostly chlorine dioxide, which is relatively expensive but therefore more selective for lignin. The selectivity makes it very interesting for the final stages of the bleaching, as it is effective even with only small amounts of remaining lignin. Elemental chlorine can react with the lignin in three ways. Under acidic conditions the chlorine can react by substitution (1) of hydrogen atoms, oxidation (2) of lignin moieties to carboxylic acid groups and by addition (3) of chlorine across carbon-carbon double bonds as displayed in Scheme 2.[65,66]

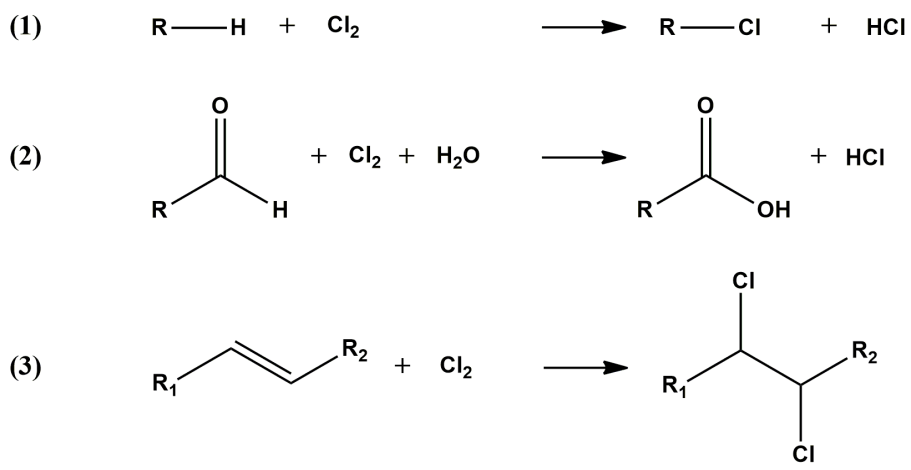

Scheme 2: Examples of the substitution (1), oxidation (2) and addition (3) reactions that occur during the chlorine bleaching process.

These reactions can occur not only with lignin, but also with cellulose and can cause degradation of cellulose, which results in a decrease in pulp strength. Especially the amorphous regions are attacked and dissolved due to the better accessibility.[67] After each stage of bleaching, the treated pulp is washed to remove any remaining chlorine and any resulting degradation products in order to minimize the use of the following chemicals. Therefore, the pulp is placed in a hot NaOH solution to displace the chlorine and thus solubilize the resulting lignin fragments as well as the affected cellulose.[64,68]

Paper making

For the papermaking process the bleached or unbleached pulp may first be further refined to bring the fibres to a desired length and roughness to enhance the formation and bonding of the fibres. Water is added to the pulp to prepare a dispersion, normally containing less than 1 w% fibres. At this point chemicals are added to equip the paper with the desired properties for its application and assist the paper making process. These include wet- or dry-strength chemicals, binder, fillers, pigments and retention agents.[69] Afterwards the received pulps slurry is fed into the wet end of the paper forming machine. The paper machine is divided into four major segments (Figure 7). In the forming section the pulp slurry is evenly distributed in the headbox on the continuously running fabric felt. After a set of draining elements, which remove water by gravitational and suctional mechanism in the sieve section the paper enters the press section. The press section, consisting of rolling presses, which further promote the water-removal and play an important role in the paper web formation by smoothing the surface and increasing the mechanical web strength. Entering the dryer section, the formed paper strand still has a residual moisture of about 50 %, which is then removed by steam-heated cylinders (contact drying), IR emitters (radiation drying) or hot air (convection drying). The dried paper is then calendered in a smoothing unit between two pressing rolls and rolled up on a reel. The calendering further modifies the surface and the interior properties of the paper for their desired applications.[70]

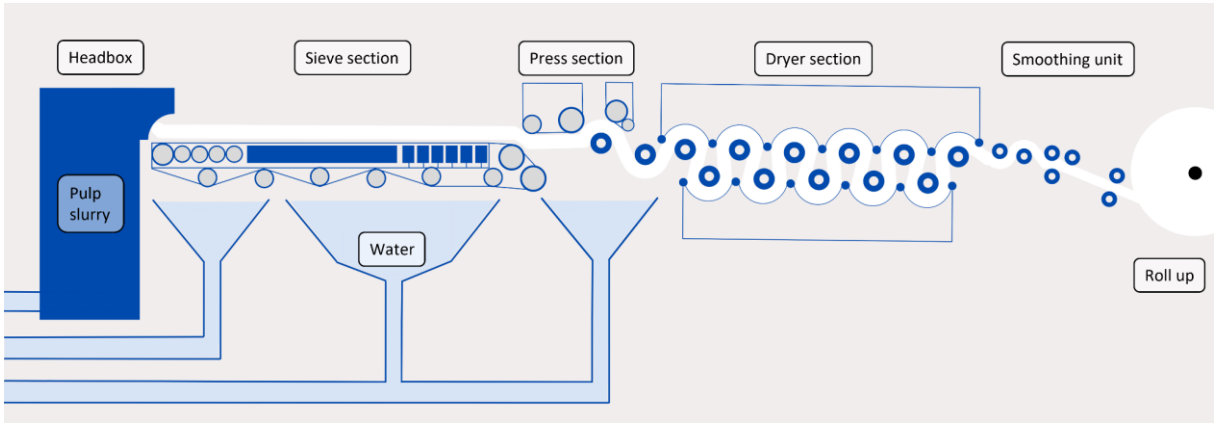

Figure 7: Basic structure of a paper machine.[70]

2.2.3. Advantages and challenges of wood/paper as construction materials

When considering wood and paper as a building material, it quickly becomes clear that wood can be described as the oldest building material of all. There is evidence that shelters were built with wood as the primary building material more than 10,000 years ago.[71] Since then, building with wood has continued to evolve through the discovery of different materials such as metal, as well as different technologies. This has resulted in new ways of joining, for example, through the use of nails and screws. The combination of wood with the adhesives developed in modern times subsequently gave rise to materials such as glued wood, chipboard and fibreboard.[72] The latter was developed from the problem of negating naturally occurring defects, as wood is still a natural material, such as knotholes or other natural deformations in the wood, which can have a negative influences on stability or the appearance. In addition, new technologies made it possible to manufacture ever smaller structural elements, which made the use of wood as a resource much more efficient.[72,73] The use of paper is also indispensable in the construction industry. It is rarely used alone, as in Japanese “Fusuma” or as insulation material, but mostly occurs in fibre composites. The best known of these is gypsum fibreboard and is used in these fibre composites as fibre reinforcement or support in the matrices. In addition, the stability that folded or corrugated cardboard brings, is also becoming more interesting.[74,75] The advantage of paper over wood is that the fibre web is reassembled in a continuous production process, the influence of natural defects in the material is minimized, and the properties and shape can be specifically tailored to the application. Furthermore, properties such as high flexibility and good recyclability offer other major advantages.

The big advantage wood and paper have compared to other materials is, that both are renewable bio-based materials. Due to their natural origin, they leave a smaller carbon footprint in comparison to other building materials, like cement, as they are recyclable.[76] After the end of the life cycle within the construction they can be fed back into a recycling chain or be composted. This initially only refers to the raw material, as the use of additives or coatings can reduce the biodegradability of both

materials and thus also have a negative impact on recyclability and compostability.[77] Furthermore, both materials have very good mechanical properties in terms of specific strength. Regarding the tensile strength of both materials, they can keep up with conventional building materials like steel or concrete.[78,79] Wood displays in addition also good pressure load properties, whereas the stability to pressure is significantly lower for plain paper. To negate this, constructive solutions were found, as they were mentioned before, in the form of tubes or honeycomb panels as well as corrugated cardboard, which increases the possible pressure load for the paper materials due to their structure.[80] However, the natural origin also has some disadvantages for the materials, which must be taken into account and addressed during construction. These disadvantages include the influence of moisture, biodegradability by fungi and bacteria and flammability.

Whereas water only has a minor impact on wood at first glance, it poses a major challenge for the use of paper. The stability of paper results, as written in chapter 2.2.1, from the large number of different hydrogen bonds between cellulose fibres. Through the introduction of water, these can be interrupted and replaced, which leads to a loss of stability.[81] For this reason, wet strength agents are used in the application of paper, which protect the fibre contact points through various mechanisms and prevent the disintegration of the fibre web. In addition, the use of sizing agents on paper can reduce water penetration to further neglect the loss in stability. If a closer look at the influence of moisture on both materials is taken, one important aspect becomes apparent. The absorption or release of moisture can cause the two materials to expand or contract, which can lead to unwanted tensions and displacements in the material, which further leads to damage or loss of stability.[82,83] Since this process is reversible, it can lead to repeated deformations. The influence of moisture is also accompanied by the decomposition of wood and paper by fungi and microorganisms. These need a moist environment to grow and decompose the wood and paper with enzymes (cellulase).[84] The decomposition leads to a loss in stability of the materials. In addition, mould, poses a health risk with repeated exposure to elevated concentrations. The final challenge for the use of wood or paper is flammability. Since hydrocarbon-based materials are capable of burning, this hazard must also be taken into account. A fire is not only a heat hazard but also reduces the stability of the structures and can lead to a collapse. The smoke produced during the combustion additionally needs to be addressed, as it can be toxic if inhaled.

To prevent or negate these influences which have a negative effect on the materials, coatings can be applied onto the materials surface or the material can be impregnated. In this respect, wood and paper differ greatly from each other. Since paper can be functionalized during production by incorporating the corresponding additives into the pulp, a deep and even distribution in the material is possible. Paper also offers increased accessibility for subsequent functionalisation. Not only do the cellulose fibres have better opportunity for possible modifications due to the removal of hemicellulose and

lignin, but also the higher porosity and the large surface area relative to the low volume enables easier penetration of the coating into the material, and even into the fibres.[85,86] Wood has a more closed surface compared to paper and the material is less porous. It is important to note, that depending on the processing and treatment of wood, these parameters can vary greatly. The surface of wood is usually coated and if a deeper impregnation of the pores under the surface is needed, they can be filled by using a vacuum-pressure technique or low-viscosity compounds. Currently, other technologies, like plasma treatments, to functionalise wood are being investigated.[87] For wood coatings to be successful, they need to be adhesive as well as have UV resistances due to the influence of light.[88] To apply protective surface coatings wood is typically painted, sprayed or dipped, which results in a comparatively small amount of coating material required. However, the problems to be considered here are a possible need for reapplication and damage to the surface from outdoor application. As wood and paper are materials of natural origin, the chemical composition and structure differ with origin or type and the coatings need to be addressed individually. To achieve an optimised effect, for example for flame retardancy, the interactions between the coating and the material need to be understood. Therefore, it is advantageous first to understand the behaviour of the raw material in order to adapt the protection accordingly. In relation to this thesis, the thermal decompositions of cellulose and lignin, the main components of wood and paper, are explained in more detail in the next chapter.

2.3. Thermal decomposition of cellulose

The first fundamental studies on the interesting decomposition phenomena of cellulose were carried out by the group of BROIDO as early as 1960. The decomposition was described as two competing reactions that are favoured depending on temperature and heating rates (Figure 8). At lower temperatures (below 280 °C) and slow heating rates, a formation of anhydrocellulose was dominant, whereas at temperatures above 280 °C, more unzipping reactions in the cellulose chain were initiated, causing tar formation. The emerging anhydrocellulose would then further decompose into char and gases.[89,90]

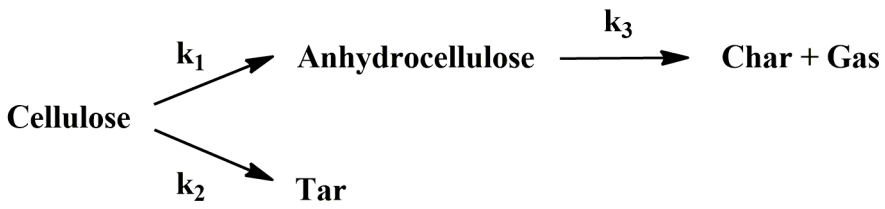

Figure 8: Kinetic model of cellulose pyrolysis proposed by BROIDO and WEINSTEIN[89,91]

Despite large amounts of research being done, the chemical reaction mechanisms for cellulose decomposition are still ambiguous and controversial. Further advancement in analytical equipment

revealed the formation of an intermediate cellulose, now called “active cellulose”, as a key step in cellulose decomposition. This was first observed by LEDE ET AL. in 2002, where cellulose was heated by radiant flash pyrolysis and analysed via HPLC/MS, which showed, in addition to the formation of levoglucosan, cellobiosan and cellotriosan, a transient intermediate liquid compound.[92] Following this observation WOOTEN ET AL. revealed that intermediate compound as an ephemeral cellulose compound.[93] It was then proven by HOSOYA ET AL. that the char formation partly results from the repolymerization of anhydrosugars like levoglucosan.[94] With these discoveries, the kinetic models of DIEBOLD[95] and WOOTEN ET AL.[93], adapted from BROIDO´s proposal, reflect the current understanding of the pyrolysis of cellulose (Figure 9).

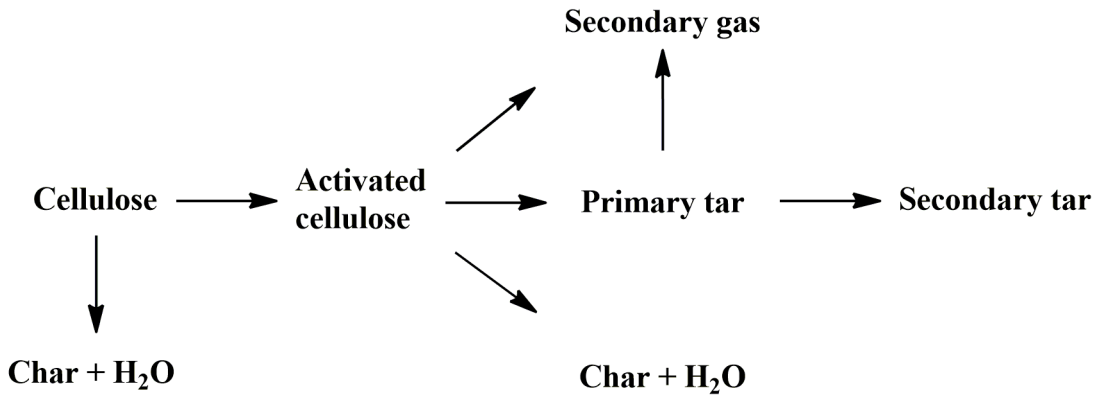

Figure 9: Kinetic model of cellulose pyrolysis proposed by DIEBOLD[95] and similarly by WOOTEN ET AL.[93]

This model describes the reduction of the cellulose polymerization degree and the formation of the “active cellulose”. It also elucidates the pyrolysis at higher temperatures by two competitive degradation reactions. The first degradation reaction describes the decomposition of cellulose to char and gases, whereas the second one describes the formation of tars containing mainly levoglucosan and other anhydrosugars. However, these kinetic models only give an overview and simplify the complex primary and secondary reactions in cellulose pyrolysis. To further investigate the pyrolysis, analytical methods like TGA-FTIR-MS, PY-GC-MS, HPLC and NMR were used to identify the emerging volatiles. The typical compounds found resulting from cellulose pyrolysis are displayed in the following Figure 10.

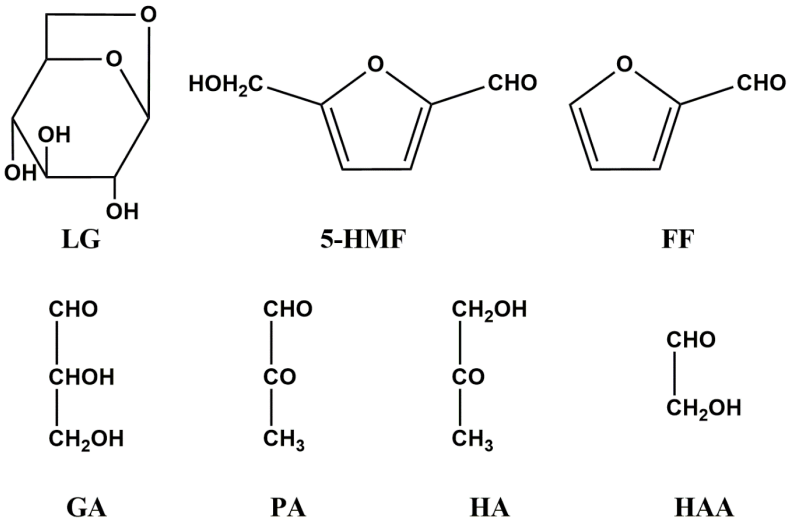

Figure 10: Typical compounds resulting from cellulose pyrolysis. LG: levoglucosan, 5-HMF: 5-hydroxymethyl-furfural, FF: furfural, GA: glyceraldehyde, PA: pyruvic aldehyde, HA: hydroxy acetone, HAA: hydroxy acetaldehyde.[96]

It is important to note, that the patterns and yields of the results are highly affected by the operating conditions and the sample source. It is generally agreed, that the formation of levoglucosan, which is the first step in the decomposition chain, is initiated with the cleavage of the β-(1-4) glycosidic linkage.[96–98] The following formation mechanism of levoglucosan remains controversial. There are several proposals ranging from a free radical mechanism by GOLOVA[99] to a heterolytic mechanism by SHAFIZADEH[98] to possible further depolymerisations due to terminal hydroxyl groups by ESSIG ET AL.[100], but none have yet been proven. The further decomposition mechanism of cellulose and, by extension, that of levoglucosan was investigated and described by SHEN ET AL.[96] and POUWELS ET AL.[101] as well as SHAFIZADEH ET AL.[102] The possible thermal decomposition pathways for cellulose molecules are shown in Scheme 3.

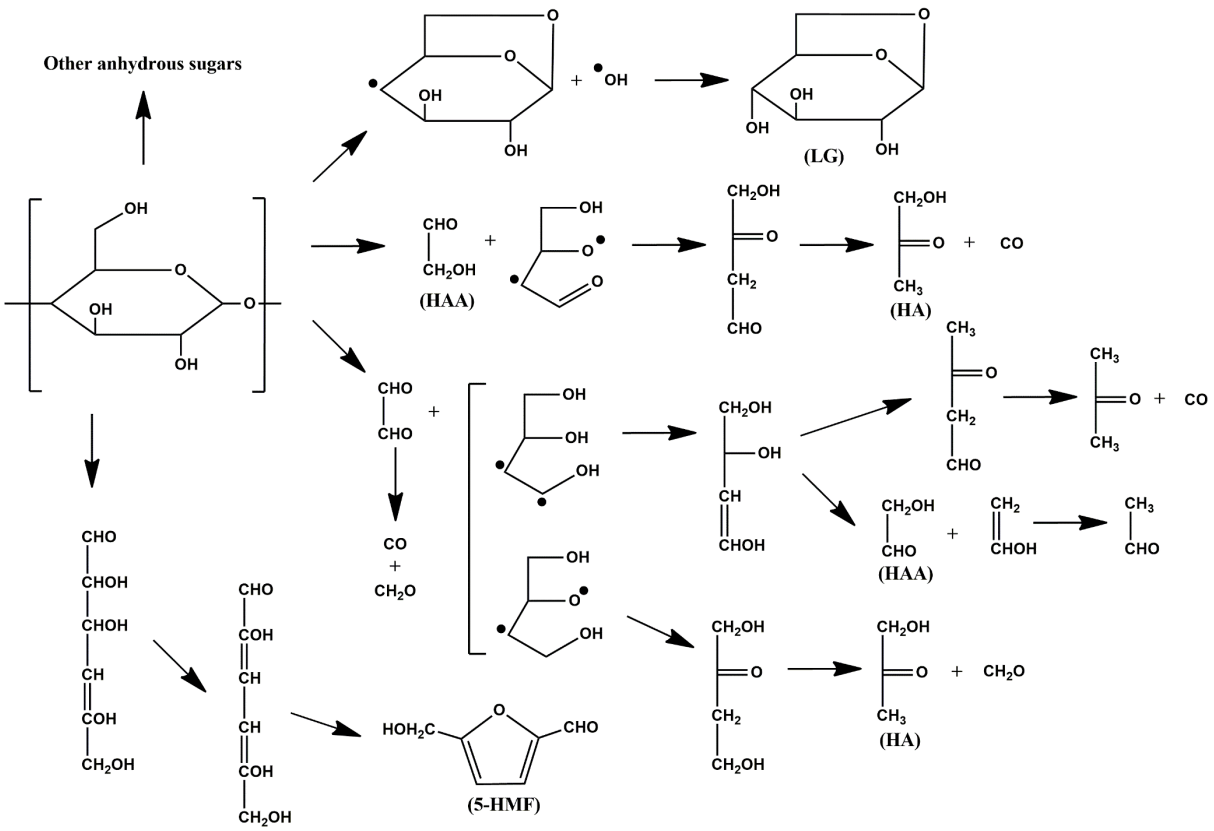

Scheme 3: Predicted chemical pathway for the thermal decomposition of cellulose.[96]

Among the various anhydrosugar derivatives that result from the decomposition of cellulose, levoglucosan occurs most frequently. Thereby, the yield of levoglucosan is affected by the source of cellulose as well as the experimental conditions, with the yield decreasing as temperature increases.[102] With decreasing yield of levoglucosan, the portions of emerging other products, displayed in Figure 10, increase. This leads to the assumption, that the formation of levoglucosan and the ring opening reaction of cellulose are competing decomposition reactions.[103] Other emerging anhydrous sugars are isomers of levoglucosan, which undergo a chemical structure rearrangement during the formation process. These require more energy as the formation of levoglucosan and therefore these anhydrosugars appear in smaller portions.[104,105] The secondary decomposition of these sugars is shown in the following Scheme 4.

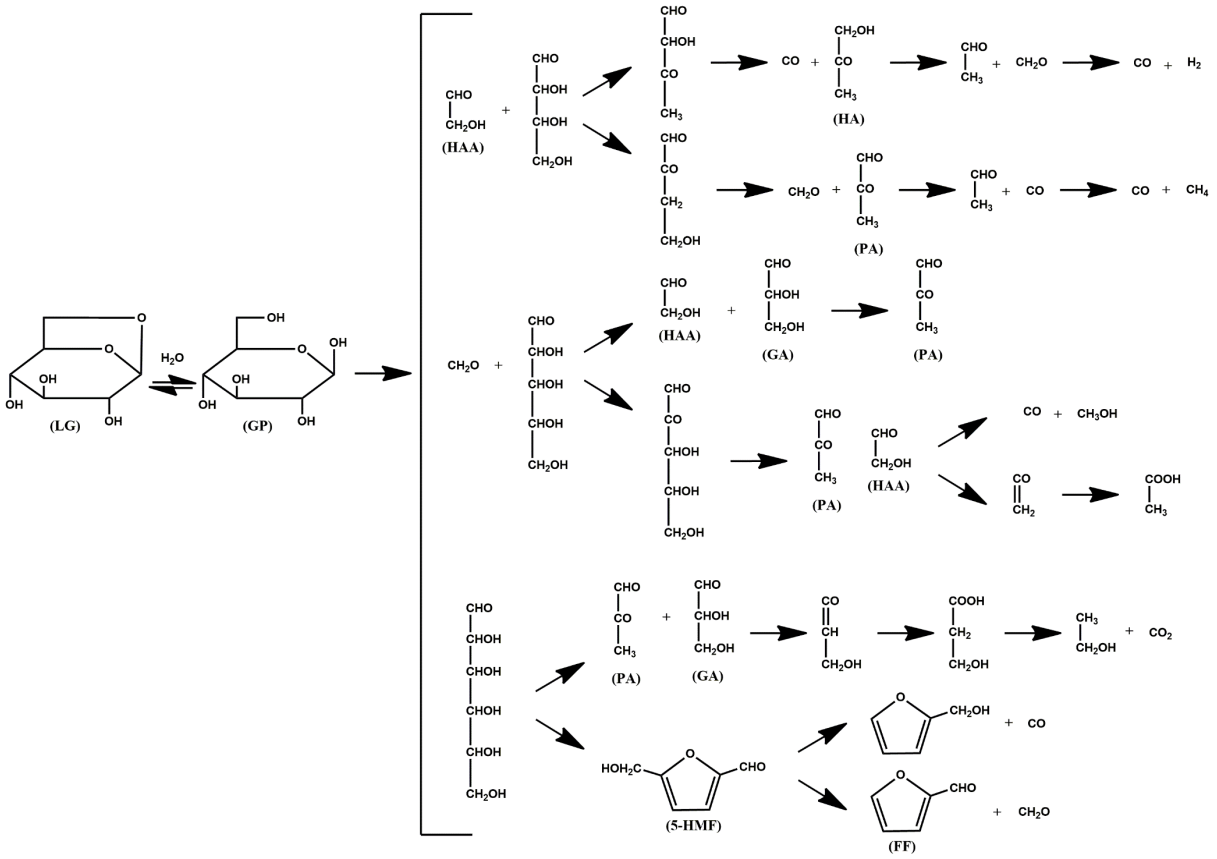

Scheme 4: Predicted chemical pathway for the secondary decomposition of the anhydrosugars.[96]

The investigation of KAWAMOTO ET AL.[103] and HOSOYA ET AL.[106] shows, that the thermal decompositions of the anhydrosugars are initiated with the ring-opening of the 1,6 - acetal bond and the rehydration to form glucopyranose (GP). For the subsequent secondary decomposition reaction, three possible pathways are proposed. The first pathway describes a ring-opening mechanism, which cause HAA and a tetrose to form. The second possible reaction mechanism breaks down the ring to form formaldehyde and a pentose. The third pathway is initiated with the formation of a hexose chain. The products resulting from the three possible reaction pathways then perform, as shown in Scheme 4, a variation of different dehydration, hydration, fission, decarbonylation and decarboxylation reactions to form the end products shown in Figure 10 as well as gases like methane, carbon monoxide and carbon dioxide. It is important to mention, that in most of the investigations of cellulose pyrolysis, an absence of HAA and acetol as pyrolysis products could be observed.[94,96,104,107] BYRNE ET AL. investigated this phenomenon in his work and found, that the proportions of both HAA, glyoxal and 5-HMF were much higher due to the use of flame retardants.[108] Following this work PIKORZ ET AL. showed that already slight impurities in the cellulose, as for example salts, could also increase the formation of HAA.[107] These results, in combination with the influencing factors of the applied method, measurement conditions and sample origin, show how

easily the decomposition of the cellulose can be affected and why the determination of this process is so challenging.[109]

2.4. Thermal decomposition of lignin

Many studies were carried out on the pyrolysis behaviour of lignin and the determination of kinetic models. Due to its non-uniform composition and complex structure, the degradation behaviour of lignin is strongly influenced by its respective origin, reaction temperatures, heating rate and measurement conditions and elucidating the reactions has proven to be even more difficult than with cellulose.[110] Further it is important to note, that in order to analyse lignin it needs to be extracted first. During this process the lignin molecule gets broken down, for example as described in chapter 2.2.2, and this can influence further analyses by introducing new functional groups, which affect the course of decomposition. In general the lignin decomposition is considered a first order reaction[111], but recently more complex kinetic models were proposed. CABALLERO ET AL. proposed in their work, that the decomposition of lignin would form various fragments, which then further decompose at individual characteristic temperatures.[112] Taking up this research, VARHEGYI ET AL. considered that a complex network thermal decomposition reactions in parallel, successive and competitive relation take place in pseudo-first order reactions.[113] None of these models have been proven as of yet, but a general viewpoint has established that the decomposition of lignin is driven by two different competing decomposition pathways (Figure 11).

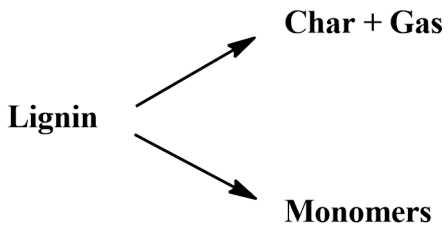

Figure 11: Lignin decomposition by two competing reaction pathways.[114]

Due to various oxygen functional groups in lignin and their different thermal stabilities, lignin thermally decomposes over a broad temperature range (150 – 500 °C). Studies showed that lignins of low methoxy group content produce the highest char yield, whereas hardwood lignins are having a generally higher methoxy group content produce lower amounts of char.[115] This results from the fact, that softwood lignins consist to a larger amount of guaiacyl units than hardwood lignins, which leads to a higher condensed structure throughout the lignin molecule and therefore a higher thermal stability. Further these guaiacyl units are prone to thermally initiated condensation reactions to a higher extent than the more prominent syringyl units in hardwood lignins, resulting in a different charring behaviour.

To further explain the decomposition of lignin LIU ET AL. and WANG ET AL. divided the process in their research into three stages.[116,117] During the initial stage the primary products are water and CO_2. First the absorbed water within the lignin is released by evaporation. With increasing temperature, the aliphatic hydroxyl groups in the lateral chains as well as the lateral C-C bonds start cracking, forming water and CO_2. Progressing into the primary stage H_2O, CO and CO_2 continue to be released due to the break of lateral chains in the lignin polymer, such as the aliphatic hydroxyl groups and C-C bonds.[118] In addition the formation of smaller quantities of aldehydes and acids was observed. At temperatures around 240 – 260 °C LIU ET AL. was able to observe, using FTIR spectroscopy, the appearance of formaldehyde, alcohols and phenols. The formation of formaldehyde was attributed to the fragmentation of the hydroxymetyhlene groups present. The majority of the emerging alcohols is methanol, although the formation of methanol is relatively lower than the phenols. With rising temperature the β-O-4 bonds and C-C linkages between lignin monomeric units cleave between 275 and 350 °C forming guaiacyl and syringyl compounds due to radicals recombination.[119–121] Depending on the origin of the lignin, softwood lignin mainly forms guaiacols whereas hardwood lignin gives both guaiacols and syringols.[122] During the last stage at temperatures around 425 °C the release of larger molecular volatiles deceases and the formation of CO and CO_2 becomes more prominent and considerable amounts of CH_4 and methanol emerge. The formation of methanol is attributed to the fragmentation of the remaining methoxyl substituents in the lignin structure. CO is formed during two different steps in this stage. The first step is attributed to the dissociation of diaryl ether and the second step is the cracking of the hydrocarbonous volatiles. This break down of these volatile products simultaneously results in the formation of methane as the methylene bonds as well as the methoxy bonds are weakened.[112,117,123,124] These possible decomposition pathways were visualised in the studies of MU ET AL. and shown in the following Figure 12.[125]

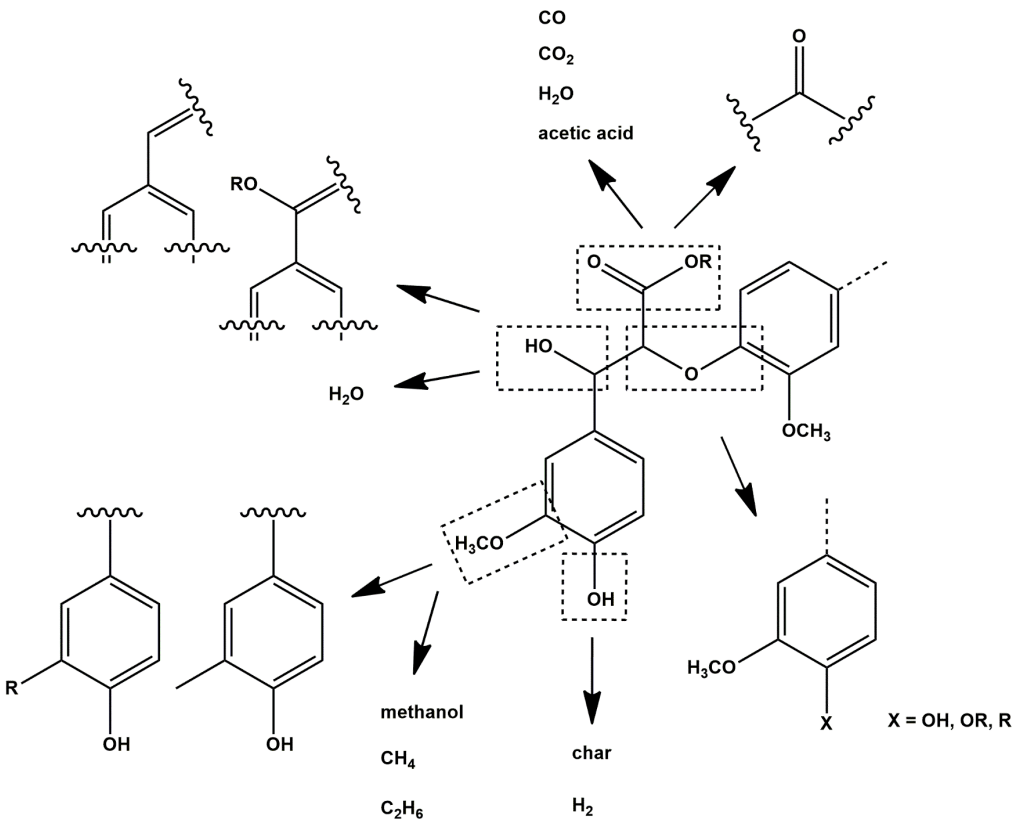

Figure 12: Visualisation of possible decomposition pathways of lignin [125]

2.5. Flame retardants and their mode of action

Flame retardants are chemicals that are added to materials or used in applications to reduce the risk of an ever-present fire threat. They cover a wide range of different chemistries and continue to develop as driving factors like global economics, changing regulations, health and safety or advances in technologies come into play. Thereby the choice of which flame retardant to use is always based on the material to be protected, the application the material is used in, the thermostability of the material, the compatibility with the material, the toxicity of the flame retardant and the price. The mode of action of flame retardants interfering with the combustion cycle may be physical, chemical, or a combination of both. The main physical protection mechanisms are the following:

- Promotion of endothermic reactions → cooling the substrate below the degradation temperature
- Generation of inert gases → diluting the gas phase to suffocate the fire due to lack of oxygen and diluting the volatile flammable decomposition products to reduce the fuel concentration
- Formation of a protecting coating → reducing the accessibility of heat, oxygen and stripping of the volatile flammable gases to interrupt the decomposition cycle

On the other hand, the possibilities with which the fire can be interrupted via chemical modes are:

- Inhibition of oxidation reactions → trapping of free-radical species by radical scavengers to negate further degradation
- Formation of carbonaceous layers → promoting carbonisation of the material to create a protecting barrier
- Acceleration of material degradation → causing pronounced dripping to withdraw the fuel from the flame (especially used with synthetic polymers)

It is important to note that the protective mechanisms mentioned do not take place separately but rather in combination. Due to this, the protective mechanism of flame retardants can be very complex and consist of multiple stages.[126,127] Figure 13 shows the basic processes involved in the combustion of organic matter and potential points of intervention (dashed lines) for flame retardants.

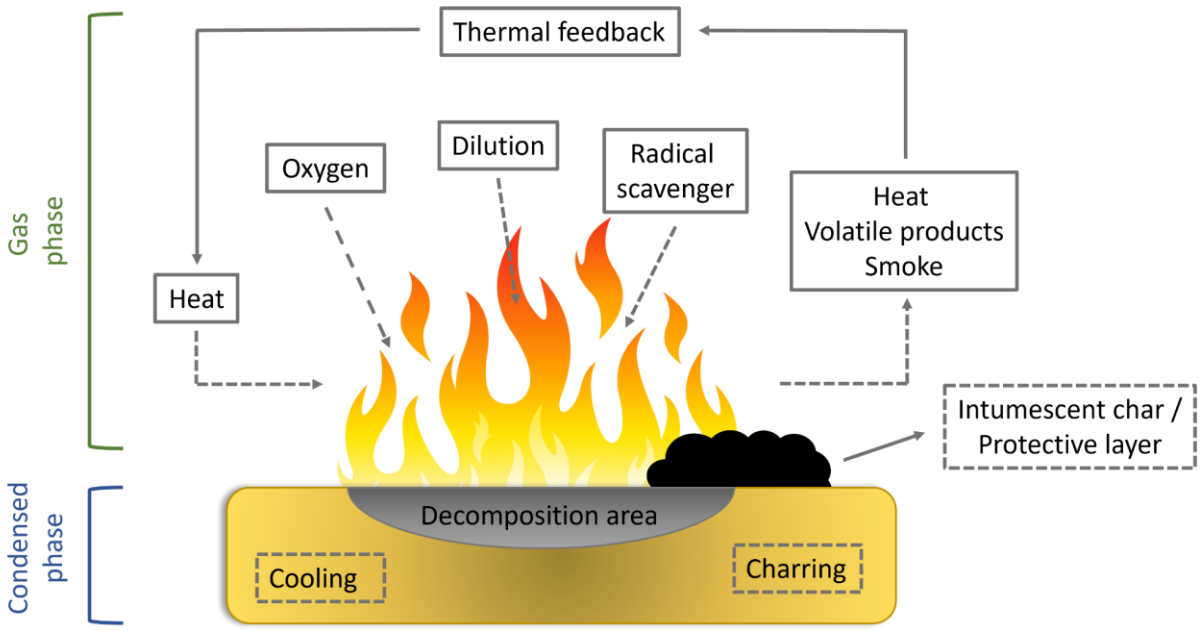

Figure 13: Processes during a fire with potential intervention points (dashed lines) of flame retardants.

With increasing concerns about the toxicity and the negative environmental impact of halogen-based compounds, the flame retardants are divided into two categories: halogenated and non-halogenated. Thereby the category of non-halogenated flame retardants can be further subdivided into phosphorous-based, nitrogen-based, intumescent systems and mineral flame retardants. To obtain increased protection, these different flame retardant systems can also be used in combination. By combining the systems, synergistic effects can be achieved that lead to a reduction in the required amount of flame retardants while increasing their effectiveness.[128,129] However, not all flame retardants can be freely combined, since antagonisms can also arise, resulting in worse protection than the sum of the efficiency of the individual flame retardants.[130] In the following the different modes of action of each group will be described separately.

2.5.1. Halogen-based flame retardants

Halogen-based flame retardants have long been used because of their efficiency and availability, as well as their low cost. With increasing concern about their toxicity to living organisms, as well as possible bioaccumulation, their use is being restricted and alternatives are being sought.[4,5] Their mode of action is the interference with the combustion cycle primarily through free-radical scavenging mechanism. As research has shown, an important step in the continuous combustion cycle results from reactions within the flame involving active radicals of fuel, hydroxyl, hydrogen and oxygen. By using halogen radicals as radical scavengers, this cycle can be interrupted and the fire extinguished. The mechanism begins (1) with the formation of halogen radicals by either reaction with a hydrogen radical from the combustion or due to degradation of the flame retardant molecule upon heating, as shown in Scheme 5. In the next step (2) the hydrogen halides emerge, produced from the reaction between the halogen radical and the decomposing materials. These hydrogen halides are considered the actual flame inhibitors, as they further react with the highly reactive hydrogen and hydroxyl radicals to decrease reactive species and thereby initiate a cycle of protection through the regeneration of the halogen radicals (3). [3,131]

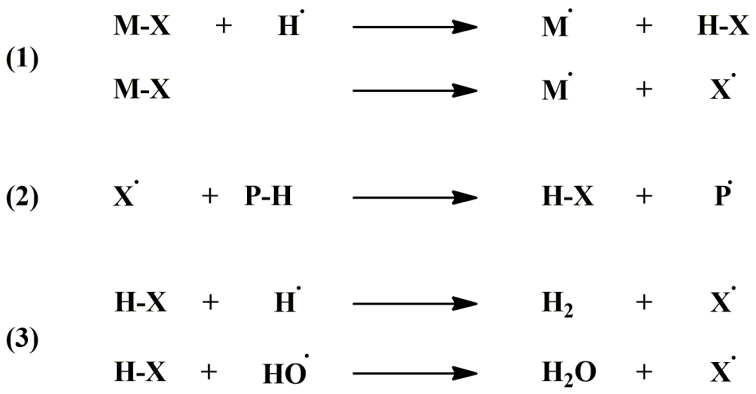

Scheme 5: Mode of action of halogenated flame retardants. (X = halogen; M = residue of flame retardant molecule; P = decomposing material)[3]

Other factors that halogen-based flame retardants contribute to the protection of the material are reducing the heat of combustion due to the high heat capacities of the halogens, and causing the formation of a solid protective layer on the surface of the material, which prevents further burning.[132]

2.5.2. Phosphorous-based flame retardants

Due to the increasing interest in using halogen-free flame retardants, phosphorus-containing flame retardants are increasingly being considered. These include a number of different phosphorus compounds, such as phosphines, phosphinates, phosphonates, phosphates and red phosphorus. Among these, there are many variations that include P-S and P-N compounds, which, depending on

the chemical environment of the phosphorus atom, have different modes of action. Phosphorous-containing flame retardants can function in either the condensed or gas phases, as well as a combination of both and thus have a very wide range of applications. In the condensed phase, these flame retardants are most efficient in oxygen-rich environments or when the material to be protected is oxygen- or nitrogen-containing. In the event of fire, phosphorus anhydrides or acids are formed, which act as dehydrating agents (Scheme 6). These dehydrogenation reactions lead to the formation of double bonds, which can crosslink at these elevated temperatures, causing carbonisation due to incomplete combustion. This leads to an increase in char formation rather than the formation of CO and CO_2.

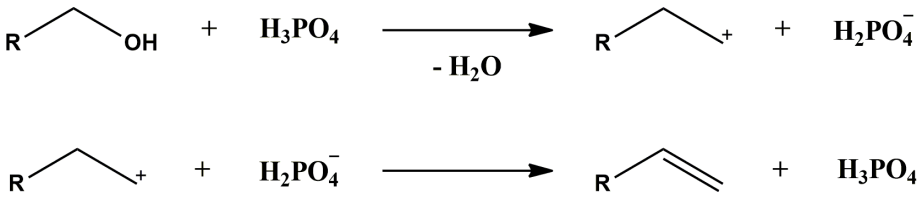

Scheme 6: Dehydration reaction of phosphoric acid with subsequent formation of a double bond.[133]

As the dehydration reaction is endothermic, it acts as a heat sink. Further forming the char layer, a diffusion barrier for oxygen, volatile decomposition products and heat, it causes an interruption in the combustion cycle at multiple points. In the gas phase, the phosphorous-based flame retardants act analogues to the halogen flame retardants. Under the influence of heat, PO-radicals can emerge that function as radical scavengers. These PO-radicals are at the same molecular concentration much more efficient than bromine or chlorine radicals. [131,134,135]

2.5.3. Nitrogen-based flame retardants

Nitrogen-based flame retardants have a very important advantage over halogen- and phosphor-based flame retardants. In case of a fire, the nitrogen-based flame retardants cause a reduced smoke production in comparison to other flame retardants. In addition, some of these nitrogen-based flame retardants are also considered eco-friendly, which makes them very interesting for many applications in synthetic polymers. Common representatives of this flame retardant class are melamine or melamine derivatives, as well as related heterocyclic compounds. They perform in the condensed phase and act as heat sinks, which reduces the temperature of the burning material and thereby hinders further decomposition. At elevated temperatures the compounds also decompose and release ammonia, which dilutes the gas phase and thus suffocates the fire. Due to their mode of action, the nitrogen-based flame retardants are not suited as flame retardants for every material, as they provide no protection against continuous exposure to fire. Because of this, they are often used in combination with other flame retardants, especially in intumescent systems.[136–138]

2.5.4. Intumescent systems

The word “intumescere” comes from Latin and means “to swell up”. This aptly describes the functional principle of intumescent flame retardants, as the effect of these systems is based on a protective voluminous layer of carbon that forms and expands, when exposed to heat. These protection barriers, as mentioned before, have multiple influences on the combustion cycle. Firstly, the physical barrier limits the transfer of heat to reduce the ongoing decomposition of the fuel, which is caused by the heat radiation of the flame. Further, it hinders the diffusion of oxygen to the decomposing material and of burnable volatile gases to the flame. Thereby the protective barrier strips the flame from the important criteria that are required to continue the combustion cycle, as shown in Figure 1. To achieve this formation of a protecting char barrier, the intumescent flame retardant system consists of three components: an acid source, a carbonization compound and a blowing agent. The emergence of the protective layer is a multistage process. Initially the acid source decomposes to a mineral acid, which initiates the dehydration reaction within the carbonization compound that causes char formation. During the decomposition of the carbonization compound, the blowing agent starts to degrade and forms non-flammable gases, diluting the gas phase and expanding the char layer (Figure 14). These gases usually are nitrogen, ammonia, water and CO_2.[139,140]

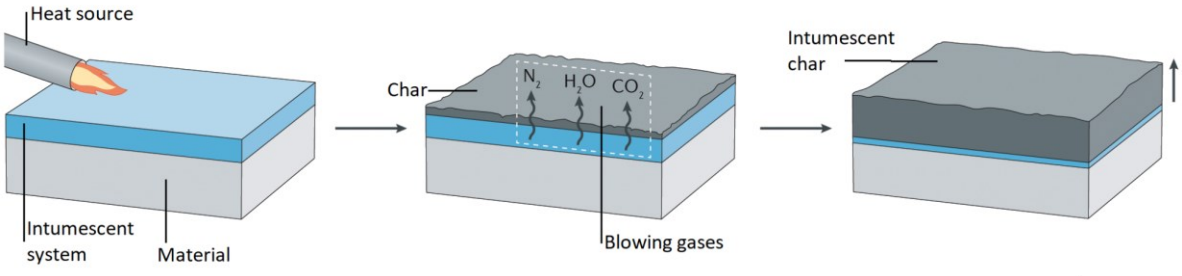

Figure 14: Step-by-step formation of the intumescent protective layer.[133]

The interaction of the three components is very important for the efficiency of the intumescent flame retardants. For example, a premature release of the blowing agents before the formation of the char layer defeats the purpose. In addition to the fire extinguishing properties, the formed char barrier has another advantage. It maintains the stability of the material to be protected, which makes it especially interesting for applications in the construction industry. Despite the many benefits of an intumescent system, it also possesses some limitations. One major problem is the water solubility of the intumescent system that causes leaching. In addition, due to their working mechanism, the thermal stability is relatively low, which makes it unsuitable for some thermally stable materials. This is especially true for materials that are involved in the intumescence process, polymers for example as carbon donors, and less so for materials such as steel, which are not involved in the flame retardant

system. Furthermore, intumescent systems are relatively expensive and the necessary application quantity to achieve protection comparatively high. [141]

2.5.5. Mineral flame retardants

At a basic level, any type of inorganic filler influences the fire behaviour, as it reduces the combustible products, changes thermal conductivity and rheology. The minerals considered as flame retardants are metal hydroxides and hydroxycarbonates. These flame retardants work on the principle of minimising the heat release during combustion in order to extinguish the fire. Metal hydroxides, like aluminium trihydroxide (ATH) and magnesium dihydroxide (MDH) as well as the hydroxycarbonate hydromagnesite (mixture of magnesium carbonate and magnesium hydroxide) release large amounts of water due to the influence of heat. Thus, they act as a heat sink for the heat released by the material decomposition process and therefore slow down the further decomposition process. [142] In addition, the evaporated water dilutes the gas phase, reducing the exothermic radical reactions. In comparison to the metal hydroxides the hydroxycarbonate releases CO_2 on top of this, which further dilutes the gas phase. Another contribution of the mineral flame retardants is smoke suppression. The exact mechanism how the smoke suppression is caused by the mineral flame retardants has not been elucidated yet, but the effect was observed in several studies.[143,144] These minerals are often used due to their low costs, non-toxicity, non-corrosiveness and their easy handling. In contrast to halogen- or phosphorus-containing flame retardants, the mineral flame retardants can only protect the material up to a certain limit. After the evaporation of the water within the minerals, the protection mechanism becomes weaker as they don't promote charring or the formation of another layer of protection, which is a disadvantage of this type of flame retardant. This can be counteracted with a high proportion of mineral flame retardant in the material, but the mineral fillers affect the mechanical properties of the materials, which is why there are upper limits for used. [145]

2.6. Flame retardants for wood

The first recorded flame retardant used to treat wood to protect it from the dangers of fire was alum, by the Egyptian.[146] Since then, the interactions of all flame retardants from halogenated to phosphorus-based have been widely researched and used in a large number of products. With the realisation of the toxicity of halogenated as well as boron-based flame retardants, these have been discouraged and the use of the remaining categories of flame retardants increasingly promoted. The best known flame retardant treatments for wood are the phosphorous containing compounds. Since they primarily work in the condensed phase by promoting char formation, they synergise very well with the natural charring properties of wood and thus provide effective protection.[147,148] Due to the several oxidative states that phosphor can have, a wide range of different phosphorous compounds exist. Although the phosphorous-containing flame retardants are considered

environmentally friendly, organophosphates can be hazardous. A study by ARAKI ET AL. demonstrated that the health issues, like asthma or allergies, can arise due to the use of the two phosphor-containing flame retardants tributyl phosphate and tris(1,3- dichlorisopropyl) phosphate.[149] In addition, the mode of action of phosphor-based flame retardants has a further disadvantage, as the dehydration reaction of the phosphates initiates at relative low temperatures. This can lead to an undesirable reduction in the stability of the wood due to premature onset of degradation reactions, especially in hot or sunny areas, as reported by LEVAN and COLLET.[150] Further, these organophosphorous compounds have an increased volatility and therefore they are rarely used alone in products and are usually combined with halogens, nitrogen-containing compounds or in intumescent systems.[151–153] Since phosphorus is also a source of nourishment for bacteria and fungi, studies have been carried out to protect the material from biodegradation. By incorporating copper into the flame retardant, MARNEY ET AL. were able to show that improved protection against this decay can be achieved.[154]

One of the combinations of phosphorous and nitrogen compounds that displays, due to their synergy, good flame retardant properties, is ammonium polyphosphate (APP). This is an inorganic salt consisting of polyphosphoric acid and ammonia and is a stable, non-volatile compound. Ammonium polyphosphate has a low water solubility due to its branched chain with variable length, making it useful for exterior applications. As the length of the polymer chain decreases the solubility of APP in water increases, which can results in leaching and cause the requirement of subsequent application.[154] To reduces this effect APP, can be mixed with other coatings, like latex inks or resin coatings, to prolong the flame retardant retention on wood.[155] Similar commonly used flame retardants are diammonium phosphate (DAP) and monoammonium phosphate (MAO). They interfere with the combustion analogous to APP, however as they are salts, they have the potential to increase the moisture content of wood making them more suitable for interior applications.[156] For exterior applications, coatings incorporated with flame retardants are used. GAO ET AL., for example, coated wood in their investigations with amino resins modified with phosphates. Due to the combination of the resin with a phosphate, they were able to increase the char yield of 7 % from untreated wood up to 35 %. Samples with the pure amino resin only yielded char residues of 18 % and did not display any further influences on the decomposition temperature or the heat release like the modified resin did.[157] Another flame retardant compound that is often used in coatings is silicon-based. In contrast to phosphates, the silicon-based compounds are not chemically working flame retardants. Instead, in case of a fire, they form a physical barrier preventing the transfer of heat and volatiles as well as oxygen.[158] For the treatment of wood, alkaline silicates are used. Many studies have focused on optimising the formulation and application of these silicate coatings in order to achieve a better performance. The treatment of wood with alkaline silicates provides a wide range of advantages, as they not only provide a high fire retardancy, but also decrease the thermal expansion and smoke

production.[159–161]. In addition, combinations of silicon, phosphor and nitrogen-based flame retardants have become popular. The synergising effects of each provide a comprehensive protection as the nitrogen compounds dilute the gas phase, the phosphor compounds improve the charring behaviour and the silicon compounds offer an increased thermal stability due to protective layer over the forming char.[162]

Recent developments address the implementation of nanocomposites into the material. The very high specific surface area of nanomaterials causes a higher efficiency at lower concentrations and therefore have great potential. In case of fire, this high specific surface allows the activation of a larger amount of flame retardant at a specific time, thus obtaining an enhanced effect. In this context the efficiency of different nano-sized inorganic fillers such as layered SiO_2[163], various vermiculite-sodium silicate composites[164] and silver nanoparticles[165] have been studied in regards to flame retardancy. Even clay nanocomposites with a specific brick and mortar structure were proposed by CAROSIO ET AL. as a sustainable flame retardant coating for wood.[166]

2.7. Flame retardants in cellulose fibre materials

Attempts to create flame retardant cellulose fibres have been made since the early nineteenth century.[167] Since these natural fibres such as cotton, jute and linen burn relatively easily, the approach to produce flame-resistant fibres was through a chemical finishing. The focus was on the development of flame retardants that remained on the fibres over several washing cycles and at the same time did not negatively affect the properties such as tensile strength, air permeability and dyeability. The flame retardants used for this purpose can be divided into the following groups: non-covalently bonded inorganic and organic compounds as well as compounds covalently bonded to the cellulose fibre.[3]

The use of inorganic phosphates like ammonium phosphates or ammonium polyphosphates is the technically simplest approach to achieve flame retardant properties on cellulosic fibres, since the inorganic flame retardant can be added to the fibre dispersion in paper making. Usually, a phosphorous content of 1-2 w% is sufficient to receive flame retardant fibres.[167] The challenge is to incorporate these water-soluble salts into a durable coating that meets the requirements for the application of the fibres. This task was addressed by HAWKES ET AL.[168] as well as WEBB ET AL.[169] by introducing multifunctional isocyanates to create a cross-link to minimise solubility. Further examples of phosphates used for non-durable treatments are monoguanidine dihydrogen phosphate and diguanidine hydrogen phosphate. The effects of both phosphates on the reduction of the limiting oxygen index (LOI) and the increase in char formation was investigated by VROMAN ET AL.[170] Organophosphorus flame retardants that have been used for a long time are formulations of 3-(dimethylphosphono)-N-methylolpropionamide (DMPMP) and tetra-kis (hydroxymethyl)

phosphonium chloride (THPC). To create durable formulations, DMPMP and THPC are crosslinked using a formaldehyde-based cross-linker such as melamine formaldehyde. The formaldehyde cross-linker causes possible environmental difficulties due to the subsequent release of formaldehyde, but these compounds are among the most durable and efficient flame retardant finishing treatments for cellulose fibres.[171,172] In order to reduce the negative impact of formaldehydes, research has been conducted with trimethylolmelamine or dimethyloldihydroxylethyleneurea as cross-linkers. In combination with oligomeric hydroxyl functional organophosphorus compounds YANG ET AL.[173] and STOWELL ET AL.[174] showed good flame retardant properties for these, while maintaining the properties after multiple washing cycles.

Besides the implementation of flame retardants onto the cellulose fibres, the functionalisation of the cellulose chains itself via grafting is another possibility. The advantage of graft polymerisation on the cellulose chains is the increased durability of the functionalisation due to the covalent connection between flame retardant and material. In pursuing this strategy, KAUR ET AL. grafted methacrylamide using UV radiations and benzophenone onto cotton, which then was further phosphorylated. Due to the synergising effects of nitrogen and phosphor, an improvement in the flammability behaviour, as well as the increase of char formation, was determined.[175] In addition to grafts using UV irradiation, modifications using plasma are becoming increasingly important in research due to its greater environmental friendliness. TSAFACK ET AL. investigated this method in more detail using microwave argon plasma and concluded that the resulting flame retardancy is influenced not only by the amount of phosphorus in the grafted monomer, but also by its surface structure. The larger specific surface area increased the efficiency, similar to the flame retardant nanoparticles, of the via plasma applied flame retardants.[176,177] But not only phosphorous-containing monomers are suitable for plasma-based application, as TOTOLIN ET AL. grafted sodium silicates into cellulose fibres, which later showed excellent flame retardant properties as well as a good durability.[178] It is important to mention that the grafting method also has a disadvantage. Since the hydroxy groups of the cellulose are modified during the functionalisation of the fibres with no further cross-linking, this has a negative effect on the strength of the cellulose materials. A change in the draw ratio of the fibres, as well as fewer inter- and intramolecular hydrogen bonds, lead to a reduction of the connections between the fibres and thus to fabric with decreased mechanical properties.[79,179]

2.7.1. Flame retardants in paper

Compared to the amount of research that takes place in the field of flame retardancy of textiles and wood, the research directed towards the fire protection of paper and paper products such as corrugated and honeycomb cardboard is relatively small. The strategies of optimising the flame retardancy of paper resulting from these investigations can be differentiated into the use of additive

flame retardants and reactive flame retardants. In industry, additive flame retardants, especially inorganic fillers, which can be introduced into paper by direct application in the wet end or fibre loading, are common. In addition to their flame retardant properties, these inorganic fillers can also contribute to the paper brightness as well as the ink receptivity. One example therefore is aluminium trihydrate, which carries a flame retardant effect due to the bound water.[180] Further TAKE ET AL. patented the method of implementing calcium silicate as well as aluminium hydroxide as fillers to create flame retardant papers.[181] Further research has been put into the study of Mg-Al hydrotalcites. With its high whiteness and good flame retardant performance WANG ET AL. showed in their studies an increase of the LOI of 25 %. However, the disadvantage of introducing such inorganic fillers was also documented. Since a large amount of these fillers has to be added to achieve sufficient flame retardancy, the mechanical properties of the paper decrease.[182] To circumvent this problem, increased efforts have been made to develop plastic coatings suitable for use as topcoats for papers. Flame retardants based on azoalkanes have been implemented in low density polyethylene and extruded onto paper. Thereby achieving good flame retardant properties as well as good interfacial adhesion with the cellulosic substrate.[183] Without such linking materials, like low density polyethylene, the correlation between increasing flame retardancy and decreasing stability is a major problem for the modification of paper, causing research to move from the additive to covalently bound flame retardants. The good accessibility of the OH-groups of the cellulose enables many esterification and etherification reactions which allow a direct functionalisation of the fibres. An example of this is the phosphorylation of cellulose using phosphorus pentoxide, which was investigated by ZHANG ET AL. By introducing melamine as a binder, the synergistic effects of the phosphorus- and nitrogen-containing flame retardants were utilised.[184] Different methods of introducing phosphorus functionalities were investigated and the success of the incorporated flame retardants was confirmed. However, these modifications also caused a decrease in the mechanical stability of the papers.[184–186] This functionalisation of the fibres can take place on the paper either before or after sheet formation. Before sheet formation, some of the fibres to be introduced are functionalised, which can have a negative effect on sheet formation and as mentioned above, on the mechanical properties of the paper. After sheet formation, the size of the product to be functionalised is a factor to be considered in surface functionalisation. Coatings, as they are used for the application on wood, are therefore another possibility to protect paper. In this context modifications via layer-by-layer (LBL) coatings have moved into focus. Thin layers with different functionalities are applied one after the other to the material to obtain various modifications like flame retardancy, water repellent properties or an increase in strength. The advantage of this application method is that good flame retardant properties can be applied to the cellulose fibres with a minimal amount of coating. Investigation of LI ET AL. have revealed that the described LBL assembly with nitrogen and phosphor-containing

polyelectrolytes creates very effective intumescent flame retardant coatings.[187] This method is also suitable for the use of bio-based materials, as shown in the research by MAGOVAC ET AL., in which multilayers of chitosan and phytic acid generate an environmentally friendly flame retardant.[188] The different layers in the LBL assembly are usually applied via a dipping process, which limits the entire functionalisation process to certain areas of application, since the size of the material to be functionalised is essential.[189]

Summarising the state of research for the flame retardancy of paper, it is clear that a large number of flame retardants already exist. Some flame retardants have been used in manufactured products for some time, but it is also clear that the introduction of a flame retardant into the paper fabric can have negative effects on its properties. Therefore, an optimal solution must be found for each application in order to obtain the desired degree of flame retardancy while maintaining the intrinsic properties of the paper. In the research on the effectiveness of the different flame retardants on the cellulosic fibres, all important parameters that enable a classification of the flame retardancy are investigated, from the LOI to the charring behaviour to cone calorimeter measurements. However, what is neglected in all investigations is the possible influence of the cellulose on the flame retardancy. Since cellulose, and its fibres, are a natural product that is influenced by multiple factors, the resulting changes in the composition can affect the protection mechanism of the flame retardants. It is noticeable that, despite the increasing attention to environmental friendliness and ecology, the proportion of bio-based flame retardants is still very low. Therefore, in-depth knowledge should be generated on the following topics:

- Influencing factors of paper intrinsic properties on the burning behaviour of paper
- Differences in the burning behaviour of paper due to the presence of lignin on the fibres
- Influence of lignin on the mechanisms of action of flame retardants
- Comparison of bio-based and commercially used flame retardants

3. Goals and Strategy

3.1. Goals

The main objective of this work is to gain a better understanding of the influence of the intrinsic properties of paper on its burning behaviour and the subsequent protection with flame retardants. In particular, the impact of remaining lignin on the fibres shall be considered. In addition, bio-based flame retardants will be considered and evaluated as viable substitutes for commercial flame retardants. Therefore, the following guiding questions shall be addressed:

- How can the intrinsic properties of paper be influenced?
- What influence do different fibre compositions have?
- How can the burning behaviour of paper be determined?
- What relationships can be identified between the changed burning behaviour and the varied intrinsic properties?
- What is the influence of remaining lignin on the fibres in this context?
- How can the proportion of flame retardant in the paper be determined?
- To what extent do the different proportions of flame retardant produce a protective effect?
- What effect do different fibre compositions have on the flame retardant effect?

3.2. Strategy

For the investigation of the fire behaviour of paper, an investigation matrix is to be set up that covers the various factors influencing the fire behaviour. For this purpose, a bleached and an unbleached pulp, i.e. a pulp containing residual lignin, from pine and spruce are used. In order to generate the different paper-intrinsic properties, papers with three grammages are produced from both pulps. These will then be gradually calendered to induce an increase in density in the different samples. The characterisation of the changes in the paper samples caused by the calendering will then not only refer to the increase in density or change in porosity but will also include other parameters that can have an effect on the fire behaviour. These include residual moisture, heat release, decomposition behaviour, crystallinity and thermal conductivity. To determine the burning behaviour of paper, which is defined as burning speed, it was necessary to establish a valid measurement method as a basis for this research. By correlating the change in burning speed due to calendering with the results of the changed intrinsic properties of the papers, conclusions are to be drawn about the main influencing factors. By examining papers made of bleached and unbleached pulp, influences of the lignin can also be taken into account. These findings should make it possible to optimise the material paper in terms of flame retardancy.

In the second part of the work, the results obtained from the investigation of the burning behaviour will be used as a baseline to investigate the impact of three different flame retardants on these papers. The commercially used ammonium polyphosphate is used as a reference and a carbamated and phosphated starch and ammonium phytate are used as bio-based flame retardants (Figure 15).

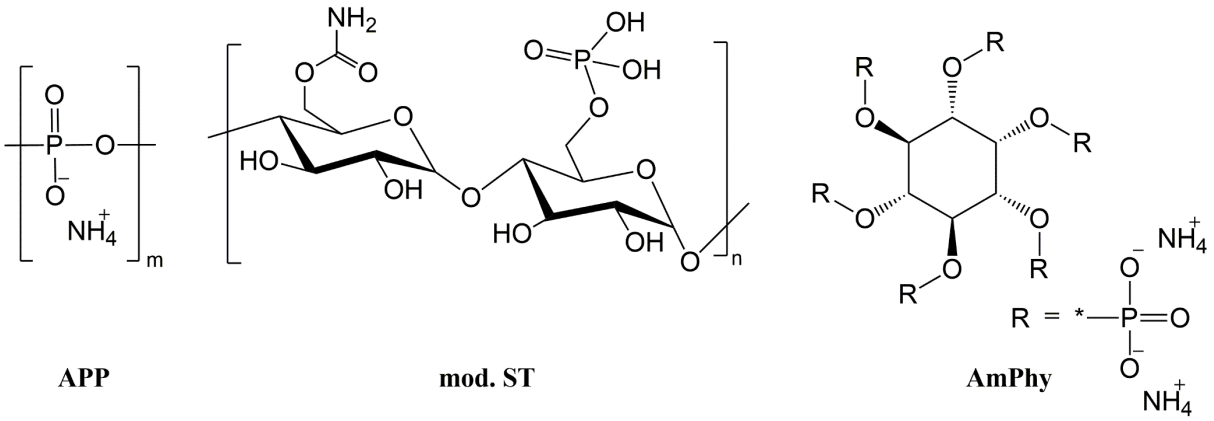

Figure 15: Structures of the flame retardants used: Ammonium polyphosphate (APP); modified starch (mod. ST); Ammonium phytate (AmPhy)

The flame retardants are to be used in different concentrations and the respective amounts will be quantified via the phosphorous content. Subsequently, the effectiveness of the flame retardants on the two types of paper are to be determined as a function of their concentration by means of cone calorimetry. The influence of the individual flame retardants on the decomposition behaviour of the papers will then be investigated by means of a combined analysis method of thermogravimetry analysis, Fourier transformed infrared spectroscopy and mass spectroscopy. In this way, a comparison can be made between the individual flame retardants in terms of effectiveness and functional mechanism. The influence of the remaining lignin on the mechanism of the flame retardants will also be investigated.

4. Methods

This chapter explains and summarises the methods used in this study. The descriptions include the burning speed test of the calendered papers (Chapter 4.1) and the solid-state NMR (Chapter 4.2) for the crystallinity measurements of the corresponding cellulosic fibres. For the investigations of the flame-retardant papers, the analysis of the phosphorus content of the samples via inductively coupled plasma atomic emission spectroscopy (ICP-AES) (Chapter 4.3) and that of the fire properties in the cone calorimeter (Chapter 4.4) are explained.

4.1. Burning Speed test

The determination of the burning speed of any sample is typically determined by measuring the elapsed time *s* required for the flame front to travel a defined distance *x*.

$$Burning\ speed = {}^{x}/_{s} = {}^{cm}/_{sec}$$

Generally, markings are made on the sample and the time is measured with a stopwatch. As a result, especially at faster or proportionally similar burning speeds, a large error in the measurements can occur due to the human reaction time. For this study, in order to negate this error, an evaluation method for the measurements of the burning speed was developed. To determine the burning speed of paper, videos of both horizontally and vertically aligned burning paper stripes were recorded. The camera was affixed in a defined place for each recording to ensure the angle and distance between the camera and the sample was uniform. The videos were recorded with a frame rate of 24 Hz. In addition to the camera, a light emitter strong enough to outshine the emerging flames during the measurements was installed, eliminating their visibility in the recorded images. The papers were ignited using a roaring blue flame of a Bunsen burner.

The videos of the fire tests were processed by *Fiji ImageJ* and converted into an 8-bit visual stack of singular pictures. A threshold was set to further convert the images into a black and white image as evident from the following Figure 16.

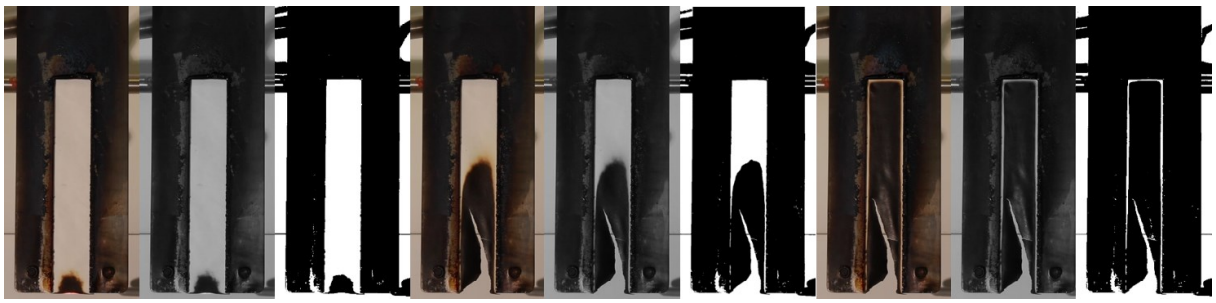

Figure 16: Conversion of the recorded picture stacks into black and white images.

For each sample, an analysis area was defined at several points in form of a gradient area (Figure 17a). Within this yellow area, the advancing flame front was detected using *MatLab* by determining the length of the black area in pixels for each image. If a flame could still be seen on the images at this time, white spots would appear at random points, which would negatively influence the subsequent evaluation. A graph created from the analysed images shows the progression of the combustion front (Figure 17b).

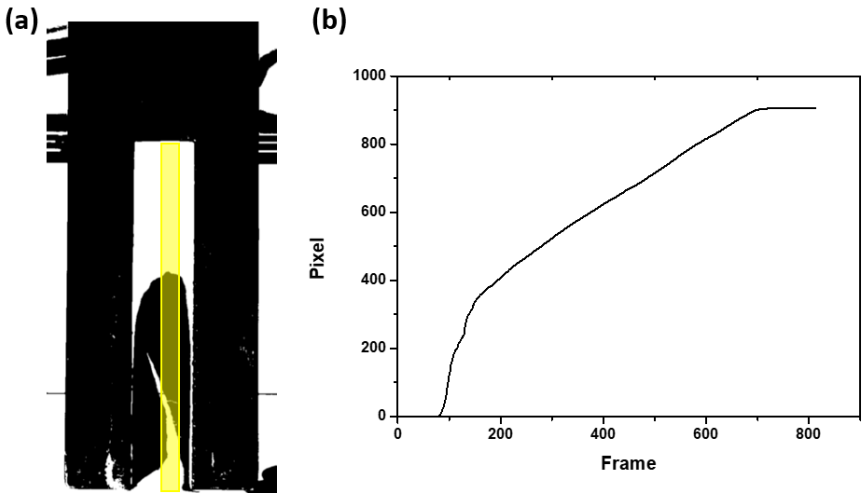

Figure 17: Conversion of the tracked progress of the flame front from the selected area (a) in correlation to the frames into a plot (b).

With the knowledge of the sample length and the frame rate of the recording, the pixels and the frame number can be converted to length and time. Thus, the gradient of the resulting curve corresponds to the burning speed (Figure 18).

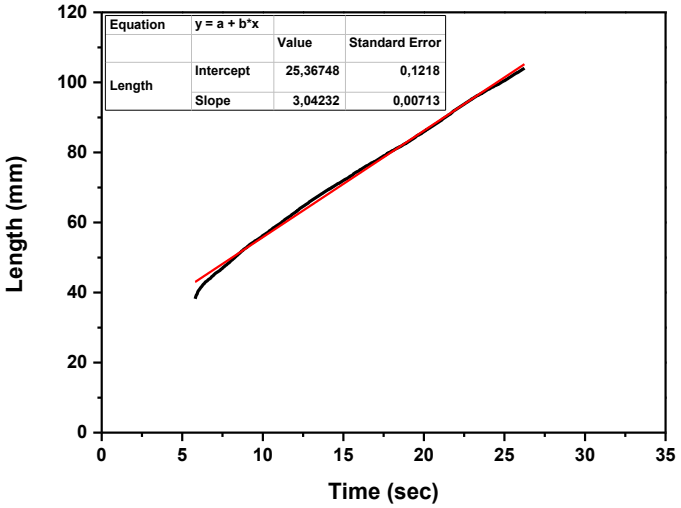

Figure 18: Determination of the burning speed using the slope of the trend line.

Burning speed is determined by averaging the results of six paper stripes obtained for one sample. In contrast to the conventional evaluation method, in which the burning speed is only determined

between two points, the evaluation method developed here is a continuous approach, which is significantly less prone to error. Due to the frame-dependent evaluation, it would also be possible to record burning speed changes within samples, if they are for example just partially coated with another material.

4.2. Determination of crystallinity using solid-state NMR

The crystallinity of cellulose is an important character in the study of the material, as it correlates with many mechanical, morphological and chemical properties. For example it has already been shown in studies that crystalline regions can have an influence on the gas and water permeability of cellulose films[190] as well as on chemical and biological reactions.[191] The most common techniques to determine the degree of crystallinity are Wide Angle X-Ray Scattering, solid-state NMR spectroscopy and Raman spectroscopy. The advantage of using solid-state NMR spectroscopy is that this measurement method allows the proportions of amorphous and crystalline cellulose to be determined directly from the obtained data.[192] The idea of using solid-state NMR spectroscopy to determine the crystallinity of cellulose is based on the fact, that even though carbon atoms can be chemically equivalent, they can be distinguished as long as they are not magnetically equivalent. Accordingly, as long as the analysed material has differently packed chains or distinct conformations, it can cause a shift of the peaks for the respecting carbon atoms.[193] Separate signals are therefore detected in the cellulose spectra for amorphous and crystalline domains and the degree of crystallinity can be determined as a crystallinity index (CrI) by deconvolution. In case of cellulose, these shifts occur for the C_4 and C_6 atoms of the anhydroglucose unit (Figure 19). The crystalline areas are addressed for C_4 in the range of 86 – 92 ppm and for C_6 in the range of 63 – 68 ppm. Signals at 79 – 86 ppm and 60 – 63 ppm are assigned to C_4 and C_6 atoms, respectively, present in amorphous regions.[194,195] The signals for the $C_{2,3,5}$ atoms are less suitable for the evaluation, because their peaks are not as distinct as the peaks for C_4 and C_6.

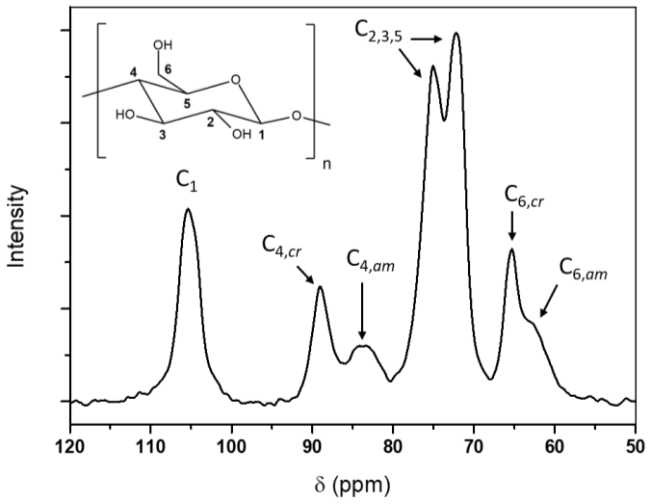

Figure 19: Assignment of NMR spectrum ranges for the differentiation of amorphous and crystalline fractions in cellulose.

As the separation of the peaks for C_4 are more distinct than for C_6, these will be used for further analysis. For the evaluation, the spectra do not need to be normalized as it would not change the ratio between both domains and the integral quantities of the respective peaks can be directly compared.

4.3. Inductively coupled plasma atomic emission spectroscopy (ICP-AES)

Inductively coupled plasma atomic emission spectroscopy (ICP-AES) is a spectral method used to determine the elemental composition of samples (Figure 20). This analytical method utilises the emission of photons produced by the excitation of an analyte by using high-energy plasma. The plasma is created when an inert gas, typically argon, passes through an alternating electric field generated by an inductively coupled coil. By insertion of the analyte into the plasma, the electrons of the atoms within are excited to a higher energetic state. Afterwards, they try to dissipate the introduced energy by falling back to the ground state. The return to the lower state of energy is accompanied by emission of light with specific wavelength, which can be used to determine the elements present. The difference of energy between the excited and ground states is specific to each element. In the case of a high concentration of a specific element, there is an accumulative effect that increases the intensity of the light emitted and this is reflected in the detector´s output signal.[196,197] Due to this effect, it is possible to create a calibration curve from analyte solutions of known element concentrations. It is important to mention that elements with similar atomic structure can cause a potential wavelength to overlap. Transition metals that are next to each other on the periodic table, like iron with an emission wavelength at 238.20 nm and cobalt at 238.94 nm, can be difficult to distinguish.[197] The wavelength of the phosphorous peak, used for this work, is located at 213.61 nm and had no overlap with the other atoms in the flame retardant papers.

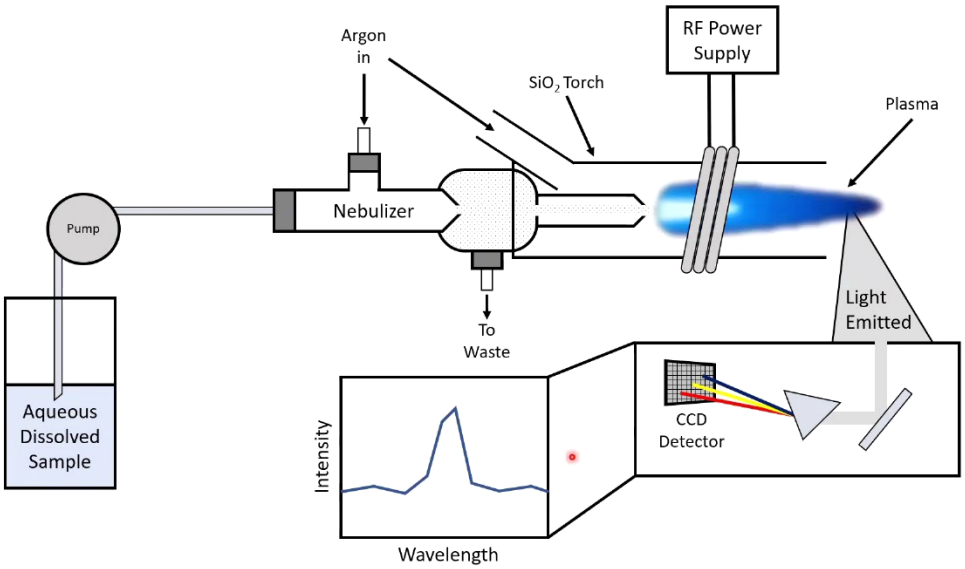

Figure 20: Schematic representation of the structure of an inductively coupled plasma atomic emission spectrometer.[198]

4.4. Cone calorimetry

Cone calorimetry (ASTME 1354 / ISO 5660) is an elaborate method used to determine numerous fire properties of a material.[199] By using a single measurement in a cone calorimeter, the heat release rate (HRR), the peak of heat release rate (pHRR), the time to ignition (TTI), the total heat released (THR), the mass loss rate (MLR), the peak of mass loss rate (pMLR) and the specific extinction area reflecting the smoke production, can all be measured (Figure 21). Out of these different measured properties the HRR and the pHRR have the greatest significance. The HRR describes the driving force of the fire due to the continuous release of heat and the pHRR, the potential of the fire propagation. The higher the peak of the heat release rate, the more the fire inclines to spread further and ignite adjacent objects. To obtain a measurement, the sample (100 mm x 100 mm x up to 50 mm) is placed on a load cell that allows the tracking of the mass loss during the test. A conical electrical radiant heater uniformly irradiates the sample at a defined heat flux from above. The ignition is then triggered by an electric spark, which inflames the gases evolving from the decomposing sample. An exhaust duct system is located above the heater that collects the emerging gases. These collected gases are analysed by a continuous gas analyser for the components O_2, CO and CO_2 and then used to calculate the HRR based on the defined relationship between the mass of oxygen consumed from air and the amount of released heat during polymer combustion. The proportionality factor is constant for every material and is equal to 13,1 kJ/g of consumed oxygen. Inside the fume cupboard, the smoke density is determined with the help of a white beam laser.[200,201]

An important note should be made regarding the investigations using the cone calorimeter, as this analysis method is designed for materials with a certain mass and thickness. Therefore, slight errors may occur when analysing thin materials such as foils or paper. As a methodological adaptation to the

thin and flexible material paper, the samples were fixed to the sample plate with a wide-meshed grid to negate the deformation resulting from the combustion, and thus maintain a constant distance between the sample and the heat emitter.

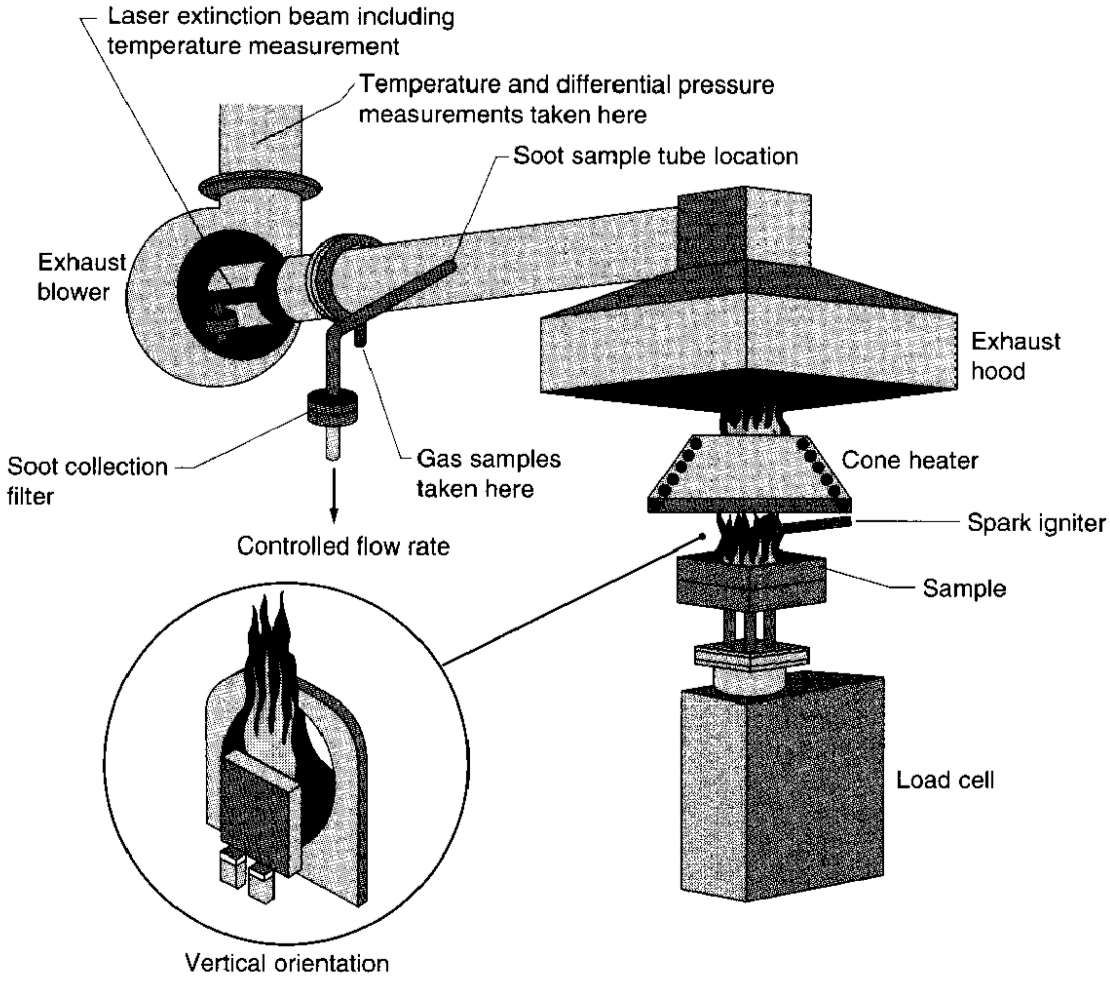

Figure 21: Schematic view of a cone calorimeter.[202]

5. Burning behaviour of paper

This chapter reports and critically discusses the influence of the paper's intrinsic properties on the burning behaviour of the material. First, the results of the burning speed measurements for the different papers made from northern bleached softwood kraft (NBSK) and unbleached kraft pulps (UKP) are presented (Chapter 5.1). The resulting differences are then correlated with the changed intrinsic properties of the paper to explain the variations in burning speeds. The parameters investigated include structural changes of the paper regarding porosity (Chapter 5.1.1) or residual moisture (Chapter 5.1.2), as well as compositional alterations in terms of variations in crystallinity (Chapter 5.1.5) of the fibres and thus changes of the thermal conductivity (Chapter 5.1.6). Influences on thermal decomposition are investigated by means of cone calorimetry (Chapter 5.1.3) and thermogravimetric analysis (Chapter 5.1.4). A summary of these results can be found at the end of this chapter.

5.1. Burning speed measurements

Before a material can be protected by flame retardants, both the fire and decomposition behaviour of the base materials must be evaluated. Afterwards, the flame retardant should be adapted to the material in order to achieve an optimal efficiency. For example, the effectiveness of the flame retardants is reduced if it begins to act drastically below or above the decomposition temperature of the material to be protected. In addition, there are various flame retardants that protect the material by different mechanisms due to their chemical composition, which can be unsuitable and thereby minimise the efficiency.[203] This raised the question of whether paper can be influenced in terms of flammability before flame retardancy is applied to further increase the protective effect. To address this open research question, a matrix of different paper samples with different intrinsic properties was created to detect possible influences. The changes included a variation of grammage from 100 g/m², 150 g/m² and 200 g/m² and four increasing calendering levels, which represent a gradual change in the intrinsic properties. Additionally, the influence of different pulps was considered. Besides a bleached pulp, an unbleached pulp with a residual lignin content of 8 w% was investigated. In previous research, possible influences on the burning behaviour have been studied for various cellulosic materials. It was concluded that factors including density[204], moisture content [205], heat release rate[206] and charring rates[207] have major influences.

In the work of GILKA-BÖTZOW ET AL.[208], for example, the dependence of the burning rate β of wood on its density ρ was investigated and the following correlation was established.

$$\beta = \sqrt{\frac{x}{\rho}} \qquad \text{(Eq. 5.1)}$$

x = wood-specific factor

It shows that with increasing density, the burning rate of wood decreases. This behaviour was explained by WOLGAST ET AL.[209]. His study of the rate of degradation of wood as a function of the density showed that the increased flame propagation speed correlated with increasing void volume, which is equivalent to a decreasing density. The bigger void volume could cause a localized overheating and simultaneous heat accumulation, which would benefit a faster flame spread. Another important factor influencing the combustion of cellulose is moisture. With increasing amounts of moisture within the cellulosic materials, the rate of combustion decreases as the energy needed for the water evaporation increases.[210]

In order to investigate the extent to which the properties mentioned above affect the burning behaviour of the processed papers, the burning rate itself was determined. To analyse different burning processes, vertical and horizontal burning was tested. In the following Figure 22 the burning speed for the NBSK papers in both burning directions are displayed, which were determined using the computer-based evaluation method described in chapter 4.1. The burning speed of the paper is plotted against the grammage to show the respecting dependencies, as well as the influence of the increasing compressions. The settings of the calendering are listed in Table 26 in the experimental section.

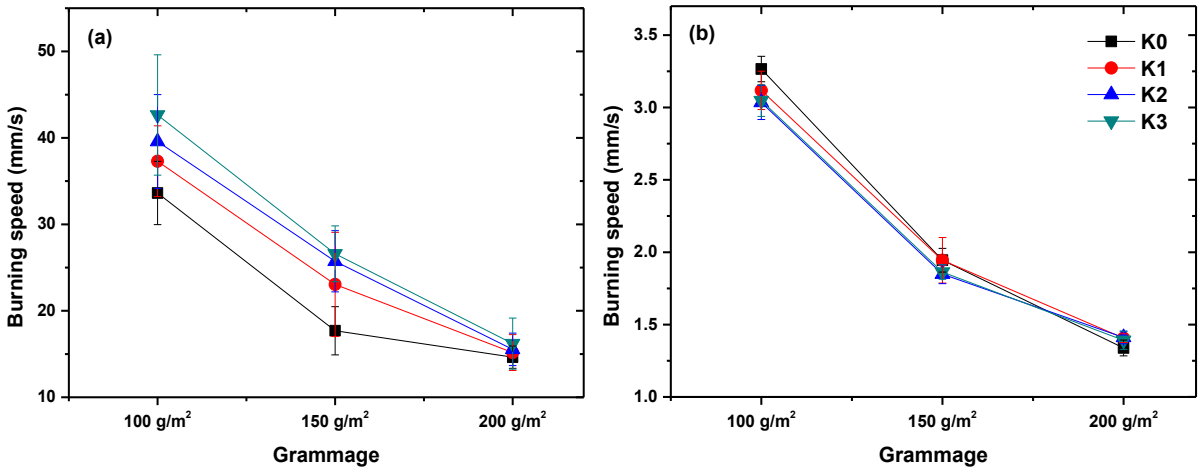

Figure 22: Determined burning speeds for NBSK papers in vertical (a) and horizontal (b) burning direction plotted against the grammage. K0 (black); K1 (red); K2 (blue) and K3 (green) correspond to the increasing degree of compression.

Looking at the course of the graphs for the vertical burning direction (Figure 22a), significant dependencies of the burning speed on varying grammage can be seen. The burning speed decreases with increasing grammage. For example, the burning speed of the uncalendered paper decreases from 33.6 mm/s to 14.6 mm/s. Under the assumption that the heat capacities of the individual paper samples do not, or only minimally change, the higher mass sample needs to absorb a higher amount of heat to reach the degradation temperature. For this reason, the decomposition of the material is slowed down, which results in a reduced burning speed.[207] In addition to the effect of the grammage, it is noticeable that burning speed is also affected by the different compression levels. An increase in compression causes the papers to burn faster. For the 100 g/m^2 papers the burning speed increases from 33.6 mm/s to 42.6 mm/s, whereas for the highest grammage, the burning speed only increases from 14.6 mm/s to 16.2 mm/s. This indicates that the effect seems to be reduced with increasing mass as the influence of the compression decreases with increasing grammage. When considering a horizontal burning direction (Figure 22b), the effect of compression does not seem to be as significant as for the vertical scenario, or is generally smaller due to the slower burning speed. Comparing the burning speeds of the NBSK samples in both directions, the burning speed in the horizontal direction is reduced by a factor of about ten. Furthermore, increasing grammages also cause reduced burning speeds in horizontal direction. The difference in burning rates for the two burning directions can be explained by the different mechanisms of fire progression. Due to convection of the rising heat, the material above the flames is pre-dried and pre-heated and can already begin to decompose, which leads to faster burning in vertical direction. On the other hand, in the horizontal plane, the rising heat plays a subordinate role for the progression of the flames, as explained by LIN JIANG ET AL.[211] Here, the main portion of the burning speed results only from heat radiation of the emerging flames from the decomposing neighbouring material, and does not accumulate as it does with the rising heat. As a result, the heat participating in the horizontal burning process is only a proportion of the heat that drives combustion in the vertical direction, resulting in slower burning.

Analogous to the NBSK papers, the determined burning speeds of the lignin-containing papers (UKP), displayed in Figure 23, show a similar progression. In both burning directions, the burning speed decreases. Furthermore, the influence on the paper samples of the compression can be recognized as well.

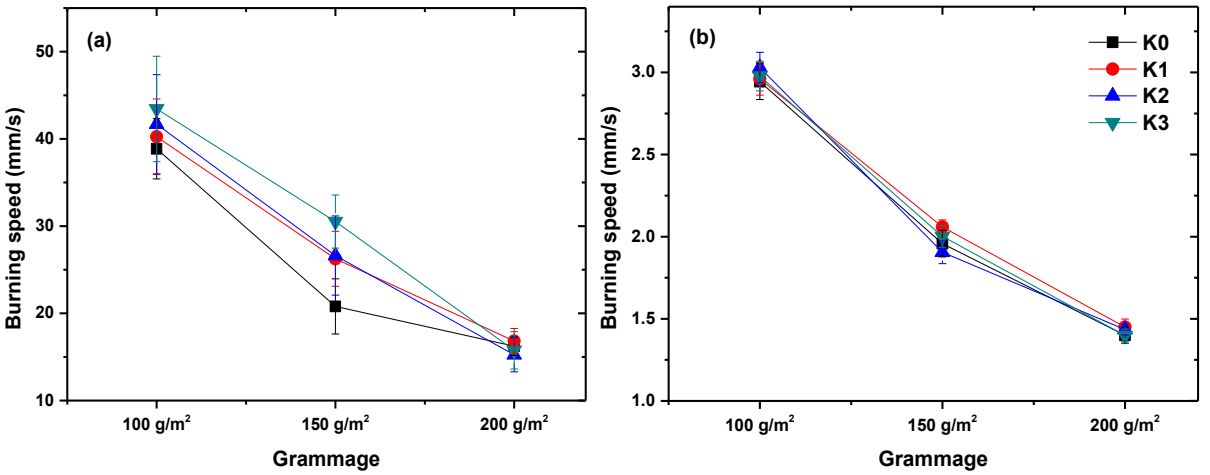

Figure 23: Determined burning speeds for UKP papers in vertical (a) and horizontal (b) burning direction plotted against the grammage. K0 (black); K1 (red); K2 (blue) and K3 (green) correspond to the increasing degree of compression.

When comparing the results of the NBSK and UPK papers (Figure 24) at various grammages and calendering steps as indicated in the figure, it is noticeable, that the lignin-containing papers burn faster than the comparable NBSK papers, which is particular evident in the vertical burning test. Since both pulps consist of a comparable ratio of pine and spruce fibres and have the same refining grade, this influence can be exclusively attributed to the remaining lignin. According to KALTSCHMITT ET AL. lignin has a net-heat of combustion of 27.0 MJ/kg and cellulose of 17.3 MJ/kg.[212] This higher combustion heat of lignin within the UKP papers could cause the increase in burning speed, because of the higher amount of released heat. Nevertheless, the low amount of lignin (8 w%) in the UKP fibres, as well as the small sample masses, should be considered as it could lead to small influences.

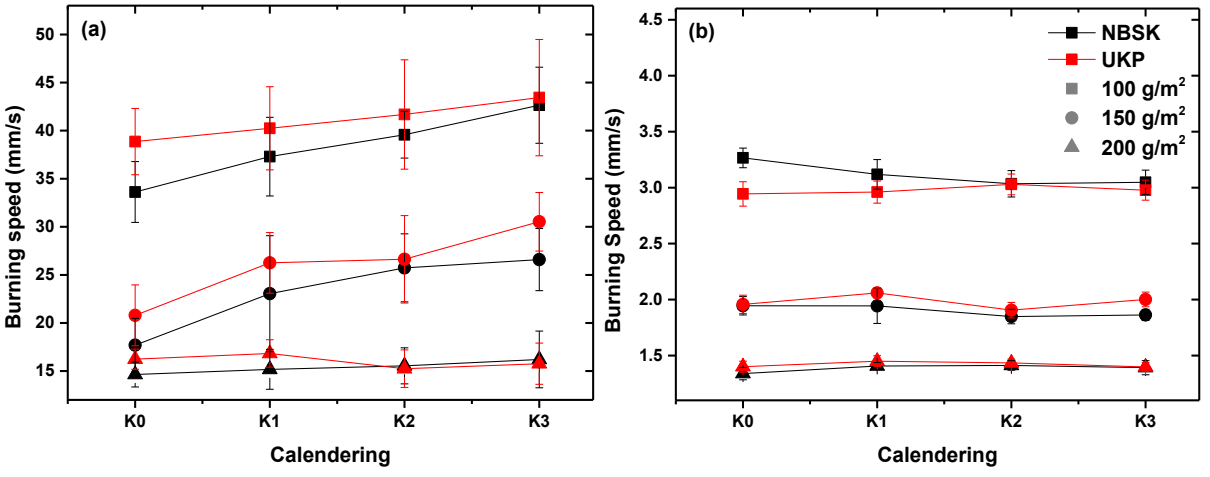

Figure 24: Comparison of the burning speeds of the bleached NBSK (black) and unbleached UKP (red) papers in vertical (a) and horizontal (b) burning direction.

The burning speed of the uncompressed UKP papers in vertical direction (Figure 24a) starts at 38.8 mm/s and increases to 43.4 mm/s with highest calendering stage, whereas the NBSK papers start with a burning speed of 33.6 mm/s and goes up to 42.6 mm/s. Similar to other grammages

investigated, the burning speed equalises with increasing compression. In addition, the differences of the burning speeds between both pulps seem to be influenced by the grammage, as well as the reduction of differences with increasing grammage. For the burning in horizontal direction (Figure 24b) the calendering seems to have almost no influence on the burning behaviour and therefore, the burning behaviour is only affected by grammage.

Contradicting the findings of the previous research by Wolgast[209] and Golka-Bötzow[208], the increasing compression of the papers caused an increase in the burning speed for both paper types. The previous works displayed a reduction in burning speed with increasing density. In order to determine the causes of these changes in the burning behaviour, the effects of calendering on the intrinsic paper properties are investigated. Therefore, the aforementioned properties, which have influences on the burning characteristics, are studied in more depth in the following chapters.

5.1.1. Changes in porosity and density

To examine the changes in the papers caused by the calendering process, the porosity of the papers was analysed using mercury porosimetry. Because the pore size distribution of laboratory hand sheets as well as commercial paper sheets is bimodal, the different influences for both types of pores are considered. In Figure 25 this bimodal pore size distribution is displayed. The pores larger than approximately 10 µm (dark grey area) predominantly are located at the surface of the sample and pores smaller than 10 µm (light grey area) correspond to the internal porosity.[86]

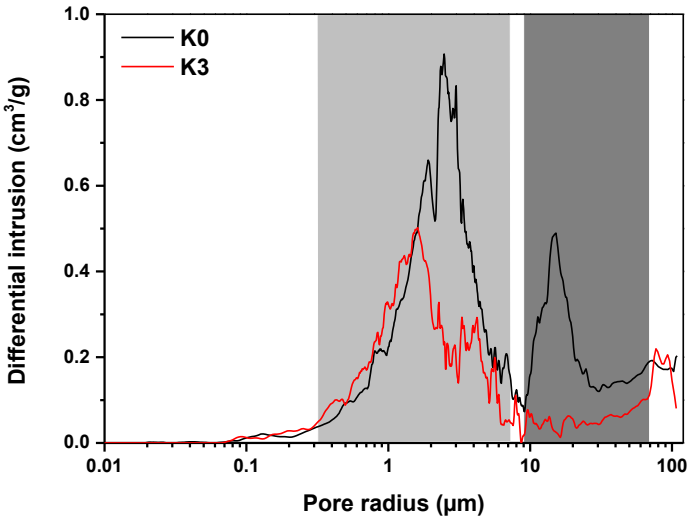

Figure 25: Pore size distribution of the uncompressed (black) and highest compressed (red) 100 g/m² NBSK paper.

By comparing the results of the uncompressed (K0) and highest compressed (K3) papers, it is noticeable that the overall porosity reduces (26.5 % → 11.8 %) with increasing compression. This decrease is most noticeable for the pores that are assigned to the surface porosity with a pore radius above 10 µm. The internal porosity (r < 10 µm) also reduces, but not in the same extent as the pores

at the surface. These changes of the cellulose material verified by means of SEM as shown in the following Figure 26 and Figure 27.

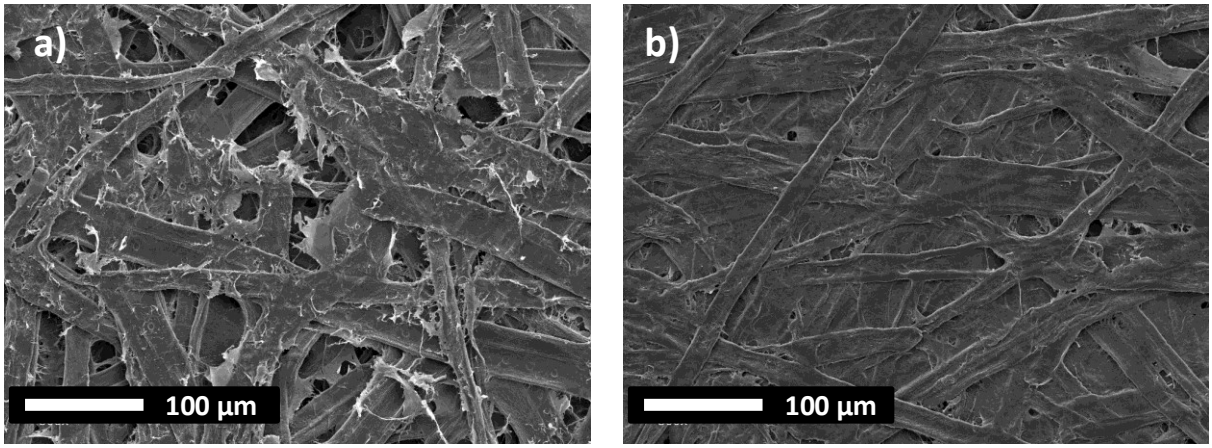

Figure 26: Top view SEM images of the uncompressed (a) and most compressed (b) 100 g/m^2 NBSK paper.

From these images, it can be observed that the compression of the paper samples made a change to the surface that was already predicted by the results of the mercury porosimetry. It becomes evident, that the compression not only affects the surface pores, but also moulds in the fibrils that originate from the milling process. This implies that the compressed samples have a reduced specific surface area, as the surfaces is qualitatively smoother. It is important to note is, that although we did not intend to study specific surface areas in a quantitative fashion, the latter is not trivial. Combining the statements of the smaller specific surface area with the minimized oxygen accessibility would usually lead to the conclusion that there is a slowing down in the burning speed, but this is not the case, as shown in the burning speed tests before.[213] Cross-sectional images of the papers (Figure 27) visualise the influence on the internal porosity.

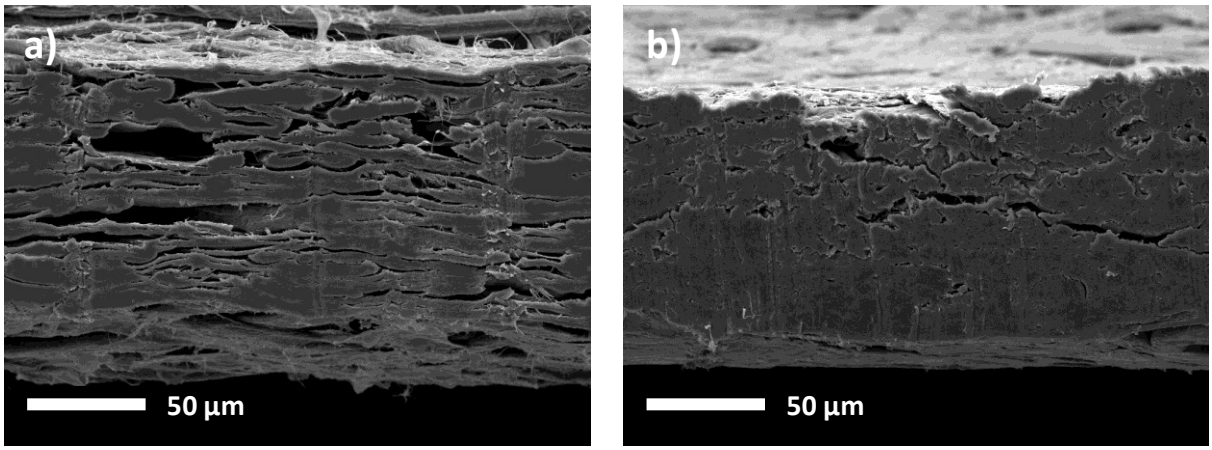

Figure 27: Cross section SEM images of the uncompressed (a) and most compressed (b) 100 g/m^2 NBSK paper.

Comparing these images of the uncompressed and compressed paper samples it is visible, that the calendered paper displays a moulding throughout the whole paper. For the most compressed paper,

only few pores are present whereas for the untreated paper the pores as well as the fibre lumen are visible. However, one has to be careful in treating these results in a quantitively manner as the cutting process in preparing the samples itself can have an influence on the cross-section morphology. All changes in the porosities of the different paper samples with the increasing calendering levels are presented in the following Figure 28.

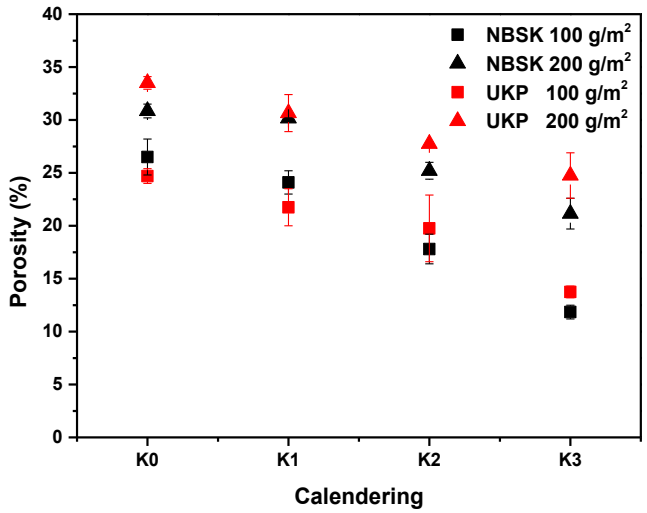

Figure 28: Measured porosities of the NBSK and UKP papers with increasing degree of calendering.

The results for the mercury porosimetry measurements show a constant decrease in porosities for the NBSK and UKP papers with increasing calendering level. For the lower grammages the porosity reduces 14 % for the NBSK and 11 % for the UKP papers whereas for the higher grammages it only reduces 10 % and 8.8 % respectively. It can be seen that for the lower grammages the porosity decreases to a greater extent than for higher grammages and furthermore, the respective decrease in porosity is greater for the NBSK papers than their UKP equivalent. The same roller pressure, in the respective calendering levels, was applied for each grammage. Therefore, less force was exerted, relative to the mass, to papers with higher grammages, which lead to decreasing compressions. The difference between the NBSK papers and the UKP papers results from the properties of the residual lignin. Lignin acts as a more compression-resistant matrix material in wood and in this case very likely minimises the effectiveness of compression.[42] In consideration of the porosimetry determination, the results of the burning speed measurements are revisited in Figure 29.

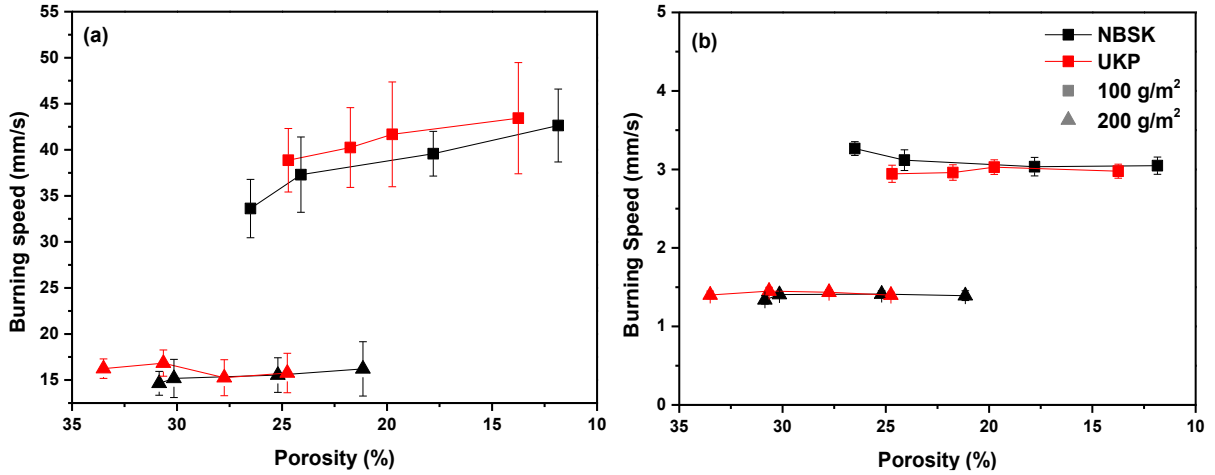

Figure 29: Comparison of the burning speeds of the bleached NBSK (black) and unbleached UKP (red) papers in vertical (a) and horizontal (b) burning direction in relation to the porosity.

When comparing the burning rates in correlation with the actual porosities, it becomes apparent that a comparable statement to the results of chapter 5.1 can be made. Despite the fact that the actual porosities of the two fibre materials do not correspond directly to the calendering levels and slight shifts occur, the influence of the compression on the lower grammage remains evident. The burning speed continues to increase with increasing density and thus decreasing porosity, whereas it does not seem to have any influence on the higher grammages. For this reason, the calendering levels are from now on used as a reference for easier comparison.

5.1.2. Moisture residue

A factor that can influence the burning speed to a greater extent is the moisture present in a material. The energy required to heat up and evaporate the residual moisture within materials can leads to a major slowdown of the burning speed. To increase the temperature of water 4.19 kJ/(kg K) of energy are needed and in addition the evaporation process of water requires another 2257 kJ/kg. Compared to other liquids, water has a much higher specific heat of vaporisation, which is why residual moisture can be an essential factor in influencing the burning speed. The differences of the measured burning speeds, in chapter 4.1, can result from changes of the residual moisture due to calendering. Therefore, the influence of calendering on the residual moisture in the papers was determined using a dry balance. The obtained results are shown in Figure 30.

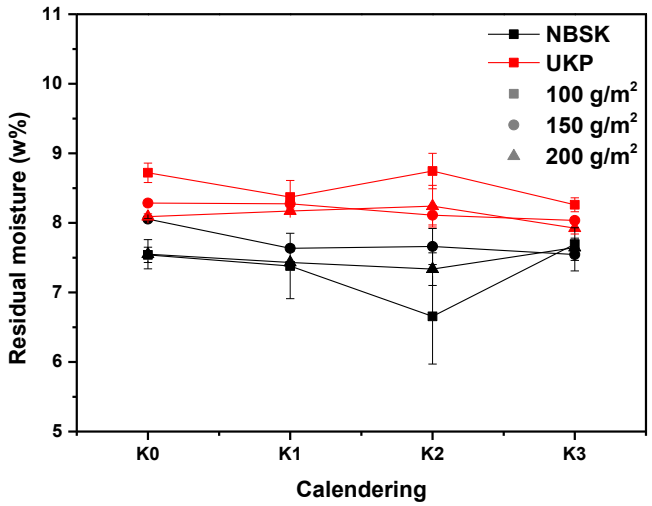

Figure 30: Determined residual moisture for NBSK (black) and UKP (red) within the differently calendered papers.

Measuring the residual moisture, it becomes evident, that the proportions of moisture does not change due to calendering within the papers. In addition, the grammage does not seem to have any influence either. The only difference that can be observed from the measurements is the difference between UKP and NBSK papers of which the UKP papers contain about 1 w% more residual moisture. But since it was previously found that the NBSK papers burn more slowly than the UKP papers, the residual moisture does not seem to contribute to the different burning behaviours in this case and can be neglected in respect to the burning speed measurements.

5.1.3. Cone calorimetry

As mentioned in chapter 4.4 the cone calorimeter is a powerful tool to determine various fire properties of a material. To examine the causes of the increased burning speed with the increasing compression the heat release rate (HRR) and total heat released (THR) was analysed. These information are beneficial, because they can indicate influences of the changed properties on the heat release and hint the origin of the increase in burning speed. In addition, the results can also be used to make an initial assessment on the influences of the residual lignin within the UKP papers. The increased burning speed of the lignin-containing papers, for example, could be explained with the difference of the net heat release of cellulose and lignin as mentioned in chapter 5.1. In addition, the earlier start of the lignin decomposition at around 150 – 300 °C, depending on the structure of the lignin, in comparison to the decomposition temperature of cellulose at 250 – 300 °C can be influential as well.[214] The following Figure 31 shows the course of the HRR for 100 g/m^2 papers of both fibres. For a better comparability of the graphs, they were normalised to the moment of ignition.

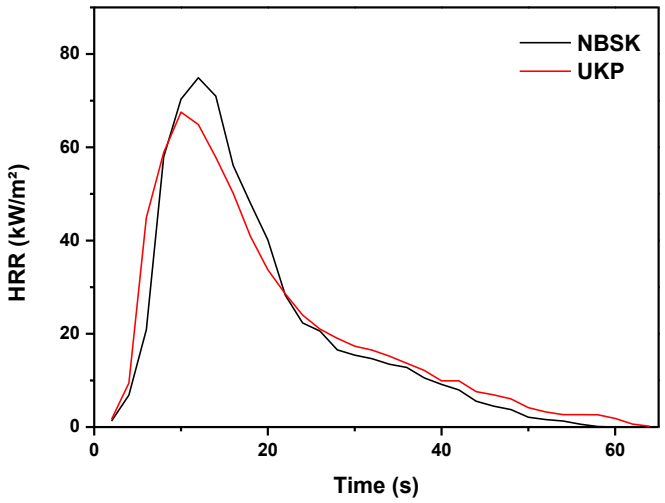

Figure 31: Course of the heat release rates of NBSK (black) and UKP (red).

Comparing the HRR-courses of both fibre types it is evident that they behave relatively similar. Two slight differences stand out in the curves of the NBSK and UKP papers. First the peak of the heat release of the NBSK fibres differs, as it is higher. The peak of heat release occurs when the decomposition process of a material is at its fastest rate and is considered as a parameter, which indicates the maximum flammability and flashover potential and can be correlated to the burning rate. The second difference is a steeper slope at the beginning of the UKP curve for the released heat and an earlier reaching of the maximum. This steeper slope could hint that during the burning more heat is released at an earlier point of time and the earlier maximum therefore indicates a faster progression.

The burning speed test revealed increased values for UKP papers compared to the NBSK equivalents. Thus, the higher burning speed of the UKP fibres cannot origin from a higher peak heat release rate (pHRR). The earlier onset of the lignin decomposition, in which the scission of the various functional groups occur, could therefor cause a steeper increase in HRR for the UKP papers. Evaluating the results of the cone calorimetry measurements regarding the time from the ignition till the pHRR, both the NBSK and the UKP papers showed similar results. On average, the time from ignition to pHRR was 10.2 ± 1.7 s for NBSK and 10.5 ± 1.8 s for UKP, and neither influences of varying grammages nor increasing compression could be observed. Based on these results, this cannot be clearly determined as a possible influencing factor for the differences in the burning rates of NBSK and UKP and will therefore not be considered further.

To further investigate the differences between the NBSK and UKP papers the pHRR of both papers was compared and it was investigated whether the compression or the grammage has an effect on the pHRR. The following Figure 32 shows the results of the corresponding cone calorimeter measurements. In order to create comparability between the different grammages, the data obtained was normalised (*n*) to the samples initial mass.

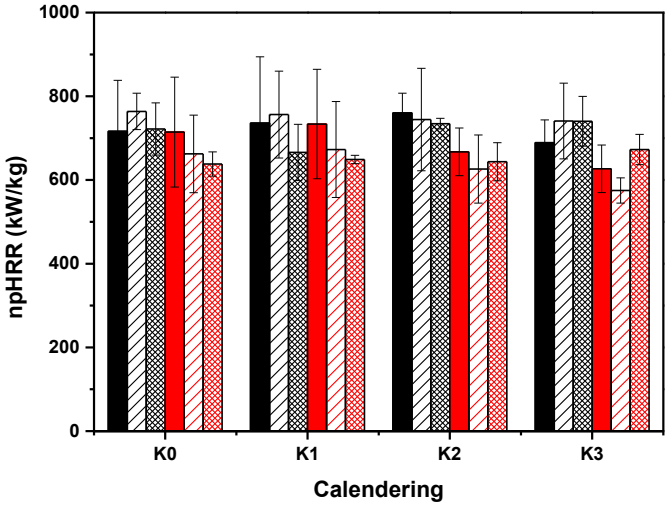

Figure 32: Normalised results of the pHRR measurements for NBSK (black) and UKP (red) papers for the grammages 100 g/m² (full), 150 g/m² (spare) and 200 g/m² (crossed) plotted against the degree of compression.

The results of the npHRR measurements show, that there is no significant influence of the compression on the heat release rate. For each compression level the values of the npHRR stays approximately the same, within the error bars of the multiple determinations. Also, the values normalised to the weight of the increased grammage for each calendering stage show no particular deviations on the heat release. It is evident, that the npHRR of the UKP papers in every variation are lower than the respecting npHRR of the NBSK papers, as already shown in Figure 31 before. This behaviour indicates, that the pHRR does not affect the burning speed in this case and the influence must origin due to other changes within the papers. To complete the analysis, a possible change within the THR was also examined. The THR corresponds to the integral of the HRR and sums up all energy release due to combustion. The results were also normalised (*n*) to the weight for comparison (Figure 33).

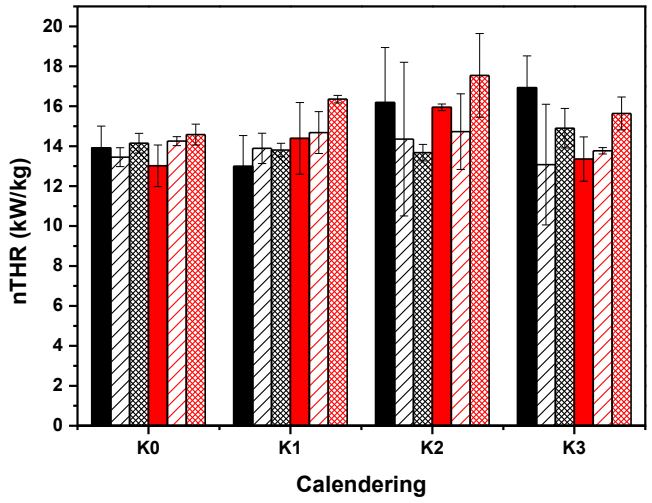

Figure 33: Normalised results of the THR measurements for NBSK (black) and UKP (red) papers for the grammages 100 g/m² (full), 150 g/m² (spare) and 200 g/m² (crossed) plotted against the degree of compression.

Based on the data of the THR, no influences on the changed burning speed can be identified either. Neither the changes in compression nor the grammage indicate a connection. Also, within the error bars no difference between the two paper types can be detected. These results of the pHRR and the THR conclude, that the increase of the burning speed of the papers with the rising compression levels is not correlated to a change in the heat release and therefore must have a different origin.

5.1.4. Thermogravimetric analysis

Corresponding to the heat release of the investigated materials the thermal stability and the charring rate can have another major influence on the burning behaviour. Knowledge about the thermal stability of a material and thus also about the degradation process can provide further indications on the changes of the burning speeds. An important role within the degradation process plays the chemical composition of the degrading materials. Components in a material matrix that degrade earlier can lead to premature breakdown of the other components due to chain propagation and branching reactions and thereby cause an overall faster degradation.[23] The thermal stability and the occurring charring was investigated using thermogravimetric analysis in both O_2 and N_2 atmospheres for the different paper materials. The investigations were conducted under both atmospheres to be able to observe the degradation behaviours under oxidative and inert conditions. As reference, the degradation of a pure Kraft lignin was also investigated to be able to compare the results with the decomposition behaviour of the lignin-containing papers. The results of the thermogravimetric analysis are displayed in the following Figure 34.

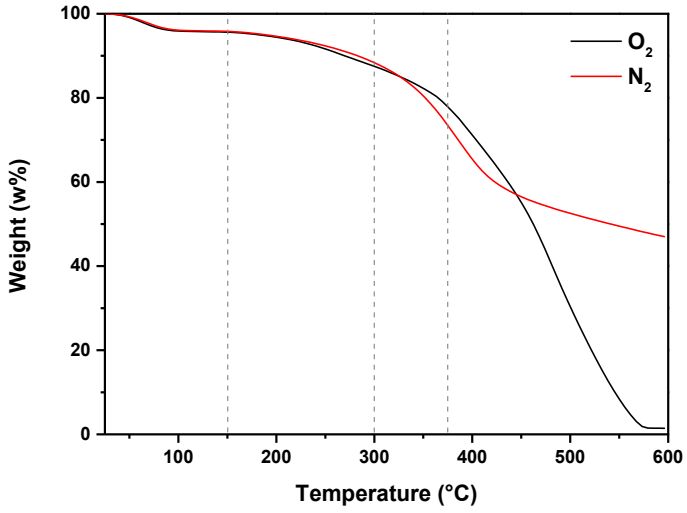

Figure 34: Decomposition behaviour measurements of Kraft lignin in O_2 and N_2 via TGA.

Using TGA it can be seen that the degradation of the Kraft lignin starts at around 200 °C after the initial evaporation of the residual water at around 100 °C. From literature it is known that the thermal degradation of lignin can be divided into three steps: 1) cleavage of the α- and β- aryl- alkyl ether bonds

at 150 – 300 °C; 2) splitting of the aliphatic side chains from the aromatic ring at about 300 °C; 3) the carbon-carbon bonds within the structural units of lignin are cleaved at 370 – 400 °C. Above the temperature of 400 °C the degradation or condensation of aromatic rings depending on the atmosphere takes place.[214] These steps can be identified as well in the results of the Kraft lignin measurements in Figure 34. With these results in mind, the thermal degradation of the NBSK and UKP will be considered in the following (Figure 35).

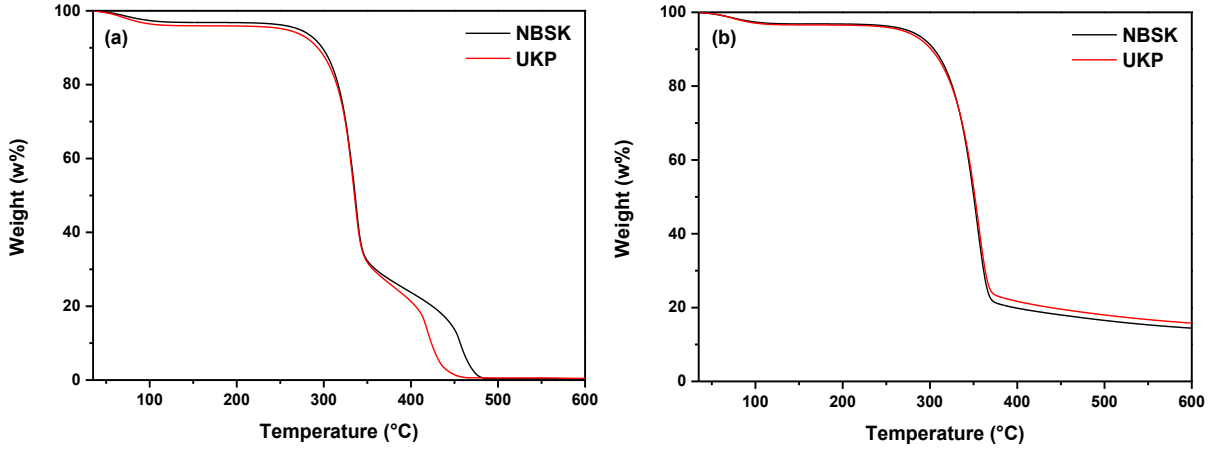

Figure 35: Determination of the degradation behaviour for the NBSK (black) and UKP (red) papers in ambient (a) and N_2 (b) atmosphere using TGA.

In accordance with the determinations of the residual moisture measurements, a greater loss of mass of 1 w% was measured in the UKP papers in the range around 100 °C when water evaporates. Under ambient atmosphere (Figure 35a) a slight influence of the lignin on the degradation behaviour is visible at around 250 °C, which is less pronounced in N_2 atmosphere (Figure 35b). Compared to the NBSK papers, the loss of mass starts presumably earlier due to the cleavage of the ether bond within the lignin as mentioned before. Both papers reach their maximum mass loss at around 327 °C (ambient atmosphere) and 344 °C (N_2) respectively. Whereas in N_2 atmosphere the residue of the lignin-containing papers is higher in comparison to the bleached pulp, under oxidative conditions it can be observed that the residues decompose earlier. The char residue of the UKP papers continuously decreases faster than the NBSK char. This is in the temperature range around 400 °C at which the carbon-carbon bonds within the structural units of lignin are split. It indicates that the resulting char or residue from the degradation of the UKP papers is lesser thermally stable then the once from the NBSK papers. As pointed out by NYDEN ET AL., fire resistant qualities are in a strong correlation with the arising char residue. Char is always formed at the expense of volatile fuel and furthermore the surface char tends to insulate the unburned material from the heat generated during the combustion.[215] With a lesser stable char, as seen in Figure 35a for the UKP papers, and therefore a reduced fire resistance, this can give a first indication why the burning speeds of NBSK and UKP differ slightly.

In addition, the influence of the compressions on the degradation of the paper materials can be observed by means of the TGA. The results for a 100 g/m^2 UKP paper are shown in the Figure 36 below.

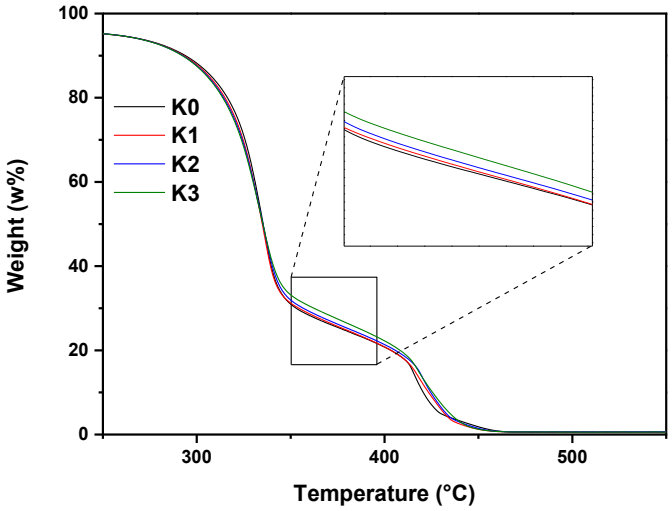

Figure 36: Analysis of the influence of calendering on the degradation behaviour in ambient atmosphere using TGA.

The differences caused by the calendering process are minimal but show the fundamental influence of material compression on the thermal degradation. The higher compression and thus reduced porosity minimises the accessibility of oxygen into the material, resulting in incomplete combustions, which lead to an increase in char formation.[204] Due to the increased temporary char residue, there is the possibility of better heat conduction due to remaining solid material in comparison to air, which would benefit a faster rate of burning. It is important to note, that these deviations are relatively small and can probably be classified as negligible with regard to the issues discussed here.

5.1.5. Crystallinity

In order to further investigate the decomposition behaviour, the influence of the calendering process on the crystallinity of the papers was examined. In the work of KIM ET AL. it was shown, that the initial temperature of thermal decomposition shifted to higher temperatures with increasing crystallite size, crystallinity index and degree of polymerization.[216] It was stated that the initial oxidative degradation takes place in in the amorphous regions of cellulose[217] and the decomposition occurs at the crystalline-amorphous boundaries.[218] The following Figure 37 shows the amorphous to crystallinity ratio determined by solid-state NMR of the calendered samples.

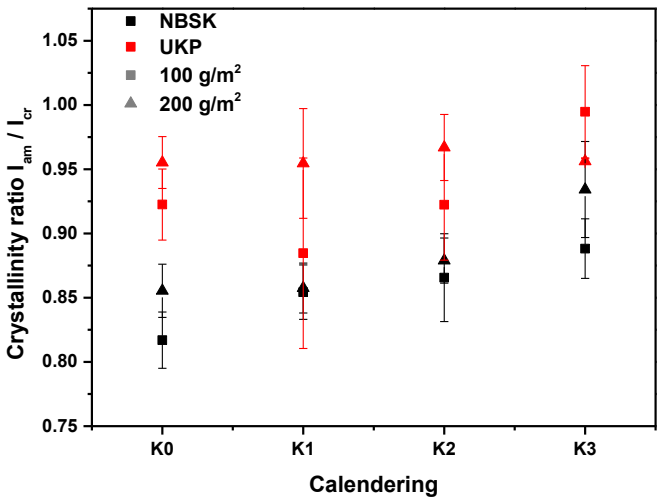

Figure 37: Results of the solid-state NMR analysis to determine the changes of the paper matrixes crystallinity caused by calendering.

The results of the solid-state NMR measurements indicate an influence of the calendering process as well as other factors on the crystallinity index. Comparing the morphology of both paper types, it is evident that the UKP papers have a higher amorphous content. On the one hand, the higher amorphous content may be due to the different pulping process of the corresponding fibres. Previous work has shown that during pulping, small cellulose crystallites as well as certain amounts of disordered cellulose are extracted from the material, which would cause in an increase in crystallinity.[67] On the other hand, the bleaching process also affects to a larger extend the amorphous areas of the pulp. The bleaching chemicals break down the amorphous lignin and remove it from the fibres, but the amorphous areas of the cellulose can also be damaged by oxidative degradation processes and removed during the subsequent extraction.[219] The removal of these amorphous parts of the cellulose would thus lead to an increase in the crystalline content, which would be the case for the NBSK papers. Another factor that could influence the crystallinity is the preparation of the laboratory papers. After the production of the sheets, a drying step is carried out, in which the papers are dried under vacuum and at elevated temperatures (93 °C). As all papers are dried in the same device, thicker sample sizes resulting from higher grammages can also affect the crystallinity during the drying process due to higher compression. In addition to these possible influences on the ratio between amorphous and crystalline regions before the calendering treatment, an influence of the calendering process can also be clearly recognised from the results shown in Figure 37. In all samples, the amorphous content in the papers increases with the degree of compression. It can be assumed that the crystalline areas within the samples are ground up by the pressure applied to the paper samples. This increased proportion of amorphous areas can subsequently affect the thermal decomposition temperature and thereby benefits the increase in burning speed, as explained in the previous mentioned investigations.

5.1.6. Thermal conductivity

Apart from the changes in porosity and crystallinity that have already been described, it is necessary to investigate another influencing factor that could be related to the increased burning speed of compressed papers: the thermal conductivity. The thermal conductivity indicates how well a material conducts heat and can be correlated with the increased pre-treatment or pre-drying of the papers, which would benefit a faster burning speed. To determine the thermal conductivity λ, the thermal diffusivity α was measured using Lock-in thermography and calculated using the following equation.

$$\lambda = \alpha \cdot c_p \cdot \rho \qquad \text{(Eq. 5.2)}$$

with c_p = heat capacity

ρ = density

The results for the measured thermal diffusivity are shown in the following Figure 38.

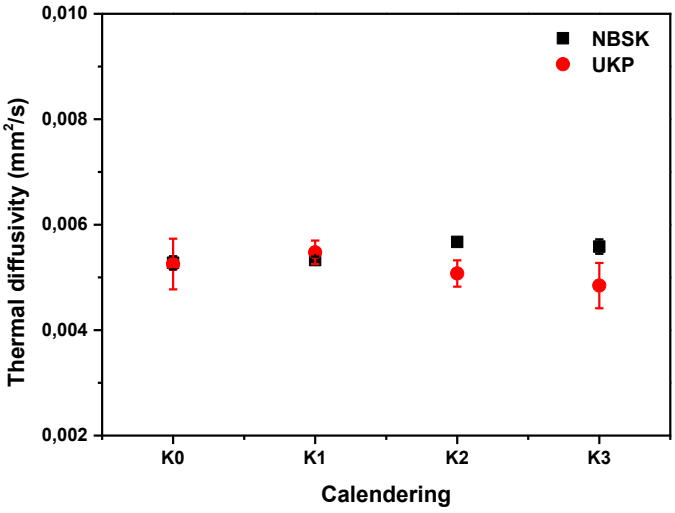

Figure 38: Results for the thermal diffusivity via Lock-in thermography for 100 g/m² NBSK (black) and UKP (red) papers.

The results of the Lock-in thermography measurements show that the process of calendering has no major impact on the thermal diffusivity. With increasing calendering level, the values barely differ from each other. In addition, within the margin of the errors no bigger difference between the NBSK and UKP papers can be observed.

For the heat capacity measurements, the sapphire method using DSC was selected. The heat capacities for the calendering levels K0 and K3 were measured and used to determine the heat capacities for the remaining calendering levels with the correlation established by HATAKEYAMA ET AL.[220] Within this work the linear dependency of the heat capacities on crystallinity was shown and expressed in equation 5.3.

$$c_p = X_c \cdot c_{p_c} + (1 - X_c) \cdot c_{p_a} \qquad \text{(Eq. 5.3)}$$

with X_c = fraction of crystalline cellulose

c_{pc}/c_{pa} = c_p of complete crystalline/amorphous cellulose

Using this relation to extrapolate the heat capacity, every crystallinity composition can be calculated (Figure 39).

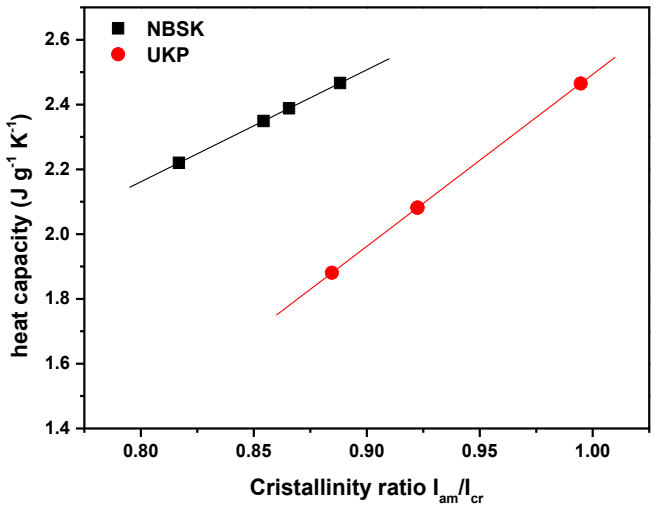

Figure 39: Extrapolation of the heat capacities for the different calendering levels of NBSK (black) and UKP (red) papers.

The calculated values for the different heat capacities of the paper samples as well as the density values from the mercury porosimetry measurements and the thermal diffusivity data are summarised in the Table 2 below.

Table 2: Results for the determinations of thermal diffusivity, density and heat capacity.

NBSK	Thermal diffusivity [cm^2/s]	Density [g/cm^3]	Heat capacity [J/g*K]	UKP	Thermal diffusivity [cm^2/s]	Density [g/cm^3]	Heat capacity [J/g*K]
K0	5,28E-03	0,79	2,22	**K0**	5,25E-03	0,66	2,08
K1	5,33E-03	0,90	2,35	**K1**	5,48E-03	0,78	1,88
K2	5,67E-03	1,11	2,39	**K2**	5,07E-03	0,97	2,08
K3	5,58E-03	1,40	2,47	**K3**	4,84E-03	1,07	2,47

Inserting the calculated heat capacities, the density from the porosity determinations and the measured thermal diffusivity in equation 5.2, the following values for λ are obtained (Figure 40).

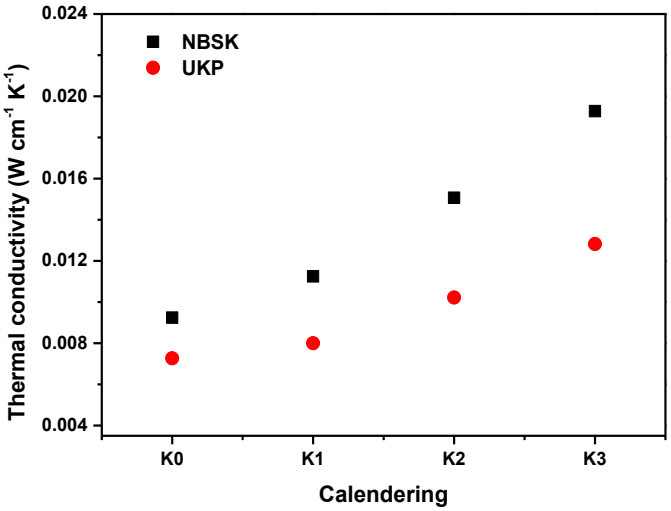

Figure 40: Calculated values for the thermal conductivities of the 100 g/m^2 NBSK (black) and UKP (red) paper samples.

From the obtained thermal conductivity data, it can be seen that with increasing calendering level the thermal conductivity increases. In addition, the unpressed NBSK papers have a higher thermal conductivity than the UKP papers. This higher thermal conductivity can be attributed to the different crystallinities of the papers. In literature it is reported that higher crystallinity of base fibres leads to higher thermal conductivity of paper sheets.[221] However, since the thermal diffusivity only changes slightly with increasing compression, as shown in Figure 38, and the crystallinity of the samples decreases with increasing compression, the increase in density may be attributed to the increase in thermal conductivity. Note, this increase in thermal conductivity also correlates with the increase in burning speed as shown in the following Figure 41.

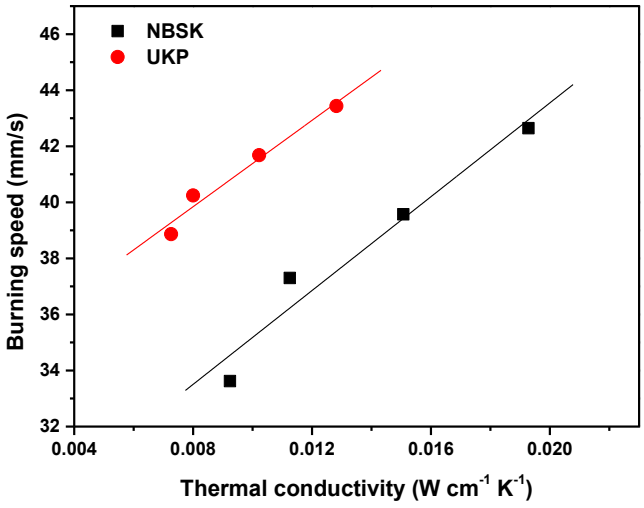

Figure 41: Correlation between the increase in thermal conductivity with the increasing burning speed of 100 g/m^2 paper due to calendering.

Correlating the thermal conductivity to the measured burning speeds of the paper samples a linear progression can be detected. Based on these results, the thermal conductivity can be confirmed as an influencing factor on the burning speed.

5.2. Discussion & Conclusion

The burning behaviour of papers made of bleached and unbleached pulp was investigated to consider possible influences of remaining lignin within the pulp. Regarding the flammability, the burning speed in horizontal and vertical burning direction was selected as a comparative factor and successfully evaluated with a computer-based method. It was found that the burning rate decreases with increasing grammage and that the unbleached UKP papers burn faster than the bleached NBSK papers. In addition, an increase in the burning rate in the vertical burning direction with increasing compression ratio was observed for the lower grammages. This effect was much less pronounced in the horizontal direction. Since this increase in the burning speed in the vertical burning direction is different to previous research and results, in which an increase in density resulted in a decrease in the burning rate, the properties of the compressed papers were then examined. First, the degree of compression was determined in order to determine the effectiveness of the calendering process. It was shown that the porosity of the papers decreased as the degree of calendering increased. The first differences were detected, as the calendering process had different effects on the two paper types. Due to the residual lignin, which may have a stiffening effect on the fibre composite, the resulting compression of the UKP papers was lower compared to the NBSK papers, although identical forces were applied. In addition, it was found that the mass of the papers had an influence on the effectiveness of the individual calendering stages, as smaller changes in porosity were observed with increasing mass at the same compression force. When correlating the determined burning speeds with the effective porosities, the increase in burning rate with increasing compression was once again confirmed. To exclude possible influences of moisture within the paper, the effect of calendering on the residual moisture in the papers was investigated. It was found that the residual moisture did not change with increasing calendering and that the UKP papers had about 1 w% more residual moisture than the NBSK papers. However, since no influence of the calendering could be determined and the UKP papers burned faster than the NBSK papers in the burning tests, the moisture could be excluded as an influencing factor. For further investigations into the fire behaviour of the papers, cone calorimeter measurements were carried out. The aim was to investigate the influence of the heat release due to the different composition of the pulps and a possible influence of the compression on this. It could be shown that neither the calendering nor the influence of the grammage had an effect on the heat release rate and the total heat released. In addition, due to the different decomposition of the cellulose and the lignin, a higher peak of the heat release rate was determined for the NBSK

papers. As the lignin decomposes over a wider temperature range, the peak HRR was lower for the UKP papers, which also contradicts the previously determined burning rates. Based on these results, a different behaviour in the release of heat during combustion could also be excluded. To further investigate the differences in thermal stability of the two pulps, thermogravimetric analyses were carried out. In this context, a slightly earlier onset of decomposition of the lignin-containing fibres was observed. The greater difference, however, lies in the enhanced oxidative degradation of these lignin-containing residues at temperatures above approximately 350 °C. It can be seen that the residue of the UKP papers decomposes faster than that of the NBSK papers. In addition, an investigation of the different degrees of compression using TGA revealed a minimal increase in residue with increasing degree of calendering, which can be attributed to a lower accessibility of oxygen and thus more incomplete combustion. Due to the higher proportion of residues, a better thermal conductivity of the combustion heat is assumed, which favours faster combustion, which was observed in the burning speed test with increasing compression. To further investigate the decomposition behaviour of the papers, the influence of calendering on crystallinity was studied. Since the thermal conductivity correlates with the crystallinity and thus contributes to the decomposition process, this parameter was investigated by means of solid-state NMR. A decrease in crystallinity due to compression within both fibre types was observed. In addition, higher proportions of amorphous regions were found within the UKP papers, which can be attributed to the amorphous lignin on the one hand and to the pulping on the other. The bleaching of the fibres causes the amorphous lignin to dissolve out, whereby amorphous parts of the cellulose are partially damaged and removed, which leads to an increase in crystalline domains in the fibres. From this, it can be assumed that with increasing proportions of amorphous regions in the cellulose, earlier decomposition and thus faster burning behaviour occurs. However, since the thermal conductivity correlates with the crystallinity and this typically decreases with increasing amorphous proportions, the thermal conductivity was also investigated. By determining the thermal diffusivity via Lock-in thermography and the heat capacity via DSC, the thermal conductivity of the paper samples was determined. A correlation of the increase in thermal conductivity with the burning speed was shown. It was found that the decisive factor for the increase in thermal conductivity is the increase in density with the calendering stages, whereas the thermal diffusivity and the heat capacity changes only slightly due to the compression. However, this effect only seems to be decisive for thin samples, since for the samples with higher grammage only a minimal influence of the calendering is recognisable. By knowing these influential factors on the burning behaviour of paper, a targeted use and optimisation of the effectiveness of flame retardants is now possible.

6. Flame retardants on/in paper

The most important results of the investigation on the influence of the flame retardants (FR) on the degradation behaviour of the papers are presented and critically discussed in the next chapter. First, the results of the coating procedure and the determination of the applied phosphorous content are presented (Chapter 6.1). The effects of the flame retardants on the decomposition of the two paper types are then investigated using cone calorimetry (Chapter 6.3). To further determine the changes of the decomposition process due to the application of the flame retardants and the possible influence of residual lignin, a coupled method of TGA, MS and FTIR is used (Chapter 6.4.2). Furthermore, the influence of the flame retardants on the mechanical properties of the papers was investigated by means of tensile tests (Chapter 6.5). A summary of these results can be found at the end of this chapter.

6.1. Application of the flame retardants

For the investigation of the modes of action and influences of three different model flame retardants, the results of the previous investigations in chapter 5 of the slowest burning paper sheets were considered. Since the uncalendered papers of each grammage showed the slowest burning speeds, papers with a grammage of 100 g/m^2 were used for further studies, as they can be impregnated with the flame retardants more homogeneously in comparison to higher grammages, although several impregnation steps are necessary to achieve similarly uniform results. To determine the efficiency of the flame retardants on the paper samples, the amount of the applied phosphorous was chosen as reference. The phosphorous content in the modified starch (mod. ST) and ammonium phytate (AmPhy) flame retardant as well as in the NBSK and UKP paper substrates were analysed by means of ICP-AES (Table 3). The phosphorous content of ammonium polyphosphate (APP) was provided by *Clariant Plastics & Coatings GmbH* (Frankfurt am Main, Germany). Theoretical values were calculated based on the structure of the flame retardants.

Table 3: Theoretical and measured phosphorous content within the papers and flame retardants.

p-content	Theo. [w%]	Measured [w%]
NBSK	0	0
UKP	0	0
APP	31.9	28.88*
mod ST	10.9	12.38
AmPhy	21.5	21.1

** The phosphor content for APP was provided by Clariant*

As expected, the results of the ICP-AES measurements show that both paper grades do not contain any traces of phosphorus. With a phosphorus content of 21.1 wt.%, the analysis of the AmPhy shows well comparable values to the theoretically calculated phosphorus content. The results of the modified starch and ammonium polyphosphate differ slightly. For the starch modified with a carbamate and phosphate group, an average substitution degree of 1 was expected in each case. However, due to the slightly increased phosphorus content, it can be assumed that the degree of substitution (DS) of the phosphate groups is greater than 1. The given phosphorous content of the APP has the largest deviations from the theoretical expected values. As the APP solution was acquired as a premixed dispersion, the deviation in phosphorous content may be attributed to the fluctuations of the production batches. These measured values were used for the subsequent determination of the effectiveness of the flame retardant.

To investigate the effectiveness of the flame retardants, preliminary tests were carried out with different concentrations in the coating solution and three concentrations were applied. The flame retardants are applied to the 100 g/m^2 papers pre-modified with 1 w% wet strength agent, using the size press as described in chapter 8.1.3. For each flame retardant the minimal amount required to achieve self-extinguishing properties on both paper types was determined. To be able to detect differences in the mode of actions of the flame retardants two other application quantities were chosen. Therefore, the applied amounts of flame retardant were cut and increased by 20 % depending on the previous determined minimum quantity necessary to generate a flame retardant property. The aim was, that the lower applied amounts did not achieve a flame retardant effect and the higher applied amounts describes an exceeding of the necessary amount of flame retardant. The applied amounts of flame retardant on the papers are determined via the “wet-pickup”. With these results, in combination with the results of the ICP-AES measurements, the respective phosphorous contents on the papers are determined (Table 4).

Table 4: Amount of applied flame retardants and the resulting w% of phosphorous in the paper samples.

Flame retardant assignments		NBSK		UKP	
		Applied FR [w%]	P-content [w%]	Applied FR [w%]	P-content [w%]
APP	Low	4,99 ± 0,15	1,44	4,88 ± 0,06	1,41
	middle	6,62 ± 0,05	1,91	6,39 ± 0,05	1,85
	high	7,93 ± 0,05	2,29	7,77 ± 0,13	2,24
mod. Starch	low	11,58 ± 0,28	1,43	11,47 ± 0,31	1,42
	middle	15,5 ± 0,6	1,92	14,76 ± 0,5	1,83
	high	18,11 ± 0,52	2,24	17,49 ± 0,32	2,17
AmPhy	low	7,38 ± 0,05	1,56	7,72 ± 0,05	1,63
	middle	9,45 ± 0,05	1,99	9,02 ± 0,07	1,90
	high	11,94 ± 0,11	2,52	11,62 ± 0,07	2,45

In the preliminary tests, to determine the required quantities of flame retardant, the burning rates for the non-self-extinguishing papers were also determined. This gave a first impression of the extent to which increasing the flame retardant content influences the burning behaviour. The following results were observed (Figure 42).

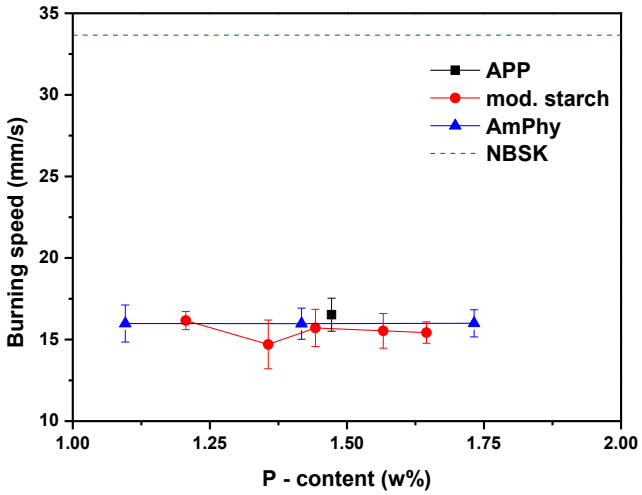

Figure 42: Influences of the flame retardants APP (black), mod. starch (red) and AmPhy (blue) on the burning speed in vertical direction of 100 g/m² NBSK paper before self-extinguishing properties compared to the untreated NBSK paper (green).

When analysing the burning speed in the vertical direction of the nonself-extinguishing coated papers, it becomes evident that even though the flames continue burning, the burning speed is reduced by the use of flame retardants. Thereby the burning speed of the NBSK papers is reduced from 33.6 mm/s (Figure 22a) for untreated papers to around 16 mm/s with flame retardants. It is noticeable, that within

the area of investigation the increasing proportions of phosphor seem to have no influence on further reducing the burning speed. It seems, that the use of the flame retardants decreases the burning speed and if a critical concentration of flame retardant is reached, the progression of combustion is inhibited. In addition, all three flame retardants decrease the burning speed to the same extent, which can be attributed to the similar mode of action, as all three flame retardants are phosphor-based flame retardants and initiate the protection mechanism via dehydration reactions of the phosphates with the OH-groups of the cellulose and by diluting the gas phase with the release of ammonia and water.

6.2. Structural characterisation via SEM

To display the effect of the flame retardants on the structure of burned paper substrates, SEM images are taken prior and after the burning experiment. Since the NBSK and UKP papers did not show any visual differences with respect to the sheet morphology, the untreated and flame retardant treated NBSK papers are compared in their condition before and after burning. The following Figure 43 shows the images of the untreated NBSK paper.

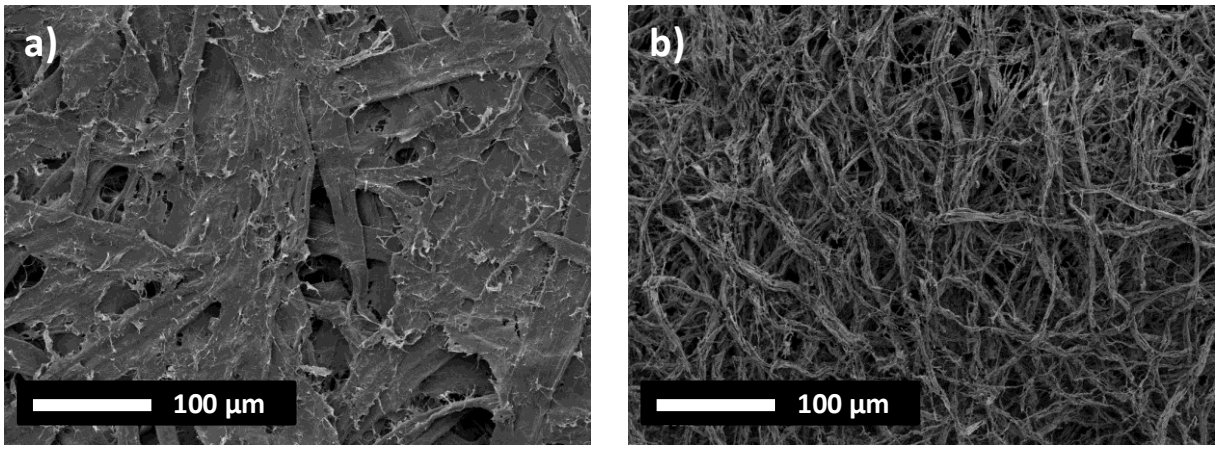

Figure 43: SEM images of the untreated NBSK paper before (a) and after (b) burning.

Before burning the NBSK paper, both the fibres and the fibrils are clearly visible in the SEM image (a). The ash remaining after incineration in (b) shows that only a kind of skeletal framework of the previous fibres remains, which have no stability and only a fraction of the original mass. Comparing this result with the following images in Figure 44, where the flame retardant APP has been applied, a significant difference in the influence of the flame retardant can be seen.

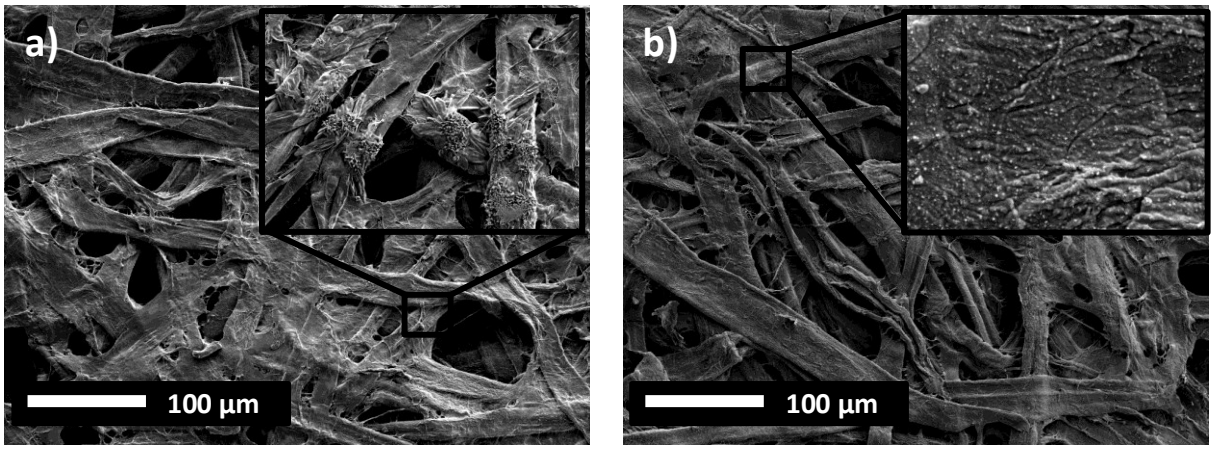

Figure 44: SEM images of the APP treated NBSK paper before (a) and after (b) burning.

In the SEM image of the APP treated NBSK paper, both the fibres and a large part of the fibrils can still be recognised. It is noticeable that crystalline structures have formed on some of the fibres, which is due to the crystallisation of the APP during the drying of the aqueous solution. Looking at the image after burning, it is noticeable that the structure of the treated fibres has been completely preserved in contrast to the untreated paper. In addition, small white dots can be seen on the surface of the fibres, which result from the combustion of the flame retardant, but which cannot be explained further in this context. The preservation of the fibre structure after the incineration can be explained by the increasing charring behaviour due to the influence of the flame retardant. As the flame retardant promotes incomplete combustion, which leads to increased charring and the formation of a more thermally stable char, the structure of the paper is preserved. Looking at the cross section of the paper, another interesting effect can be observed. The cross section of the APP treated NBSK paper before and after the incineration is displayed in Figure 45.

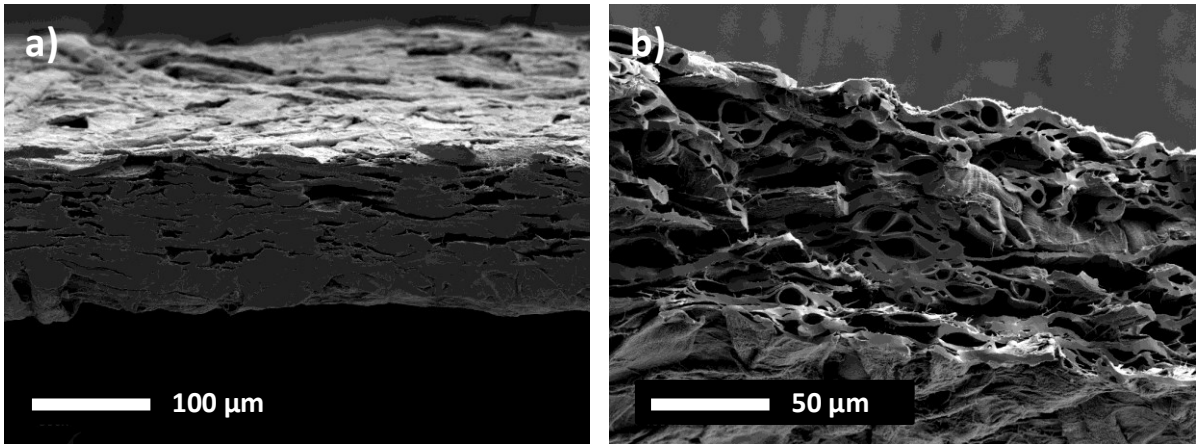

Figure 45: SEM images of the cross section of APP treated NBSK paper before (a) and after (b) burning.

The cross section of the treated NBSK paper before the incineration shows no differences to the cross section of the untreated NBSK paper displayed in Figure 27. After combustion, two interesting points can be seen with regard to the influence of the flame retardant. Compared to image (a), it can be seen

in the cross-sectional image (b) from Figure 45 that the lumen of the fibres has opened. This widening of the lumen can be explained by a combination of gases released and the reorientation of the cellulose chains during the combustion. BACON R. AND TANG M. described this behaviour of the reorientation of cellulose chains during carbonization in their studies, which would support this statement.[222] This increases the diameter of the fibres and the resulting free space further assists the heat barrier properties generated by the flame retardant. Furthermore, clean fractures can be seen on the fibres, which were created during the preparation of the cross-section. This allows conclusions to be drawn about the mechanical properties of the fibres after burning under the influence of the flame retardant. Normally, the cellulose fibres are flexible, and the preparation of cross-section causes slight pinching of the material as shown in image (a), but in image (b) the remains after the burning display a more ceramic behaviour. Therefore, some of the mechanical stability of the paper is retained, which would give great advantage in the various possible areas of application.

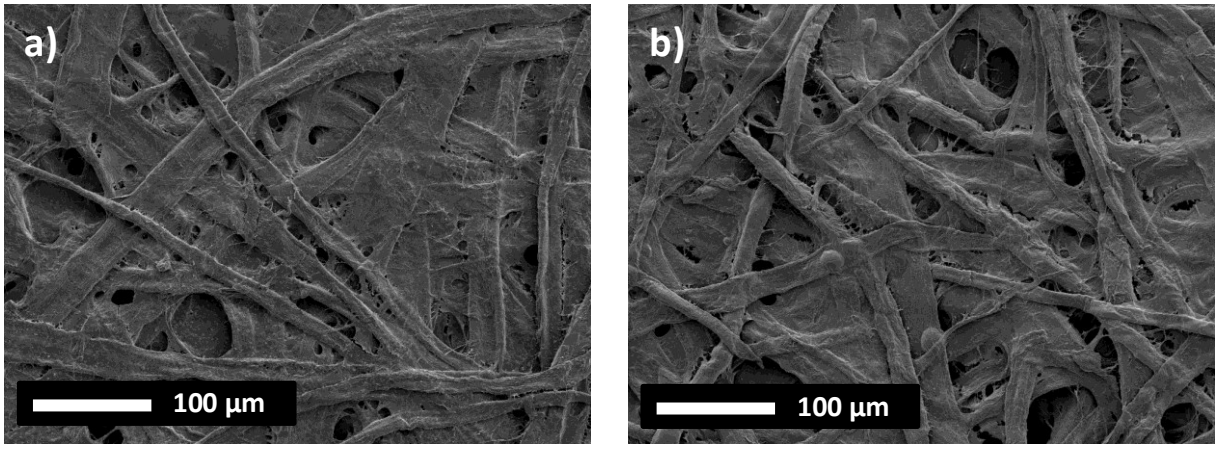

Figure 46: SEM images of the NBSK papers treated with mod. starch before (a) and after (b) burning.

Looking at the SEM images of the mod. starch before and after combustion in Figure 46, it is possible to see that the fibrils stick together due to the use of the mod. starch. In addition, the surface of the paper appears much less porous and enclosed. This behaviour of starch is well known, as it can be used as a surface sizing agent. Comparable to the results of APP, the structure remains intact even after burning the paper. In addition, bubbles can be seen on the fibres. These can result from the fact that more gases are initially released during the combustion of the mod starch, which leads to localised swelling. This effect cannot be seen in the images of the cross-section, but same as for the APP flame retardant, the swelling of the lumens and the clean fractures can be observed as well (Figure 47).

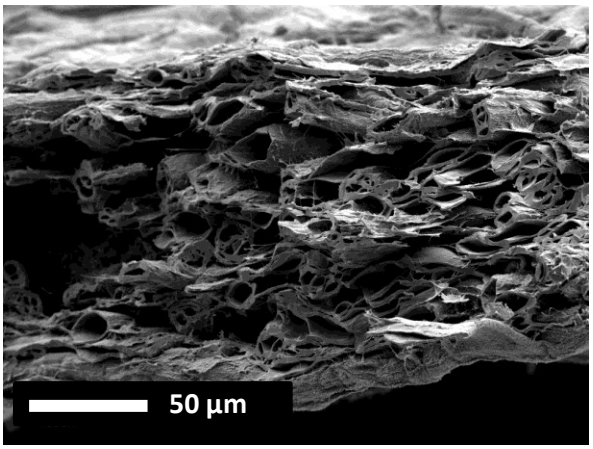

Figure 47: Cross-section SEM image of the burned NBSK paper treated with mod. starch.

In the case of the AmPhy flame retardant, the same influences of the flame retardant on the behaviour during burning as before could be observed. There were no special characteristics that can be emphasised.

6.3. Cone calorimetry

To determine the efficiency of ammonium polyphosphate (APP), the modified starch (mod. ST.) and ammonium phytate (AmPhy) flame retardants, cone calorimetry measurements were conducted. By comparing the values of the pHRR, THR and total smoke release (TSR) in relation to the amount of the applied phosphor, the efficiency of each flame retardant can be studied. In the following Figure 48 the measured results for the HRR of all flame retardants are displayed. Prior to the measurements, an assumption was made that, due to the adjusted amounts of flame retardants and the corresponding proportional gradations as well as the results of the preliminary test displayed in Figure 42 and all three flame retardants are phosphorus-based, they could affect the HRR in a similar manner.

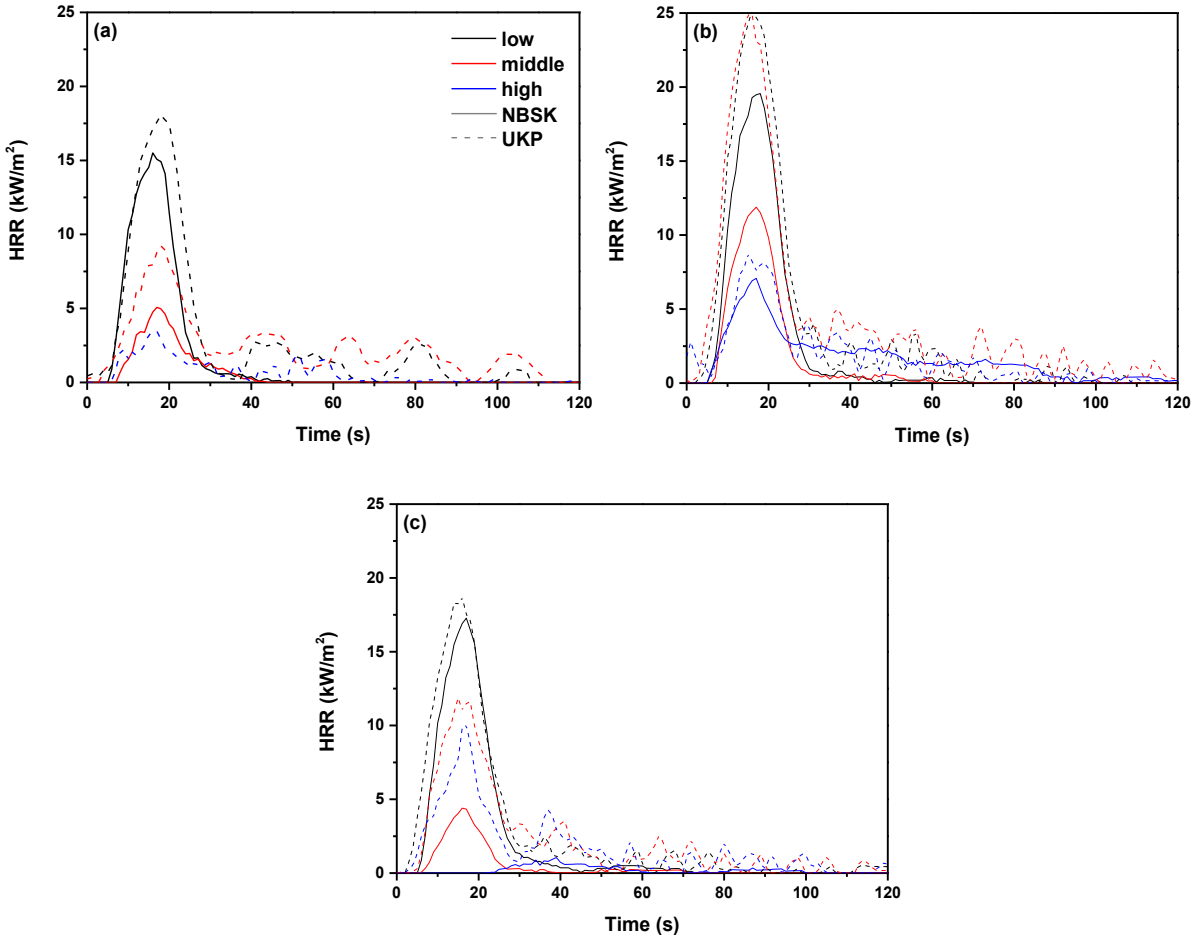

Figure 48: HRR measurements by cone calorimetry of coated NBSK (full) and UKP (dashed) papers with (a) APP, (b) mod. starch and (c) AmPhy.

Observing the HRR curves of the three flame retardants in Figure 48, it can be seen that with increasing amount of applied flame retardant the HRR reduces. It should be noted, that the HRR values for the most highly coated papers are in some cases as low that they can no longer be detected with cone calorimetry. A further comparison of the results shows that the applied amounts of flame retardants APP and AmPhy influence the HRR of both paper types comparably. The mod. starch, on the other hand, shows higher HRR values in all three concentrations, although the amounts of applied flame retardant achieve the same level of protection as the other flame retardants. Furthermore, a difference between the measurements of coated NBSK and UKP papers is visible. The lignin containing UKP papers display a recurring heat release, while the NBSK papers show only to have one peak. From these differing behaviours, it can be seen that the burning behaviour and the heat released by burning are not only influenced by the onset of the endothermic dehydration reaction of the phosphate groups in the flame retardants. Other factors such as the release of inert gases and the diffusion barrier created by charring also interfere with the combustion. To further demonstrate this difference between the introduced proportions of phosphate groups and the resulting flame retardant properties, the pHRR was selected as a reference, as it reflects the maximum flammability and

flashover potential and thus represents the driving force of combustion. These pHRR results in Figure 49 are normalised (*n*) to the weight and plotted against the phosphorous content of the samples for comparison.

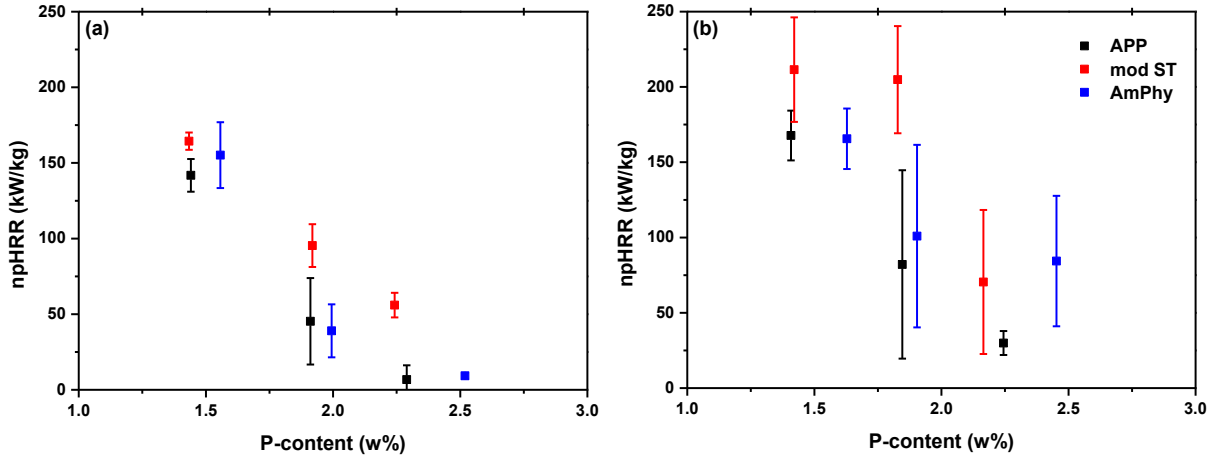

Figure 49: pHRR measured and normalised to the weight of the flame retardants APP (black), mod starch (red) and AmPhy (blue) on NBSK (a) and UKP (b) papers plotted against the applied phosphorous content.

Comparing the results of the cone calorimeter measurements with the measurements on untreated papers it becomes evident that the use of flame retardants drastically reduces the HRR. Even when using an amount of flame retardant insufficient to cause a self-extinguishing effect, the pHRR decreases from about 700 kW/kg for untreated paper (Figure 32) to 200 kW/kg. With increasing phosphor content, the pHRR continues to decrease for all flame retardants until the HRR is almost no longer measurable. Considering the effectivity of the flame retardants, APP reaches the lowest pHRR values with least amount of phosphorous content followed by AmPhy. Based on the measured data, an almost linear correlation between increasing phosphorous content and decreasing pHRR can be extrapolated. With these results from Figure 49 it is shown that not only the amount of phosphate groups introduced influences the burning behaviour. It can be concluded that other factors, such as the general chemical composition of the flame retardant or the amount of inert gases released or the charring behaviour resulting from the flame retardants, must also be taken into account.

Further, Figure 48 and Figure 49 display, that the coated UKP papers in comparison to the NBSK papers have higher pHRR values. In contrast to the cone calorimeter measurements of the calendered papers, where the NBSK papers showed a higher pHRR than the UKP papers (chapter 5.1.3). The flame retardant effect seems to be less pronounced with the UKP papers. In addition, the measurements of the UKP papers in Figure 48 show a repetitive heat release in the HRR curves. These differences can be attributed to the remaining lignin on the fibres of the UKP papers. As the mode of action of the phosphorous containing flame retardants are attributed to the endothermic dehydration reaction of the phosphate groups with the hydroxyl groups of the cellulose, it can be assumed that the remaining lignin may interfere with this mechanism. In previous works, the average hydroxyl content for Kraft

lignin was determined to be 5,94 mmol/g, while the theoretical value for cellulose is up to 18,5 mmol/g.[223] Due to the lower number of accessible hydroxyl groups, as the remaining lignin encases the cellulose fibres, the efficiency of the protective mechanism of the flame retardants for the UKP papers is lower. The latter results in a higher pHRR. The reappearing release of heat in the UKP papers can thus be attributed to this reduced protection. It is possible that due to the reduced accessibility, only less char forms, resulting in an insufficient heat barrier. Continued exposure to heat could cause the char barrier to break thus exposing unprotected material and causing further decomposition, which could result in additional heat release. The process of the char barrier formation can be recognised in the HRR curves and is shown in Figure 50 using AmPhy as an example for NBSK (Figure 50a) and UKP (Figure 50b).

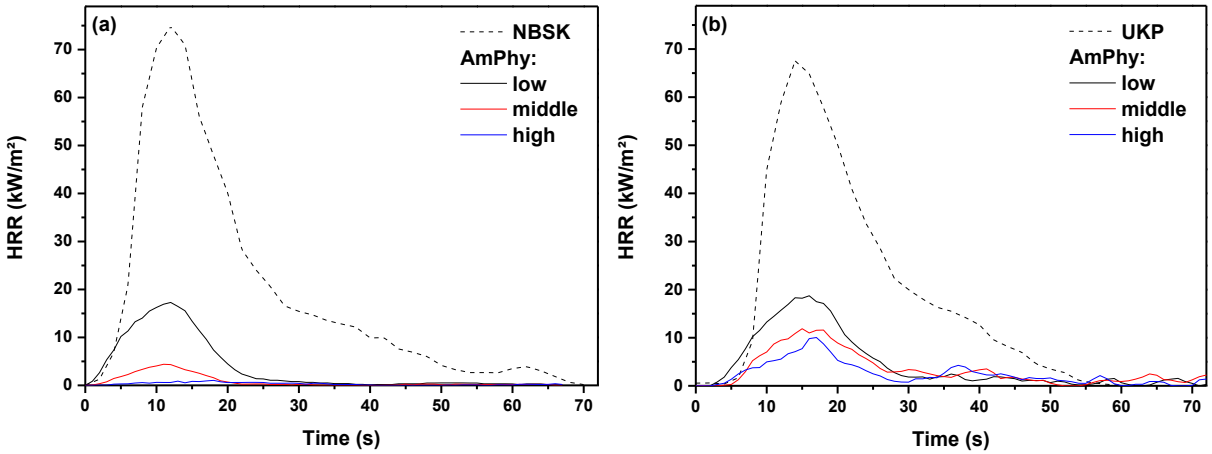

Figure 50: HRR curves of untreated and with AmPhy coated NBSK (a) and UKP (b) papers.

Previous studies displayed the influence of the developing char due to the application of flame retardants results in a broader peak shape of the HRR curves compared to the untreated papers. The incipient protection mechanism lowers and delays the heat release, resulting in the aforementioned peak broadening. The during the composition thickening char layer further results in a decrease in the HRR as it increases the efficiency of the heat barrier. This is reflected in a faster decrease of the HRR after the peak for the treated papers, while the HRR for the untreated papers decreases only slowly.[224] In the example for AmPhy (Figure 50), the broadening of the HRR curve of the treated papers in comparison to the HRR curve of the untreated papers indicates the formation of the char barrier. The latter was also shown by SCHARTEL ET AL.[224] Furthermore, the treated NBSK papers display the peak of HRR at 12 s and an extinguishing at around 22 s, whereas the treated UKP papers has its pHRR at 15 s and the end of the first HRR peak at 28 s. This broadened HRR for the UKP papers can be explained by the lower char formation due to the influence of lignin. Breaking the char barrier, as mentioned before, would further explain the continuous release of heat for the UKP papers. The renewed heat release of the UKP papers also affects the THR. While the HRR represents the potential of the progression of the fire, the THR summarises the total heat contributing to the combustion

(Figure 51). As the THR decreases, the potential amount of decomposing material decreases as less energy is available for this purpose, indicating the effect of the flame retardants.

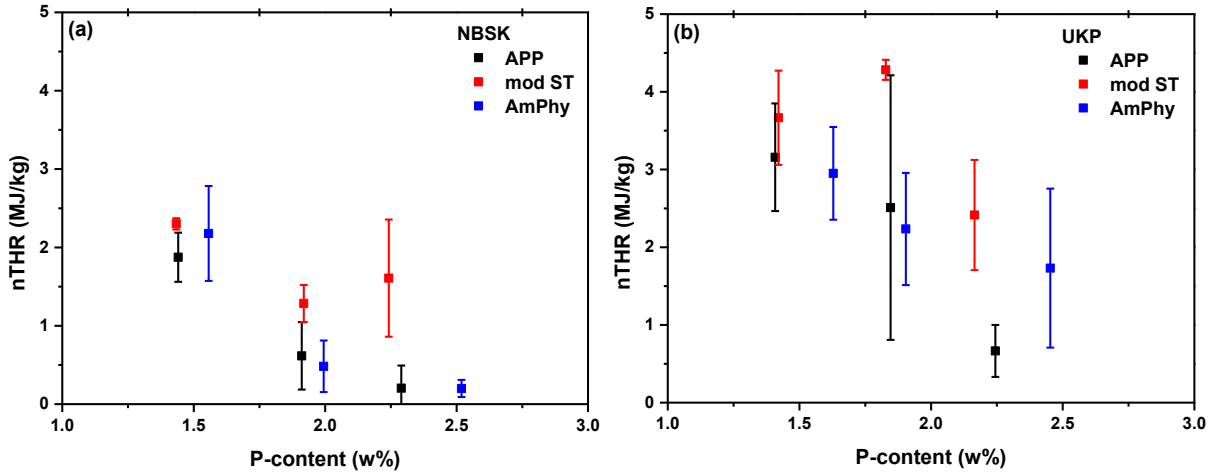

Figure 51: Normalised results of the THR measurements for NBSK (a) and UKP (b) papers coated with APP (black), mod. starch (red) and AmPhy (blue).

Similar to the pHRR values, the nTHR decreases with increasing proportions of phosphorous content in the paper samples. It becomes even more distinct that the coated UKP papers perform worse compared to the NBSK papers. Since the applied amounts of flame retardant are comparable between the respective coatings, the resulting difference can only be attributed to the influence of the remaining lignin on the UKP and the rerelease of heat shown in Figure 48. During the decomposition the aromatic structures of the lignin can undergo aromatic condensation reactions, which promotes the formation of carbonous char. The resulting high carbon content, as shown by SONNIER ET AL., has a decreased thermo oxidative stability in comparison to the phosphor-carbonaceous complexes formed in the presence of phosphates.[225]

Considering the efficiencies of the flame retardants APP displays the strongest flame retardant properties as it reduces the amount of heat generated the most. AmPhy shows similar good results in the ratio of phosphorous used to heat released and mod. starch shows a lower capacity if compared to the other flame retardants. It is important to note, that as displayed in Table 3, APP and AmPhy contain a higher proportion of phosphorous than the mod. starch. This means that lower amounts of these flame retardants are necessary to achieve flame protection if compared to mod. starch, which additionally implies a higher efficiency. Another important factor to consider when protecting a material with a flame retardant is smoke production. Usually, the aim is to reduce the amount of smoke to a minimum, as the smoke can be hazardous if inhaled. For example, the use of halogenated flame retardants, has been discontinued because the smoke produced by these flame retardants can be toxic and is therefore as dangerous to those exposed as the fire. In Figure 52 the results for the measured TSR of the samples are displayed.

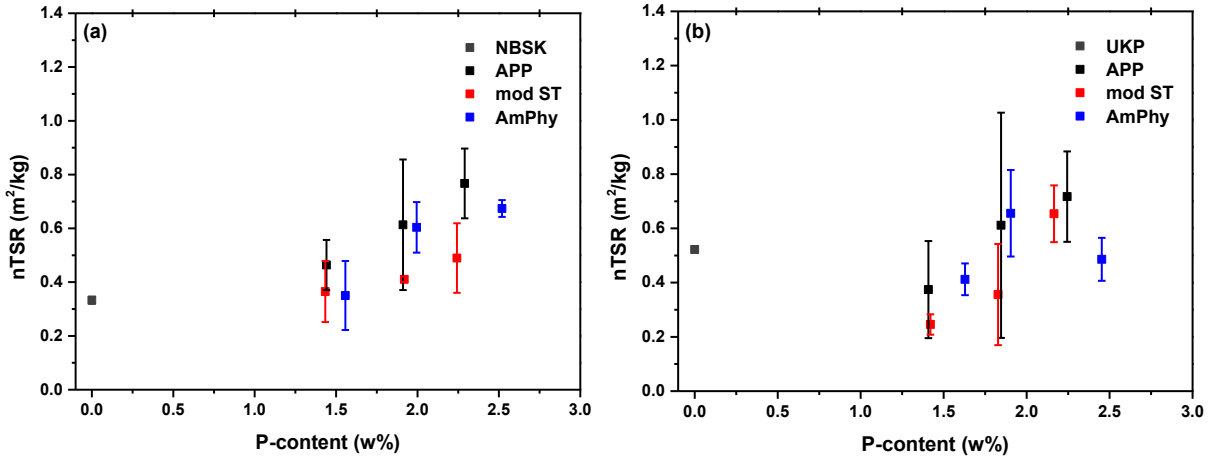

Figure 52: Normalised to weight values of the TSR of NBSK (al) and UKP (b) paper samples coated with APP (black), mod.starch (red) and AmPhy (blue).

Since cellulose is a material that burns almost completely without producing large amounts of smoke, only small amounts of TSR are to be expected. Considering the uncoated papers first, it can be seen that due to the remaining lignin in the UKP papers, a higher smoke production of 0.52 m^2/kg was measured in contrast to 0.33 m^2/kg for the NBSK papers. By using only small amounts of flame retardants, this smoke emission can be slightly reduced for the UKP papers resulting in nTSR values similar to NBSK papers. Increasing the amount of applied flame retardants then leads to an increase in smoke production. Since the flame retardants cause incomplete decomposition of the material and thus promote charring, a larger amount of char particles can be released from the material. Increasing quantities of flame retardants thereby lead to an increasing nTSR. Since the cone calorimeter was close to the measurement limit for the small amounts of smoke released, relatively large errors in the measurements were obtained here. However, looking at the smoke released from UKP and NBSK papers, it is noticeable that the use of flame retardants on the UKP papers results in lower smoke production. When this reduced smoke production is combined with the previous results, it can be further concluded that lignin impedes the functioning of the flame retardants. The lower proportion of OH-groups, which reduces the dehydrogenation reaction of the phosphate groups, and the more thermally unstable char formed from the condensed aromatic compounds of the lignin suggests a generally reduced charring behaviour, which results in a reduced smoke production.

6.4. Effectivity of the flame retardants

Since the flame retardants mod. ST and AmPhy are based on phosphorus modified organic materials and contain phosphates, like the reference flame retardant APP, as functional groups, it was further investigated whether the flame retardants have different effects on the decomposition pathway of the paper materials and whether the flame retardants are further influenced by the remaining lignin on the UKP fibres.

To detect the differences within the decomposition behaviour of the paper materials by using flame retardants the behaviour was analysed by TGA-FTIR-MS. By using TGA-FTIR-MS, it is possible to obtain data from three different analysis methods simultaneously to conclude about the decomposition behaviour by analysing the emerging decomposition products. TGA is used to determine the thermal stability of the material and its weight fractions of emerging volatile components. The first derivative of the TGA curve (i.e. derivative thermogravimetry (DTG) curve) can help indicate the pattern of the decomposition reaction and determine overlapping reactions by showing changes in the slope of the TGA curve. By coupling TGA with FTIR and MS, the real time emerging gaseous products can be detected during the whole pyrolysis process. The FTIR data can be processed into a three-dimensional FTIR spectrum with the coordinates of absorption, wavenumber and point of emergence to help visualising the decomposition process. The possible assignment of the functional groups determined in the FTIR spectra, correlated to the corresponding mass spectra allows conclusions about the decomposition products formed. To determine points of interest in the ongoing decomposition process, the Gram-Schmidt (G.S.) curve was used. This curve shows the total intensity of the detected substances measured by the FTIR and thus enables a more precise determination of the most important decomposition points.

The analysis by TGA-FTIR-MS could only detect fragments up to approx. m/z = 96 u when examining the papers with regard to the MS analysis. This is caused by condensation effects within the capillary that transports the gaseous components from the oven chamber to the MS detector. This capillary consists of fused silica with a length of 1.5 m and is heated to 280 °C. Because temperatures of up to 600 °C are reached in the oven during the TGA measurements, it is possible that larger gaseous components of the sample decomposition condense in the capillary and do not reach the detector. Furthermore, it should be noted that due to the capillary length, delays of around 2 min between the MS and FTIR measurements can occur, which results in a shift of the emerging temperatures up to 10 – 15 °C.

6.4.1. Cellulose

Determining the influences of the flame retardants on the decomposition of NBSK and UKP papers, the decomposition behaviour of untreated papers are measured first. The results of the TGA measurement (N_2 atmosphere; heating rate 5 K/min) and the DTG curves derived as well as the Gram-Schmidt (G.S.) curve of untreated NBSK is shown in the following Figure 53 and summarised in Table 5.

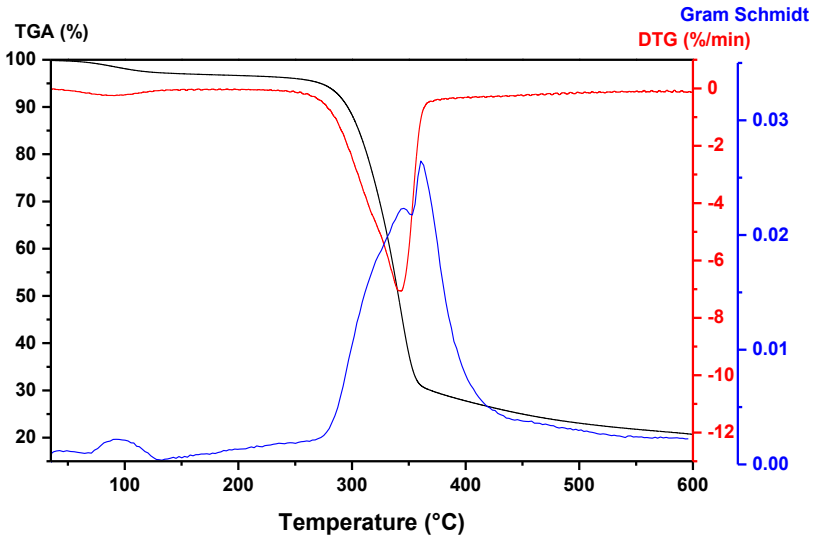

Figure 53: TGA, DTG and Gram Schmidt curves of 100 g/m² NBSK paper under N_2 atmosphere.

Table 5: Summary of mass losses, DTG and Gram Schmidt peaks of 100 g/m² NBSK paper.

Range Temperature (°C)	Mass loss (%)	DTG Peak (°C)	G.S. Peak (°C)	Residue (%)
35 – 266	4.6	95	95	20.6
266 – 367	65.2	342	345	
367 – 600	9.6		360	

The decomposition of the NBSK paper displayed in the TGA curve shows a slight weight loss of 4.6 % in the temperature range of 35 – 266 °C, which can be attributed to the release of water in small quantities at around 100 °C. After evaporation of the residual water within the paper, decomposition starts at 266 °C and occurs in one peak, as displayed in the DTG curve, with a maximum decomposition rate at 342 °C. The occurrence of a peak indicates that the pyrolysis of the NBSK paper is completed in a single step. Reaching 367 °C, the speed of the mass loss decreases, and the residue reaches a mass percent of 30.2 %. Thereafter, the residues continues to decompose slowly until the end of the measurement, where a residue of 20.6 % remains. The G.S. curve indicates two peaks at 345 °C and 360 °C. The detection of the various gaseous products in the FTIR increase gradually with proceeding time and decrease rapidly after attaining the second maximum. The peak at 345 °C can be attributed to the decomposition of cellulose, while the peak at 360 °C rather relates to the breakdown of the previous formed residues. In order to be able to assign these measured pinpoints of the cellulose decomposition, the results obtained are correlated with the results of the TGA-MS measurements, which are visualized in the following Figure 54.

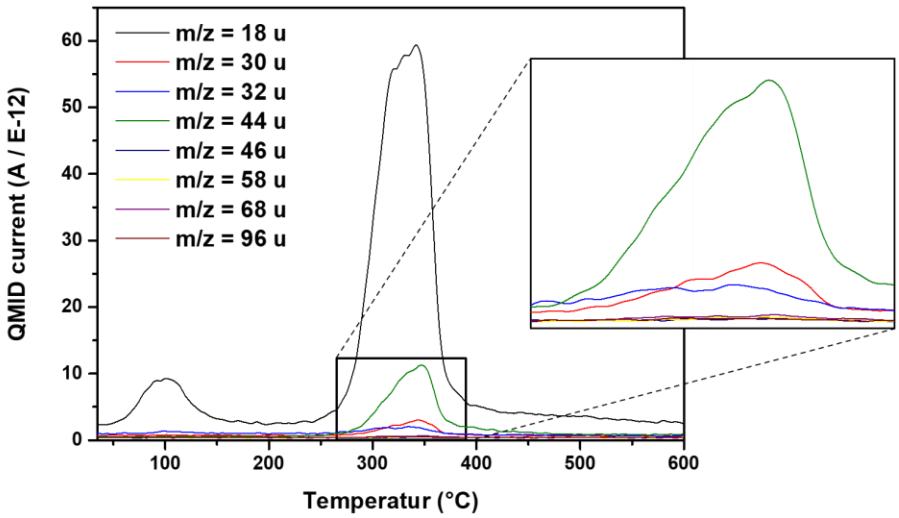

Figure 54: Detected molecular ions of the NBSK paper decomposition in the TGA-MS measurements.

In the decomposition of the NBSK paper, the molecule ions with the highest intensities measured by TGA-MS are water (m/z = 18 u), formaldehyde (m/z = 30 u) and methanol (m/z = 32 u). The resulting mass/charge – ratio of 44 can be assigned to either carbon dioxide or acetaldehyde. These fragments are typical for the decomposition of cellulose, as shown by SHEN ET AL.[96] Carbon monoxide (m/z = 28 u) as another occurring decomposition product was not directly identifiable as its detection overlaps with the nitrogen peak, which is the atmosphere used for the measurements. Furthermore, trace amounts of molecule ions with a mass/charge – ratio of 46 u, 58 u, 68 u and 96 u where measured, which can be attributed to ethanol, acetone or glyoxal, furan and furfural. Due to the small amounts detected, these cannot be further evaluated by FTIR. To determine these resulting compounds, the characteristic base and fragment peaks of these compounds were considered. To display the base and fragment peaks of the decomposition products, the MS spectrum at a temperature of 345 °C is shown in the following Figure 55. The corresponding molecular, base and fragment peaks of these compounds necessary for the characterisation are listed beforehand in Table 6.

Table 6: Listing of the fragmentations of the individual compounds from the decomposition of NBSK paper.[226]

	Molecular peak [m/z]	Base peak [m/z]	Fragment peaks [m/z]
Ethanol	46	31	27,29,43,45
Acetone	58	43	15,27,39,42
Glyoxal	58	29	28,30,31,32,44,56
Furan	68	68	29,37,38,39,40,42
Furfural	96	96	29,37,38,39,40,42,50,67,95

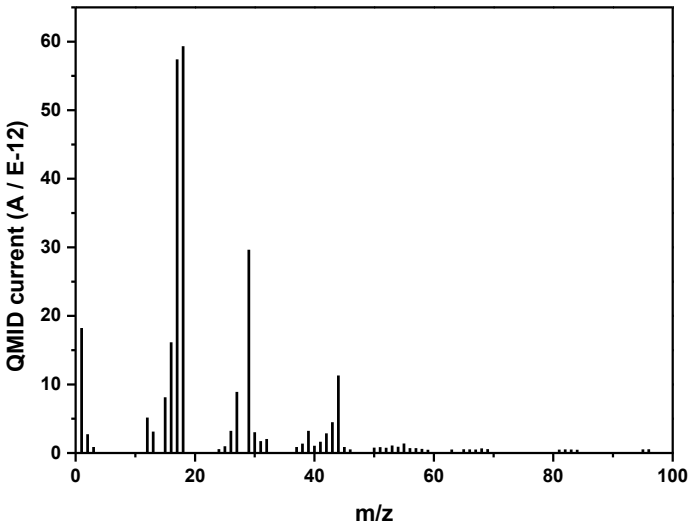

Figure 55: MS spectrum of the NBSK decomposition at 345°C.

For the analysis it should be noted that many compounds generate fragments with the same mass/charge – ratio and therefore the relative ion abundances from the fragmentations of the individual compounds are less reliable. In the case of carbon dioxide and acetaldehyde, as they share the same mass/charge – ratio, the emergence and distinction cannot be determined with MS alone. The results of the FTIR measurements therefore allow not only the confirmation of the measured decomposition products, but also the differentiation of the formation times of compounds with the same mass/charge – ratio. The following Table 7 summarizes these peak temperatures of the MS and FTIR measurements. The selected FTIR absorption bands represent characteristic bands of the individual compounds.

Table 7: Detected peak temperatures of the TGA-MS and -FTIR measurements of the NBSK paper and their assignments.

TGA - MS			**TGA - FTIR**	
Mass/Charge ratio	**Peak-Temperature [°C]**	**Molecule**	**Absorption bands**	**Peak-Temperature [°C]**
m/z = 18 u	99 / 342	H_2O	1701 – 1694 cm^{-1}	104 / 350
m/z = 28 u	-	CO	2191 – 2164 cm^{-1}	349
m/z = 30 u	345	CH_2O	1760 – 1720 cm^{-1}	350
m/z = 32 u	341	CH_3OH	-	-
m/z = 44 u	340	CO_2	2378 – 2302 cm^{-1}	345
m/z = 44 u	346	CH_3CHO	1813 – 1787 cm^{-1}	350

Using the data from the FITR measurements displayed in Figure 56, the formation of carbon dioxide can be confirmed with characteristic absorption bands at 2116-2094 cm^{-1} and 2191-2164 cm^{-1}. Carbon

dioxide causes two absorption bands at 669-667 cm^{-1} and 2378-2302 cm^{-1} and for water absorption bands at 1561-1471 cm^{-1}, 1701-1694 cm^{-1} and 3760-3721 cm^{-1} are characteristic. As the mass/charge – ratio of 44 can be assigned to carbon dioxide or acetaldehyde, the formation of acetaldehyde during the decomposition process can be identified by the characteristic bands at 1127-1073 cm^{-1} (C-C stretching vibrations), 1381-1353 cm^{-1} (CH_3 deformation vibrations), 1813-1787 cm^{-1} (C=O stretching vibrations) and 2844-2792 cm^{-1} (C-H stretching vibrations). The C=O stretching vibration at 1760-1720 cm^{-1} is attributed to the formation of formaldehyde but the C-H stretching vibrations at 2800 cm^{-1} of formaldehyde overlap with the vibrations of acetaldehyde, which prevents this compound from being unequivocally proven herewith. Similar is the case with the results for methanol. The characteristic C-O vibrations of methanol at bands of 1100 cm^{-1} are in the same range as the C-C stretching vibrations of acetaldehyde.

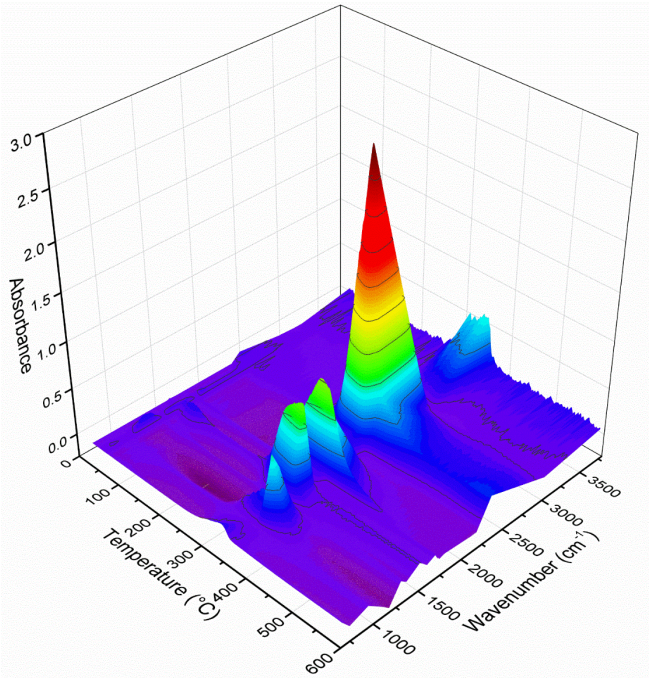

Figure 56: 3D FTIR-spectra of the detected decomposition products of the NBSK paper.

Regarding the decomposition of cellulose, the results show that water, carbon monoxide and carbon dioxide are initially formed. According to YANG ET AL., the formation of water during the decomposition of cellulose is initially ascribed to cross-linking reactions between glucose molecules and dehydrations within the pyran ring.[227] CO_2 as the major gas product is primarily generated via decarboxylation reactions and the release of carboxyl groups, whereas the emergence of CO is attributed to the decomposition of ether and carbonyl groups via decarbonylation reactions.[228] The formation of formaldehyde, methanol and acetaldehyde begins at slightly higher temperatures. These decomposition products result from the cleavage of the hemiacetal in depolymerisation as well as bond cleavage reactions. The earlier appearance of water, CO_2 and CO suggest that the cross-linking,

ring-opening, decarboxylation and decarbonylation reactions require less energy than the depolymerization and bond cleavage reactions. The subsequent formation of CO_2 and CO displayed in Figure 56 results from the further decomposition of the previously generated cellulose fragments, the residue formed.

Comparing these results of the decomposition of NBSK to the decomposition of the lignin containing UKP paper the TGA, DTG and G.S. curves of the UKP measurements are shown in Figure 57.

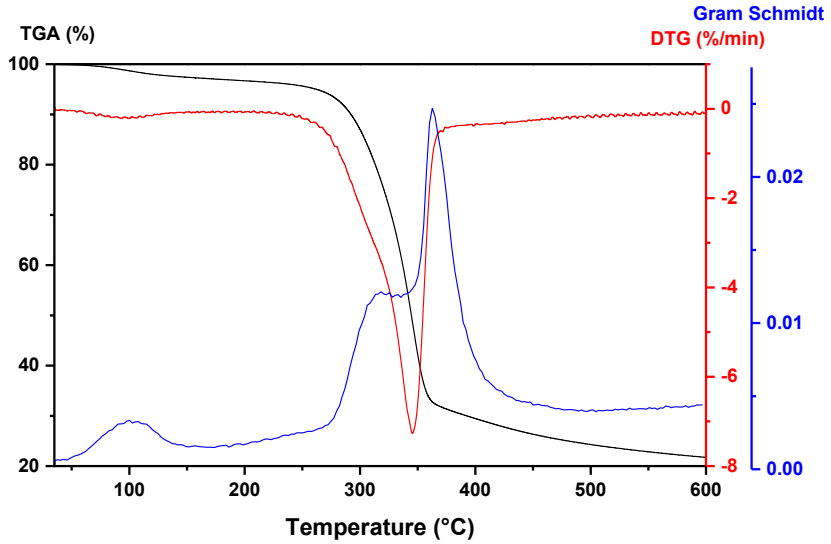

Figure 57: TGA, DTG and Gram Schmidt curves of 100 g/m² UKP paper.

Table 8: Summary of mass losses, DTG and Gram Schmidt peaks of 100 g/m² UKP paper.

Range Temperature (°C)	Mass loss (%)	DTG Peak (°C)	G.S. Peak (°C)	Residue (%)
35 - 221	3.7	98	100	21.7
221 - 369	65.3	345	318	
379 - 600	9.3		362	

Comparable to the results of the decomposition of the NBSK paper in Figure 53, the UKP paper also displays an initial weight loss at around 100 °C, which equally correlates with the evaporation of the residual moisture. Afterwards the decomposition occurs in one step in the temperature range from 221 – 369 °C with a maximum decomposition rate at 345 °C. Noticeable is the earlier onset of the decomposition and a change in the slope of the DTG curve at 318 °C. The increase in the slope is more pronounced than in the case of the decomposition of the NBSK paper and indicates a faster mass loss, which can be assigned to a faster decomposition. At 361 °C, the DTG curve shows the completion of this decomposition step with a residual fraction of 32.2 %, which decreases to 21.7 % over the remaining measuring period. This completion of the decomposition of the cellulose consequently takes place at the same temperature in both papers. The earlier onset of decomposition in combination with

the change in decomposition rate and the simultaneous completion of decomposition indicates that two separate decompositions reactions of lignin and cellulose are involved. The resulting decomposition products of the UKP paper are displayed in the following Figure 58.

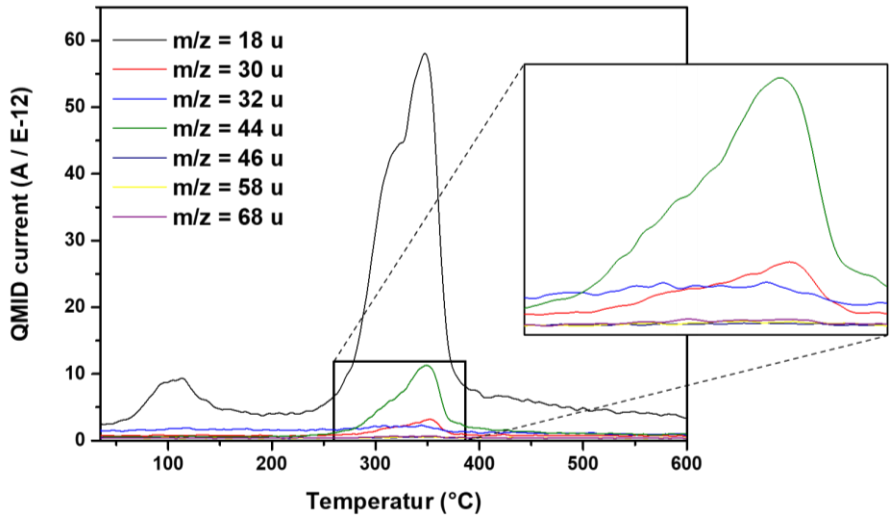

Figure 58: Detected molecular ions of the UKP paper decomposition in the TGA-MS measurements.

For the decomposition of the UKP paper similar molecule ions as for the decomposition of NSBK paper emerge. The formation of water (m/z = 18 u), formaldehyde (m/z = 30 u) and methanol (m/z = 32 u) as well as either carbon dioxide or acetaldehyde (m/z = 44 u) can be detected. Traces of molecule ions occur which can be assigned to ethanol, glyoxal and furan. The following Table 9 lists the peak temperatures of the MS and FTIR measurements.

Table 9: Detected peak temperatures of the TGA-MS and -FTIR measurements of the UKP paper and their assignments.

TGA - MS			**TGA - FTIR**	
Mass/Charge ratio	**Peak-Temperature [°C]**	**Molecule**	**Absorption bands**	**Peak-Temperature [°C]**
m/z = 18 u	113 / 347	H_2O	1701 – 1694 cm^{-1}	100 / 353
m/z = 28 u	-	CO	2191 – 2164 cm^{-1}	349
m/z = 30 u	352	CH_2O	1760 – 1720 cm^{-1}	357
m/z = 32 u	344	CH_3OH	-	-
m/z = 44 u	343	CO_2	2378 – 2302 cm^{-1}	350
m/z = 44 u	350	CH_3CHO	1813 – 1787 cm^{-1}	355

The correlation of the data from the MS measurements with the results of the FTIR measurements show that the results obtained for UKP paper follows a similar pattern as the decomposition of NBSK paper. The FTIR-spectrum for the UKP decomposition is displayed in the following Figure 59.

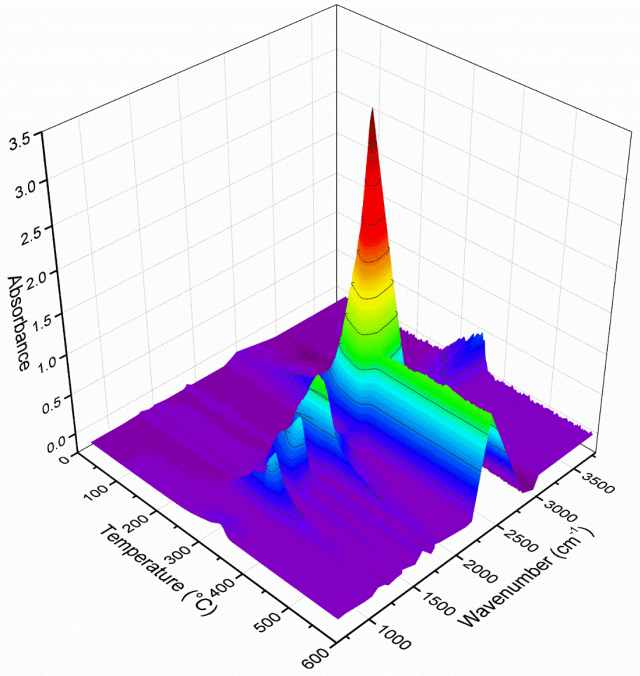

Figure 59: 3D FTIR-spectra of the detected decomposition products of the UKP paper.

In order to be able to derive the differences in the decomposition of NBSK and UKP papers, the G.S. curves of both samples are first considered. As already explained in chapter 5.1.4, lignin begins to decompose earlier than cellulose with the cleavage of α- and β- aryl- alkyl ether bonds in the temperature range of 150 – 300 °C, which can be observed by comparing the onset of decomposition between Figure 53 and Figure 57. In the case of the UKP paper, the first G.S. peak is at 318 °C, excluding the release of water, and thus about 30 °C before the first G.S. peak in the decomposition of the NBSK paper. An earlier release CO, CO_2 and water can be detected with the FTIR measurements for the UKP paper result from the decomposition of the substituted groups and aliphatic structures within the from the weakly bound oxygen groups, such as aldehyde groups. Comparably, these reactions can also occur in the cellulose chain, but the aromatic composition of the lignin leads this earlier decomposition mechanisms. The stability of the resulting decomposition products of these aromatic radicals with a radical stabilisation energy (RSE) of 43 kJ/mol are much more stable than secondary alkyl radicals with an RSE of 31 kJ/mol due to the aromatic delocalisation of the radical, resulting in an earlier decomposition.[229] The second G.S. peak, on the other hand, occurs at the same temperature for both samples, indicating that the residues decompose independently of the lignin in the UKP papers. In both cases, the main emerging gases detected by MS spectroscopy in this decomposition step of the remaining carbonous structure are water, carbon dioxide, formaldehyde and methanol. As MS spectroscopy is not an absolute measuring method, the values for the occurrence of the molecules cannot directly be compared. For this purpose, the ratio of the individual products formed can be

compared to obtain information about the composition of the products formed. Figure 60 shows this ratio for NBSK and UKP.

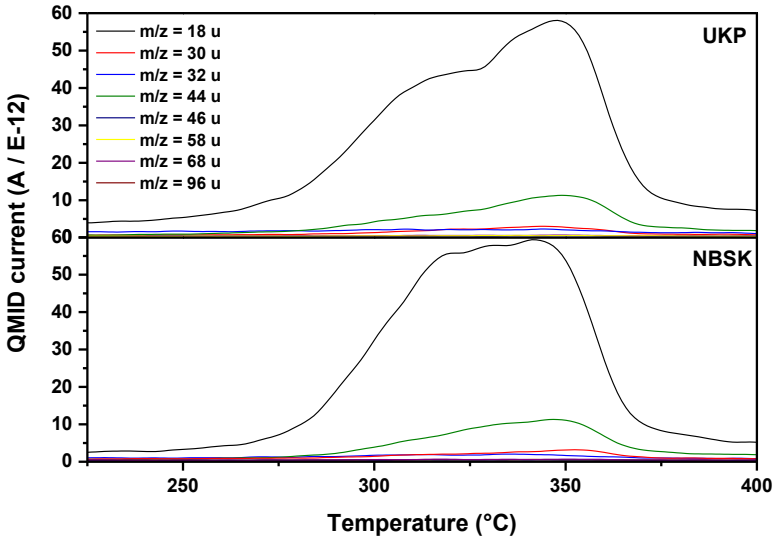

Figure 60: Comparison of the MS-spectra of NBSK and UKP paper.

Comparing the graphs/diagrams for NBSK and UKP paper, it becomes evident that the lignin in the UKP papers initiates an earlier degradation of the material in comparison to bleached NBSK fibres. This statement is based on the assumption that the cellulosic matrix consists of fibres of the same origin and thus the same composition, and that they therefore only differ in the remaining lignin content on the fibres. The earlier onset of water formation comes from different degradation process of multiple O-containing functional groups present in the lignin and the increased stability of the resulting decomposition products, as described before. Furthermore, this earlier decomposition/degradation seems to delay the decomposition of the cellulose as a second peak in the water formation arises at around 327 °C. The possible earlier charring due to incomplete combustion of lignin could create a char barrier that delays the decomposition of the cellulose fibres. This follows the previous made statement, that the more stable aromatic radicals resulting from the cleavage of low molecular gaseous molecules like CO_2 or water at lower temperatures cause this shift. These aromatic radicals can further undergo condensation reactions with other lignin structural units or the cellulose forming a carbonous complex which initially protects the fibre material. Regarding the formation of carbon dioxide, a similar behaviour can be observed. The onset of CO_2 emergence appears at the same temperature but displays over this temperature range, which is attributed to the lignin decomposition, a lower expression for the UKP paper. This lower emergence of CO_2 can therefore be explained by a smaller number of carboxyl-groups in the lignin than on the bleached cellulose fibres. Because of the small peaks of the other decomposition products, no reliable statement can be made about the influence of the lignin content in the papers on these other decomposition products.

6.4.2. Flame retardants – TGA-FTIR-MS analysis

Following the investigation of the untreated paper decomposition within the next section the influence of the flame retardant on the papers is analysed. Therefore, the decomposition of the pure flame retardants is always investigated first. The received information of these measurements can be used to separate decomposition product arising from the flame retardants from the decomposition products of the papers and can generate a first insight on thermal decomposition behaviours.

APP

APP, which is increasingly used in industry as a non-bio-based flame retardant, is analysed first to provide a reference for the other two bio-based flame retardants used in this work. In the following Figure 61 the TGA, DTG and G.S. curves of the flame retardant APP measurements are shown. The results of these measurements are summarised in Table 10. This information can be used to determine the onset and decomposition behaviour of the flame retardant and its influence when applied to the cellulose substrate.

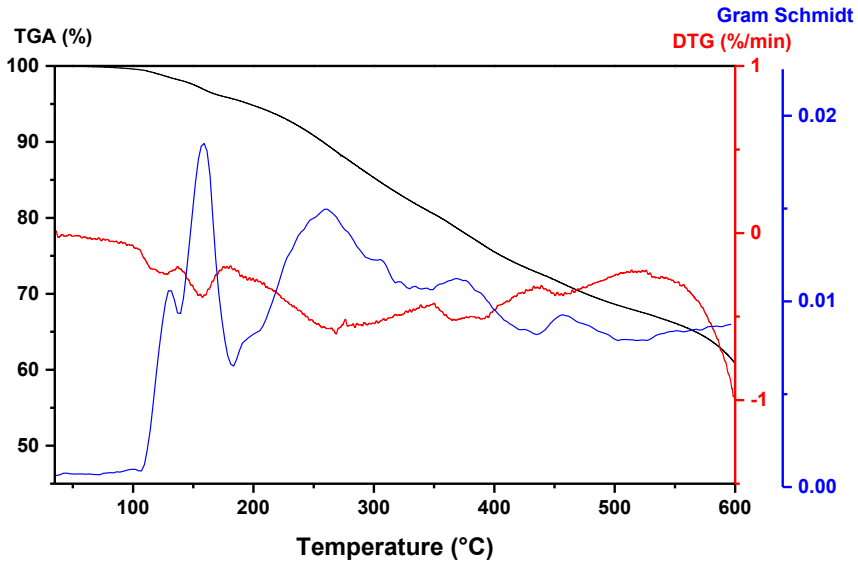

Figure 61: TGA, DTG and Gram Schmidt curves of the flame retardant APP.

Table 10: Summary of mass losses, DTG and Gram Schmidt peaks of APP.

Range Temperature (°C)	Mass loss (%)	DTG Peak (°C)	G.S. Peak (°C)	Residue (%)
35 - 136	1.8	127	129	60.7
136 - 178	2.4	158	159	
178 - 350	15.4	267	259	
350 - 438	7.8	367	369	
438 - 520	5.0	456	456	
520 - 600	6.9			

Looking first at the course of the TGA curve of the APP flame retardant decomposition, it shows a slow but constant decrease in mass. Analysing these results, it can be concluded that in a first step the remaining water is removed from the compound at around 104 °C and that in the second step at 127 °C the decomposition of the flame retardant begins. CAMINO ET AL. suggests that the onset of decomposition can be attributed to the release of ammonia from terminal NH_3 compounds.[230] In a following step, ranging from 136 – 178 °C, NH_3 and water are eliminated in small amounts from less stable functional groups within the APP chain. At temperatures above 210 °C CAMINO ET AL. describes the formation of thermally more stable P-O-P or P-NH-P bridges, the formation which further releases NH_3 and water through condensation reactions. The residue obtained in the TGA analysis accounts for 60.7 w% of the initial mass, indicating the thermal stability of the formed residue. The repeated release of NH_3 and water observed in the TGA analysis, can be confirmed by the MS measurements (see Figure 62).

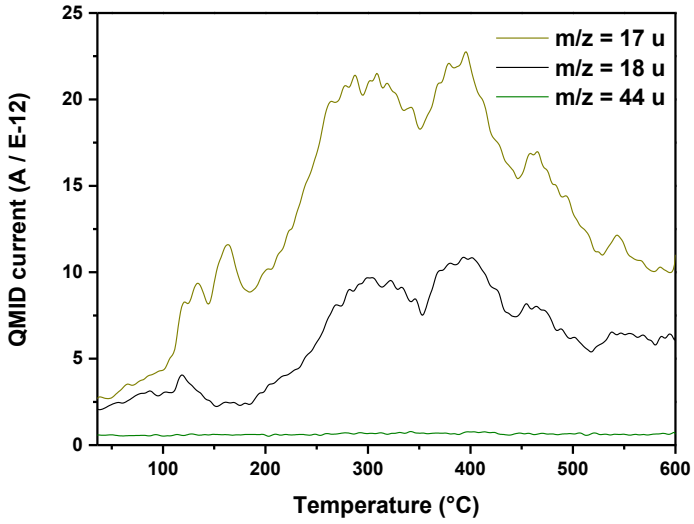

Figure 62: Detected molecular ions of the APP flame retardant decomposition in the TGA-MS measurements.

Table 11: Detected peak temperatures of the TGA-MS and -FTIR measurements of the APP flame retardant and their assignments.

TGA - MS			TGA - FTIR	
Mass/Charge ratio	**Peak-Temperature [°C]**	**Molecule**	**Absorption bands**	**Peak-Temperature [°C]**
m/z = 17 u	163, 309, 395, 460	NH_3	968 – 959 cm^{-1}	160, 263, 363, 455
m/z = 18 u	119, 305, 395, 453	H_2O	1753 – 1679 cm^{-1}	159, 267, 369, 457
m/z = 44 u	-	CO_2	2378 – 2302 cm^{-1}	-

As APP repeatedly releases NH_3 and water during decomposition, only the largest peaks are mentioned in Table 11. Comparing the MS graph/diagram from Figure 62 with the decomposition steps described by CAMINO ET AL., the described decomposition pattern can be recognised.[230] Following this decomposition pattern, the evaporation of water followed by the release of terminal NH_3 groups at around 125 °C can be identified in the beginning of the measurements. Furthermore, the formation of the P-O-P and P-NH-P crosslinks during decomposition, leading to the simultaneous release of water and NH_3 can be attributed to peaks building up from 210 °C to 310 °C. The emergence of CO_2 is only indicated in very small quantities in the MS spectrum but is detected in the FTIR spectrum in Figure 63, at higher temperatures, which may be due to the decomposition of additives within the APP solution from *Clariant* at higher temperatures, as otherwise no other carbon source should be included in the flame retardant.

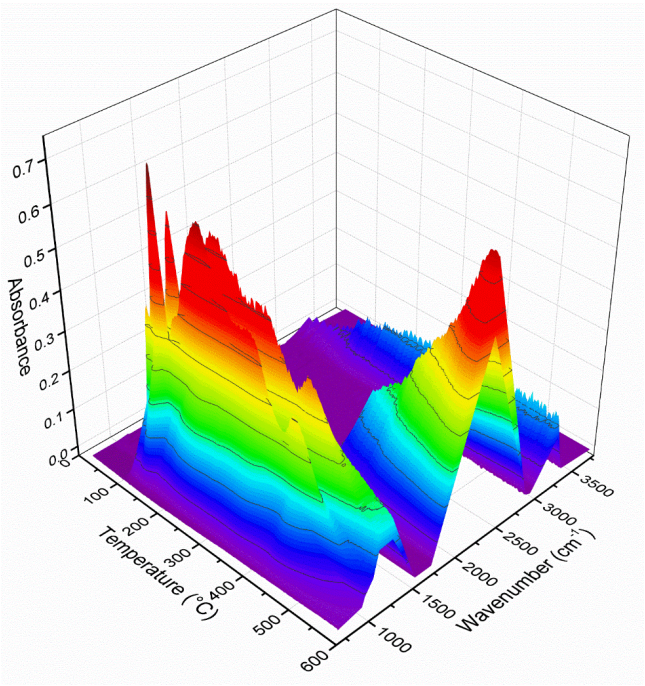

Figure 63: 3D FTIR-spectra of the detected decomposition products of the flame retardant APP.

It is important to note that the increasing peak at approx. 2350 cm^{-1} cannot only be attributed to the formation of CO_2, but could also represent the formation of compounds containing P-H groups, since this functional group also exhibits vibrations within the same range.[231] However, no evidence for the emergence of phosphor-containing compounds could be found in the MS spectrum, therefore the formation of phosphorous-containing gaseous products is unlikely. Summarising these results, APP decomposes in successive steps releasing NH_3 and water at several temperature pinpoints. Both emerging gases should have no further influence on the evaluation of the decomposition of the paper treated with the APP flame retardant.

In the following Figure 64 the TGA, DTG and G.S curves are displayed for the measurements of the NBSK paper prepared with the medium applied amount of the APP flame retardant (6.62 w%). The amount of flame retardant applied was chosen to generate self-extinguishing properties on the paper material when ignited and should therefore be able to represent the influence of the flame retardant.

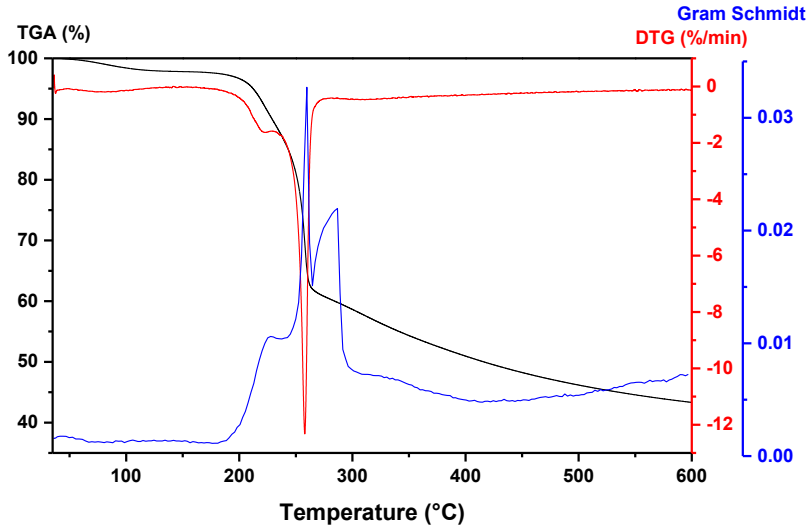

Figure 64: TGA, DTG and Gram Schmidt curves of NBSK paper coated with APP (6.62 w%).

Table 12: Summary of mass losses, DTG and Gram Schmidt peaks of NBSK paper coated with APP (6.62 w%).

Range Temperature (°C)	Mass loss (%)	DTG Peak (°C)	G.S. Peak (°C)	Residue (%)
35 – 183	2.6	-	-	43.3
183 – 230	7.8	223	227	
230 – 278	29.1	257	259	
278 – 600	17.2		286	

Comparing the results of the TGA measurements of untreated NBSK paper, shown in Table 5, with the results of the NBSK paper impregnated with APP, shown in Table 12, it becomes evident, that the presence of APP on the cellulosic material changes the decomposition behaviour of the paper. The

decomposition for untreated NBSK paper starts at temperatures of 266 °C, whereas the decomposition of NBSK paper treated with APP is indicated at a temperature of 183 °C. This temperature corresponds to the same temperature at which APP begins to decompose. In contrast to the decomposition behaviour of NBSK paper in the TGA measurements for the flame retardant treated paper three peaks appear in the G.S. curve. The first appearing peak in the G.S. curve can be attributed to the reaction of APP with the cellulose as shown in Scheme 6 in chapter 2.5.2. The loss of mass determined in the TGA results on the one hand from the release of NH_3 and water from the flame retardant APP and on the other hand from the evaporation of water due to the dehydration reaction of the phosphate groups with the OH-groups of the cellulose. This leads to the formation of phosphor-carbonaceous complexes. The residues formed from these P-O-C complexes have a higher thermal stability, which initially acts as a first heat and diffusion barrier.[232–234] With increasing temperature, these complexes disintegrate forming C-C double bonds, which are capable of cross-linking. This cross-linking and the onset of further cellulose decomposition is assigned to the second step in the TGA investigations. Due to cross-linking, incomplete decomposition occurs, resulting in a higher remain of residue. The remaining residue increases from 31.3 w% for NBSK paper to 62.2 w% for NBSK paper treated with APP. However, as the temperature continues to rise, the remaining residue also begins to decompose forming CO and CO_2, which is reflected in the third peak of the G.S. curve. The gaseous products formed during these three steps are shown in the MS spectrum in Figure 65.

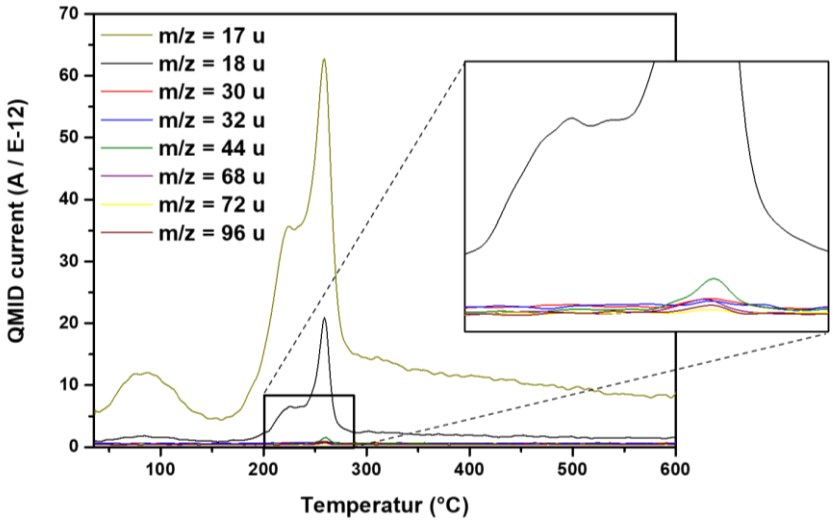

Figure 65: Detected molecular ions of the APP treated NBSK paper decomposition in the TGA-MS measurements.

Table 13: Detected peak temperatures of the TGA-MS and -FTIR measurements of the APP treated NBSK papers and their assignments.

TGA - MS			TGA - FTIR	
Mass/Charge ratio	**Peak-Temperatures [°C]**	**Molecule**	**Absorption bands**	**Peak-Temperatures [°C]**
m/z = 17 u	224, 258	NH_3	967 – 905 cm^{-1}	261
m/z = 18 u	225, 258	H_2O	1701 – 1694 cm^{-1}	227, 283
m/z = 28 u	-	CO	2191 – 2164 cm^{-1}	261, 392
m/z = 30 u	259	CH_2O	-	-
m/z = 32 u	259	CH_3OH	-	-
m/z = 44 u	260	CO_2	2378 – 2302 cm^{-1}	261, 322

Analysing the mass spectrum of the TGA-FTIR-MS measurements for the NBSK paper flame retarded with APP, shown in Figure 65, the presence of NH_3 can clearly be observed. As shown in the investigations on APP previously, the release of NH_3 is attributable to the decomposition of APP. Furthermore, it can be seen that the gas products formed from the first peak, excluding the evaporation of water at 100 °C, are mainly NH_3 and water. This confirms the previous assumption that NH_3 and water are released from less stable functional groups within the APP in the first step and that water is formed by the dehydration reaction of the phosphate groups with the OH-groups of the cellulose. At approx. 260 °C, in the temperature range of the second G.S. peak, the resulting decomposition products can be assigned to cellulose in addition to water and NH_3. It is noticeable that these decomposition products occur to a significantly lesser extent than without the flame retardants applied. In general, fewer gaseous products containing carbon are formed, which can be attributed to the formation of char and the phosphor-carbon complex and the therefore entrapping of carbon within the residue. Comparing the resulting decomposition products with the formed products from untreated cellulose, similar results can be observed. The only difference is the formation of pyruvic aldehyde (m/z = 72 u). As pyruvic aldehyde is usually formed during the cellulose decomposition through a dehydration reaction of decomposition intermediate glyceraldehyde and did not occur in the MS measurements of the NBSK paper.[96] This is another indication that the flame retardant influences the decomposition pathway of the cellulose. TETSUO HONMA ET AL. described in their studies the influences on the conversion of glyceraldehyde to pyruvic aldehyde. They discussed that the formation of pyruvic aldehyde is catalysed by the presence of water, as the water molecule can form ring-like hydrogen bonds causing a reduction of the threshold energy for the conversion.[235] As the influence of the flame retardant promotes the formation of water, this could explain the increased occurrence of pyruvic aldehyde. Following pyruvic aldehyde decomposes further to CO and

acetaldehyde, which both were detected in the MS and FTIR studies of NBSK. The subsequent decomposition of the residues with the formation of CO and CO_2 cannot be clearly demonstrated in the MS measurements. However, these can be recognised in the following Figure 66 of the FTIR measurements at around 320 °C.

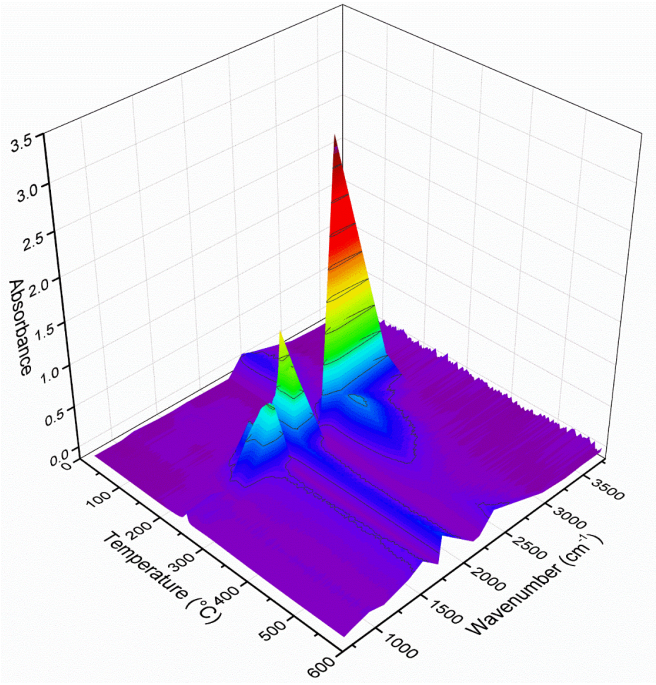

Figure 66: 3D FTIR-spectra of the detected decomposition products of the NBSK paper treated with APP.

Comparing the results of the FTIR measurements of NBSK paper treated with APP, shown in Figure 66, with the results for NBSK in Figure 56, the reduced occurrence of emerging decomposition products can be observed as well. In particular, the missing peak in Figure 66 at around 1100 cm^{-1} attributed to C-C or C-O stretching vibrations indicates very clearly the reduced emergence of the carbon containing decomposition products, such as acetaldehyde or methanol.

Subsequently, the UKP paper treated with APP flame retardant is investigated. As with the NBSK paper, the thermal decomposition of the flame retardant paper is first analysed using TGA, displayed in Figure 67.

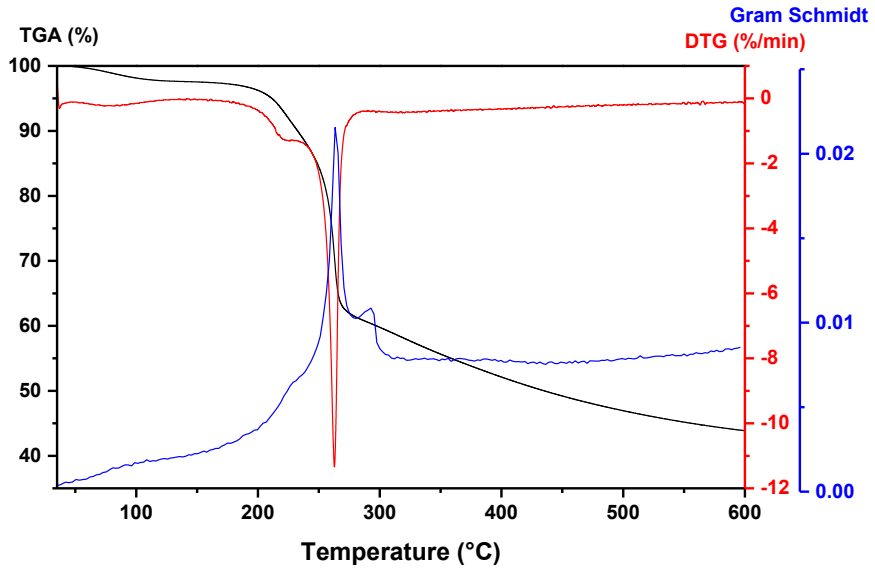

Figure 67: TGA, DTG and Gram Schmidt curves of UKP paper coated with APP (6.39 w%).

Table 14: Summary of mass losses, DTG and Gram Schmidt peaks of UKP paper coated with APP (6.39 w%).

Range Temperature (°C)	Mass loss (%)	DTG Peak (°C)	G.S. Peak (°C)	Residue (%)
35 - 169	2.7	-	-	43.8
169 - 229	6.4	223.4	228.8	
229 - 286	30.1	262.7	263.4	
286 - 600	17		292.7	

Comparing the TGA results of the measurements with the APP treated UKP paper with the results of the NBSK paper displays a significant difference in the course of decomposition. The first and third G.S. peaks are significantly less pronounced in the measurements of the APP treated UKP paper than in the flame retardant NBSK paper. In contrast to before, when the untreated UKP paper had an earlier onset of decomposition due to the remaining lignin on the cellulose fibres, the decomposition of both papers treated with the APP flame retardant starts at the same temperatures. This earlier onset temperature can be attributed to the reaction of the phosphates with the OH-groups within the papers, which initiates at the same temperature and therefore causes the earlier mass loss in both papers. In the case of UKP paper, this first peak is less pronounced, which can be ascribed to the influence of the lignin. With fewer available OH-groups, the dehydration reaction of the phosphate groups turns out lower, resulting in lower amounts of released gaseous products. Looking at the following steps of the decomposition it becomes apparent, that both paper types undergo the remaining decomposition steps at the same temperatures (Table 12/Table 14). This leads to the conclusion that the influence of the flame retardant causes a uniform decomposition of the cellulosic materials. In addition, the

resulting amount of residue remains for both paper types after the end of the measurements are the same.

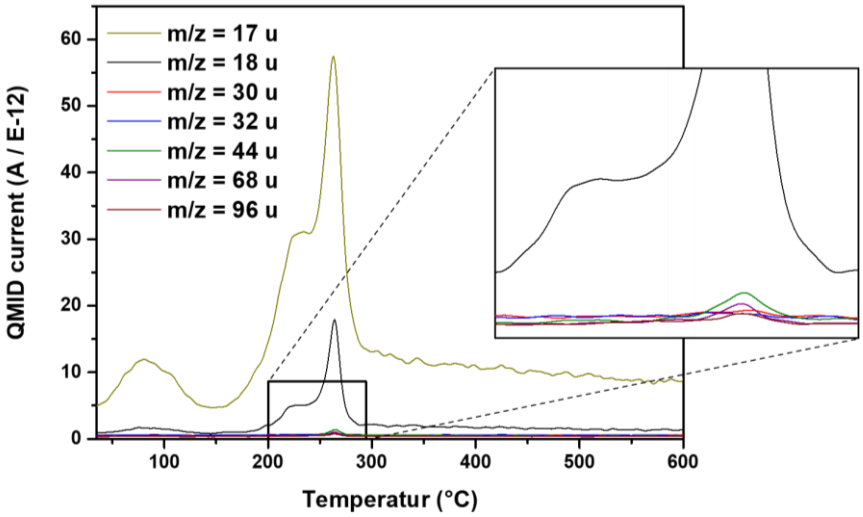

Figure 68: Detected molecular ions of the APP treated UKP paper decomposition in the TGA-MS measurements.

The resulting decomposition products of APP treated UKP papers are similar to the products emerging in the APP treated NBSK paper decomposition. With the application of the flame retardant, the emergence of NH_3 and water can be detected at around 210 °C. The occurrence of carbon-containing products in the following decomposition step such as formaldehyde or methanol is compared to the untreated UKP paper drastically decreased. It is noteworthy that in these measurements no pyruvic aldehyde arises. While it has been argued for the flame retardant NBSK paper, that the flame retardant influences the decomposition process of the cellulosic material and causes an increased emergence of pyruvic aldehyde, this is not the case for the UKP paper. The absence of this formed compound could therefore be a sign for a reduction on the efficiency of the flame retardant on lignin containing material. As the dehydration reaction of the phosphate groups increases the formation of water during the decomposition, which, as TETSUO HONMA ET AL. their studies stated, catalyses the conversion of glyceraldehyde to pyruvic aldehyde, the absence of pyruvic aldehyde in contrast to the previous results found in regards to APP on the NBSK paper leads to the conclusion that the lignin can be associated with the interference of this dehydration reaction.[235] This would further confirm the influence of the lignin on the protection mechanism of the flame retardant. Comparing the MS measurement of the NBSK in Figure 65 with the results of the UKP measurement in Figure 68, it is also notable that for the APP treated NBSK paper the main carbon-containing gas product by far is CO_2 whereas this is much less distinct to the other emerging carbon-containing gaseous products for the UKP paper.

Table 15: Detected peak temperatures of the TGA-MS and -FTIR measurements of the APP treated UKP papers and their assignments.

TGA - MS			TGA - FTIR	
Mass/Charge ratio	**Peak-Temperatures [°C]**	**Molecule**	**Absorption bands**	**Peak-Temperatures [°C]**
m/z = 17 u	225, 263	NH_3	968 – 959 cm^{-1}	198
m/z = 18 u	225, 264	H_2O	1701 – 1694 cm^{-1}	232, 291
m/z = 28 u	-	CO	2191 – 2164 cm^{-1}	265, 403
m/z = 30 u	266	CH_2O	-	-
m/z = 32 u	-	CH_3OH	1035 – 1031 cm^{-1}	267
m/z = 44 u	264	CO_2	2378 – 2302 cm^{-1}	265, 328

Comparing the results of the FTIR measurements of the APP flame retardant NBSK and UKP papers, no significant difference can be observed. However, it should be mentioned that the peak for the formation of CO_2 is much more pronounced in the UKP paper than in the NBSK paper. The assumption solidifies, that the remaining lignin interferes with the protection mechanism of the flame retardant allowing a continuing of the complete combustion of the cellulose, as stated before.

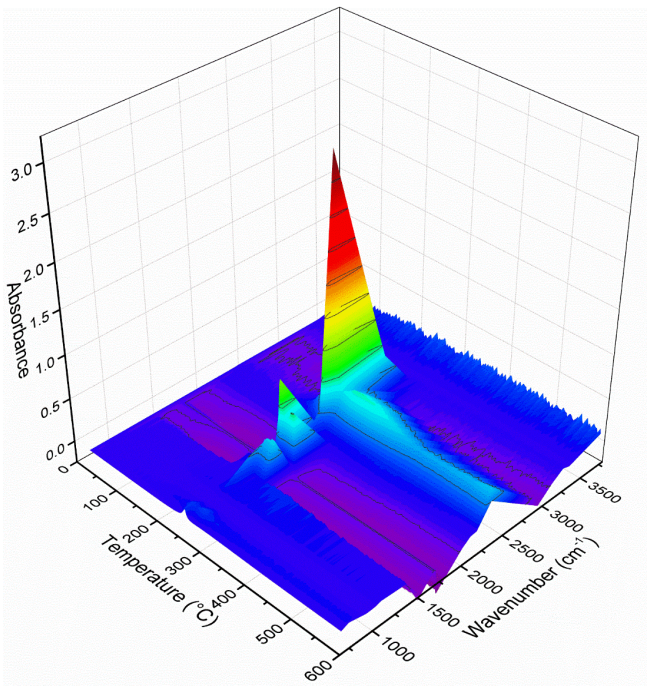

Figure 69: 3D FTIR-spectra of the detected decomposition products of the UKP paper treated with APP.

Mod. starch

After the investigations of the APP flame retardant, the next flame retardant investigated is the modified starch. Since mod. starch is a bio-based flame retardant, with a similar composition to cellulose, in which the OH-groups of starch have been functionalised with phosphate and carbamate groups, the decomposition of the mod. starch could have more interference points in the investigations of the decomposition behaviour of the paper substrates than APP. Below, Figure 70 shows the measured TGA, DTG and G.S. curves for the mod. starch flame retardant. The points of interest of these graphs are summarised in Table 16.

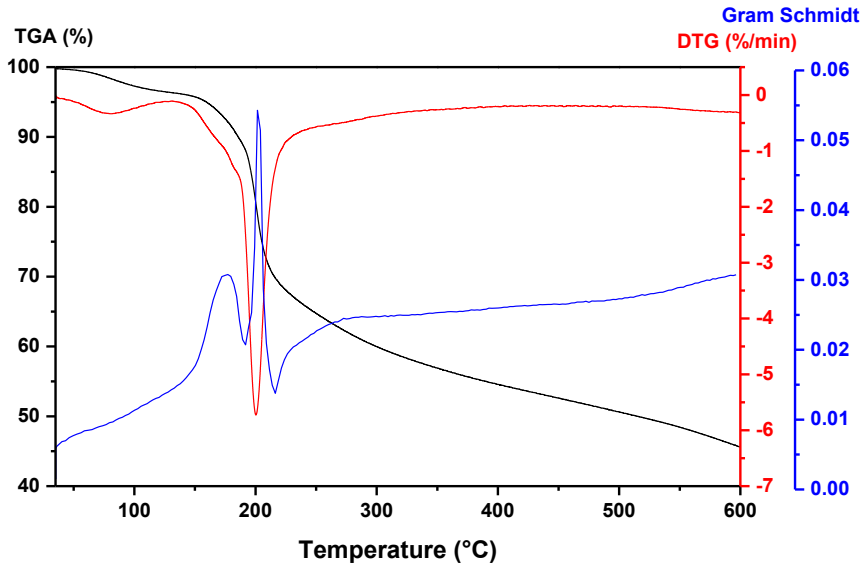

Figure 70: TGA, DTG and Gram Schmidt curves of the flame retardant mod. starch.

Table 16: Summary of mass losses, DTG and Gram Schmidt peaks of mod. starch.

Range Temperature (°C)	Mass loss (%)	DTG Peak (°C)	G.S. Peak (°C)	Residue (%)
35 - 134	3.8	79.0	-	45.5
134 - 175	3.7	168.4	177.2	
175 - 236	26.1	200.2	201.5	
236 - 600	20.9		(275.0)	

The course of the TGA curve of the mod. starch flame retardant shows a similar course to the decomposition of the untreated cellulosic materials. In contrast to the untreated paper materials, the mod. starch starts begins to decompose earlier at 175 °C. This earlier onset of decomposition, evident in the first G.S. peak, can be associated with the decomposition of the carbamate groups, as studies by LASZKIEWICZ ET AL. on cellulose carbamate have shown.[236] Beforehand, similar to the previous

investigations, the evaporation of residual water takes place. The second G.S. peak, located at 200 °C, can therefore be attributed to the decomposition of the starch and the onset of the dehydration reaction, comparable to the APP flame retardant, due to the phosphate groups. Within the mod. starch the phosphate groups can react with the remaining OH-groups in the polymer chain, which leads to the fact, that the effect, which is expected on the cellulose fibres, can be observed in a weakened version. It is interesting to note that after the completion of the decomposition step the G.S. curve indicates a resumption of emerging gaseous products. This could indicate a less stable residue that continues to decompose with the release of gaseous products, due to an incomplete realization of the dehydration reaction by the phosphate groups. In chapter 6.1 the DS for the phosphate groups or the mod. starch was determined as greater than 1 and the conversion of OH-groups to carbamate groups leading to the assumption that a not sufficient number of OH-groups within the mod. starch remained, which would further support the previous hypothesis. Following up these investigations, the MS measurements, displayed in Figure 71, are used to confirm the previously formed statements.

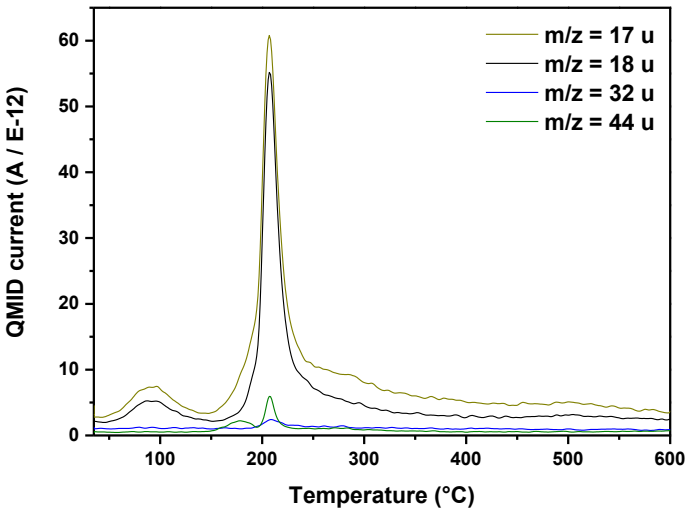

Figure 71: Detected molecular ions of the modified starch flame retardant decomposition in the TGA-MS measurements.

Table 17: Detected peak temperatures of the TGA-MS and -FTIR measurements of the modified starch flame retardant and their assignments.

TGA - MS			TGA - FTIR	
Mass/Charge ratio	**Peak-Temperatures [°C]**	**Molecule**	**Absorption bands**	**Peak-Temperatures [°C]**
m/z = 17 u	207	NH_3	968 – 959 cm^{-1}	181, 195, 317
m/z = 18 u	207	H_2O	1701 – 1694 cm^{-1}	216
m/z = 28 u	-	CO	2191 – 2164 cm^{-1}	206
m/z = 32 u	208	CH_3OH	-	-
m/z = 44 u	179, 207	CO_2	2378 – 2302 cm^{-1}	174, 203

In the MS measurements, four major emerging gaseous products are detected with the mass – charge ratio of 17, 18, 32 and 44 u are. In this order, they can be attributed to ammonia, water, methanol and carbon dioxide on the basis of the characteristic absorption bands from the FTIR measurements, displayed in Table 17. Noticeable is the early increase in the ammonia curve and the first peak in the carbon dioxide curve, which can be related to the previous considerations of the earlier decomposition of the carbamate groups. At 207 °C the main decomposition of the flame retardant takes place and the emergence peaks for all gaseous products are reached. Since the OH-groups of the starch are functionalised with carbamate and phosphate groups, fewer OH-groups are available for the dehydration reaction of the phosphates. This decreases the effectiveness of the flame retardant when considered alone and causes the continuous loss of mass after the initial decomposition of the residue. The CO_2 resulting from the decomposition of the residue can be recognised in the FTIR spectrum shown in Figure 72.

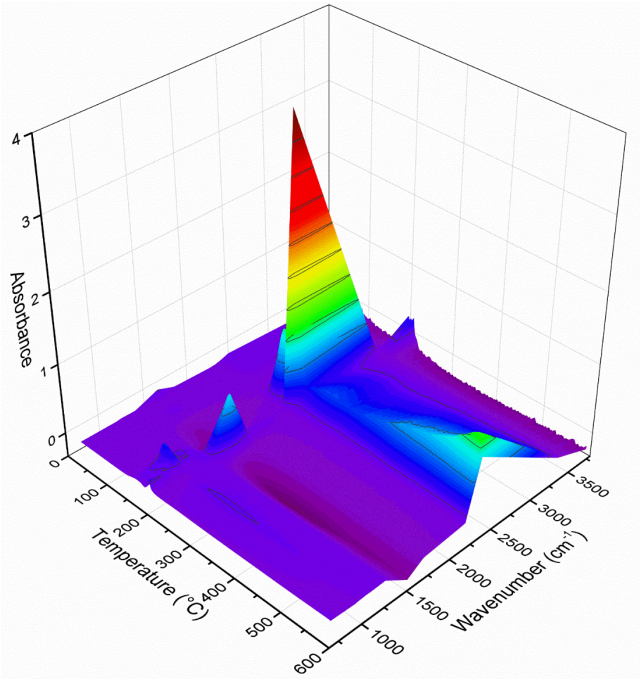

Figure 72: 3D FTIR-spectra of the detected decomposition products of the modified starch flame retardant.

Since the mod. starch has a similar chemical structure to cellulose, only modified with carbamate and phosphate groups, it is obvious that the gaseous products formed during the decomposition of the flame retardant can overlap. Similar to the decomposition of cellulose, water, methanol and carbon dioxide emerge. In order to identify the influence of the flame retardant on the decomposition behaviour of the papers, the different appearance times of the individual products can be used as a differentiation factor. In addition, since the proportion of mod. starch introduced is about 15 w%, the released gaseous products only occur in a lower ratio. Only the emerging ammonia can be directly attributed to the flame retardant.

Continuing the investigating of the influence of mod. starch flame retardant on the NBSK paper the TGA analysis displays, as shown in Figure 73, that this flame retardant also shifts the decomposition of the cellulose to a lower temperature. In addition, the onset of decomposition behaviour of the flame retardant can be recognised in the course of the graphs for the NBSK paper treated with mod. starch.

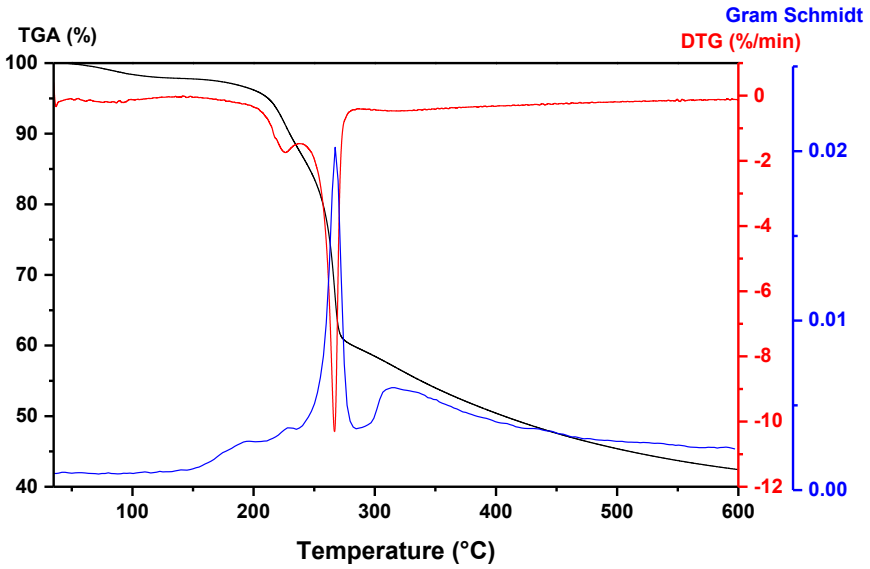

Figure 73: TGA, DTG and Gram Schmidt curves of NBSK paper coated with mod. starch (15.5 w%).

Table 18: Summary of mass losses, DTG and Gram Schmidt peaks of NBSK paper coated with mod. starch (15.5 w%).

Range Temperature (°C)	Mass loss (%)	DTG Peak (°C)	G.S. Peak (°C)	Residue (%)
35 - 153	2.3	-	-	42.4
153 - 238	10.3	-	194.1	
		225.5	228.4	
238 - 287	27.8	266.9	267.3	
287 - 600	17.1		313.0	

Comparable to the decomposition of the flame retardant, the first release of gaseous products, can be detected for the treated NBSK paper below 200 °C, which corresponds to the beginning of decomposition. This is closely followed by a further G.S. peak at around 225 °C. From the investigations on the pure mod. starch flame retardant it can be concluded that the first peak correlates with the decomposition of the carbamate groups and the subsequent with the decomposition of the starch and the onset of the dehydration reaction. The largest mass loss at 266 °C found in the TGA investigations can be attributable to the decomposition of the paper and thus of the cellulose. During the studies of the APP flame retardant, the same temperature was detected for the cellulose decomposition, which leads to the assumption that the decomposition temperature of cellulose is always lowered to the

same level due to the influence of the dehydration reaction by the phosphate groups. After the decomposition of the cellulose the TGA shows a continuous loss of mass for the residue, which is also evident in the emergence of gaseous products in the G.S. curve at 313 °C. This indicates a less stable residue due to incomplete charring or an incomplete conversion of the cellulose with the flame retardant causing continued decomposition.

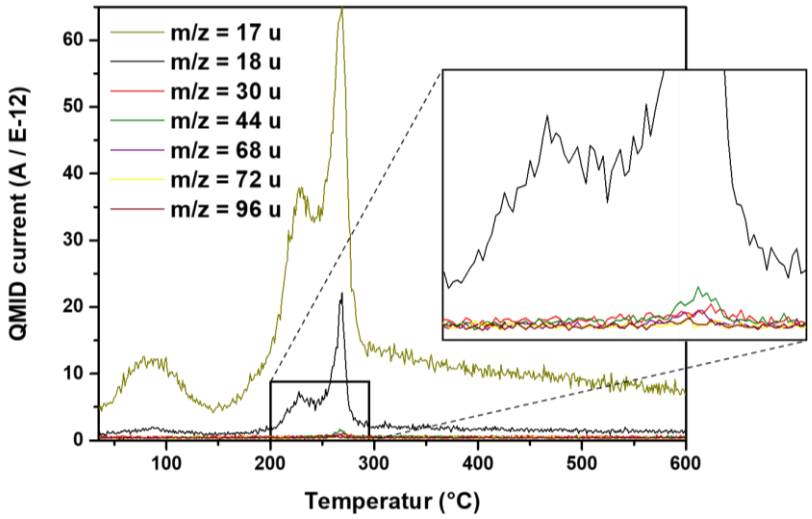

Figure 74: Detected molecular ions of the NBSK paper treated with mod. starch flame retardant decomposition in the MS measurements.

Comparing the results of the MS measurements with the results displayed in Figure 74 for the NBSK paper treated with APP flame retardant, similarities can be seen in the curves of the emerging gaseous products. Similar to the APP, the curves show three points of emergence. The first at around 100 °C, which can be assigned to the evaporation of the water remaining in the flame retardant or the paper material, and the second at 227 °C, which combined the release of NH_3 and water from the dehydration reaction. The third peak at around 270 °C, with the release of CO_2 and other carbon-containing products, can result from the further decomposition of the mod. starch flame retardant and the cellulose. In addition, the emergence of pyruvic aldehyde (m/z = 72 u) is detected. The only difference is the absence of methanol formation. Like the APP flame retardant, the mod. starch flame retardant significantly reduces the emergence of carbon-containing gaseous products. The continuous detection of gaseous products above the temperature of 300 °C, as with the APP flame retardant, are not visible in the MS spectrum, but can be seen in the FITIR spectrum in Figure 75.

Table 19: Detected peak temperatures of the TGA-MS and -FTIR measurements of the NBSK paper treated with mod. starch flame retardant and their assignments.

TGA - MS			TGA - FTIR	
Mass/Charge ratio	**Peak-Temperatures [°C]**	**Molecule**	**Absorption bands**	**Peak-Temperatures [°C]**
m/z = 17 u	227, 269	NH_3	967 – 905 cm^{-1}	197, 269
m/z = 18 u	227, 268	H_2O	1760 – 1694 cm^{-1}	236, 271, 300
m/z = 28 u	-	CO	2191 – 2164 cm^{-1}	234, 269, 394
m/z = 30 u	270	CH_2O	-	-
m/z = 44 u	266	CO_2	2378 – 2302 cm^{-1}	233, 269, 322

When further investigating the decomposition of the NBSK paper treated with mod. Starch, it is noticeable that two main peaks appear in the FTIR spectrum at absorption-bands of 1760 – 1694 cm^{-1}. Due to their occurrence at different temperatures of 270 °C and 300 °C, the first peak refers to the formation of H_2O during the decomposition of cellulose and the second to the decomposition of the formed residue.

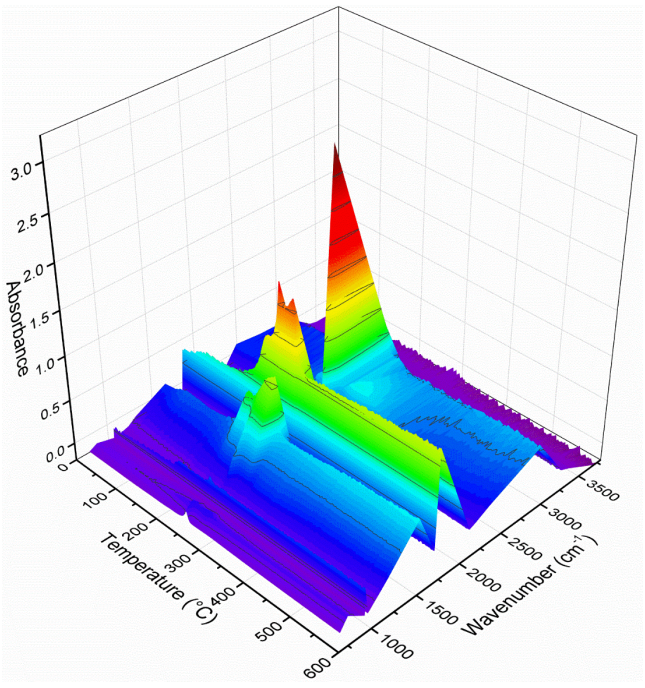

Figure 75: 3D FTIR-spectra of the detected decomposition products of the NBSK paper treated with modified starch.

Comparing the results of the measurements of the NBSK paper treated with mod. starch to the TGA analysis of the treated UKP paper, it can be seen that the decomposition of the lignin containing UKP paper treated with mod. starch behaves slightly different. The curves displayed in Figure 76 have a closer resemblance to the results of the UKP treated with APP, shown in Figure 67, than with the

previous TGA results of the NBSK paper treated with mod. starch. The TGA and DTG curves show, as in the case of the mod. Starch treated NBSK, a small mass loss at 224 °C before the main decomposition at 267 °C. In contrast, the distinct separation of the decomposition of the flame retardant before the main mass loss is not as pronounced when using the G.S. curve. As with the UKP paper treated with APP, the remaining lignin on the fibres cause an earlier mass lass that overlaps with the decomposition of the flame retardant. In addition, the gap seen in the decomposition of the mod. starch treated NBSK paper between the main mass loss and the decomposition of the residue is not seen in the G.S. curve of the UKP paper. Nevertheless, the ongoing detection of released gaseous products in the G.S. curves further support the previous assumption that the mod. starch leads to a more unstable residue or an incomplete conversion of the cellulose by the flame retardant, which then decomposes further.

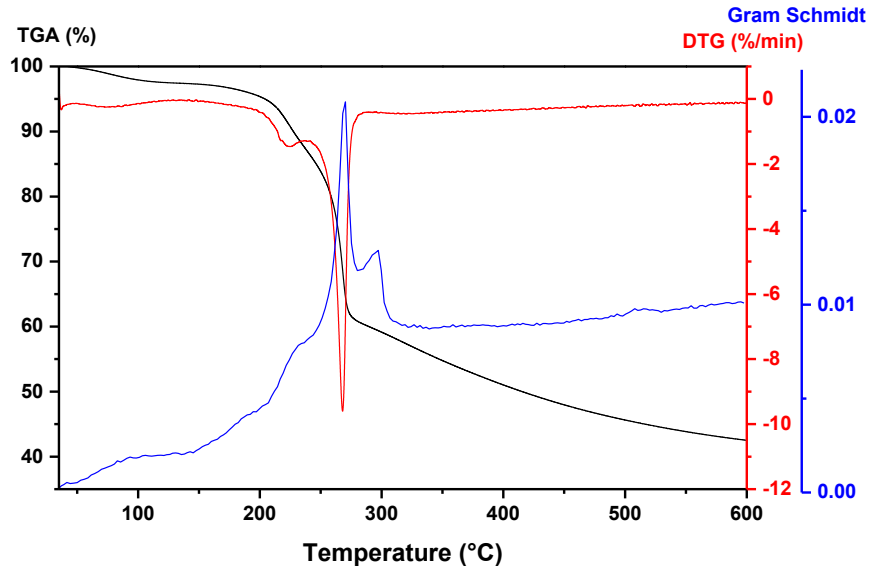

Figure 76: TGA, DTG and Gram Schmidt curves of UKP paper coated with mod. starch (14.76 w%).

A further comparison of the results of the TGA analysis summarized in Table 20 with the results of the mod. starch treated NBSK paper in Table 18, the remaining lignin on the UKP fibres doesn't seem to have an influence on the start of the decomposition temperatures and the remaining residues at the end of the measurement.

Table 20: Summary of mass losses, DTG and Gram Schmidt peaks of UKP paper coated with mod. starch (14.76 w%).

Range Temperature (°C)	Mass loss (%)	DTG Peak (°C)	G.S. Peak (°C)	Residue (%)
35 - 151	2.8	-	-	42.4
151 - 237	9.8	224.5	231.6	
237 - 285	27.1	267.7	270.3	
285 - 600	17.9		297.3	

The decomposition behaviour of the mod. starch treated UKP paper material examined by MS spectroscopy shows no significant differences with regard to the influence of the lignin to the results of the NBSK paper analysis. As already noted with the peaks regarding the decomposition steps in the TGA measurements, the gaseous products detected in the MS analysis appear at the same temperatures with similar intensities (Table 21). Noticeable is, that just as in the investigations on the flame retardant APP, the formation of pyruvic aldehyde cannot be detected in the investigation shown in Figure 77. This seems to further confirm the previously made statement in the section for the NBSK paper coated with APP, that the influence of lignin results in a decreased efficiency of the functional groups within the flame retardants, causing a reduced formation of pyruvic aldehyde.

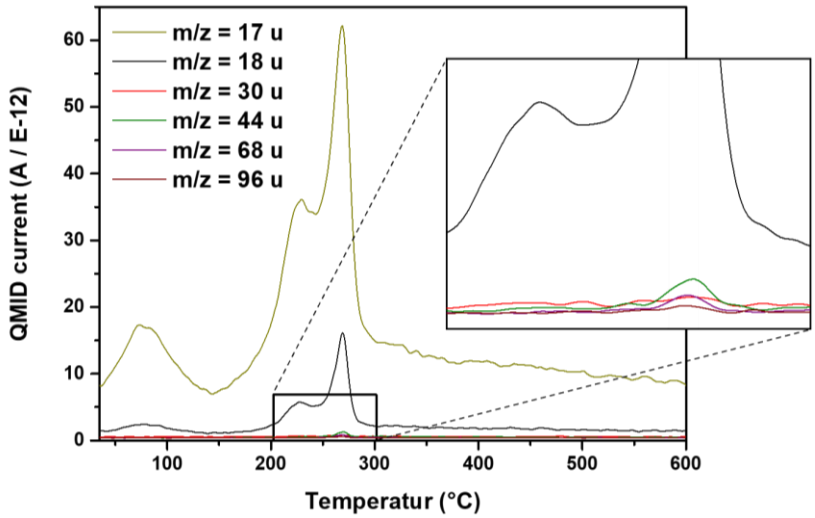

Figure 77: Detected molecular ions of the mod. starch treated UKP paper decomposition in the TGA-MS measurements.

Table 21: Detected peak temperatures of the TGA-MS and -FTIR measurements of the mod. starch treated UKP papers and their assignments.

TGA - MS			TGA - FTIR	
Mass/Charge ratio	**Peak-Temperatures [°C]**	**Molecule**	**Absorption bands**	**Peak-Temperatures [°C]**
m/z = 17 u	229, 268	NH_3	967 – 905 cm^{-1}	197, 270
m/z = 18 u	227, 268	H_2O	1701 – 1694 cm^{-1}	237, 269, 298
m/z = 28 u	-	CO	2191 – 2164 cm^{-1}	269, 394
m/z = 30 u	-	CH_2O	-	-
m/z = 44 u	270	CO_2	2378 – 2302 cm^{-1}	230, 269, 321

In the FTIR measurements, no differences can be detected due to the influence of the lignin in the UKP papers. The temperatures at which the corresponding peaks appear are almost identical in both papers (Table 19/Table 21). Since the amount of phosphate groups introduced, when applying the flame

retardant to the papers was similar between the different flame retardants, the influence of the structural composition of the flame retardant could be noticeable here.

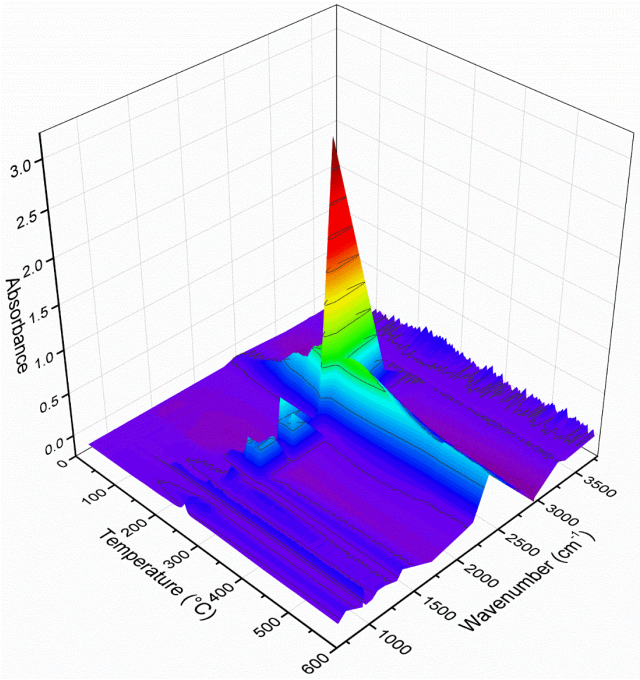

Figure 78: 3D FTIR-spectra of the detected decomposition products of the UKP paper treated with modified starch.

Amphy

The ammonium phytate flame retardant is the second bio-based flame retardant investigated on both paper materials. In contrast to the APP and mod. starch flame retardant, the AmPhy flame retardant is not polymeric and can be better described as a salt. In the following AmPhy is examined for its decomposition behaviour.

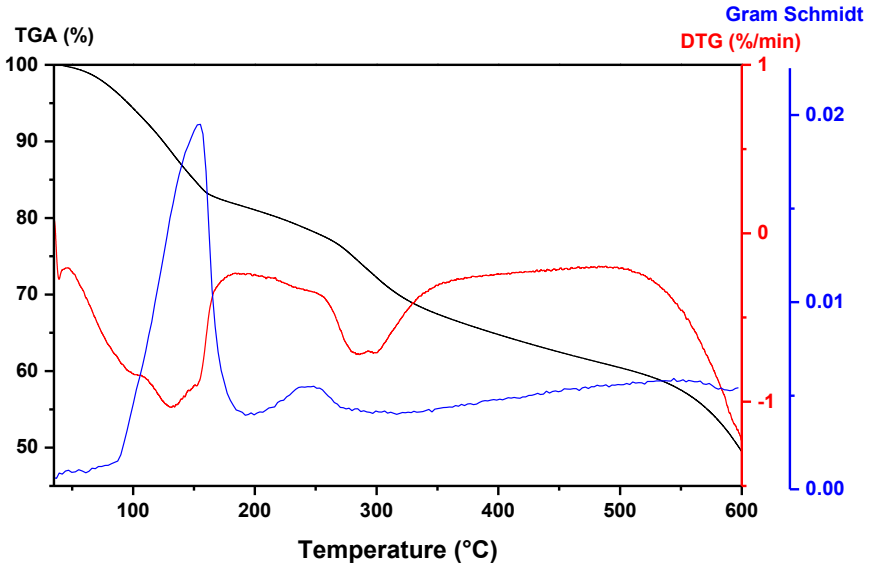

Figure 79: TGA, DTG and Gram Schmidt curves of the flame retardant AmPhy.

For the decomposition of AmPhy three steps can be determined using TGA. As AmPhy is a salt, the early mass loss in the TGA curve in the range of 35 – 185 °C, displayed in Figure 79, can be attributed to the evaporation of water due to its hygroscopic properties and in agreement with the previous investigations of the other flame retardants to the release of ammonia. Followed by a second minor step in the range of 185 – 357 °C, the flame retardant seems to decompose forming a residue, which then continues to reduce in mass until the end of the measurements. Around 50 w% of the initial mass remains as residues. The G.S. curve for the investigation of AmPhy shows two peaks during the measurement, but also indicates, that after the second peak gaseous products continue to emerge till the end of the measurement. The results of the TGA analysis are summarized in the following Table 22.

Table 22: Summary of mass losses, DTG and Gram Schmidt peaks of AmPhy.

Range Temperature (°C)	Mass loss (%)	DTG Peak (°C)	G.S. Peak (°C)	Residue (%)
35 - 185	18.3	131.6	155.2	49.3
185 - 357	14.7	286.0	245.8	
357 - 600	17.7			

The MS results obtained from the TGA-FTIR-MS measurements reflect the course of the TGA results. Over the period of the investigation two peaks can be determined. As displayed in Figure 80, only ammonia (m/z = 17 u) and water (m/z = 18 u) were detected as gaseous product emerging from the decomposition of the flame retardant and the peaks of emergence correlate with the mass loss steps detected in TGA. The release of water at around 100 °C can be attributed to the evaporation of residual water in the salt, as mentioned before, and the peak 290 °C to the release of water due to condensation reactions between the phosphate groups of AmPhy. These condensation reactions, in which the thermal more stable P-O-P bridges are formed, can also explain the high yield of residue at the end of the TGA measurements. The two different release peaks of ammonia can be explained similarly to the different releases of ammonia in the APP flame retardant. At 130 °C, ammonia is released with weaker interactions with the phosphate groups, whereas at 290 °C, with the onset of the condensation reaction the ionic interactions reduce causing the release. Important to note is that despite the cyclohexane ring forming the centre of the phytic acid, no CO_2 was detected in the MS measurements.

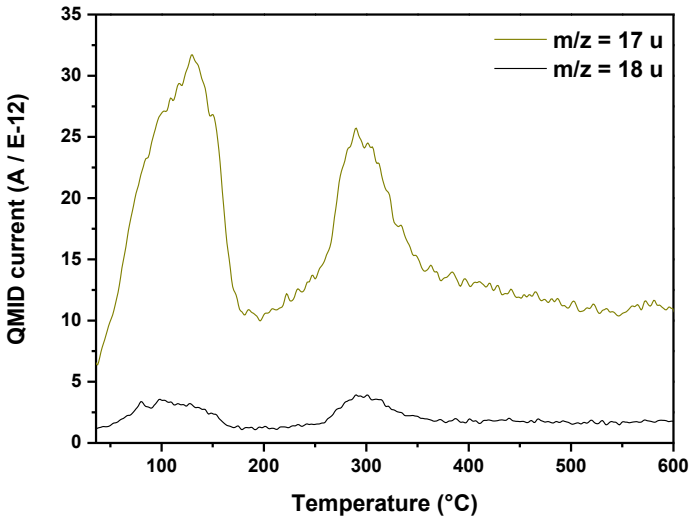

Figure 80: Detected molecular ions of the decomposition of the AmPhy flame retardant in the TGA-MS measurements.

Table 23: Detected peak temperatures of the TGA-MS and -FTIR measurements of the AmPhy flame retardant and their assignments.

TGA - MS			TGA - FTIR	
Mass/Charge ratio	**Peak-Temperatures [°C]**	**Molecule**	**Absorption bands**	**Peak-Temperatures [°C]**
m/z = 17 u	130, 290	NH_3	967 – 905 cm^{-1}	156, 242
m/z = 18 u	98, 290	H_2O	1701 – 1694 cm^{-1}	92, 294
m/z = 44 u	-	CO_2	2378 – 2302 cm^{-1}	-

The FTIR results summarised in Table 23 further confirm the results obtained by the MS measurements. In addition, as shown in Figure 81, the FTIR spectra indicates a peak at vibrational bands at 2350 cm^{-1}, which is consistent with the continuous release after the second mass loss step in the TGA measurements and would match the release of CO_2. As with the APP flame retardant studies, these vibrational bands can also indicate the release of P-H containing gaseous products. As both possible emerging products could not be further identified, no further statements can be made in this regard.

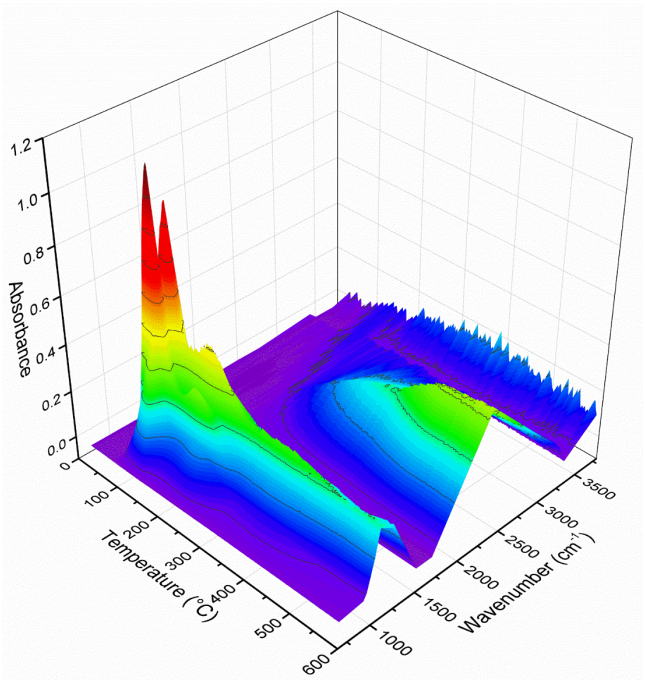

Figure 81: 3D FTIR-spectra of the detected decomposition products of the ammonium phytate flame retardant.

In summary, the decomposition products released by the decomposition of the flame retardant AmPhy are not expected to overlap with the products of the paper decomposition.

To further distinguish the influences of the flame retardant on the decomposition of the paper materials, the AmPhy flame retardant was investigated in two different concentrations. In order to achieve the largest effect for the TGA-FTIR-MS investigation, the papers with the lowest and highest amounts of applied flame retardant are used. In the following Figure 82 the results of the TGA measurements are displayed in (a) for the NBSK paper treated with the lower amount of the AmPhy flame retardant (7.38 w%), which is not sufficient to cause self-extinguishing properties, and in (b) the NBSK paper to which an excess of the AmPhy flame retardant (11.94 w%) was applied.

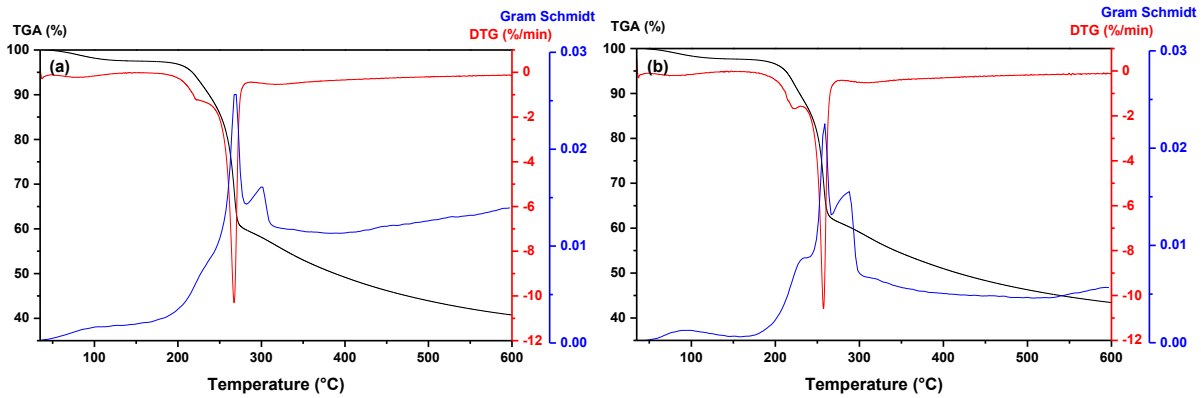

Figure 82: TGA, DTG and Gram Schmidt curves of NBSK paper coated with a low (7.38 w%) [a] and a high (11.94 w%) [b] amount of AmPhy.

Analysing the course of the TGA curves of the NBSK paper treated with AmPhy, it becomes evident that the results show similarities with the results of the APP investigations. The TGA curves displays for

both flame retardant loading amounts the decomposition occurring in one step. It is notable that for the paper with the lower amount of flame retardant the main mass loss takes place at a temperature of 266 °C, while for the higher amount the temperature is reduced to 257 °C. Since only the amount of flame retardant on the paper was varied, this shift in the onset of the decomposition of the paper can be attributed to the amount of flame retardant applied. This indicates that the thermal stability of the cellulose matrix material is as assumed beforehand reduced by the higher amounts of phosphate groups entering the dehydration reactions. In addition, the accessibility or the reactivity of the phosphate groups also seems to have an influence. The TGA results of the APP flame retardant, shown in Figure 64, indicate that the greatest mass loss also occurs at 257 °C. Comparing the phosphorous content of the average NBSK-APP sample (1.91 w%) with the most heavily loaded NBSK-AmPhy sample (2.52 w%) , it can be seen that the AmPhy sample has a higher phosphorous content. Based on the assumption that the decomposition temperature of the cellulose decreases with increasing proportion of phosphate groups, it can be concluded that the equal decrease in decomposition temperature of the APP flame retardant in comparison to the AmPhy flame retardant results from the polymeric structure and the thus resulting better accessibility of its phosphate groups to the cellulose over a larger area.

On further evaluation of the TGA measurements of both AmPhy samples, the DTG curves as well as the G.S. curves indicate smaller peaks before the main mass loss, which become more prominent with increasing amounts of applied flame retardant. These peaks appear at the same temperature of 222 °C for both samples, suggesting that this peak is due to an interaction of the flame retardant rather than the cellulose. In contrast, a greater influence of the applied amounts of flame retardants can be seen in the decomposition of the residues after the main decomposition peak. With the lower amount of Amphy, a continuous decrease of the residue can be observed up to a remaining amount of 40.7 w%. During this process, the G.S. curves show a constant stream of emerging gases. At the highest AmPhy quantities used, a decrease of the residue can be seen up to a residue of 43.3 w%, but the continues release of gaseous products remains significantly lower. Due to the small amount of flame retardant, at which the paper is not yet self-extinguishing, there is less to no complete formation of the aforementioned P-C-P bridges, which means that the residue is less thermally stable and thus begins further decomposition earlier.

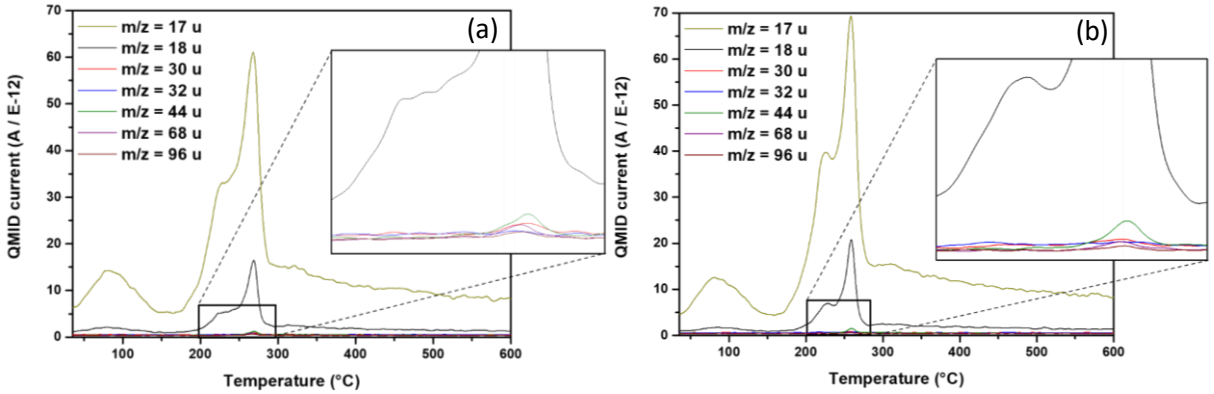

Figure 83: Detected molecular ions of the decomposition of NBSK paper coated with a low (7.38 w%) [a] and a high (11.94 w%) [b] amount of AmPhy.

The influence of the increased amount of applied AmPhy flame retardant can also be seen in the MS spectra shown in Figure 83. The first peak, displayed at 222 °C in the DTG curve, correlates to the peaks at approx. 226 °C in the MS measurements and can be attributed to the emergence of water and ammonia. The fact that the peak does not shift with the increasing flame retardant content can be attributed to the incipient decomposition of the flame retardant. This is also supported by the fact that the peak becomes more distinct as the proportion of flame retardant increases. In the case of the APP flame retardant this release relates to the release of less stable ammonia groups and the release of water due to condensation reactions. In agreement with the results of the TGA investigations, the peak in the MS spectrum relating to the decomposition of the cellulose, shifts with increasing proportions of flame retardant to lower temperatures. Furthermore, it can be observed that the proportion of the remaining emerging gaseous products shift towards CO_2 at the same time. With the increased amount of flame retardant, charring is promoted, which traps the carbon-atoms in the residue.

Table 24: Detected peak temperatures of the TGA-MS and -FTIR measurements of the NBSK paper treated with a low (7.38 w%) [a] and a high (11.94 w%) [b] amount of AmPhy flame retardant and their assignments.

TGA - MS				**TGA - FTIR**		
Mass/Charge ratio	**Peak-Temp. (low AmPhy) [°C]**	**Peak-Temp. (high AmPhy) [°C]**	**Molecule**	**Absorption bands [cm^{-1}]**	**Peak-Temp. (low AmPhy) [°C]**	**Peak-Temp. (high AmPhy) [°C]**
m/z = 17 u	227, 267	225, 258	NH_3	967 – 905	270	258
m/z = 18 u	224, 267	228, 258	H_2O	1760 – 1694	261, 297	259, 289
m/z = 28 u	-	-	CO	2191 – 2164	270, 380	258, 361
m/z = 30 u	269	-	CH_2O	-	-	
m/z = 32 u	-	-	CH_3OH	-	-	
m/z = 44 u	269	259	CO_2	2378 – 2302	270, 336, 519	258, 312

One main effect that is noticeable due to the influence of the increasing flame retardants content is the promotion of incomplete combustion, which leads to charring. Besides the appearance of water and ammonia in the FTIR measurements, shown in Figure 84, the biggest change is the reduction of emerging CO_2 as the proportion of flame retardants increases and the continuous release of water. In the NBSK sample with a lower proportion of AmPhy, complete decomposition of the cellulose to CO_2 seems to take place and the resulting charring also continues with the formation of CO_2. With the high AmPhy content, it can be clearly seen that more H_2O is produced during the decomposition of the cellulose, indicating an increased amount of condensation reactions by the phosphate groups due to the excess of flame retardant. The amount of emerging CO also increases, which results from a higher proportion of incomplete decompositions. The resulting higher flame retardant effect caused by the implementation of a higher amounts of AmPhy is therefore a synergy of several effects. The increase of released inert gaseous products like CO, CO_2 and ammonia as well as H_2O cause a dilution of the gas phase and suffocate the flames. In addition, the incomplete combustion causing charring and the higher thermal stability of the char form a heat and diffusion barrier that impedes the pyrolysis of the underlying material and the possible diffusion of oxygen and decomposition products.

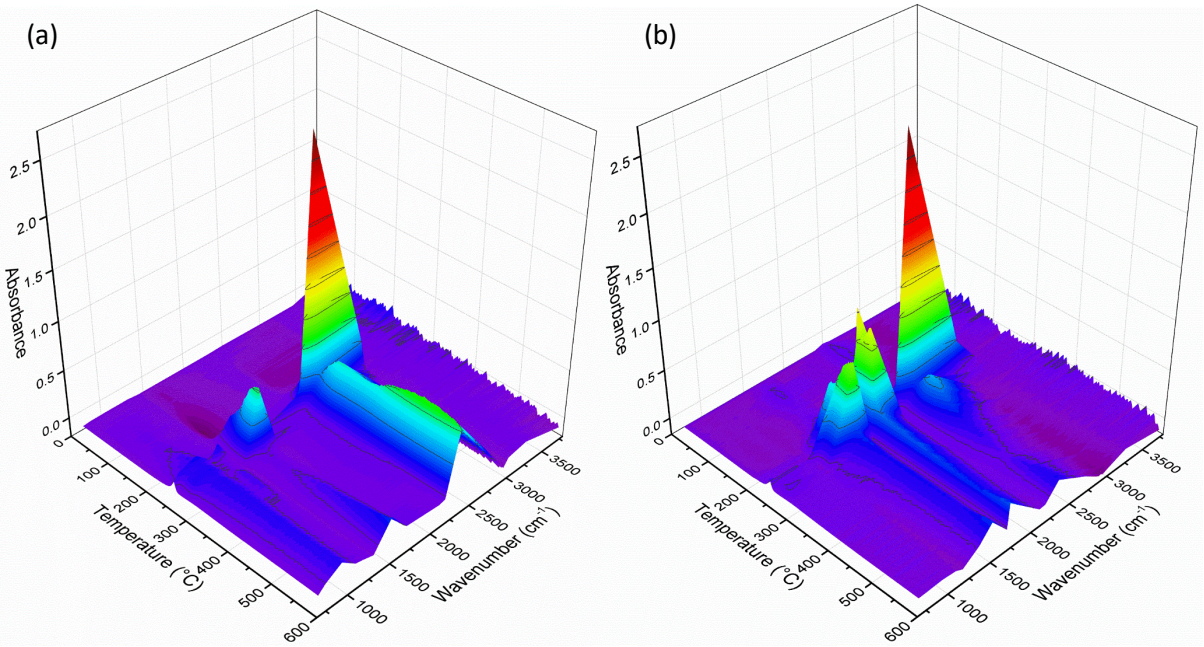

Figure 84: 3D FTIR-spectra of the detected decomposition products of the NBSK paper treated with a low (7.38 w%) [a] and a high (11.94 w%) [b] amount of AmPhy flame retardant.

Following the investigations of the AmPhy treated NBSK papers the results of the TGA measurements for the treated UKP papers treated with low (7.72 w%) [a] und high (11.62 w%) [b] amounts of AmPhy are shown in Figure 85.

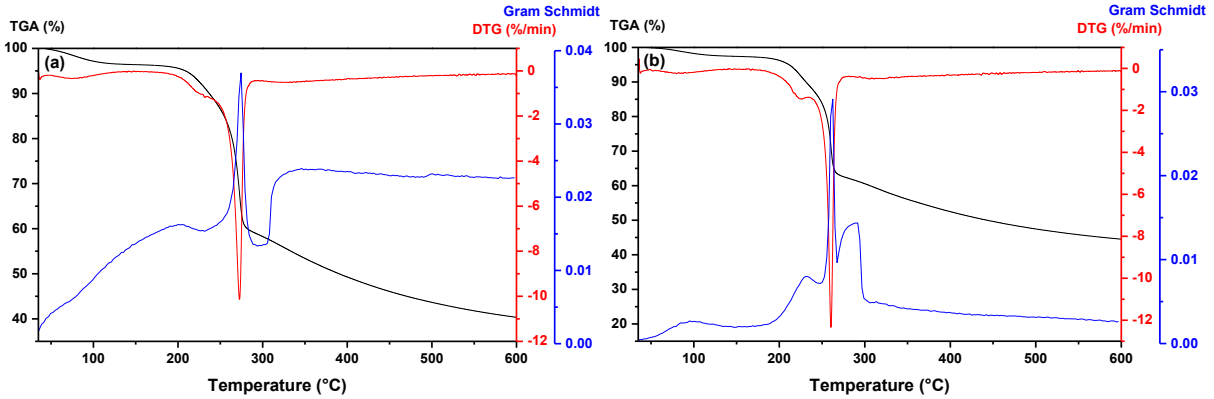

Figure 85: TGA, DTG and Gram Schmidt curves of UKP paper coated with a low (7.72 w%) [a] and a high (11.62 w%) [b] amount of AmPhy.

If the results of the UKP measurements are put in relation to the NBSK measurements, the influence of the different amounts of flame retardant used shows a comparable behaviour. As with the treated NBSK paper, a peak in the DTG curve at 225 °C for the start of the decomposition of the flame retardant can be seen for the two different quantities of flame retardant used. In the temperature range of 35 – 200 °C an increase of released gaseous products is notable in the G.S. curve for the UKP paper with lesser applied amount of AmPhy, which cannot be explained in this context. Following the onset of the decomposition of the flame retardant the main mass loss during the TGA measurements occurs. As before, this is attributed to the decomposition of the cellulosic material and the temperature of this main decomposition effect declines from 272 °C to 260 °C with increasing amount of flame retardant. When the decomposition of the resulting residue begins, a first difference between the NBSK and the lignin containing UKP paper can be seen. With the smaller amount of flame retardant introduced, a constant flow of released gas products can be seen in the G.S. curve. This is much less pronounced in the case of the examined NBSK paper and thus suggests the formation of a thermally less stable residue. The stronger pronouncement of this effect can be attributed to the influence of the lignin and the reduced effectivity of the flame retardant due to the lower number of OH-groups accessible. Since this effect is does not occur with the higher addition of flame retardant, the overloading with flame retardant and the resulting increased input of phosphate groups seems to negate this effect. At the end of the measurements, the remaining residues are 40.3 w% for the lower amount of AmPhy and 44.5 w% for the higher amount. This result of increased amount of remaining char due to a higher implementation of flame retardant follows the line with the previous results.

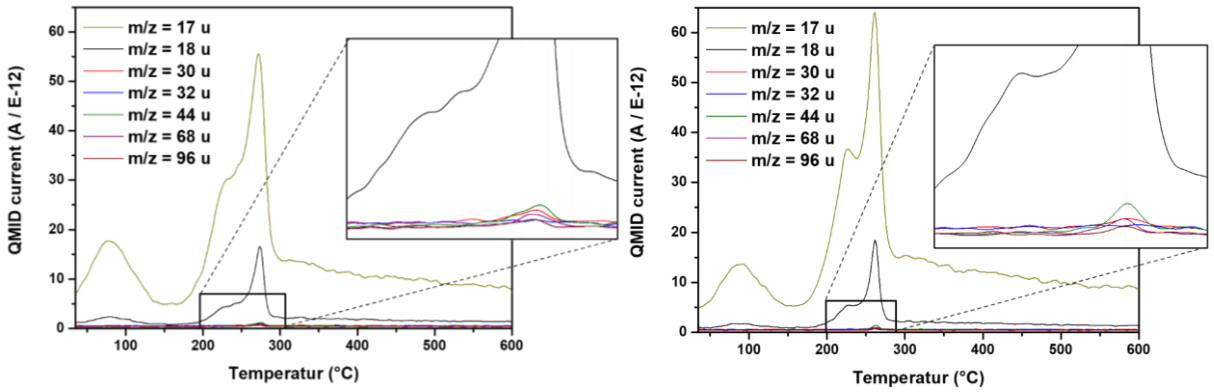

Figure 86: Detected molecular ions of the decomposition of UKP paper coated with a low (7.72 w%) [a] and a high (11.62 w%) [b] amount of AmPhy.

Following the TGA measurements, the results of UKP paper MS measurements, which are shown in Figure 86, display no significant difference to the results of the NBSK papers, which are shown in Figure 83. The peaks of the emerging gaseous decomposition products appear at similar temperatures and the course of the curves similar as well. In addition, the influence of the increasing amount of flame retardant can be observed in the resulting pronouncement of the peaks and the shift towards the emergence of CO_2. The peak temperatures of both MS measurements are listed in Table 25.

Table 25: Detected peak temperatures of the TGA-MS and -FTIR measurements of the UKP paper treated with a low (7.72 w%) [a] and a high (11.62 w%) [b] amount of AmPhy flame retardant and their assignments.

TGA - MS				TGA - FTIR		
Mass/Charge ratio	**Peak-Temp. (low AmPhy) [°C]**	**Peak-Temp. (high AmPhy) [°C]**	**Molecule**	**Absorption bands [cm^{-1}]**	**Peak-Temp. (low AmPhy) [°C]**	**Peak-Temp. (high AmPhy) [°C]**
m/z = 17 u	229, 271	226, 261	NH_3	967 – 905	275	207
m/z = 18 u	227, 273	225, 261	H_2O	1760 – 1694	275, 305	236, 263,290
m/z = 28 u	-	-	CO	2191 – 2164	275, 390	262, 375
m/z = 30 u	273	-	CH_2O	-	-	-
m/z = 32 u	-	-	CH_3OH	3004 – 2906	275	-
m/z = 44 u	274	262	CO_2	2378 – 2302	275, 330	262, 315

Looking at the results of the FTIR measurements in Figure 87, differences between the results of the NBSK paper and UKP paper measurements can be seen. Comparing the graphs of the NBSK and UKP paper with low amounts of AmPhy applied, the most striking difference is the occurring peak at 1701 – 1694 cm^{-1} for the UKP paper, which is attributed to the emergence of H_2O. As the second peak for water at 1561 – 1471 cm^{-1} is detected in the FTIR spectrum, this difference is not attributed to the influence of the lignin but can rather be attributed to an analytical error. Apart from this difference,

no further major differences can be observed, besides the continuous release of CO_2 after the main decomposition for the lower applied amount of AmPhy.

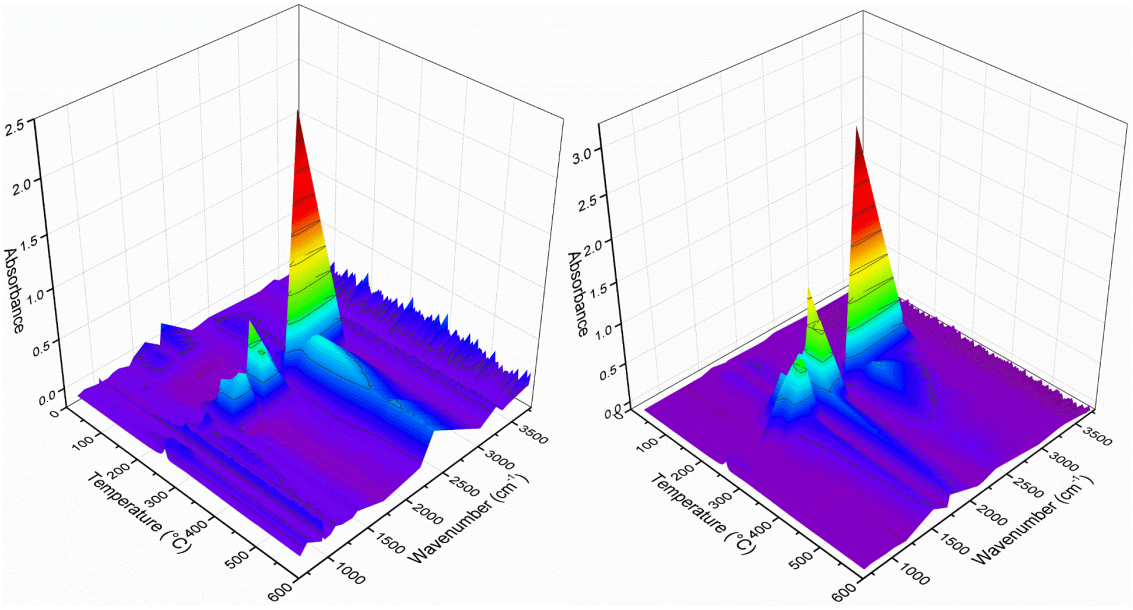

Figure 87: 3D FTIR-spectra of the detected decomposition products of the UKP paper treated with a low (7.72 w%) [a] and a high (11.62 w%) [b] amount of AmPhy flame retardant.

6.5. Influences on mechanical properties

In order to further determine the applicability of flame retardants in the "Building with Paper" project, the mechanical properties of NBSK and UKP papers coated with flame retardants were investigated in the following. As previously explained, the high mechanical properties of the papers result from the many hydrogen bonds that the cellulose fibres can form. In addition, the length and the resulting number of fibre-fibre connection points as well as the entanglements play an important role. These factors can be influenced by the addition of additives, for example reducing the number of hydrogen bonds, thus changing the mechanical properties. Therefore, the width-related breaking load was determined for the treated papers and the results are shown in the following Figure 88.

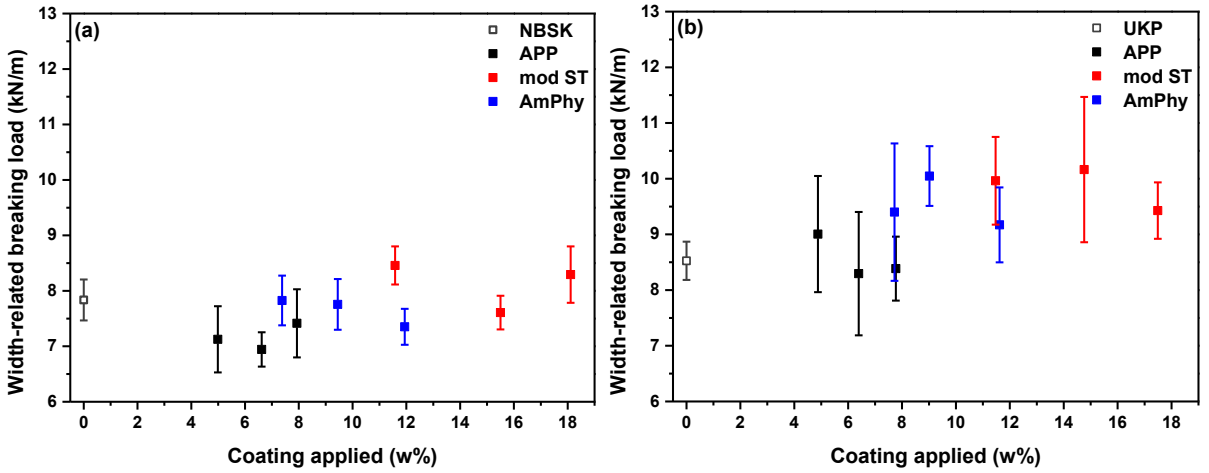

Figure 88: Width-related breaking load for the NBSK (a) and UKP (b) papers coated with different amounts of APP (black), mod. ST (red) and AmPhy (blue).

From the results of the tensile test, it becomes evident, that the three different flame retardants influence the width-related breaking load of the papers slightly differently. In addition, a difference between the NBSK and the UKP papers can be observed. Since bleaching not only removes residual lignin and accompanying substances, but also affects the cellulose fibre, this can have the effect that the strength of the bleached pulp is lower than that of the unbleached pulp. In addition, lignin, as it is an amorphous polymer, increases due to its chemical composition the breaking load. Further the research of JANNE LAINE ET AL. showed the correlation between swelling of fibres and tensile strength. Their conclusion included that swelling results in a more flexible fibre with increased surface, which results in a higher tensile strength due to the larger contact area.[237] From the results in chapter 5.1.2, we know that the remaining moisture in the UKP papers is 1 w% larger than for the NBSK papers. It can be assumed, that the higher moisture content leads to an increased swelling and thus the higher mechanical properties. Looking at the results for the NBSK papers in Figure 88 (a) it can be seen that APP overall decreases the breaking load of the NBSK paper, whereas AmPhy roughly maintains the level and mod. starch slightly increases the breaking load. With respect to the UKP papers in Figure 88 (b), the influence of the flame retardants seems to be less pronounced, since APP only minimally lowers the width-related breaking load and in the case of AmPhy and mod. starch the breaking load increases. Further it can be said, that within the error bars, the breaking strength decreases for each flame retardant as the applied amounts increase.

The increase of the breaking load due to the application of mod. starch can be explained with the similar structure of starch to cellulose. The starch chain can form hydrogen bonds with the cellulose chain, which don't negatively affect the mechanical properties and thus create an increase in fibre-fibre connections causing the increase in the breaking load. This effect is known as the "Schwimmhaut" effect.[238] However, since some of the OH-groups of the starch are converted into phosphate or carbamate groups this interaction is lower than with pure starch.

The reason why APP and Amphy have reduced mechanical properties can be explained with its ionic structure. As described in chapter 2.2.2, during the pulping as well as the bleaching process, functional groups, such as carboxyl group or sulfonic acids, are formed on the bleached and unbleached fibres. As these are negatively charged, same as the phosphate groups in the flame retardants, a repulsion occurs which can disrupt the fibre-fibre interaction and thus weakens it. This weakening therefore results in a smaller width-related breaking load. In addition, a difference in the influence of APP and Amphy can be seen. This difference can be explained by the structural composition of both flame retardants. Since APP is a polyelectrolyte and AmPhy is a salt, AmPhy can, due to its smaller structure, diffuse into the fibre, whereas APP accumulates on the surface. The penetration into the fibre reduces the previously described effect of repulsion, which is why the sheets treated with AmPhy have a higher breaking strength than the sheets with APP.[239–241]

6.6. Discussion and conclusion

The aim of the investigations of the three different phosphorous-based flame retardants was to investigate their behaviour and effectiveness on two different paper substrates. The fibre composition of these two papers was chosen similarly to create comparability. The difference between the two paper substrates was that the UKP paper, in contrast to the NBSK paper, is unbleached and thus still has a larger proportion (8 w%) of residual lignin. The influence of this residual lignin on the effect of the flame retardants was also investigated. In order to be able to investigate the influence of the flame retardants precisely, the concentrations for each flame retardant were empirically chosen so that, with minimal amount required, self-extinguishing properties are generated on the papers. For APP the required amount was around 6.5 w%, for mod. starch 15 w% and for AmPhy 9.25 w%. To be able to further investigate the flame retardants the amounts applied were cut and increased by 20 % to create non self-extinguishing papers and papers with an excess of flame retardant. The exact amounts applied were checked by ICP-AES to ensure the possibility of correlation between the three flame retardants. During the preliminary test, a first observation was made that the influence of an insufficient amounts of flame retardant causes a decrease in the burning speed/rate of the samples. It became apparent that regardless of the flame retardant, the degree of decrease was similar and did not decrease further with increasing amounts of flame retardant. This led to the conclusion that the flame retardants reduce the burning speed to a certain level and that a self-extinguishing effect is induced only when a critical amount of added flame retardant is reached. Using the prepared samples, the effectivity of the flame retardants in combination with the amounts applied to the NBSK and UKP paper was investigated using cone calorimetry. The HRR showed that UKP had a higher peak HRR in each of the cases. In addition, repetitive releases of heat were detected in the treated UKP papers, indicating an apparent initial poorer flame retardancy on the UKP paper. This assessment was also supported by the course of the

UKP HRR curves, as they were broader than the NBSK curves, which indicated lower protective properties. The treated UKP papers also perform worse with regard to the THR of the samples tested, as more heat is released overall during combustion, which further corresponds to poorer flame retardancy. Comparing the flame retardants with each other, it can be seen that mod. starch has the worst flame retardant properties on paper, as it releases the most amounts of heat. APP and AmPhy are about in the same range, although AmPhy, when relating the properties to the phosphate groups introduced, introduces slightly more groups to reach the same level as APP. Besides heat release, smoke release is an important factor when considering flame retardants. In the case of smoke development, the behaviour is the reverse of before. Here it can be seen that the papers examined, which are impregnated with mod starch, release the least amount of smoke and APP releases the largest amounts. However, it should be noted that paper or cellulose generally emits little smoke during combustion and the measured values are very close to the detection limit. In addition, an increase in TSR can be seen with increasing flame retardant content in the papers. This indicates that the more char is introduced into the material by the increase in applied flame retardant, the more smoke is produced. This also explains why mod. starch gives the best values here, where it is assumed to have the worst flame retardant properties. If the samples are viewed in an imaging analysis method such as SEM, the influences of the flame retardants on the paper matrices can be seen. When untreated paper is burnt, only the ash remains in the form of a skeletal scaffold of the fibres. Due to the influence of the flame retardants, the entire structure of the paper can be preserved because of the charring behaviour introduced. Only minor differences between the flame retardants were observed, such as the formation of white dots with APP or the swelling of individual fibres due to the mod. starch. Based on cross-section images of the burnt samples, it was also possible to recognise that the fibres swell up when they burn and thus take up a larger volume, which is further supporting the desired heat barrier properties. In addition, the fibres show clean fractions in the cutting edge, which displays a change in mechanical properties of the fibres as they show a more ceramic behaviour due to carbonization. This behaviour ensures the stability of the flame-retardant material compared to the unprotected paper even after burning and therefore gives a huge benefit when building with these materials. In order to show the differences between the flame retardants and the influence of the residual lignin on the UKP regarding the decomposition behaviour, the combined analytical method of TGA-FTIR-MS is used. To exclude possible influencing factors of the flame retardants on the evaluation of the treated NBSK and UKP papers and to investigate the decomposition behaviour of the different flame retardants, they were first examined individually. No adverse effects were detected for APP and AmPhy, and only mod starch, showed slight possibilities of overlay due to its chemical similarity to cellulose. For the untreated papers, it becomes apparent that the decomposition process of the papers is shifted by the influence of the lignin. In the case of the UKP paper, the weight loss in the TGA analysis

starts earlier than in the case of the NBSK paper due to the earlier onset of decomposition of the lignin. This is related to the decomposition of the substituted groups and aliphatic structures within the lignin structure leading to CO_2 release from the carboxyl groups, H_2O from the hydroxyl groups, CO from the weakly bound oxygen groups in the temperature range of 150 – 300 °C. However, in combination with the three flame retardants, both the NBSK and the UKP paper showed a comparable onset of decomposition at approximately 223 °C. As this temperature is below the temperature of the onset of the UKP paper, no influence of the lignin can be determined. In the corresponding FTIR and MS spectra, the release of NH_3 and water can be detected at this point, indicating that at this temperature the phosphate groups of the flame retardants react with the OH-groups of the cellulose and the lignin in a dehydration reaction. This was also confirmed by the experiments with different amounts of the flame retardant AmPhy, which had no influence on this onset temperature. It was found that the intensity of the peak increased with increasing applied amount, which can be attributed to the increased availability of phosphate groups and thus a larger amount of reaction partners. In addition, the results of the TGA analyses show that the use of flame retardants reduced the temperature of the main decomposition of the sample. This is 342 – 345 °C for the untreated NBSK and UKP papers, while it is 257 – 267 °C with the flame retardants. The investigations with the AmPhy flame retardant have shown that this reduction in temperature is related to the amounts of flame retardant used. As the proportion increases, the decomposition temperature decreases, which suggest that as the amount of phosphate groups introduced increases and the number of dehydration reactions increases, there is a decrease in the hydrogen bonds of the cellulose. The loss of these hydrogen bonds, which are a cause of the thermal stability of cellulose, leads to this drop in the temperature of the main decomposition point Furthermore, the use of flame retardants causes a change in the decomposition mechanism. Whereas various gaseous products, besides water, CO and CO_2, like formaldehyde, methanol and acetaldehyde for the untreated NBSK and UKP paper occur during the decomposition, the amounts of released gases are drastically reduced due to the use of flame retardants. Under the influence of the flame retardant the main emerging gases are water, CO and CO_2. This reduced emerging of formaldehyde, methanol and acetaldehyde can be attributed to the shift in the decomposition mechanism of the cellulose as well as to the promoted charring, which results in the entrapment of carbon in the residue. This shift in the gaseous products released can be well observed in the comparison of the different amounts of AmPhy flame retardant applied, where these decrease with increasing AmPhy content. Interesting to note is the occurrence of pyruvic aldehyde. Pyruvic aldehyde is normally a minor intermediate product in the decomposition of cellulose and does not appear in the studies of untreated cellulose. However, in the NBSK papers treated with APP or mod. starch, it is visible in the MS spectra in small amounts, which illustrates the shifted decomposition due to the use of flame retardants from the cellulose. This molecule does not appear in the analysis of the UKP paper,

which may be a further indication that the flame retardant effectivity is reduced on the lignin-containing papers. As the research of TETSUO HONMA ET AL. stated, that the formation of pyruvic aldehyde is catalysed by the presents of water, it was possible to assume, that the non-detectability with the UKP papers was due to a lower precipitation of the dehydration reaction caused by the lignin. The biggest difference between the individual flame retardants and the two types of paper can be seen in the formation of the residue and its stability. Particular attention should be paid to the difference between NBSK and UKP papers. In the case of UKP papers containing lignin, after the peak of the main decomposition of the material, a further constant flow of gases produced can be seen in the G.S. curves. With the NBSK papers, on the other hand, this release decreases rapidly after the formation of the residue or coal and is much less pronounced. However, this behaviour in the UKP papers is also found in the investigations of the AmPhy flame retardant with the lower application quantities. This leads again to the conclusion that the flame retardant is inhibited in its protective mechanism by the lignin remaining on the fibres. Comparing the amounts of residues remaining due to the increased charring behaviour of the flame retardants, it can be seen that the residue increases from about 20 w% for the untreated papers to 42 – 45 w% due to the flame retardants. There are only slight gradations for the different flame retardants, with the mod. starch generating slightly less residue than the APP flame retardant. However, even with excessive application of AmPhy to the papers, only maximum values of around 45 w% residue are obtained, which is why no clear statements can be made about the different efficacies of the flame retardants via this factor.

In addition, the influences of the applied flame retardants on the mechanical properties of the NBSK and UKP papers was investigated, since in the context of the project “Building with paper” the preservation of these is an important point. It was shown that by incorporating APP the lowest stability was obtained in the papers and by incorporating mod. starch, due to its similar chemical structure to cellulose, the highest stability was generated. The lower breaking strength in the papers due to the introduction of APP and AmPhy could be attributed to the influence of the introduced negatively charged phosphate groups on the fibre-fibre interactions. The negative influence of the AmPhy flame retardant is less pronounced, since it is a chemically small salt molecule and not a polyelectrolyte like APP and can therefore diffuse into the fibre. As a result, it has less influence on the interactions at the surface of the fibres.

7. Summary

The aim of this work was to investigate the factors influencing the burning behaviour of paper. An understanding of the combustion behaviour was to be generated, depending on the changes in the burning behaviour due to changed intrinsic properties. An adequate method had to be developed for the precise determination of the burning behaviour. The changes in the intrinsic properties of the papers were to be investigated using multi-method analysis in order to form a link between structural changes and combustion behaviour. The results of these investigations were to be used in a further step in combination with flame retardants. The influence of different phosphorus-based flame retardants as well as the influence of the varying paper matrix was to be determined, to generate an understanding of important parameters in the flame retardancy of paper. In addition, the mechanical properties obtained due to the modification with flame retardants were investigated in order to draw a conclusion for applicability in construction with paper.

In order to address the question of the factors influencing the burning behaviour of paper in the first part of the work, a matrix of different paper samples was set up. Both the change in the intrinsic properties of the paper and the influence of the grammage were taken into account. In addition, the paper samples were made from bleached and unbleached paper in order to investigate the influence factor of remaining lignin on the paper fibres. For the fundamental investigation of the paper materials with very similar burning behaviour, a computer-based optical evaluation method was developed that allowed the most accurate possible determination of the burning speed. This precise determination allowed to differentiate the burning speeds for the papers with their different properties, which in combination with the analyses of the changed intrinsic properties allowed conclusions to be drawn. In addition, both the horizontal and the vertical burning direction were investigated, to study different burning mechanism. During the investigations of the burning speed, it was found that in contrast to the horizontal burning direction, the burning speed in the vertical burning direction increases with increasing degree of calendering. Furthermore, a dependence of the burning speeds on the grammage could be observed. The effect of increasing burning speed with increasing degree of calendering decreased with increasing grammage. This untypical behaviour of increasing burning speed with increasing densification was then to be explained by means of the investigations of the changed intrinsic properties. When comparing the bleached NBSK papers with the lignin containing UKP papers, it was found that the UKP papers generally have a higher burning speed. This difference also decreased with increasing grammage and degree of calendering.

To determine the cause of the increasing burning speed with increasing degree of calendering the changes in the intrinsic properties of the papers due to calendering were investigated. The focus of the investigations was set on the analysis of the porosity, residual moisture, thermal degradation and

properties, crystallinity and thermal conductivity. With regard to the analysed changes in porosity and residual moisture due to calendering in the two paper types, no correlation was found that would explain the variations in the measured burning speeds. The investigations into the thermal decomposition of the papers showed that the UKP papers onset of decomposition starts at an earlier temperature than the NBSK papers. This earlier decomposition can was attributed to the lower onset decomposition temperature of lignin, which was caused by the cleavage of weaker C-C bonds or functional groups and is further supported by the possibility of delocalisation within the aromatic compounds. The subsequent measurements of the thermal properties by means of cone calorimetry showed that the heat release peak of the UKP papers is lower as well, which initially contradicts the faster burning of the UKP papers, since the heat release is an indication of better flammability and a higher flashpoint. But since the heat release curve of the UKP papers has a broader shape, the total heat release of the papers is comparable and the differences in the heat release rates was assumed to be minor influential on the burning speed. In addition, no influence of the calendering or the grammage was observed, what further indicates, that the heat release rate is not the decisive factor for the changes in the burning speed. Further investigation the changes in the intrinsic properties of the papers due to calendering, solid-state NMR displayed a change in crystallinity. A correlation was determined, that showed a decrease in crystallinity with increasing degree of densification due to calendering, which can be attributed to the forcible disruption of crystalline regions. As changes in the crystallinity cause a change in the thermal conductivity, the thermal conductivity for the different papers was measured. Using lock-in thermography and differential scanning calorimetry to determine thermal diffusivity and the specific heat capacity, the thermal conductivity was calculated. The results for the thermal conductivity showed an increase in thermal conductivity with increasing calendering, which correlates with the increase in burning rate and thus provided an argument for the influence of calendering on the burning speed. The better thermal conductivity causing a faster distribution of heat within the paper leading to pre-drying and initiation of decomposition of the material, which promotes faster firing. The difference in fire behaviour in horizontal and vertical fire direction could subsequently be explained by the different thermal convection of the corresponding burning direction. By combining these different analysis methods, it could therefore be shown, that the influence on the different burning behaviour of the papers is caused by a change in thermal conductivity. The differences in the burning behaviour of the NBSK paper and the UKP further results from their different onset of decomposition.

In the second part of the work, the effects and influences of flame retardants on bleached and unbleached papers as well as the changes in the degradation process were investigated. For this purpose, three different phosphorus-based flame retardants – ammonium polyphosphate, a starch modified with phosphate and carbamate groups and ammonium phytate – were applied in three

different quantities to bleached and unbleached papers. The applied amounts for the flame retardants were chosen to describe three criteria. At the lowest applied amounts, the flame retardant should not be sufficient for effective flame retardancy, while the medium amount was chosen so that a minimal application of the flame retardant would result in a self-extinguishing effect. The highest application amount represented an excess of flame retardant. The applications were analysed by ICP-AES to determine the phosphorus content applied and to be able to use this as a reference. During the preliminary tests, it was found that all flame retardants lowered the burning speed of the papers to the same level at the lower application rates. This gave a first insight into the need for a critical amount of flame retardant to achieve a self-extinguishing effect. To determine the efficiency of the three flame retardants, the heat release rate, total heat release and smoke production rate were determined using cone calorimetry. A correlation was found between the amount of applied flame retardant and the decrease in peak heat release rate and total heat release. These decreased with increasing amount of flame retardant applied. It was further noted that the bleached NBSK paper and the unbleached UKP paper differed in their behaviour. The UKP papers showed recurrent heat release and the total heat released was higher than the treated NBSK papers, which displayed a contradiction to the measurements of the untreated papers. Furthermore, the geometry of the HRR curves suggested that the two papers had different charring behaviour, indicating a negative influence of the residual lignin in the UKP papers on the protective mechanism. To further investigate possible differences in the mode of action of the flame retardants, SEM images of the protected papers were taken before and after combustion. Only minor differences between the flame retardants were found, which could be attributed to the combustion of the flame retardants themselves. However, the influence of the protection provided by the flame retardants and the preservation of the fibre structures due to increased charring were clearly evident. The influence of the flame retardants on the decomposition of the two papers was analysed via TGA FTIR-MS. When comparing the results for the decomposition of the pure papers with those of the flame retardant papers, a clear reduction in the decomposition temperature was observed. This was determined to the onset of the flame retardant mechanism by the introduced phosphate groups. In addition, due to the changed degradation behaviour, an earlier decomposition of the cellulose material was observed with regard to an increased charring behaviour. The gaseous decomposition products released in the process were further investigated and a decrease in the carbonaceous decomposition products was detected. The influence of the flame retardants, which enhances the charring behaviour of the samples and thus entrapping carbon in the residue, results in the decrease of carbonaceous decomposition products and in an increased release of water and carbon dioxide, further supporting the protective mechanism of the flame retardants. In addition, a correlation between the influence of the flame retardant and the formation of pyruvic aldehyde was found. The conjecture was made, that the increased release of water due to the dehydration reaction

of the flame retardants increased the conversion of glyceraldehyde to pyruvic aldehyde. The absence of pyruvic aldehyde was then attributed to a reduced efficacy by the lignin. Further regarding the influence of lignin, it was found that there was poorer char behaviour when flame retardants were used. In addition, further gaseous decomposition products were detected in the flame retardant NBSK papers, which did not occur in the investigations of the UKP papers. Since the influence of the flame retardants inhibits the decomposition of the matrix material, this was another indication of poor functioning of the flame retardants on the UKP papers. The combination of these and the previous results during the analysis of the influential factors of flame retardancy on papers led to the assumption, that the remaining lignin in the UKP papers lead to a lower reactivity of the flame retardant. This could be explained by a reduced number of OH-groups by the lignin, which are essential for the function of phosphate group-based flame retardants.

Using this information in combination with the results of the investigation on the influence of the flame retardants on the mechanical properties of the papers, a proposal regarding the project “Building with paper” can be made. Since sustainability plays an important role, the mod. starch and the Amphy flame retardant are directly compared to each other. This work has shown that the flame retardant effectiveness in terms of critical minimum quantity introduced, charring behaviour and reduction of heat released was in every case better with AmPhy used than with the mod. starch. While the breaking load due to the introduction of AmPhy is lower than with mod. starch, it does not fall below the measured mechanical properties of the untreated cellulose, which is why the AmPhy flame retardant would be recommended for the use of “Building with paper” within the framework of this thesis.

In summary, this work provides a detailed overview of the factors that influence the burning behaviour and also the fire protection of paper. In the process, a new method for the precise determination of the burning speed was elaborated. In addition, an understanding of the correlation between intrinsic paper properties and the fire behaviour of paper was created. The influencing factors of different flame retardants were investigated and a correlation between the matrix material and the efficiency of some phosphor-containing flame retardants could be established. To further define these influences of the paper matrix material, papers based on other pulps with other compositions would have to be compared to those results presented in this work. In addition, research of the influence of other types of flame retardants on the investigated pulps could further improve the understanding of the flame retardant – cellulose interactions.

8. Experimental Section

This chapter summarises all the experimental details. The descriptions include both the preparation of the paper substrates used and their modifications through either compression or the treatment with flame retardants. In addition, the procedures for their characterisations with the various analytical methods are explained.

8.1. Material preparations

The following experiments comprise papers with different grammages. Part of the papers, which did not contain wet strength agents, were used for the calendering tests while papers with wet strength agents were coated with flame retardants in a further step. Details of these experimental processes are described below. The pulps used for paper production were organised and milled in cooperation with the Department of Paper Manufacturing and Mechanical Process Engineering at the TU Darmstadt. The modified starch, which is used as a flame retardant, was provided by the *Jäckering* company. All the other chemicals were purchased commercially and applied without further purification.

8.1.1. Production of papers

Two different fibre types were used to produce the laboratory papers. To ensure uniformity throughout the BAMP! – project, only northern bleached softwood kraft (NBSK) and unbleached kraft pulp (UKP) with a Schopper-Riegler number of 25 ± 2 were used. Therefore, a Voith LR 40 laboratory refiner was utilised with a refiner speed of 2000 rpm and 2,231 kW power. The fibres thus prepared were then processed with a Rapid-Köthen sheet former according to DIN 54358 and ISO 5269/2. In order to ensure the stability of the manufactured sheets during the subsequent coating process in the size press 1 w%, in regard to the paperweight, wet strength agent Glyoxal was added to the sheet formation process. These papers were produced with a grammage of 100 g/m^2, whereas the papers without wet strength agents for the burning behaviour test had grammages of 100 g/m^2, 150 g/m^2 and 200 g/m^2. Only papers with a maximum error of 2 % in respect to the paperweight were used.

8.1.2. Calendering

To change the paper intrinsic properties of the laboratory sheets cold calendering was performed at room temperature. Thereby different sets of forces and rollers were deployed in a “Laborkalander” from *Sumet Systems GmbH*. The different experimental sets can be found in the following Table 26.

Table 26 : Calender settings for varying the intrinsic paper properties

Reference	Force [N/cm]	Roller
KO	0	-
K1	10	Steel / Composite
K2	150	Steel / Composite
K3	300	Steel / Steel

8.1.3. Size press application

Impregnating the paper samples with the flame retardants was performed by using the sizing press SP 6513 from Mathis. For this purpose, papers modified with a wet strength agent were used. The parameters of the sizing press were set to a contact pressure of 1 bar and a running speed of 1 m/s. All flame retardants were dissolved in water. A minimum of 35 mL for each applied solution and two impregnation steps in succession were necessary to achieve a complete impregnation of the papers. The coated papers were then placed in the fume cupboard and dried overnight. To determine the actual amount of flame retardant applied to the papers, the so-called “wet pickup” was measured. For this purpose, the papers were weight before and after coating. By knowing the concentration of the flame retardant solutions, the quantity applied could be determined.

8.1.4. Formulation of ammonium phytate

For the formulation of the ammonium phytate, 50 mL of a 25 w% ammonia solution was placed in a beaker. Next, phytic acid was added in portions to keep the solution at an adequate temperature until neutralisation, which was controlled by means of pH indicator paper. Afterwards 1 mL of ammonia solution was given to the solution in excess to ensure that all the phytic acid was converted to the respective salt. The mixture was cooled down to room temperature and then precipitated in an amount of acetone that was five-times the volume of the reaction solution. Two liquid phases arose. After sufficient mixing and subsequent separation of the two phases, the supernatant acetone was decanted and replaced by fresh acetone. The viscosity of the resulting phytate solution increases due to the water loss during the process. In the last step, the acetone was replaced with anhydrous acetone. A whitish salt precipitates. The supernatant acetone was extracted via a frit and the product was stored in an airtight container. The yield was 95%.

8.2. Instrumentation

All the analytical methods used to characterise the processed papers are described below. Since the investigation of the fire properties of the pressed papers involves changes in the intrinsic properties of

the paper, these are addressed in the first part (Chapter 8.2.1). The second part (Chapter 8.2.2) refers to the thermal analytical methods and flame retardancy tests. If not explicitly mentioned, the corresponding measurement was carried out at the Ernst-Berl-Institute of the TU Darmstadt in the working group of Prof. Dr. M. Biesalski.

8.2.1. Measurement of the paper´s intrinsic properties

Burning speed measurements

In order to measure the burning speed of the different papers, samples with dimensions of 120 x 25 mm^2 were prepared. These were clamped into a retainer, as displayed in the methods chapter 4.1 Figure 16, preventing them from bending or deforming during the burning process. The paper stripes were ignited with a Bunsen burner as the burning process was recorded with a Canon EOS 600D camera. The setup was illuminated with a Godox SL-200W spotlight. The obtained videos were imported as an image stack using Fijii Image J and converted to 8-bit photos. By adjusting the threshold, black and white images were obtained that reflect the progress of the fire front. This progress was then evaluated with the help of MatLab as explained in chapter 4.1. Each paper was measured six times.

Mercury porosimetry

For the determination of pore size distribution, specific pore volume and porosity of the samples, mercury porosimetry was conducted at the PTS Heidenau with the Poremaster® GT (33/60) from Quantachrome Instruments. Therefore approximately 200 mg of the sample were added to the sample chamber before it was filled with mercury by applying an increasing external pressure (1-5000 PSI). For each paper substrate at least, double determinations were performed. The obtained results are summarized in Table XXX.

Scanning electron microscopy (SEM)

To gain a visual impression of the influence of the calendering on the morphology of the paper structure, scanning electron microscope images were taken. The device used was a Philips XL30 FEG. The paper samples were sputter-coated by sputtering with 15 nm of a platinum-palladium alloy with a composition of 80:20 using a sputter coater 208 HR with the associated thickness measuring unit mtm 20 from Cressington.

Moisture residue

The residual moisture within the paper samples was determined with a Satorius MA 45 dry balance. Therefore, the samples were heated up to 115 °C for at least 15 min to reach dry weight and no more

weight loss was detectable. The difference of the two weight corresponds to the moisture content within the paper.

Tensile strength

Tensile strength of the paper samples was determined as an average of ten samples according to DIN ISO 1924-2 with a *Zwick Z1.0* with a 1 kN load cell using the software *testXpert II V3.71* (*ZwickRoell GmbH & Co. Kg*) in a controlled environment with 23 °C and 50% r.h..

Solid-state NMR spectroscopy

All solid-state NMR measurements were performed in the research group of Prof. Dr. G. Buntkowsky at the TU Darmstadt on a Bruker Avance III 300 MHz spectrometer at an operating frequency of 75.46 MHz for ^{13}C and 300.11 MHz for ^{1}H. The sample were placed into a 4 mm ZrO_2 rotor and measured with a broadband $^{1}H/X$ probe at a MAS spinning frequency of 5 kHz. $^{1}H \rightarrow ^{13}C$ cross-polarization (CP MAS) was used with a linear ramp at a contact time of 3 ms, an acquisition time of 49 ms and a TPPM15 [242] broadband decoupling sequence during acquisition. The recycle delay was set to 2 s and 2048 scans were used. All spectra were referenced to TMS (0 ppm) with adamantane (39.5 ppm) as an external standard. The obtained data were analysed with MestreNova.

Lock-In thermography

Thermal diffusivity measurements were conducted in the working group of Prof. Dr. M. Retsch at the University Bayreuth using lock-in thermography according to the specifications of KOPERA ET AL.[243] Samples were coated with 25 nm of carbon on one side and mounted on a sample holder. The holder was set in a vacuum chamber with an optically transparent window behind and an IR-transparent sapphire window in front of the sample. An intensity modulated line laser (Schäfter+Kirchhoff, λ=520 nm, P0=55 mW) was focused on the carbon coated back side of the sample. This caused temperature modulations inside the free-standing sample that were monitored with an Infratec ImageIR 9430 research IR-camera equipped with a M=1.0x microscopy objective. Online lock-in evaluation using the IRBIS active online software directly provided phase and amplitude images. Linearization of both signals and fitting perpendicular to the laser line allowed calculation of the thermal diffusivity.

8.2.2. Thermal properties

Thermogravimetric analysis (TGA)

Thermogravimetric analyses were carried out in a temperature range from 25 to 600 °C with a heating rate of 10 °C/min to investigate the thermal stability of the different compressed papers. The TGA

apparatus used was a Mettler Toledo TGA 1, operating in air or nitrogen environment under a 30 mL/min gas flow using 100 mg alumina crucibles.

TGA-FTIR-MS

Thermogravimetric analysis coupled with Fourier-transformed infrared spectroscopy and mass spectroscopy was performed by the working group of Prof. R. Riedel at the TU Darmstadt. The simultaneous thermal analysis was carried out using a TGA/DTA STA 449C Jupiter from NETZSCH coupled to FTIR TENSOR 27 from Bruker and a MS QMS 403C Aëolos. The heating rate was set to 5 K/min in a temperature range of 35 to 600 °C.

Inductively coupled plasma atomic emission spectroscopy (ICP-AES)

To determine the phosphorus ratio of the flame retardants on the paper samples ICP-AES was conducted at the C2MA Mines Alès, France in the group of Rodolphe Sonnier. For these measurements three samples were tested per reference. The samples were randomly cut out of the paper and had a sample weight of approximately 50 mg. In a first step the samples were mineralized with a MILESTONE 1200-MEGA. The dilution volume of the mineralisation was 50 mL with 1 mL HNO_3 (63 %) and 2 mL H_2SO_4 (98 %). The obtained solution was then analysed with the ICP-AES device HORIBA Jobin Yvon – Activa M. Beforehand the device was calibrated with phosphorous solutions of 5, 25 and 100 mg/L.

Cone Calorimetry

The resistance to heat flux of the paper samples was investigated using cone calorimetry in cooperation with Federico Carosio at the Polytechnic University of Turin and the Fraunhofer LBF Institute Darmstadt. The measurements were carried out under an irradiative heat flux of 25 kW/m^2 and the square samples had dimensions of 100 x 100 mm^2. The procedure is derived from ISO 5660 and described at TATA ET AL. 2011.[244] For this the samples were fixed with a wide-meshed stainless steel grid to prevent the samples from bending. Measured parameters were heat release rate (HRR, kW/m^2) and the respecting peak of heat release rate (PHRR, kW/m^2) as well as the total heat release (THR, kW/m^2) and the smoke production rate (SPR, m^2/m^2). All cone calorimetry experiments were repeated four time for each sample to ensure the reproducibility and significance of the data.

8.2.3. Reagents, solvents and materials

OC – Chemical dispensary of the organic and inorganic chemistry at the TU Darmstadt

Acetone	OC
Ammonia solution (25 w%)	OC
APP	*Clariant Plastics & Coatings GmbH*
Glyoxal	
NBSK fibres	APV TU Darmstadt
UKP fibres	APV TU Darmstadt
Mod. starch	Jäckering GmbH
Phytic acid	Sigma-Aldrich

List of abbreviations and symbols

5-HMF 5-hydroxymethyl-furfural
AGU ..... anhydroglucose unit
AmPhy ..... ammonium phytate
AOX ..... absorbable organic halides
APP ..... ammonium polyphosphate
ATH ..... aluminium trihydroxide
BAMP! ..... Building with Paper!
c_p ..... heat capacity
CrI ..... crystallinity index
DAP ..... diammonium phosphate
DMPMP ..... 3-(dimethylphosphono)-N-methylolpropionamide
DP ..... degree of polymerisation
DS ..... degree of substitution
DTA ..... differential thermal analysis
DTG ..... derivative thermogravimetry
ECF ..... Elemental chlorine-free process
FR ..... flame retardant
FTIR ..... fourier-transform infrarad spectroscopy
G.S. ..... Gram-Schmidt
GA ..... glyceraldehyde
GC ..... gas chromatography
GP ..... glucopyranose
HA ..... hydroxyacetone
HAA ..... hydroxyacetaldehyde
HPLC ..... high-performance liquid chromatography
HRR ..... heat release rate
ICP-AES ..... Inductively coupled plasma atomic emission spectroscopy
IR ..... infrared
LBL ..... layer-by-layer
LG ..... levoglucosan
LOI ..... limiting oxygen index
MAO ..... monoammonium phosphate
MDH ..... magnesium dihydroxide
MLR ..... mass loss rate
mod. ST ..... modified starch
MS ..... mass spectrometry
NBSK ..... northern bleached softwood kraft pulp
NMR ..... nuclear magnetic resonance spectroscopy
PA ..... pyruvic aldehyde
PHRR ..... peak heat release rate
pMLR ..... peak mass loss rate
PY ..... pyrolysis
RSE ..... radical stanilisation energy

SEM ..... scanning electron microscopy
SPR ..... smoke production rate
TCF ..... Total chlorine-free process
T_g ..... glass-transition temperature
TGA ..... thermogravimetric analysis
THPC ..... tetra-kis (hydroxymethyl) phosphonium chloride
THR ..... total heat release
TSR ..... total smoke release
TTI ..... time to ignition
UKP ..... unbleached kraft pulp
UV ..... ultraviolet
w% ..... weight percent
X_c ..... fraction of crystalline cellulose
α ..... thermal diffusivity
λ ..... thermal conductivity
ρ ..... density

List of figures

Table directory

Scheme directory

9. References

[1] N. N. Brushlinsky, M. Ahrens, S. V. Sokolov, P. Wagner, *World Fire Statistics*: *Report No. 23*, 2018.

[2] "DIN 4102-1:1998-05, Brandverhalten von Baustoffen und Bauteilen_- Teil_1: Baustoffe; Begriffe, Anforderungen und Prüfungen,".

[3] A. R. Horrocks and D. Price, *Fire Retardant Materials*, Elsevier Reference Monographs, s.l., 2001.

[4] R. Weber, "Relevance of BFRs and thermal conditions on the formation pathways of brominated and brominated–chlorinated dibenzodioxins and dibenzofurans," *Environment international*, vol. 29, no. 6, pp. 699–710, 2003.

[5] R. J. Law, A. Covaci, S. Harrad et al., "Levels and trends of PBDEs and HBCDs in the global environment: status at the end of 2012," *Environment international*, vol. 65, pp. 147–158, 2014.

[6] S. D. Jadhav, "A review of non-halogenated flame retardant," *The Pharma Innovation*, vol. 7, 5, Part F, p. 380, 2018.

[7] S. V. Levchik and E. D. Weil, "A Review of Recent Progress in Phosphorus-based Flame Retardants," *Journal of Fire Sciences*, vol. 24, no. 5, pp. 345–364, 2006.

[8] E. Schmitt, "Phosphorus-based flame retardants for thermoplastics," *Plastics, Additives and Compounding*, vol. 9, no. 3, pp. 26–30, 2007.

[9] R. Pfaendner and T. Melz, "Biogenic Plastic Additives," in *Biological Transformation*, pp. 161–178, Springer, 2020.

[10] Global Alliance for Buildings and Construction, International Energy Agency and the United Nations Environment Programme, "2019 Global status report for buildings and construction: Towards a zero-emission, efficient and resilient buildings and construction sector,".

[11] A. H. Buchanan and S. B. Levine, "Wood-based building materials and atmospheric carbon emissions," *Environmental Science & Policy*, vol. 2, no. 6, pp. 427–437, 1999.

[12] A. Torres, J. Brandt, K. Lear et al., "A looming tragedy of the sand commons," *Science (New York, N.Y.)*, vol. 357, no. 6355, pp. 970–971, 2017.

[13] D. M. J. S. Bowman, J. K. Balch, P. Artaxo et al., "Fire in the Earth system," *Science (New York, N.Y.)*, vol. 324, no. 5926, pp. 481–484, 2009.

[14] R. A. Corry, "Fundamentals of fire investigation," in *Handbook on firesetting in children and youth*, pp. 75–98, Elsevier, 2002.

[15] H. W. Emmons, "Fire and fire protection," *Scientific American*, vol. 231, no. 1, pp. 21–27, 1974.

[16] P. Atkins and J. de Paula, "Atkins' physical chemistry - 4th edition: Black-body radiation," pp. 284–286.

[17] R. Stephen, *An introduction to combustion: concepts and applications - 2nd edition*, McGraw-Hill, 1996 p. 305-362.

[18] C. L. Tien and S. C. Lee, "Flame radiation," *Progress in Energy and Combustion Science*, vol. 8, no. 1, pp. 41–59, 1982.

[19] P. Boulet, G. Parent, Z. Acem et al., "On the emission of radiation by flames and corresponding absorption by vegetation in forest fires," *Fire Safety Journal*, vol. 46, 1-2, pp. 21–26, 2011.

[20] R. Siegel, *Thermal radiation heat transfer - 4th edition*, CRC press, 2001, p.530 - 547.

[21] J. C. Biordi, "Molecular beam mass spectrometry for studying the fundamental chemistry of flames," *Progress in Energy and Combustion Science*, vol. 3, no. 3, pp. 151–173, 1977.

[22] W. C. Gardiner, "The Chemistry of Flames," *Scientific American*, vol. 246, no. 2, pp. 110–125, 1982.

[23] J. Troitzsch, *Plastics flammability handbook: principles, regulations, testing, and approval*, Hanser Munich, Germany, 2004.

[24] C. A. Wilkie and A. B. Morgan, *Fire retardancy of polymeric materials*, CRC press, 2009.
[25] K. Schmidt-Rohr, "Why Combustions Are Always Exothermic, Yielding About 418 kJ per Mole of O 2," *Journal of Chemical Education*, vol. 92, no. 12, pp. 2094–2099, 2015.
[26] A. Kylili and P. A. Fokaides, "Policy trends for the sustainability assessment of construction materials: A review," *Sustainable Cities and Society*, vol. 35, pp. 280–288, 2017.
[27] R. J. Thomas, "Wood: Structure and chemical composition," ACS Publications, 1977.
[28] J. E. Jakes, C. G. Hunt, S. L. Zelinka et al., "Effects of moisture on diffusion in unmodified wood cell walls: a phenomenological polymer science approach," *Forests*, vol. 10, no. 12, p. 1084, 2019.
[29] D. N.-S. Hon, "Cellulose: a random walk along its historical path," *Cellulose*, vol. 1, no. 1, pp. 1–25, 1994.
[30] J. Credou and T. Berthelot, "Cellulose: from biocompatible to bioactive material," *Journal of Materials Chemistry B*, vol. 2, no. 30, pp. 4767–4788, 2014.
[31] D. Klemm, B. Philpp, T. Heinze et al., *Comprehensive cellulose chemistry. Volume 1: Fundamentals and analytical methods*, Wiley-VCH Verlag GmbH, 1998.
[32] H. A. Krässig, *Cellulose: structure, accessibility and reactivity*, Gordon and Breach Science Publ, 1993.
[33] D. Roy, M. Semsarilar, J. T. Guthrie et al., "Cellulose modification by polymer grafting: a review," *Chemical Society Reviews*, vol. 38, no. 7, pp. 2046–2064, 2009.
[34] R. M. Rowell, *Handbook of wood chemistry and wood composites*, CRC press, 2012.
[35] D. Fengel and G. Wegener, *Wood: chemistry, ultrastructure, reactions*, Walter de Gruyter, 2011.
[36] L. Szcześniak, A. Rachocki, and J. Tritt-Goc, "Glass transition temperature and thermal decomposition of cellulose powder," *Cellulose*, vol. 15, no. 3, pp. 445–451, 2008.
[37] M. Takai and J. R. Colvin, "Mechanism of transition between cellulose I and cellulose II during mercerization," *Journal of Polymer Science: Polymer Chemistry Edition*, vol. 16, no. 6, pp. 1335–1342, 1978.
[38] M. Pauly, S. Gille, L. Liu et al., "Hemicellulose biosynthesis," *Planta*, vol. 238, no. 4, pp. 627–642, 2013.
[39] Ö. Eriksson, D. A. Goring, and B. O. Lindgren, "Structural studies on the chemical bonds between lignins and carbohydrates in spruce wood," *Wood science and technology*, vol. 14, no. 4, pp. 267–279, 1980.
[40] F. M. AL-Oqla and M. S. Salit, "Natural fiber composites," in *Materials Selection for Natural Fiber Composites,* F. M. AL-Oqla and M. S. Salit, Eds., pp. 23–48, Woodhead Publishing, 2017.
[41] A. Sakakibara and Y. Sano, "Chemistry of lignin," *Wood and cellulosic chemistry*, vol. 2, pp. 109–173, 2000.
[42] K. Freudenberg and A. C. Neish, "Constitution and biosynthesis of lignin," *Constitution and biosynthesis of lignin*, 1968.
[43] Fachuang Lu and John Ralph, "Cereal Straw as a Resource for Sustainable Biomaterials and Biofuels: Chapter 6 - Lignin," pp. 169–207.
[44] J. H. Bos and M. Staberock, *Das Papierbuch*: *Handbuch der Papierherstellung*, ECA Pulp & Paper, Houten, 2006.
[45] Q. Wang, M. S. Jahan, S. Liu et al., "Lignin removal enhancement from prehydrolysis liquor of kraft-based dissolving pulp production by laccase-induced polymerization," *Bioresource technology*, vol. 164, pp. 380–385, 2014.
[46] T. K. Das and C. Houtman, "Evaluating chemical-, mechanical-, and bio-pulping processes and their sustainability characterization using life-cycle assessment," *Environmental Progress*, vol. 23, no. 4, pp. 347–357, 2004.

[47] P. Bajpai, ed., *Biotechnology for Pulp and Paper Processing*: *Chapter 7 - Biopulping*, Springer US, Boston, MA, 2012.
[48] H. L. Hintz, "Paper: Pulping and Bleaching," in *Encyclopedia of Materials: Science and Technology,* K. J. Buschow, R. W. Cahn, M. C. Flemings et al., Eds., pp. 6707–6711, Elsevier, Oxford, 2001.
[49] X. Han, R. Bi, H. Oguzlu et al., "Potential To Produce Sugars and Lignin-Containing Cellulose Nanofibrils from Enzymatically Hydrolyzed Chemi-Thermomechanical Pulps," *ACS Sustainable Chemistry & Engineering*, vol. 8, no. 39, pp. 14955–14963, 2020.
[50] X. Lei, Y. Zhao, K. Li et al., "Improved surface properties of CTMP fibers with enzymatic pretreatment of wood chips prior to refining," *Cellulose*, vol. 19, no. 6, pp. 2205–2215, 2012.
[51] G. K. Gupta, H. Liu, and P. Shukla, "Pulp and paper industry–based pollutants, their health hazards and environmental risks," *Current Opinion in Environmental Science & Health*, vol. 12, pp. 48–56, 2019.
[52] G. Singh, S. Kaur, M. Khatri et al., "Biobleaching for pulp and paper industry in India: Emerging enzyme technology," *Biocatalysis and Agricultural Biotechnology*, vol. 17, pp. 558–565, 2019.
[53] M. I. Fonseca, J. I. Fariña, M. L. Castrillo et al., "Biopulping of wood chips with Phlebia brevispora BAFC 633 reduces lignin content and improves pulp quality," *International Biodeterioration & Biodegradation*, vol. 90, pp. 29–35, 2014.
[54] C. J. Behrendt, R. A. Blanchette, M. Akhtar et al., "Biomechanical pulping with Phlebiopsis gigantea reduced energy consumption and increased paper strength:[summary]," *Tappi journal. Vol. 83, no. 9 (Sept. 2000). p. 65.*, 2000.
[55] A. Gonzalo, F. Bimbela, J. L. Sánchez et al., "Evaluation of different agricultural residues as raw materials for pulp and paper production using a semichemical process," *Journal of Cleaner Production*, vol. 156, pp. 184–193, 2017.
[56] D. E. Teixeira, "Recycled old corrugated container fibers for wood-fiber cement sheets," *International Scholarly Research Notices*, vol. 2012, 2012.
[57] B. A. Malo, "Semichemical hardwood pulping and effluent treatment," *Journal (Water Pollution Control Federation)*, pp. 1875–1891, 1967.
[58] H. Wallmo, H. Theliander, A.-S. Jönsson et al., "The influence of hemicelluloses during the precipitation of lignin in kraft black liquor," *Nordic Pulp & Paper Research Journal*, vol. 24, no. 2, pp. 165–171, 2009.
[59] G. Gellerstedt, "Chemistry of chemical pulping," *Pulping chemistry and technology*, vol. 2, pp. 91–120, 2009.
[60] H. Tran and E. K. Vakkilainnen, "The kraft chemical recovery process," *Tappi Kraft Pulping Short Course*, pp. 1–8, 2008.
[61] G. Annergren and U. Germgard, "Process aspects for sulfite pulping," *Appita: Technology, Innovation, Manufacturing, Environment*, vol. 67, no. 4, p. 270, 2014.
[62] Lopes, Alice do Carmo Precci, C. M. Silva, A. P. Rosa et al., "Biogas production from thermophilic anaerobic digestion of kraft pulp mill sludge," *Renewable Energy*, vol. 124, pp. 40–49, 2018.
[63] G. Gellerstedt, "The chemistry of bleaching and post-color formation in kraft pulps," *3rd International Colloqium on Eucalyptus Pulp (ICEP). Belo Horizonte, Brazil. doi*, vol. 10, 2007.
[64] P. Bajpai, *Biermann's Handbook of Pulp and Paper: Volume 1: Raw Material and Pulp Making*: *Chapter 19 - Pulp Bleaching*, Elsevier, 2018.
[65] K. R. Solomon, "Chlorine in the bleaching of pulp and paper," *Pure and applied chemistry*, vol. 68, no. 9, pp. 1721–1730, 1996.
[66] G. Gellerstedt, E. Lindfors, M. Pettersson et al., "Reactions of lignin in chlorine dioxide bleaching of kraft pulps," *Research on chemical intermediates*, vol. 21, no. 3, pp. 441–456, 1995.

[67] R. Evans, R. H. Newman, U. C. Roick et al., “Changes in cellulose crystallinity during kraft pulping. Comparison of infrared, X-ray diffraction and solid state NMR results,” *0018-3830*, 1995.
[68] N. Sharma, N. K. Bhardwaj, and R. B. P. Singh, “Environmental issues of pulp bleaching and prospects of peracetic acid pulp bleaching: A review,” *Journal of Cleaner Production*, vol. 256, p. 120338, 2020.
[69] P. Bajpai, *Pulp and paper industry: chemicals*, Elsevier, 2015.
[70] D. Chu, M. Forbes, J. Backström et al., “Model Predictive Control and Optimization,” *Advanced model predictive control*, p. 309, 2011.
[71] G. Wimmers, “Wood: a construction material for tall buildings,” *Nature Reviews Materials*, vol. 2, no. 12, pp. 1–2, 2017.
[72] R. J. Ross, “Wood handbook: wood as an engineering material,” *USDA Forest Service, Forest Products Laboratory, General Technical Report FPL-GTR-190, 2010: 509 p. 1 v.*, vol. 190, 2010.
[73] N. As, Y. Goker, and T. Dundar, “Effect of Knots on the physical and mechanical properties of scots pine,” *Wood Research*, vol. 51, no. 3, pp. 51–58, 2006.
[74] Ö. Ayan, *Cardboard in architectural technology and structural engineering: A Conceptual approach to cardboard buildings in architecture*, ETH Zurich, 2009.
[75] A. Cripps, “Cardboard as a construction material: a case study,” *Building Research & Information*, vol. 32, no. 3, pp. 207–219, 2004.
[76] A. Buchanan, ed., *Energy and CO2 advantages of wood for sustainable buildings*, Citeseer, 2007.
[77] J. K. Borchardt, “Recycling, paper,” *Kirk-Othmer Encyclopedia of Chemical Technology*, 2000.
[78] A. Zink-Sharp, “The mechanical properties of wood,” *Wood Quality and its Biological Basis. Blackwell Publishing-CRC Press. Biological Sciences Series. Boca Raton, Fla., EUA*, pp. 187–210, 2003.
[79] T. Huber, J. Müssig, O. Curnow et al., “A critical review of all-cellulose composites,” *Journal of materials science*, vol. 47, no. 3, pp. 1171–1186, 2012.
[80] J. Schönwälder and J. Rots, “Mechanical behaviour of cardboard in Construction,” *Cardboard in Architecture*, vol. 7, p. 131, 2008.
[81] H. W. Haslach, “The moisture and rate-dependent mechanical properties of paper: a review,” *Mechanics of time-dependent materials*, vol. 4, no. 3, pp. 169–210, 2000.
[82] H. W. Haslach, “The moisture and rate-dependent mechanical properties of paper: a review,” *Mechanics of time-dependent materials*, vol. 4, no. 3, pp. 169–210, 2000.
[83] H. D. Tiemann, *Effect of moisture upon the strength and stiffness of wood*, US Department of Agriculture, Forest Service, 1906.
[84] M. P. Coughlan and F. Mayer, “The cellulose-decomposing bacteria and their enzyme systems,” *The prokaryotes: a handbook on the biology of bacteria: ecophysiology, isolation, identification, applications, vol. I.,* Ed. 2, pp. 460–516, 1992.
[85] M. Plötze and P. Niemz, “Porosity and pore size distribution of different wood types as determined by mercury intrusion porosimetry,” *European Journal of Wood and Wood Products*, vol. 69, no. 4, pp. 649–657, 2011.
[86] M. J. Moura, P. J. Ferreira, and M. M. Figueiredo, “Mercury intrusion porosimetry in pulp and paper technology,” *Powder Technology*, vol. 160, no. 2, pp. 61–66, 2005.
[87] K. G. Pabeliña, C. O. Lumban, and H. J. Ramos, “Plasma impregnation of wood with fire retardants,” *Nuclear Instruments and Methods in Physics Research Section B: Beam Interactions with Materials and Atoms*, vol. 272, pp. 365–369, 2012.
[88] F. Bulian and J. Graystone, *Wood coatings: Theory and practice*, Elsevier, 2009.
[89] F. J. Kilzer and A. Broido, “Speculations on the nature of cellulose pyrolysis,” *Pyrodynamics. 2: 151-163*, vol. 2, pp. 151–163, 1965.

[90] A. Broido and F. J. Kilzer, “A critique of the present state of knowledge of the mechanism of cellulose pyrolysis,” *Fire Research Abstracts and Reviews. 5 (2): 157-161.*, vol. 5, no. 2, pp. 157–161, 1963.
[91] A. Broido and M. Weinstein, “Low temperature isothermal pyrolysis of cellulose,” in *Thermal analysis*, pp. 285–296, Springer, 1972.
[92] J. Lédé, F. Blanchard, and O. Boutin, “Radiant flash pyrolysis of cellulose pellets: products and mechanisms involved in transient and steady state conditions,” *Fuel*, vol. 81, no. 10, pp. 1269–1279, 2002.
[93] J. B. Wooten, J. I. Seeman, and M. R. Hajaligol, “Observation and characterization of cellulose pyrolysis intermediates by 13C CPMAS NMR. A new mechanistic model,” *Energy & fuels*, vol. 18, no. 1, pp. 1–15, 2004.
[94] T. Hosoya, H. Kawamoto, and S. Saka, “Pyrolysis behaviors of wood and its constituent polymers at gasification temperature,” *Journal of Analytical and Applied Pyrolysis*, vol. 78, no. 2, pp. 328–336, 2007.
[95] J. P. Diebold, “A unified, global model for the pyrolysis of cellulose,” *Biomass and Bioenergy*, vol. 7, 1-6, pp. 75–85, 1994.
[96] D. K. Shen and S. Gu, “The mechanism for thermal decomposition of cellulose and its main products,” *Bioresource technology*, vol. 100, no. 24, pp. 6496–6504, 2009.
[97] S. Li, J. Lyons-Hart, J. Banyasz et al., “Real-time evolved gas analysis by FTIR method: an experimental study of cellulose pyrolysis,” *Fuel*, vol. 80, no. 12, pp. 1809–1817, 2001.
[98] F. Shafizadeh, R. H. Furneaux, T. G. Cochran et al., “Production of levoglucosan and glucose from pyrolysis of cellulosic materials,” *Journal of Applied Polymer Science*, vol. 23, no. 12, pp. 3525–3539, 1979.
[99] O. P. Golova, “Chemical effects of heat on cellulose,” *Russian Chemical Reviews*, vol. 44, no. 8, p. 687, 1975.
[100] M. Essig, “Mechanism of fromation on the major volatile products from the pyrolysis of cellulose,” *Cellulose and Wood*, vol. 841, 1989.
[101] A. D. Pouwels, G. B. Eijkel, and J. J. Boon, “Curie-point pyrolysis-capillary gas chromatography-high-resolution mass spectrometry of microcrystalline cellulose,” *Journal of Analytical and Applied Pyrolysis*, vol. 14, no. 4, pp. 237–280, 1989.
[102] F. Shafizadeh and Y. Z. Lai, “Thermal degradation of 1, 6-anhydro-. beta.-D-glucopyranose,” *The Journal of Organic Chemistry*, vol. 37, no. 2, pp. 278–284, 1972.
[103] H. Kawamoto, H. Morisaki, and S. Saka, “Secondary decomposition of levoglucosan in pyrolytic production from cellulosic biomass,” *Journal of Analytical and Applied Pyrolysis*, vol. 85, 1-2, pp. 247–251, 2009.
[104] Y. F. Liao, “Mechanism study of cellulose pyrolysis,” *HangZhou, China: ZheJiang University*, 2003.
[105] G. N. Richards, “Glycolaldehyde from pyrolysis of cellulose,” *Journal of Analytical and Applied Pyrolysis*, vol. 10, no. 3, pp. 251–255, 1987.
[106] T. Hosoya, H. Kawamoto, and S. Saka, “Different pyrolytic pathways of levoglucosan in vapor- and liquid/solid-phases,” *Journal of Analytical and Applied Pyrolysis*, vol. 83, no. 1, pp. 64–70, 2008.
[107] J. Piskorz, D. Radlein, and D. S. Scott, “On the mechanism of the rapid pyrolysis of cellulose,” *Journal of Analytical and Applied Pyrolysis*, vol. 9, no. 2, pp. 121–137, 1986.
[108] G. A. Byrne, D. Gardiner, and F. H. Holmes, “The pyrolysis of cellulose and the action of flame-retardants,” *Journal of Applied Chemistry*, vol. 16, no. 3, pp. 81–88, 1966.

[109] D. Shen, R. Xiao, S. Gu et al., "The overview of thermal decomposition of cellulose in lignocellulosic biomass," *Cellulose-biomass conversion*, pp. 193–226, 2013.
[110] J. Li, B. Li, and X. Zhang, "Comparative studies of thermal degradation between larch lignin and manchurian ash lignin," *Polymer Degradation and Stability*, vol. 78, no. 2, pp. 279–285, 2002.
[111] M. V. Ramiah, "Thermogravimetric and differential thermal analysis of cellulose, hemicellulose, and lignin," *Journal of Applied Polymer Science*, vol. 14, no. 5, pp. 1323–1337, 1970.
[112] J. A. Caballero, R. Font, and A. Marcilla, "Study of the primary pyrolysis of Kraft lignin at high heating rates: yields and kinetics," *Journal of Analytical and Applied Pyrolysis*, vol. 36, no. 2, pp. 159–178, 1996.
[113] G. Varhegyi, M. J. Antal Jr, E. Jakab et al., "Kinetic modeling of biomass pyrolysis," *Journal of Analytical and Applied Pyrolysis*, vol. 42, no. 1, pp. 73–87, 1997.
[114] J. A. Caballero, J. A. Conesa, R. Font et al., "Pyrolysis kinetics of almond shells and olive stones considering their organic fractions," *Journal of Analytical and Applied Pyrolysis*, vol. 42, no. 2, pp. 159–175, 1997.
[115] E. Jakab, O. Faix, and F. Till, "Thermal decomposition of milled wood lignins studied by thermogravimetry/mass spectrometry," *Journal of Analytical and Applied Pyrolysis*, vol. 40, pp. 171–186, 1997.
[116] Q. Liu, S. Wang, Y. Zheng et al., "Mechanism study of wood lignin pyrolysis by using TG–FTIR analysis," *Journal of Analytical and Applied Pyrolysis*, vol. 82, no. 1, pp. 170–177, 2008.
[117] S. Wang, K. Wang, Q. Liu et al., "Comparison of the pyrolysis behavior of lignins from different tree species," *Biotechnology Advances*, vol. 27, no. 5, pp. 562–567, 2009.
[118] R. A. Fenner and J. O. Lephardt, "Examination of the thermal decomposition of kraft pine lignin by Fourier transform infrared evolved gas analysis," *Journal of agricultural and food chemistry*, vol. 29, no. 4, pp. 846–849, 1981.
[119] K. V. Sarkanen and C. H. Ludwig, *Liguins. Occurrence, formation, structure, and reactions*, 1971.
[120] R. Wittkowski, *Phenole im Räucherrauch: Nachweis und Identifizierung*, VCH, 1985.
[121] W. Fiddler, W. E. Parker, A. E. Wasserman et al., "Thermal decomposition of ferulic acid," *Journal of agricultural and food chemistry*, vol. 15, no. 5, pp. 757–761, 1967.
[122] J. Zhao, W. Xiuwen, J. Hu et al., "Thermal degradation of softwood lignin and hardwood lignin by TG-FTIR and Py-GC/MS," *Polymer Degradation and Stability*, vol. 108, pp. 133–138, 2014.
[123] F. Shafizadeh, *Thermal uses and properties of carbohydrates and lignins*, Elsevier, 2012.
[124] M. Brebu and C. Vasile, "Thermal degradation of lignin—a review," *Cellulose Chemistry & Technology*, vol. 44, no. 9, p. 353, 2010.
[125] W. Mu, H. Ben, A. Ragauskas et al., "Lignin Pyrolysis Components and Upgrading—Technology Review," *BioEnergy Research*, vol. 6, no. 4, pp. 1183–1204, 2013.
[126] P. Kiliaris and C. D. Papaspyrides, "Polymers on fire," in *Polymer green flame retardants*, pp. 1–43, Elsevier, 2014.
[127] J. Green, "Mechanisms for flame retardancy and smoke suppression-a review," *Journal of Fire Sciences*, vol. 14, no. 6, pp. 426–442, 1996.
[128] M. Lewin, "Synergism and catalysis in flame retardancy of polymers," *Polymers for Advanced Technologies*, vol. 12, 3-4, pp. 215–222, 2001.
[129] J. Wagner, P. Deglmann, S. Fuchs et al., "A flame retardant synergism of organic disulfides and phosphorous compounds," *Polymer Degradation and Stability*, vol. 129, pp. 63–76, 2016.

[130] M. Le Bras and S. Bourbigot, “Mineral fillers in intumescent fire retardant formulations—criteria for the choice of a natural clay filler for the ammonium polyphosphate/pentaerythritol/polypropylene system,” *Fire and Materials*, vol. 20, no. 1, pp. 39–49, 1996.
[131] M. Lewin and E. D. Weil, “Mechanisms and modes of action in flame retardancy of polymers,” *Fire retardant materials*, vol. 1, pp. 31–68, 2001.
[132] P. Georlette, J. Simons, and L. Costa, “Halogen-containing Fire Retardant Compounds” in Ed. A. and C.,(2000),” *08247887*, 2000.
[133] S. T. Lazar, T. J. Kolibaba, and J. C. Grunlan, “Flame-retardant surface treatments,” *Nature Reviews Materials*, vol. 5, no. 4, pp. 259–275, 2020.
[134] J. Green, “Phosphorus-containing flame retardants,” *Fire Retardency of Polymeric Materials. Marcel! Dekker, Inc, 270 Madison Avenue, New York, NY 10016, USA, 2000.*, pp. 147–170, 2000.
[135] B. Schartel, “Phosphorus-based flame retardancy mechanisms—old hat or a starting point for future development?,” *Materials*, vol. 3, no. 10, pp. 4710–4745, 2010.
[136] S. M. Lomakin and G. E. Zaikov, *Ecological aspects of polymer flame retardancy*, Vsp, 1999.
[137] Horacek, H., and W. Grabner, ed., *Nitrogen based flame retardants for nitrogen containing polymers*, Wiley Online Library, 1993.
[138] H. Horacek and R. Grabner, “Advantages of flame retardants based on nitrogen compounds,” *Polymer Degradation and Stability*, vol. 54, 2-3, pp. 205–215, 1996.
[139] S. Bourbigot, M. Le Bras, S. Duquesne et al., “Recent advances for intumescent polymers,” *Macromolecular Materials and Engineering*, vol. 289, no. 6, pp. 499–511, 2004.
[140] A. R. Horrocks, “Developments in flame retardants for heat and fire resistant textiles—the role of char formation and intumescence,” *Polymer Degradation and Stability*, vol. 54, 2-3, pp. 143–154, 1996.
[141] E. D. Weil, “Fire-Protective and Flame-Retardant Coatings - A State-of-the-Art Review,” *Journal of Fire Sciences*, vol. 29, no. 3, pp. 259–296, 2011.
[142] La Hollingbery and T. R. Hull, “The fire retardant behaviour of huntite and hydromagnesite–A review,” *Polymer Degradation and Stability*, vol. 95, no. 12, pp. 2213–2225, 2010.
[143] P. R. Hornsby, “The application of magnesium hydroxide as a fire retardant and smoke-suppressing additive for polymers,” *Fire and Materials*, vol. 18, no. 5, pp. 269–276, 1994.
[144] T. R. Hull, A. Witkowski, and L. Hollingbery, “Fire retardant action of mineral fillers,” *Polymer Degradation and Stability*, vol. 96, no. 8, pp. 1462–1469, 2011.
[145] F. Hewitt and T. R. Hull, “Mineral Filler Fire Retardants 17,” *Fillers for Polymer Applications*, p. 329, 2017.
[146] T. R. Hull, R. J. Law, and Å. Bergman, “Chapter 4 - Environmental Drivers for Replacement of Halogenated Flame Retardants,” in *Polymer Green Flame Retardants,* C. D. Papaspyrides and P. Kiliaris, Eds., pp. 119–179, Elsevier, Amsterdam, 2014.
[147] B. Schartel, “Phosphorus-based flame retardancy mechanisms—old hat or a starting point for future development?,” *Materials*, vol. 3, no. 10, pp. 4710–4745, 2010.
[148] I. van der Veen and J. de Boer, “Phosphorus flame retardants: properties, production, environmental occurrence, toxicity and analysis,” *Chemosphere*, vol. 88, no. 10, pp. 1119–1153, 2012.
[149] A. Araki, I. Saito, A. Kanazawa et al., “Phosphorus flame retardants in indoor dust and their relation to asthma and allergies of inhabitants,” *Indoor air*, vol. 24, no. 1, pp. 3–15, 2014.
[150] S. LeVan, *Choosing and applying fire-retardant-treated plywood and lumber for roof designs*, US Department of Agriculture, Forest Service, Forest Products Laboratory, 1989.

[151] K. Katsuura and N. Inagaki, “Flame-retardant properties of cellulose phenylthiophosphonate,” *Journal of Applied Polymer Science*, vol. 22, no. 3, pp. 679–687, 1978.
[152] R. Stevens, D. S. van Es, R. Bezemer et al., “The structure–activity relationship of fire retardant phosphorus compounds in wood,” *Polymer Degradation and Stability*, vol. 91, no. 4, pp. 832–841, 2006.
[153] B. Sjögren, A. Iregren, and J. Järnberg, “The Nordic Expert Group for Criteria Documentation of Health Risks from Chemicals. 143. Phosphate triesters with flame retardant properties,” *Arbete och Hälsa*, vol. 44, no. 6, 2010.
[154] D. C. Marney, L. J. Russell, and R. Mann, “Fire performance of wood (Pinus radiata) treated with fire retardants and a wood preservative,” *Fire and Materials*, vol. 32, no. 6, pp. 357–370, 2008.
[155] O. L. Diniz, “Flame retardant for wood application,”.
[156] S. Liodakis, D. Vorisis, and I. P. Agiovlasitis, “Testing the retardancy effect of various inorganic chemicals on smoldering combustion of Pinus halepensis needles,” *Thermochimica Acta*, vol. 444, no. 2, pp. 157–165, 2006.
[157] M. Gao, K. Zhu, Y. J. Sun et al., “Thermal degradation of wood treated with amino resins and amino resins modified with phosphate in nitrogen,” *Journal of Fire Sciences*, vol. 22, no. 6, pp. 505–515, 2004.
[158] S. Hamdani, C. Longuet, D. Perrin et al., “Flame retardancy of silicone-based materials,” *Polymer Degradation and Stability*, vol. 94, no. 4, pp. 465–495, 2009.
[159] S. A. Eastman, A. J. Lesser, and T. J. McCarthy, “Supercritical CO 2-assisted, silicone-modified wood for enhanced fire resistance,” *Journal of materials science*, vol. 44, no. 5, pp. 1275–1282, 2009.
[160] C. A. Giudice and A. M. Pereyra, “Silica nanoparticles in high silica/alkali molar ratio solutions as fire-retardant impregnants for woods,” *Fire and Materials*, vol. 34, no. 4, pp. 177–187, 2010.
[161] A. M. Pereyra and C. A. Giudice, “Ethyl silicates with different hydrolysis degree like non-flammable impregnating material for wood,” *Maderas. Ciencia y tecnología*, vol. 10, no. 2, pp. 113–127, 2008.
[162] Z. Yang, B. Fei, X. Wang et al., “A novel halogen-free and formaldehyde-free flame retardant for cotton fabrics,” *Fire and Materials*, vol. 36, no. 1, pp. 31–39, 2012.
[163] Bueno, AB Francés, et al., ed., *Treatment of natural wood veneers with nano-oxides to improve their fire behaviour*, IOP Publishing, 2014.
[164] S. P. Kumar, S. Takamori, H. Araki et al., “Flame retardancy of clay–sodium silicate composite coatings on wood for construction purposes,” *Rsc Advances*, vol. 5, no. 43, pp. 34109–34116, 2015.
[165] T. Cai, X. Shen, E. Huang et al., “Ag nanoparticles supported on MgAl-LDH decorated wood veneer with enhanced flame retardancy, water repellency and antimicrobial activity,” *Colloids and Surfaces A: Physicochemical and Engineering Aspects*, vol. 598, p. 124878, 2020.
[166] F. Carosio, F. Cuttica, L. Medina et al., “Clay nanopaper as multifunctional brick and mortar fire protection coating—wood case study,” *Materials & Design*, vol. 93, pp. 357–363, 2016.
[167] A. R. Horrocks, B. K. Kandola, P. J. Davies et al., “Developments in flame retardant textiles–a review,” *Polymer Degradation and Stability*, vol. 88, no. 1, pp. 3–12, 2005.
[168] J. A. Hawkes, P. Webb, D. M. Lewis et al., *Method and composition; WO2009030947 (A1)*, 9/3/2008.
[169] P. Webb, D. M. Lewis, J. A. Hawkes et al., *Composition and method ; WO2007099343 (A1)*, 3/2/2007.

[170] I. Vroman, E. Lecoeur, S. Bourbigot et al., “Guanidine hydrogen phosphate-based flame-retardant formulations for cotton,” *Journal of industrial textiles*, vol. 34, no. 1, pp. 27–38, 2004.
[171] S. Gaan and G. Sun, “Effect of phosphorus flame retardants on thermo-oxidative decomposition of cotton,” *Polymer Degradation and Stability*, vol. 92, no. 6, pp. 968–974, 2007.
[172] W. A. Reeves, G. L. Drake Jr, L. H. Chance et al., “Flame Retardants for Cotton Using APO and APS-THPC Resins,” *Textile Research Journal*, vol. 27, no. 3, pp. 260–266, 1957.
[173] C. Q. Yang, W. Wu, and Y. Xu, “The combination of a hydroxy-functional organophosphorus oligomer and melamine-formaldehyde as a flame retarding finishing system for cotton,” *Fire and Materials*, vol. 29, no. 2, pp. 109–120, 2005.
[174] J. K. Stowell and C. Q. Yang, “A Durable Low-Formaldehyde Flame Retardant Finish for Cotton Fabrics,” *AATCC review*, vol. 3, no. 2, 2003.
[175] I. Kaur and R. Sharma, “Development of flame retardant cotton fabric through grafting and post-grafting reactions,” *0971-0426*, 2007.
[176] M. J. Tsafack and J. Levalois-Grützmacher, “Plasma-induced graft-polymerization of flame retardant monomers onto PAN fabrics,” *Surface and Coatings Technology*, vol. 200, no. 11, pp. 3503–3510, 2006.
[177] M. J. Tsafack and J. Levalois-Grützmacher, “Towards multifunctional surfaces using the plasma-induced graft-polymerization (PIGP) process: Flame and waterproof cotton textiles,” *Surface and Coatings Technology*, vol. 201, no. 12, pp. 5789–5795, 2007.
[178] V. Totolin, M. Sarmadi, S. O. Manolache et al., “Low Pressure, Nonequilibrium-Plasma-Assisted Generation of Flame Retardant Cotton,” *AATCC review*, vol. 9, no. 6, 2009.
[179] K. Kong and S. J. Eichhorn, “Crystalline and amorphous deformation of process-controlled cellulose-II fibres,” *Polymer*, vol. 46, no. 17, pp. 6380–6390, 2005.
[180] H. Holik, *Handbook of paper and board*, John Wiley & Sons, 2006.
[181] T. Take, K. Nakahara, and K. Kaneko, *Nonflammable paper*: *U.S. Patent No. 4780180*, 1988.
[182] S. Wang, J. Huang, and F. Chen, “Study on Mg-Al hydrotalcites in flame retardant paper preparation,” *BioResources*, vol. 7, no. 1, pp. 997–1007, 2012.
[183] W. Pawelec, T. Tirri, M. Aubert et al., “Toward halogen-free flame resistant polyethylene extrusion coated paper facings,” *Progress in Organic Coatings*, vol. 78, pp. 67–72, 2015.
[184] T. Zhang, M. Wu, S. Kuga et al., “Cellulose Nanofibril-Based Flame Retardant and Its Application to Paper,” *ACS Sustainable Chemistry & Engineering*, vol. 8, no. 27, pp. 10222–10229, 2020.
[185] F. Xu, L. Zhong, Y. Xu et al., “Highly efficient flame-retardant kraft paper,” *Journal of materials science*, vol. 54, no. 2, pp. 1884–1897, 2019.
[186] D. Katović, S. Bischof-Vukušić, S. Flinčec-Grgac et al., “Flame retardancy of paper obtained with environmentally friendly agents,” *Fibres & Textiles in Eastern Europe,* 3 (74), 90--94, 2009.
[187] Y.-C. Li, S. Mannen, A. B. Morgan et al., “Intumescent all-polymer multilayer nanocoating capable of extinguishing flame on fabric,” *Advanced Materials*, vol. 23, no. 34, pp. 3926–3931, 2011.
[188] E. Magovac, I. Jordanov, J. C. Grunlan et al., “Environmentally-Benign Phytic Acid-Based Multilayer Coating for Flame Retardant Cotton,” *Materials*, vol. 13, no. 23, p. 5492, 2020.
[189] K. Ariga, J. P. Hill, and Q. Ji, “Layer-by-layer assembly as a versatile bottom-up nanofabrication technique for exploratory research and realistic application,” *Physical Chemistry Chemical Physics*, vol. 9, no. 19, pp. 2319–2340, 2007.
[190] J.-W. Kim, S. Park, D. P. Harper et al., “Structure and thermomechanical properties of stretched cellulose films,” *Journal of Applied Polymer Science*, vol. 128, no. 1, pp. 181–187, 2013.

[191] D. Klemm, F. Kramer, S. Moritz et al., “Nanocelluloses: a new family of nature-based materials,” *Angewandte Chemie International Edition*, vol. 50, no. 24, pp. 5438–5466, 2011.
[192] S. Park, J. O. Baker, M. E. Himmel et al., “Cellulose crystallinity index: measurement techniques and their impact on interpreting cellulase performance,” *Biotechnology for biofuels*, vol. 3, no. 1, pp. 1–10, 2010.
[193] T. Liitiä, S. L. Maunu, and B. Hortling, “Solid state NMR studies on cellulose crystallinity in fines and bulk fibres separated from refined kraft pulp,” *Holzforschung*, vol. 54, no. 6, pp. 618–624, 2000.
[194] K. Wickholm, P. T. Larsson, and T. Iversen, “Assignment of non-crystalline forms in cellulose I by CP/MAS 13C NMR spectroscopy,” *Carbohydrate research*, vol. 312, no. 3, pp. 123–129, 1998.
[195] S. Maunu, T. Liitiä, S. Kauliomäki et al., “13C CPMAS NMR investigations of cellulose polymorphs in different pulps,” *Cellulose*, vol. 7, no. 2, pp. 147–159, 2000.
[196] H. J. van de Wiel, “Determination of elements by ICP-AES and ICP-MS,” *National Institute of Public Health and the Environment (RIVM). Bilthoven, The Netherlands*, pp. 1–19, 2003.
[197] “1.5: ICP-AES Analysis of Nanoparticles,” *Libretexts*, 14.7.2016.
[198] Zachary Neale, “Inductively coupled plasma optical emission spectroscopy (ICP-OES) Overview,” https://youtu.be/InFhIHPZYIc.
[199] ISO, “Reaction-to-fire tests — Heat release, smoke production and mass loss rate: Part 1: Heat release rate (cone calorimeter method) and smoke production rate (dynamic measurement),” 01-2021, vol. 13.220.50, 5660-1:2015.
[200] V. Babrauskas, “The cone calorimeter,” in *SFPE handbook of fire protection engineering*, pp. 952–980, Springer, 2016.
[201] J. Troitzsch and E. Antonatus, *Plastics flammability handbook: principles, regulations, testing, and approval*, Carl Hanser Verlag GmbH Co KG, 2021.
[202] Günther Beyer, “Nanocomposites : a new calss of flame retradants for polymers,” *Plastics, Additives and Compounding,* no. 4,1, pp. 22–28, 2002.
[203] C. D. Papaspyrides and P. Kiliaris, *Polymer green flame retardants*: *Chapter 1 - Polymers on Fire*, Newnes, 2014.
[204] S. M. Mostashari, S. Z. Mostashari, and S. M. Mostashari, “The effect of weight content or density on the burning behavior of some cellulosic specimens,” *Polymer-Plastics Technology and Engineering*, vol. 47, no. 8, pp. 819–823, 2008.
[205] M. M. Khan, J. L. de Ris, and S. D. Ogden, “Effect of moisture on ignition time of cellulosic materials,” *Fire Safety Science*, vol. 9, pp. 167–178, 2008.
[206] Ö. Ceylan, J. Alongi, L. van Landuyt et al., “Combustion characteristics of cellulosic loose fibres,” *Fire and Materials*, vol. 37, no. 6, pp. 482–490, 2013.
[207] E. L. Schaffer, *Charring Rate of Selected Woods--traverse to Grain*, US Department of Agriculture, 1967.
[208] A. Gilka-Bötzow, A. Heiduschke, and P. Haller, “Zur Abbrandrate von Holz in Abhängigkeit der Rohdichte,” *European Journal of Wood and Wood Products*, vol. 69, no. 1, pp. 159–162, 2011.
[209] R. Wolgast, “Flame retarding building materials,” *VFBD Forschung und Technik im Brandschutz*, vol. 1961, no. 10, pp. 2–4.
[210] B. Miller, J. R. Martin, B. C. Goswami et al., “The effects of moisture on the flammability characteristics of textile materials,” *Textile Research Journal*, vol. 45, no. 4, pp. 328–337, 1975.
[211] L. Jiang, Z. Zhao, W. Tang et al., “Flame spread and burning rates through vertical arrays of wooden dowels,” *Proceedings of the Combustion Institute*, vol. 37, no. 3, pp. 3767–3774, 2019.
[212] H. Hofbauer, M. Kaltschmitt, and T. Nussbaumer, “Energie aus Biomasse–Grundlagen, Techniken, Verfahren,”.

[213] H. W. Yii, “Effect of surface area and thickness on fire loads,” *1173-5996*, 2000.
[214] K. Wang, F. Xu, and R. Sun, “Molecular characteristics of kraft-AQ pulping lignin fractionated by sequential organic solvent extraction,” *International journal of molecular sciences*, vol. 11, no. 8, pp. 2988–3001, 2010.
[215] M. R. Nyden, G. P. Forney, and J. E. Brown, “Molecular modeling of polymer flammability: application to the design of flame-resistant polyethylene,” *Macromolecules*, vol. 25, no. 6, pp. 1658–1666, 1992.
[216] U.-J. Kim, S. H. Eom, and M. Wada, “Thermal decomposition of native cellulose: influence on crystallite size,” *Polymer Degradation and Stability*, vol. 95, no. 5, pp. 778–781, 2010.
[217] W. D. Major, *The degradation of cellulose in oxygen and nitrogen at high temperatures*, Georgia Institute of Technology, 1958.
[218] A. Broido, A. C. Javier-Son, A. C. Ouano et al., “Molecular weight decrease in the early pyrolysis of crystalline and amorphous cellulose,” *Journal of Applied Polymer Science*, vol. 17, no. 12, pp. 3627–3635, 1973.
[219] J. Krishnan, S. Sunil Kumar, and R. Krishna Prasad, “Characterization of kraft pulp delignification using sodium dithionite as bleaching agent,” *Chemical Engineering Communications*, vol. 207, no. 6, pp. 837–846, 2020.
[220] T. Hatakeyama, K. Nakamura, and H. Hatakeyama, “Studies on heat capacity of cellulose and lignin by differential scanning calorimetry,” *Polymer*, vol. 23, no. 12, pp. 1801–1804, 1982.
[221] H. Ma, Y. Ma, and Z. Tian, “Simple theoretical model for thermal conductivity of crystalline polymers,” *ACS Applied Polymer Materials*, vol. 1, no. 10, pp. 2566–2570, 2019.
[222] R. Bacon and M. M. Tang, “Carbonization of cellulose fibers—II. Physical property study,” *Carbon*, vol. 2, no. 3, pp. 221–225, 1964.
[223] M. Zieglowski, “Synthese und Charakterisierung von Polyurethanschäumen und–beschichtungen ausgehend von Lignin und Ligninderivaten,” 2020.
[224] B. Schartel and T. R. Hull, “Development of fire-retarded materials—interpretation of cone calorimeter data,” *Fire and Materials*, vol. 31, no. 5, pp. 327–354, 2007.
[225] R. Sonnier, A. Viretto, B. Otazaghine et al., “Studying the thermo-oxidative stability of chars using pyrolysis-combustion flow calorimetry,” *Polymer Degradation and Stability*, vol. 134, pp. 340–348, 2016.
[226] P. Linstrom, “NIST Chemistry WebBook, NIST Standard Reference Database 69,” 1997.
[227] H. Yang, R. Yan, H. Chen et al., “Characteristics of hemicellulose, cellulose and lignin pyrolysis,” *Fuel*, vol. 86, 12-13, pp. 1781–1788, 2007.
[228] X. Yang, Z. Fu, D. Han et al., “Unveiling the pyrolysis mechanisms of cellulose: Experimental and theoretical studies,” *Renewable Energy*, vol. 147, pp. 1120–1130, 2020.
[229] J. Hioe and H. Zipse, “Radical Stability—Thermochemical Aspects,” *Encyclopedia of Radicals in Chemistry, Biology and Materials*, 2012.
[230] G. Camino, L. Costa, and L. Trossarelli, “Study of the mechanism of intumescence in fire retardant polymers: Part V—Mechanism of formation of gaseous products in the thermal degradation of ammonium polyphosphate,” *Polymer Degradation and Stability*, vol. 12, no. 3, pp. 203–211, 1985.
[231] C. Dayanand, G. Bhikshamaiah, V. J. Tyagaraju et al., “Structural investigations of phosphate glasses: a detailed infrared study of the x (PbO)-(1− x) P 2 O 5 vitreous system,” *Journal of materials science*, vol. 31, no. 8, pp. 1945–1967, 1996.
[232] X. Lai, J. Qiu, H. Li et al., “Thermal degradation and combustion behavior of novel intumescent flame retardant polypropylene with N-alkoxy hindered amine,” *Journal of Analytical and Applied Pyrolysis*, vol. 120, pp. 361–370, 2016.

[233] B. Qu and R. Xie, “Intumescent char structures and flame-retardant mechanism of expandable graphite-based halogen-free flame-retardant linear low density polyethylene blends,” *Polymer International*, vol. 52, no. 9, pp. 1415–1422, 2003.
[234] F. Zhang, J. Zhang, and C. Jiao, “Study on char structure of intumescent flame-retardant polypropylene,” *Polymer-Plastics Technology and Engineering*, vol. 47, no. 11, pp. 1179–1186, 2008.
[235] Honma, T., Hakamada, M., Sato, Y., Tajima, K., Hattori, H., Inomata, H., ed., *Density Functional Theory Study of Glyceraldehyde Hydrolysis in Supercritical Water*, 2006.
[236] B. Łaszkiewicz and B. Domasik, “Thermal properties of cellulose carbamate,” *Journal of Thermal Analysis and Calorimetry*, vol. 35, no. 7, pp. 2235–2242, 1989.
[237] Laine Janne, R. Hynynen, and P. Stenius, ed., *The effect of surface chemical composition and charge on the fibre and paper properties of unbleached and bleached kraft pulps*, Pira International, 1997.
[238] E. Gruber, “Papier-und Polymerchemie,” *Vorlesungsskriptum zum Lehrgang „Papiertechnik “an der Dualen Hochschule Karlsruhe*, 2011.
[239] M. Zhao, L. Robertsén, L. Wågberg et al., “Adsorption of paper strength additives to hardwood fibres with different surface charges and their effect on paper strength,” *Cellulose*, vol. 29, no. 4, pp. 2617–2632, 2022.
[240] L. Wågberg, “Polyelectrolyte adsorption onto cellulose fibres–A review,” *Nordic Pulp & Paper Research Journal*, vol. 15, no. 5, pp. 586–597, 2000.
[241] J. Laine, “Effect of ECF and TCF bleaching on the charge properties of kraft pulp,” *Paperi Ja Puu-Paper and Timber*, vol. 79, no. 8, pp. 551–559, 1997.
[242] A. E. Bennett, C. M. Rienstra, M. Auger et al., “Heteronuclear decoupling in rotating solids,” *The Journal of Chemical Physics*, vol. 103, no. 16, pp. 6951–6958, 1995.
[243] B. af Kopera and M. Retsch, “Multiplexed lock-in thermography,” *Review of Scientific Instruments*, vol. 92, no. 1, p. 14902, 2021.
[244] J. Tata, J. Alongi, F. Carosio et al., “Optimization of the procedure to burn textile fabrics by cone calorimeter: Part I. Combustion behavior of polyester,” *Fire and Materials*, vol. 35, no. 6, pp. 397–409, 2011.

10. Appendix

Fiji Image J macro

```
macro "Stack profile Data" {
    if (!(selectionType()==0 || selectionType==5 || selectionType==6))
      exit("Line or Rectangle Selection Required");
    setBatchMode(true);

    run("Plot Profile");
    Plot.getValues(x, y);
    run("Clear Results");
    for (i=0; i<x.length; i++)
       setResult("x", i, x[i]);
    close();

    n = nSlices;
    for (slice=1; slice<=n; slice++) {
       showProgress(slice, n);
       setSlice(slice);
       profile = getProfile();
       sliceLabel = toString(slice);
       sliceData = split(getMetadata("Label"),"\n");
       if (sliceData.length>0) {
          line0 = sliceData[0];
          if (lengthOf(sliceLabel) > 0)
             sliceLabel = sliceLabel+ " ("+ line0 + ")";
       }
       for (i=0; i<profile.length; i++)
          setResult(sliceLabel, i, profile[i]);
    }
    setBatchMode(false);
    updateResults;
}
```

MathLab macro

Start wave:

```
clear;clc;
q1='Ordner';
q2='Datei';
q3='Kaffee holen';
answer=questdlg('Was soll geladen werden','Ladeauswahl',q1,q2,q3,q3);
if strcmp(answer,q1)
   ordner=dir('*.csv');
   ordner={ordner.name};
   for i=1:size(ordner,2)
      filename = ordner{i};
      delimiter = ',';
      fileID = fopen(filename,'r');
      data = textscan(fileID, '%s', 'Delimiter', delimiter,  'ReturnOnError', false);
      fclose(fileID);
      wave_finder(data,filename,delimiter);
   end
else
   if strcmp(answer,q2)
      filename =  uigetfile({'*.csv'},'Input Datei');
      delimiter = ',';
      fileID = fopen(filename,'r');
      data = textscan(fileID, '%s', 'Delimiter', delimiter,  'ReturnOnError', false);
      fclose(fileID);
      wave_finder(data,filename,delimiter);
   else
      if strcmp(answer,q3)
         msgbox('Hol dir selber ein Kaffee')
      end
   end
end
```

Wave finder:

```
unction [  ] = wave_finder(data,filename,delimiter)
% clear;
% filename =  uigetfile({'*.csv'},'Input Datei');
% delimiter = ',';
% fileID = fopen(filename,'r');
% data = textscan(fileID, '%s', 'Delimiter', delimiter,  'ReturnOnError', false);
% fclose(fileID);
lauf=0;
i=4;
while lauf==0
   if strcmp(data{1,1}{i,1},'1')
      lauf=1;
   end
   i=i+1;
end
```

```
formatSpec='%f %s';
for j=3:i-2
   formatSpec=[formatSpec,' %f'];
end
fileID = fopen(filename,'r');
data = textscan(fileID, formatSpec, 'Delimiter', delimiter,  'ReturnOnError', false);
fclose(fileID);
%erg=zeros(size(data,2)-2,2);
erg_lauf=1;
erg_fehler_lauf=1;
for i=3:size(data,2)
   lauf=0;
      %    time(i-2,1)=data{1,i}(1);
   %     [wert,pos]=max(data{1,i}(2:end));
   %     if wert==255
   %         erg(i-2,2)=data{1,1}(pos(end)+1);
   %     else
   %         erg(i-2,2)=0;
   %     end
   j=size(data{1,i},1);
      while lauf==0
         if data{1,i}(j)==255
            erg(erg_lauf,1)=data{1,i}(1);
            erg(erg_lauf,2)=data{1,1}(j);
            lauf=1;
            erg_lauf=erg_lauf+1;
         else if j==2
                lauf=1;
                [wert,pos]=max(data{1,i}(2:end));
                erg(erg_fehler_lauf,4)=data{1,i}(1);
                erg(erg_fehler_lauf,5)=data{1,1}(pos(1)+1);
                erg(erg_fehler_lauf,6)=wert;
                erg_fehler_lauf=erg_fehler_lauf+1;
            end
         end
         j=j-1;
      end
end
delete([filename(1:length(filename)-4),'.xlsx']);
xlswrite([filename(1:length(filename)-4),'.xlsx'],erg);
end
```

Pore size distributions

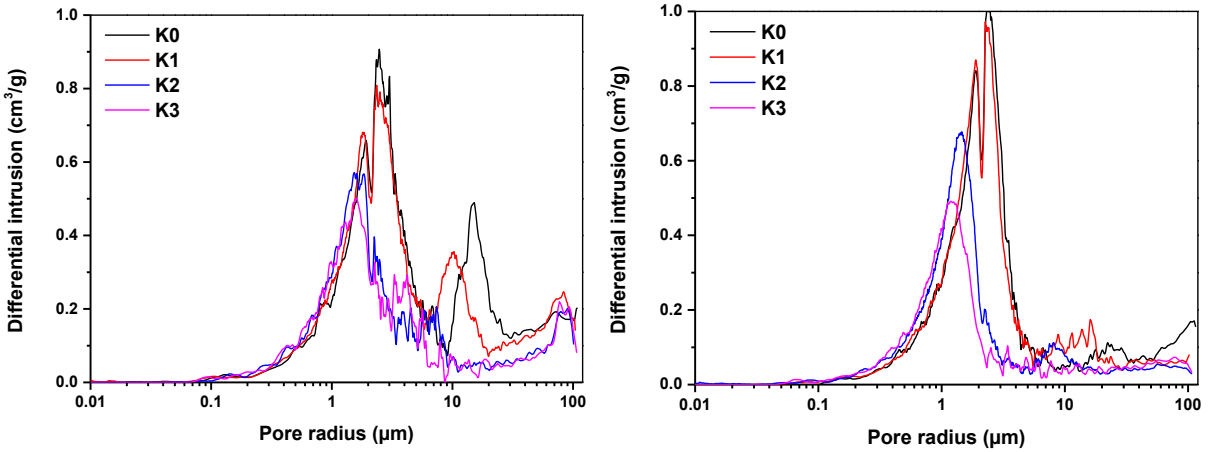

Figure 89: Pore size distribution of the 4 different calendaring stages of 100 g/m² (left) and 200 g/m² (right) NBSK paper.

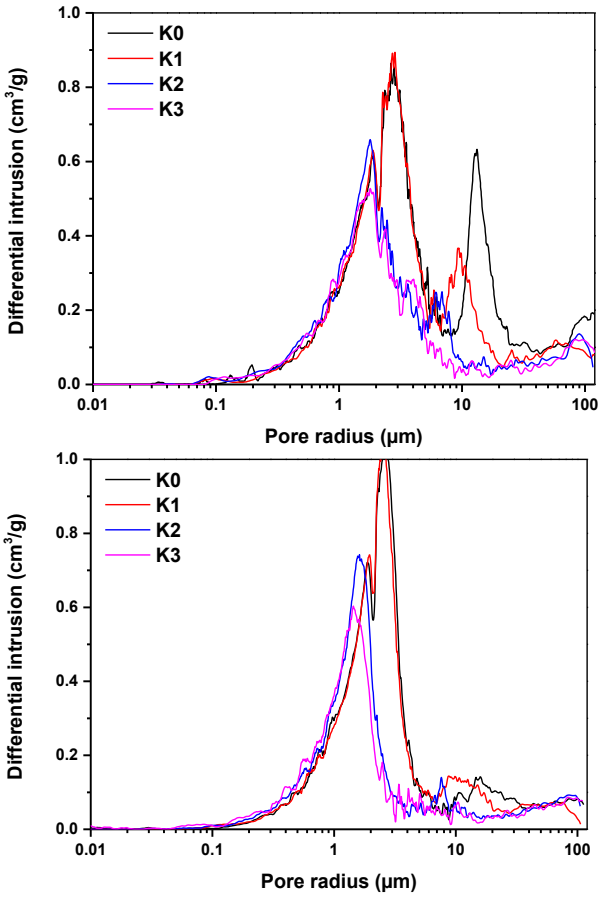

Figure 90: Pore size distribution of the 4 different calendaring stages of 100 g/m² (left) and 200 g/m² (right) UKP paper.

Thermogravimetric Analysis

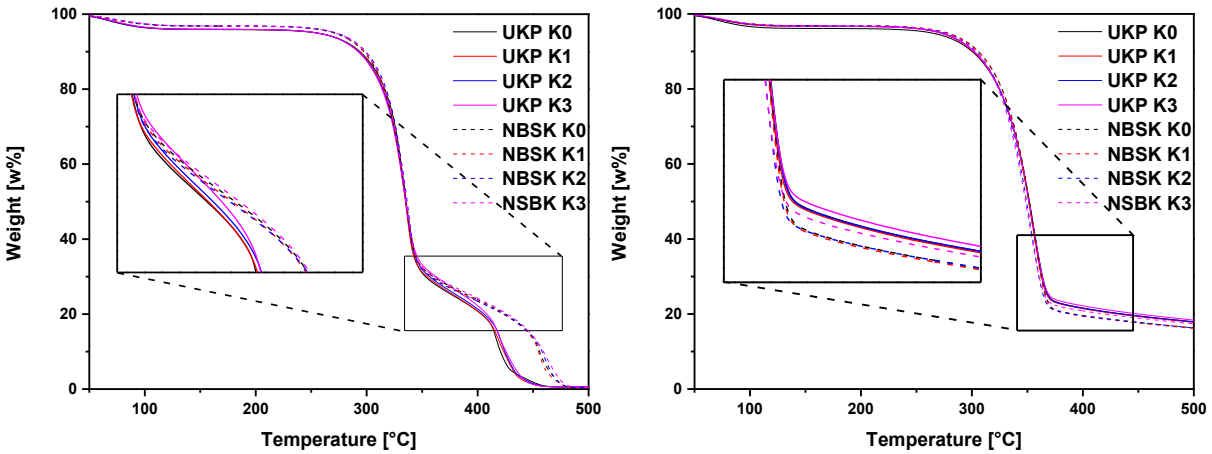

Figure 91: Analysis of the influence of calendering on the degradation behaviour in ambient (left) and N_2 atmosphere (right) for NBSK (dashed) and UKP (solid) 100 g/m² papers using TGA.

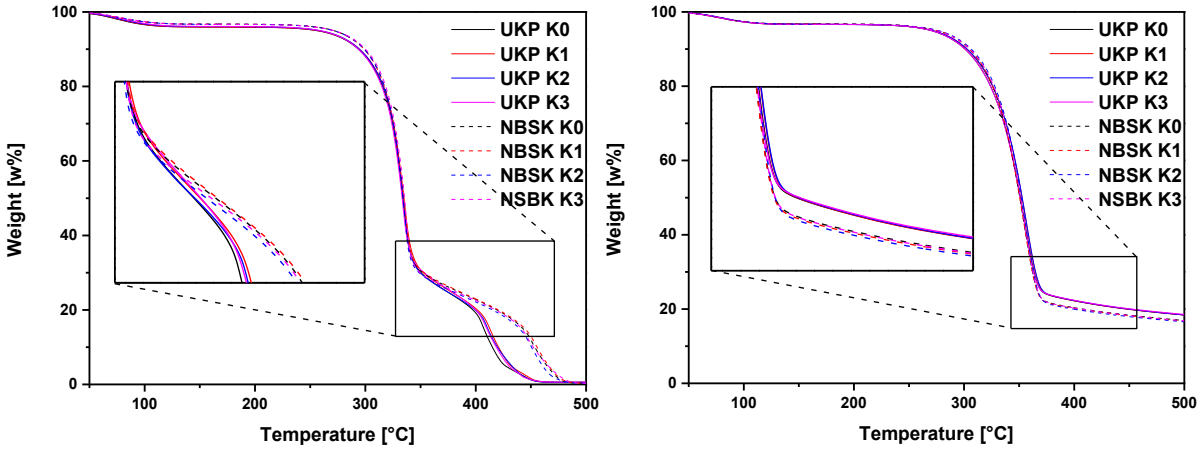

Figure 92: Analysis of the influence of calendering on the degradation behaviour in ambient (left) and N_2 atmosphere (right) for NBSK (dashed) and UKP (solid) 150 g/m² papers using TGA.

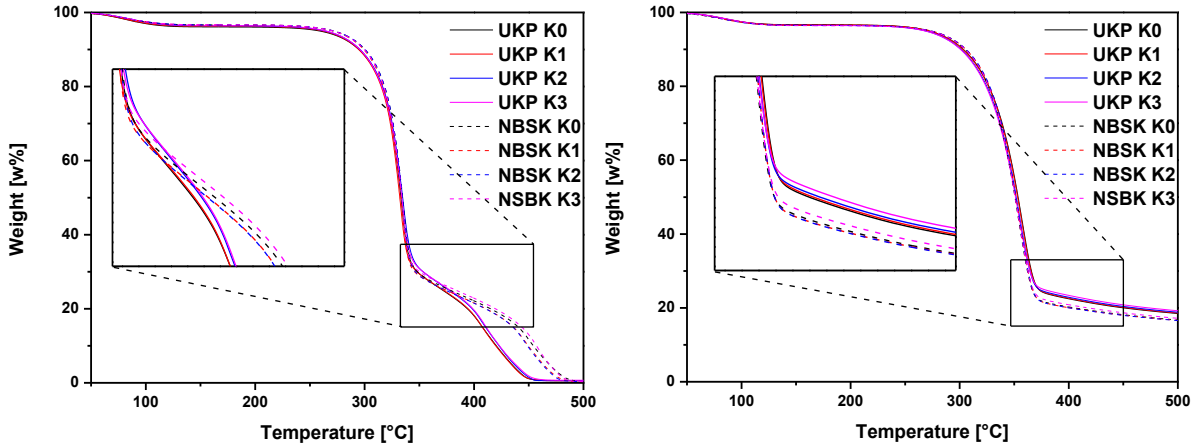

Figure 93: Analysis of the influence of calendering on the degradation behaviour in ambient (left) and N_2 atmosphere (right) for NBSK (dashed) and UKP (solid) 200 g/m^2 papers using TGA.

Crystallinity determinations via NMR

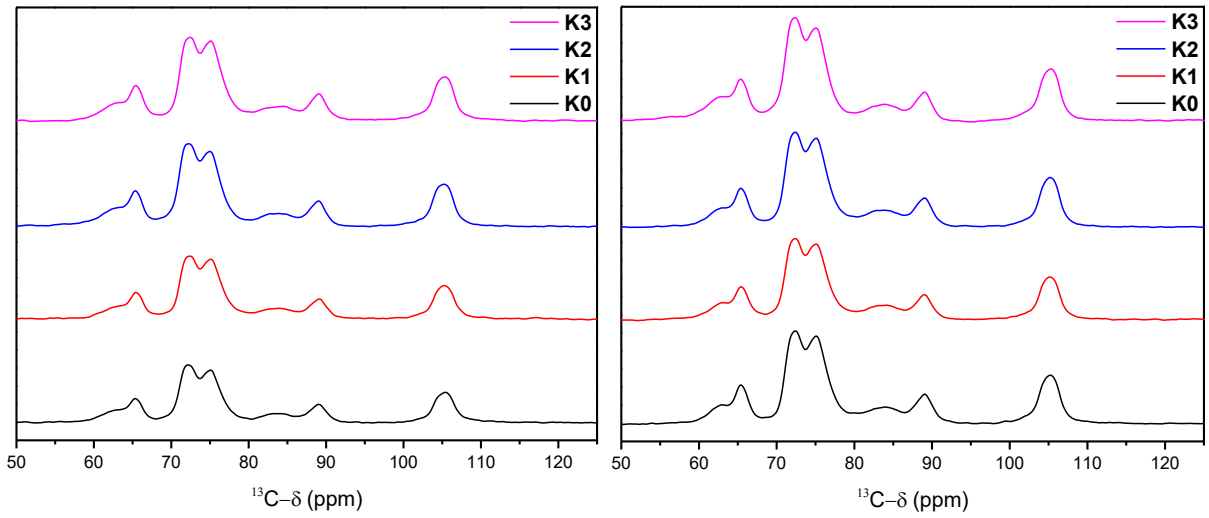

Figure 94: ^{13}C CP MAS ssNMR spectra of 100 g/m^2 NBSK (left) and UKP (right) papers with their 4 different calendering stages.

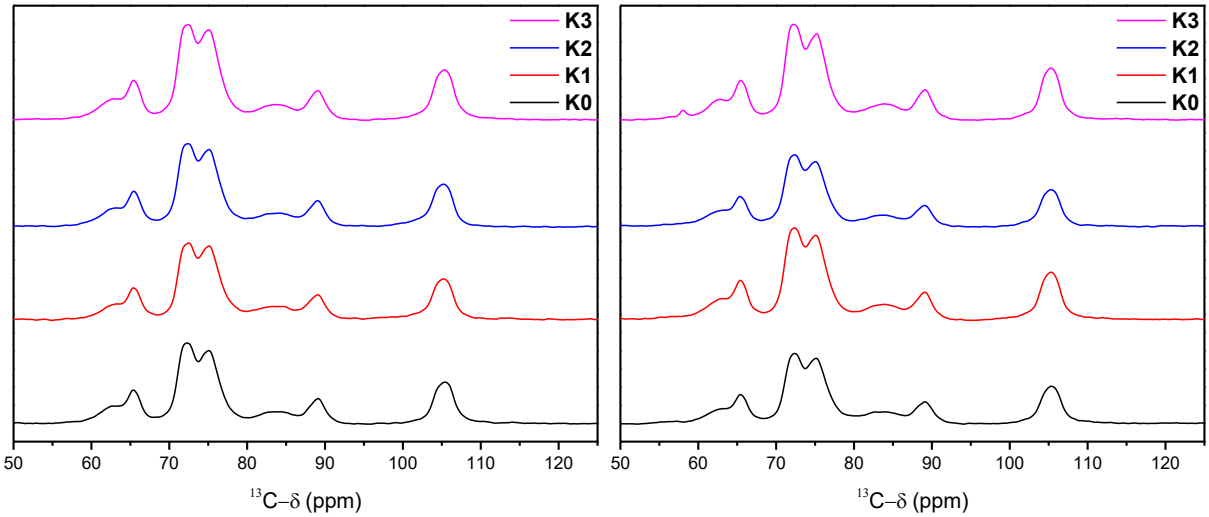

Figure 95: ^{13}C CP MAS ssNMR spectra of 200 g/m^2 NBSK (left) and UKP (right) papers with their 4 different calendering stages.

11. Declarations

Erklärungen laut Promotionsordnung

§8 Abs. 1 lit. c PromO

Ich versichere hiermit, dass die elektronische Version meiner Dissertation mit der schriftlichen Version übereinstimmt und für die Durchführung des Promotionsverfahrens vorliegt.

§8 Abs. 1 lit. d PromO

Ich versichere hiermit, dass zu einem vorherigen Zeitpunkt noch keine Promotion versucht wurde und zu keinem früheren Zeitpunkt an einer in- oder ausländischen Hochschule eingereicht wurde. In diesem Fall sind nähere Angaben über Zeitpunkt, Hochschule, Dissertationsthema und Ergebnis dieses Versuchs mitzuteilen.

§9 Abs. 1 PromO

Ich versichere hiermit, dass die vorliegende Dissertation selbstständig und nur unter Verwendung der angegeben Quellen verfasst wurde.

§9 Abs. 2 PromO

Die Arbeit hat bisher noch nicht zu Prüfungszwecken gedient.

Darmstadt,

_____

(Unterschrift)